Trinity College Dublin
Coláiste na Tríonóide, Baile Átha Cliath
The University of Dublin

THE INNATE IMMUNOMODULATORY EFFECTS OF AQUAMIN IN THE CONTEXT OF THE METABOLIC SYNDROME

A thesis submitted to Trinity College Dublin,

The University of Dublin

In the fulfilment of the requirement

For the degree of

Doctor of Philosophy

2023

By

Emmanouil Lioudakis

Mgr.Pharmacy, M.Sc.

Supervisor: Dr Margaret Lucitt

Department of Pharmacology and Therapeutics, School of Medicine, Trinity College Dublin

DECLARATION

I declare that this thesis has not been submitted as an exercise for a degree at this or any other university and it is entirely my own work.

I agree to deposit this thesis in the University's open access institutional repository or allow the library to do so on my behalf, subject to Irish Copyright Legislation and Trinity College Library conditions of use and acknowledgement.

_____

Emmanouil Lioudakis

SUMMARY

Metabolic disease is a combination of conditions that manifest together, elevating the risk for cardiovascular disease, type 2 diabetes and stroke. Inflammation is a major contributor in the pathophysiology of metabolic syndrome. Toll-like receptor (TLR) yields one of the main targets for anti-inflammatory pharmacotherapy. As macrophages and associated cytokines are strongly implicated in the inflammatory component of obesity, and metabolic disease, we aimed to investigate the effect of supplementation with Aquamin™ a mineral extract from red marine algae – rich in calcium (34%), in modulating inflammatory responses in vitro.

Using ELISA, and RT-PCR, it was demonstrated that Aquamin significantly reduces the protein and RNA expression of signature inflammatory cytokines such as TNF-α and IL-6 in dendritic cells, human monocytes, as well as murine and human macrophages that were exposed to LPS which is a TLR4 ligand.

To empower our insight concerning the anti-inflammatory effect of Aquamin, the protein expression of iNOS was measured by western blotting. The results revealed notable reduction of LPS-induced iNOS expression in murine macrophages by Aquamin.

Furthermore, significant reduction of TNF-α and IL-6 of TLR3 driven macrophages upon Aquamin treatment was reported by ELISA by exposing the cells to dsRNA, while no significant alteration was observed in TLR9-stimulated macrophages. That finding led to the conceivable assumption that Aquamin exerts its anti-inflammatory effect by exhibiting a TRIF-dependent immunomodulary role. Murine macrophages were exposed to LPS and transcriptional levels of MyD88 and TICAM1 adaptor molecules were measure by RT-PCR. Interestingly, our results revealed that gene expression of TICAM1 is significantly reduced by Aquamin, while no effect was seen on MyD88. These results further corroborate the hypothesis that Aquamin blocks TLR in a TRIF-dependent manner. IFN regulatory factor 3 (IRF3) is a transcription factor downstream of TLR3 as well as TRIF (TICAM1)-dependent TLR4 signaling. Activation of the receptors results to nuclear translocation of IRF3 and

subsequent production of IFN-β. Using immunohistochemistry, the effect of Aquamin in the activation of IRF3 was assessed. The results demonstrate significant reduction of Poly(I:C)-induced nuclear translocation of IRF3 as well as reduction of the IFN-β gene expression which was measured by RT-PCR.

Analysis of the macrophage transcriptome under LPS alone and NLRP3 exposure in the presence and absence of Aquamin and simvastatin can shed light on the mechanisms associated with Aquamin treatment. Here, the results of an in vitro study of murine BMDMs transcriptome response during LPS and LPS with cholesterol crystals (CC) stimulation using RNA-seq are described. Primary macrophages were extracted from murine bone marrow and were treated with Aquamin and simvastatin prior to exposure to TLR4 and NLRP3 stimulants. Initially ELISA was carried out to determine the TNF-α and IL-1β protein concentration. Our results highlighted that Aquamin has a more potent inhibitory effect than simvastatin against both cytokines in vitro. Treatment with Aquamin led to a significantly higher number of differentially expressed genes (DEGs) compared to simvastatin, both when compared to untreated control and in comparison, with LPS or LPS- and CC-induced samples. Functional analyses of these DEGs, including pathway enrichment, revealed potential functional roles for genes that have not been previously described. Verification of some relative genes was performed by RT-PCR.

Interestingly, this study evaluated the effect of Aquamin in a clinically relevant model of diet-induced obesity and inflammation. The mineral extract was formulated into a high fat diet and fed to C57BL/6 mice over 10 weeks, where diet induced obesity markers are assessed. A decreasing pattern in actual and percentage weight gain in animals fed the mineral extract supplemented diet was observed compared to control high fat fed animals. No change in food and water intake between the animal groups is observed. Mineral supplemented animals also responded better to insulin and glucose tolerance tests.

Collectively, the data generated in this thesis suggests that Aquamin's anti-inflammatory effects under TLR4 and TLR3 stimulation might be a result of TRIF dependent signaling mechanism. In summary the natural marine mineral extract may be beneficial in ameliorating diet induced obesity and modulates the associated inflammation in a TRIF-dependent manner.

ACKNOWLEDGMENTS

First and foremost, I am deeply indebted to my supervisor Dr. Margaret Lucitt. I cannot thank you enough for offering me the opportunity to do a PhD under your guidance and for your unwavering support. Not only for the unparalleled input you provided, but also for your patience throughout the whole duration of the PhD which cannot be underestimated. I could not have imagined having a better mentor for my PhD.

I would also like to extend my deepest gratitude to our collaborator Professor Patrick Walsh and all the members of his lab, especially Dr. Eirini Giannoudaki for their invaluable contribution to this project. Apart from their constructive advice all these years, I gratefully acknowledge their substantial help in flow cytometry and the in vivo part of this project.

This PhD would not have been possible without the support of Marigot Ltd. I very much appreciate their profound belief in our abilities to carry out this project.

I am also extremely grateful to Prof. Paul Spiers. Paul, you allowed me to work in your lab so I cannot thank you enough for your great hospitality and the insightful scientific conversations, which extended my practical and theoretical knowledge.

Furthermore, I cannot begin to express my thanks to Dr Pierce Kavanagh and Mr Kenneth Scott. Every laboratory needs gentlemen like yourselves. You had the willingness and expertise to provide me continuous support and encouragement throughout the duration of this project. I am delighted that I had the chance to meet both of you.

I cannot leave Pharmacology without mentioning my intimate friends Fawza and Dr Ismail Elgenaidi that never wavered in their support and helped me physically and mentally to complete this project. You are both hard workers and greatly inspired me to keep going every time I felt overwhelmed.

Thanks should also go to Dr Bashir Mohamed for his relentless help whenever it was requested. I cannot help but express my gratitude for all the social and scientific chats I had with you and Dr Steven Gray. Stephen, thank you for the access to the nanodrop.

I’d like to recognize the assistance and the precious advice I received from Prof. Aideen Long and Dr Stephen Maher upon assessing my transfer report.

Another reason I consider myself extremely lucky to be part of Pharmacology and Therapeutics is Teresa. Teresa, I hope you enjoy your well-deserved retirement to its fullest. Thank you for making my life easier every time paperwork had to be sorted. Most importantly, thank you for setting up those lovely morning coffee meetings with endless supply of cake.

To my partner, my family and friends, thank you for the unconditional love and support you provided me over the years. You have always been supporting and nurturing me and all this would not have been possible without having you in my corner.

PUBLICATIONS AND PRESENTATIONS

Lioudakis E, Lucitt M. Statin Disruption of Cholesterol Metabolism and Altered Innate Inflammatory Responses in Atherosclerosis. Immunometabolism. 2021;3(3):e210023

Papers in preparation:

- Lioudakis E, Lucitt M. Soluble Aquamin exerts anti-inflammatory effects by targeting TRIF-dependent Toll-like receptor signaling.
- Transcriptome analysis of Aquamin-treated BMDMs

Poster presentation:
Irish Association of Pharmacology 20th Annual Meeting, National University of Galway, Ireland, 30th November 2019. Title: The effects of Aquamin™ a marine mineral supplement from red algae on metabolic function.

LIST OF UNITS

g	grams
h	hours
kg	kilograms
L	liter
M	molar
mg	milligrams
ml	milliliter
mM	millimolar
ng	nanograms
pg	picograms

LIST OF ABBREVIATIONS

AMPK	Adenosine monophosphate-activated protein kinase
Ang II	Angiotensin II
ANOVA	Analysis of Variance
AP-1	Activator protein 1
APCs	Antigen-presenting cells
ASC	Apoptosis-associated speck-like protein containing a CARD)
BCA	Bicinchoninic acid
BMDMs	Bone marrow-derived macrophages
BP	Biological processes
CC	Cholesterol crystals
CD14	cluster of differentiation 14
CKD	Chronic kidney disease
CLR	C-type lectin receptors
CRP	C-reactive protein
DAMPS	Danger associate molecular patterns
DCs	Dendritic cells
DEGs	Differentially expressed genes
DMEM	Dulbecco's modified eagle medium
dsRNA	Double-stranded RNA
ELISA	Enzyme-linked Immunosorbent Assay
eNOS	Endothelial nitric oxide synthase
FFAs	Free fatty acids
FMO	Fluoresscence Minus One
FOXO1	Forkhead box protein O1
FPKM	fragments per kilobase of exon per million mapped fragments
FSP27	Fat-specific protein 27
GO	Gene ontology
GTT	Glucose tolerance test
HFD	High fat diet
HMGCR	HMG-CoA reductase
HPA	Hypothalamic-pituitary-adrenal
IBD	Inflammatory bowel disease
IBTS	Irish Blood Transfusion Service
IFN	Interferon
IGT	impaired glucose tolerance
IKK	Ik kinase
IL-6	Interleukin-6
iNOS	Inducible nitric oxide synthase
IRAK	Interleukin-1-receptor associated Kinase
IRF3	Interferon regulatory factor 3
IκBα	Inhibitor of nuclear factor kappa B
IκBα	Inhibitor of nuclear factor kappa B
KEGG	Kyoto Encyclopedia of Genes and Genomes
LD	Live Dead
LDL	Low density lipoprotein
LDLr	low-density lipoprotein receptor

LPS	Lipopolysaccharide
LRR	Leucine-rich repeats
LTA	lipoteichoic acid
MAPKs	mitogen-activated protein kinases
M-CSF	Macrophage colony-stimulating factor
MD-2	Myeloid Differentiation factor 2
MetS	Metabolic syndrome
MF	Molecular function
MyD88	Myeloid differentiation primary-response gene 88
NADPH	Nicotinamide adenine dinucleotide phosphate
NAFLD	Nonalcoholic fatty liver disease
NF-κB	nuclear factor-κB
NGS	New Generation Sequencing
NLR	NOD-like receptor
NLRP3	NLR family pyrin domain containing 3
NSAIDs	Non-steroidal anti-inflammatory drugs
OA	Osteoarthritis
PAI-1	Plasminogen activator inhibitor-1
PAMPs	Pathogen associated molecular patterns
PBMCs	Peripheral blood mononuclear cells
PCA	Principal component analysis
PGN	Peptidoglycan
PRRs	Pattern-recognition receptors
RAAS	Renin–angiotensin–aldosterone system
ROCKs	Rho kinases
ROS	Reactive oxygen species
RPMI	Rosswell Park Memorial Institute
RT-qPCR	Real time-quantitative polymerase chain reaction
TAK1	TGF-β-activated kinase 1
TBK1	TANK-binding kinase 1
TBST	Tris Buffered Saline with Tween®20
Th1	T-helper 1
TIR	Toll-Interleukin-1 receptor
TIRAP	Toll Interleukin 1 Receptor Adaptor Protein
TLR	Toll-like receptor
TNF-α	Tumour necrosis factor α
TRAF-6	TNF Receptor Associated Factor 6
TRAM	TRIF related adaptor molecule
TRIF	TIR-domain-containing adaptor inducing interferon-β

LIST OF TABLES

LIST OF FIGURES

TABLE OF CONTENTS

1. GENERAL INTRODUCTION

1.1 Metabolic disease

1.1.1 Definition, pathophysiology and risk factors

Metabolic disease is one of the major causes of morbidity and mortality worldwide (1). Over the past century, there has been a dramatic increase in the prevalence of type II diabetes as well as obesity which is increasingly recognized as a serious worldwide public health concern. Obesity, in combination with abnormal cholesterol and triglyceride levels, increased blood sugar and high blood pressure is collectively known as the metabolic syndrome (MetS). The MetS is recognised as a major risk and contributor to heart disease, insulin resistance, glucose intolerance, type 2 diabetes and stroke (2-4). Metabolic syndrome is characterized as a chronic pro-inflammatory and prothrombotic state in which the visceral fat component of adipose tissue is centrally associated with the disease pathophysiology (5, 6).

Free fatty acids (FFAs) released from adipose tissue sites contribute to lipoprotein abnormalities and hyperinsulinemia (Fig. 1.1). The accumulation of lipids for example in liver and muscle tissue leads to worsening over time of insulin resistance and dyslipidemias. Insulin resistance leads to impairment of lipolysis which is carried out by insulin under normal conditions and thus results to further increase circulating FFAs (7). The release of FFAs also harms pancreatic β-cells leading to reduced insulin secretion (8). Adipocytes may also cause endocrine alterations and elevate the risk for cardiovascular events (9). Adipose tissue releases an adipokine known as leptin which is responsible for controlling energy homeostasis and triggers the activation of type 1 T helper (Th1) cells, a subset of T

lymphocytes, a pathway which is associated with increased cardiovascular risk associated with obesity and diabetes (10). On the other hand, high adipose tissue mass contributes to the reduction of adiponectin which is involved in insulin sensitization as well as having anti-inflammatory effects. This anti-inflammatory adipokine exerts protective mechanisms against the development of cardiometabolic diseases by enhancing atherosclerotic plaque stability and lowering smooth cell proliferation as well as muscular reactivity (11-13).

Insulin resistance can result to MetS simply by exhibiting a negative correlation with blood pressure causing hypertension due to reduced vasodilation as a result of impaired insulin, as well as increased vasoconstriction from FFA due to elevated levels of ROS (14). Insulin resistance yields one of the most predominant features of MetS and thus detecting insulin resistance may assist in the diagnosis of MetS. Previous evidence have demonstrated technics which are cost effective and less invasive in order to predict insulin resistance (15-17). As per previous research by Hrebicek et al. as well as Singh and Saxena, calculating homeostatic model assessment–insulin resistance (HOMA-IR) index and quantitative insulin sensitivity check index (QUICKI) can yield a useful tool in the evaluation of insulin resistance.

The development of MetS can also be attributed to Angiotensin II (Ang II) a product of the renin–angiotensin–aldosterone system (RAAS) that regulates blood pressure. Increased adiposity increases angiotensin converting enzyme activation and the formation of Ang II (18). Ang II produces reactive oxygen species (ROS) which are linked to a series of events such as platelet aggregation, oxidation of low density lipoprotein (LDL), as well as activation of nuclear factor kappa B (NF-kB) transcription factor which promotes inflammation (19,

20). Overall a state of accumulating pro-inflammatory [tumour necrosis factor-a (TNF-a) and interleukin-6 (IL-6)] and pro-thrombotic [plasminogen activator inhibitor-1 (PAI-1)] mediators result following the excessive release of FFAs, as summarized in Fig. 1.1 (21, 22).

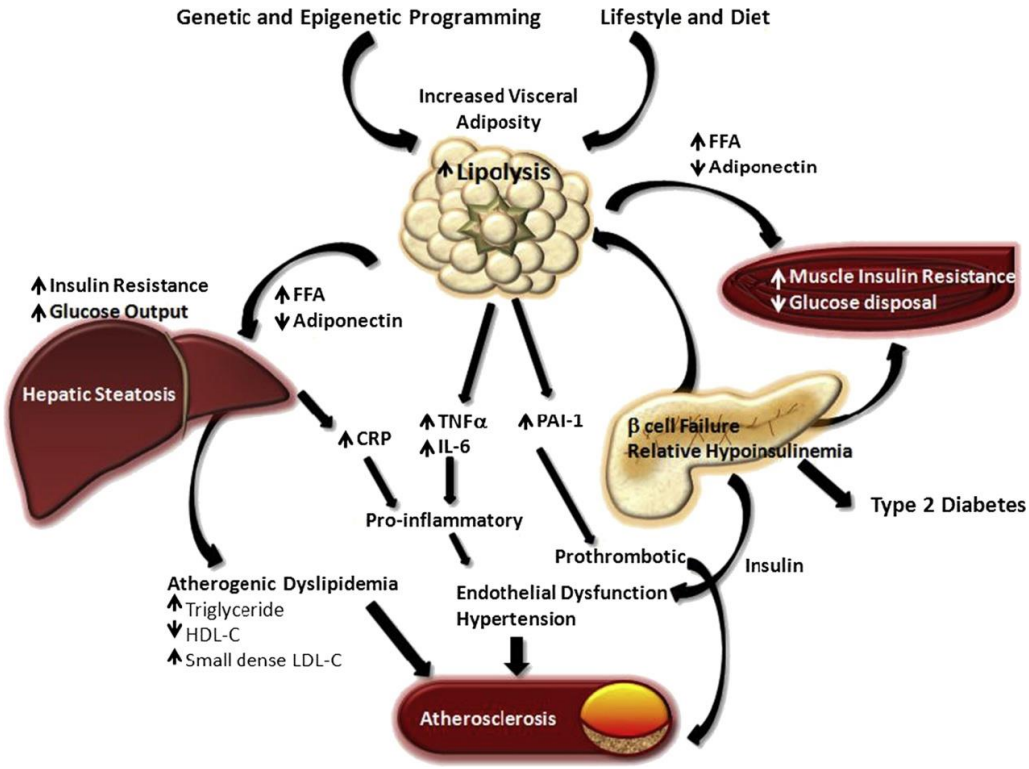

Figure 1.1 Pathophysiology of metabolic syndrome.

Schematic shows the pathogenic effects and multisystemic effects associated with increased visceral adiposity accompanied by production of pro-inflammatory mediators which in turn leads to pathological events that constitute the metabolic syndrome. *Adapted from "Metabolic Syndrome" by Samson SL, Garber AJ. Endocrinology and Metabolism Clinics. 2014;43(1):1-23.* (23)

The research to date has not fully elucidated the mechanisms that result in the worsening of the medical conditions associated with MetS. There is ample support to the claim that most people suffering from the condition are obese and they live a sedentary lifestyle. On the other hand, people can feature insulin resistance despite having normal weight and hence be prone to develop MetS. Even though Stress is not as major of a determinant as obesity and diabetes, it can yield an additional risk factor to the development of MetS according to previous evidence. Chronic stress could impair hypothalamic-pituitary-adrenal axis (HPA-axis) balance (24). Elevated cortisol levels are positively correlated with insulin resistance as well as glucose intolerance. Dyslipidemia and high blood pressure could also be attributed to dysregulated cortisol levels (25), indicating that stress could be a key player to the pathophysiology of cardiometabolic disease which is supported by previous research that had discovered a linkage between dysregulated HPA-axis and heart disease (26).

1.1.2 MetS biomarkers in more detail

As mentioned earlier, high leptin levels are known to be positively correlated to elevated body fat levels and hence metabolic events (27). Leptin is responsible for regulation of insulin sensitivity and glucose homeostasis (28). However, loss of sensitivity to leptin also know as leptin resistance can lead to impairment of the above functions leading to metabolic imbalance (29). Since elevated leptin is associated with cardiovascular events as well as inflammation, it exhibits an influential marker that links cardiovascular and metabolic disease.

In opposition to the role of leptin, adiponectin can yield a protective effect in cardiovascular and metabolic diseases such as atherosclerosis and diabetes (30, 31). As briefly stated previously,

adiponectin can be beneficiary to insulin sensitivity (32) and can function as a stabilizer of atheromatous plaque (33). Proper adiponectin levels are linked with protection against hypertension and insulin resistance. Previous research had established that individuals that feature low levels of adiponectin have higher predisposition to MetS (34).

Existing evidence has identified another biomarker of MetS which is generated from adipocytes and associated with glucose regulation, inflammation and adipogenesis in vivo and in vitro (35). Individuals that display MetS manifestation also demonstrate high levels of circulating chemerin which is a chemoattractant (36-38). Despite the fact that previous studies had shown that a high chemerin/adiponectin ration could serve as a diagnostic tool for MetS (39), further research needs to be conducted to validate its reliability.

Several publications have documented the link of Toll-like to MetS. Mice that were exposed to high fat diet to develop a MetS phenotype have demonstrated high expression of TLR4 (40). Along similar lines, murine models with TLR2 deficiency have presented low insulin resistance and diminished expression of pro-inflammatory cytokines as well as macrophage infiltration as opposed to TLR2 controls (41).

1.2 Inflammation

Inflammation is the mechanism which the body aims to retain its integrity with, upon tissue injury. When the body senses danger signals such as physical injury, infection, and trauma, inflammation is initiated (42). Exposure to pathogenic stimuli leads to activation of immune cells which leads to the release of pro-inflammatory cytokines and inhibition of anti-inflammatory cytokines (43). Again, the inflammatory response is driven by generation of chemokines

and cytokines as a result of transcription factor signaling such as NF-κB, AP-1 as well as type I interferons. Among the most popular cytokines and chemokines used are TNF-α, IL-1 and CCL2 respectively (44).

Symptomatology of inflammation includes pain, swelling and redness mainly (45). The clinical manifestation of inflammation is facilitated by histamine which permits the migration of phagocytes (46). Bradykinin yields another inflammatory mediator which increases the sensitivity of peripheral neurons that detect pain signals known as nociceptors and lead to loss of function as a response to pain (47, 48). Inflammation is aided by TNF-α, IL-6 and IL-1. On the contrary it is blocked by factors such as TGF-β and IL-10, while other cytokines like IL-4 are known to both aid inflammation in allergies but inhibit it in tumorigenesis exerting dual function (42).

The majority of acute and chronic diseases are characterized by inflammation which leads to excessive immune cell activity. Impairment of anti-inflammatory mechanisms leads to increased expression of cytokines and hence activation of NF-κB (49-51). Autoimmune diseases, asthma, as well as cardiovascular diseases such as arrhythmia and coronary artery disease all result from inflammation (42).

1.3 Obesity and associated diseases

Obesity is characterized by excess central abdominal fat which is an issue that has dominated the interest of the scientific community for many years. The disproportionate enlargement of the adipose tissue occurs due to immune cell infiltration and adipocyte hypertrophy (52, 53). Nowadays the increased accessibility of energy-dense foods in combination with the low need for physical activity has contributed to the development of obesity. Other key

factors which increases the risk for obesity is genetic predisposition since an increasing number of individuals displays susceptibility to develop obesity and related health problems due to heritability **(54, 55)**. Maternal nutrition can play a crucial role in the development of obesity as nutrient exposure during pregnancy can cause epigenetic modifications in certain genes elevating the risk of obesity and diabetes later in life **(56)**.

Obesity can lead to a range of health conditions such as Type II diabetes, heart disease, cancer risk, liver disease, mood as well as reproductive disorders (57, 58). Increased adipogenesis can also cause harmful effects in a variety of organs such as pancreas, liver, kidney, brain, heart, testis and muscles as well as causing sleep disturbances (59). Previous literature has shown that increased adipokine synthesis is linked with a high risk for diabetes (60). Increased adiposity can have detrimental effects in the liver by leading to nonalcoholic fatty liver disease (NAFLD) and subsequent liver cirrhosis (61, 62). Prior research has also emphasized that increased adiposity can escalate chronic kidney disease (CKD). However the deterioration of CKD is likely to be mediated by the obesity-induced diabetes and hypertension rather than directly (63). Another organ that is affected by obesity is the brain. Furthermore, excessive intake of nutrients that promote obesity such as carbohydrates and fats may also impair cerebral glucose metabolism by affecting insulin secretion and hence brain function (64). As has been previously reported in the literature, an obese state could negatively impact the blood supply to the brain, which might result in memory impairment and long term dementia (65, 66).Overall a diverse range of pathogenic effects across numerous body systems associate with the obese state which characterize the metabolic syndrome. As stated previously, chronic inflammation in the adipose tissue contributes to the development of insulin resistance and type 2 diabetes (67).

A growing body of literature has examined the significance of inflammation as an evolving mechanism in the development of a broad spectrum of disorders. When the immune system detects pathogens and other harmful stimuli, the removal of toxic molecules as well as the tissue repair process are initiated (68, 69). Hence inflammation is a defense mechanism which is crucial for health and homeostasis (70). Tissue injury triggers acute inflammatory response to attenuate the potential infection at the site of injury. It is well-established that acute inflammation if dysregulated can cause chronic inflammation, leading to inflammatory diseases (71). Highly prevalent diseases are driven by inflammation and the dysregulation of the immune system. Examples of inflammation-based diseases are heart disease, stroke, diabetes mellitus and autoimmune diseases (72). Adipose tissue is central to the inflammatory pathophysiology associated with the cardiometabolic syndrome. Increase in dietary fat intake triggers adipocyte hyperplasia (73). Consequently, the increase in adipose tissue mass can outgrow its own blood supply. A state of adipose tissue hypoxia can occur inducing cell necrosis, macrophage infiltration and the production of pro-inflammatory mediators such as IL-6 and TNF-alpha (74, 75).

A state of low-grade inflammation as a result from the release of the pro-inflammatory cytokines can maximize the risk of obesity-related co-morbidities. The inflammatory response which is facilitated by macrophages is a key factor of obesity-related tissue inflammation and insulin resistance. As explained below, there are many different types of infiltrating macrophages known to exist and associated with tissue inflammatory pathologies. Simplified here is the inflammatory, classical, or M1 macrophages, and the reparative, alternative, or M2 macrophages. Analysis of cell populations isolated from adipose tissue in both human and animal models of obesity has demonstrated that adipose tissue

macrophages are responsible for almost all adipose tissue TNF-alpha expression and significant amounts of IL-6 expression (76).

Epidemiology studies have pointed out IL-6 and TNF-alpha as inflammatory cytokines both linked to insulin resistance, type II diabetes and aggravation of cardiovascular events (77). In rodent models, it has been highlighted that infusion of human recombinant IL-6 could induce gluconeogenesis and a hyperglycemic state (78). A similar metabolic response to glucose regulation is manifested in humans after administration of subcutaneous recombinant IL-6 (79). The role of TNF-α in insulin resistance is less clear. In animal models of diet induced obesity blocking TNF-α signaling is beneficial against development of the metabolic syndrome (80). In human studies, neutralization of TNF-α also improves insulin sensitivity in patients suffering from a chronic inflammatory disease (81). However, TNF-α neutralization in type II diabetic patients has failed to show an improvement in insulin sensitivity (82).

The differences in the blocking effects seen with TNF-α may relate to the overall underlying inflammation across the patient cohorts studied. Perhaps a closer look at disease staging and timing of interventions with anti-inflammatory therapeutic strategies may provide better outcomes. Despite these difference in targeting TNF-α, inflammation overall is seen as a key component in driving the metabolic syndrome. Microbial pathogens induce inflammation which yields a fundamental mechanism of innate immunity (83).

1.4 Innate immune system overview

Immune cells identify tissue injury or infection, and they initiate an inflammatory response. The immune system of vertebrates is composed of innate and acquired immunity. Excessive dietary intake can lead to the activation of innate and

adaptive immune system. While innate immune system responds rapidly to foreign substances producing a nonspecific immune response, acquired immune system is associated with elimination of pathogen molecules in the latter phase of infection and the production of immunological memory (84, 85). Initially, during the first encounter with a pathogen, the adaptive immune response is slow. However, at the next encounter with the same pathogen the adaptive immune system acts rapidly with precision. Notwithstanding the fact that innate immune response is more generalized in comparison to adaptive immunity, innate immune response is a pivotal function of the immune system as it yields the first line of defense against an infection (86). The innate immune system is highly conserved across species providing the initial responses to infection and disease. Components of the innate immune system consists of physical barriers such as the skin and gastrointestinal tract, humoral responses in the form of the complement system and various cellular components. Cells such as macrophages (expanded on section 1.6), monocytes, dendritic cells (DCs), as well as neutrophils and mast cells identify invading pathogens during tissue damage by surface expressed pattern recognition receptors (PRRs) (87). Neutrophils possess a short life span and do not play a predominant regulatory role in the adaptive immune system (88). They rapidly act as phagocytes which occurs within minutes prior to phagocytosis-triggered cell death. Although phagocytosis is predominantly significant for engulfing of small pathogen molecules, the release of granules in the neutrophils is also induced by larger pathogens (89). To begin with, secretory vesicles consisting of surface receptors are put in motion before the release of tertiary granules consisting of matrix metalloproteases. Those metalloproteases aid migration through the extracellular matrix (90). Necrotic or damaged cells can function as sterile stimuli (91) and along with microbiological pathogens stimulate the

release of antimicrobial peptides as well as proteases that degrade fungi and bacteria in an efficient manner. Finally, neutrophils undergo apoptosis or other form of cell death upon prolonged interaction with microorganisms (92, 93).

Contrary to neutrophils that serve mainly innate immunity, dendritic cells yield a link between innate and adaptive immune response by capturing antigens and just like macrophages (94), they function as antigen-presenting cells to adaptive immune cells and hence facilitate their differentiation into effector cells (95). Based on the available evidence, dendritic cells are categorized to pasmacytoid (pDC) and myeloid (mDC) DCs and they recognize PAMPs via PRRs (96, 97). Therefore, DCs trigger T-cell responses against antigens as well as coordinate with Natural Killer cells mediating the early stage of innate immunity as well as the consecutive adaptive immune response (98).

Pathogen-associated molecular pattern molecules (PAMPs), for example, lipopolysaccharide (LPS), from microbial species and damage- associated molecular patterns (DAMPs), which are endogenous molecules released from dying or damaged cells are identified by PRRs on the surface of immune cells leading to the receptor activation (99). This activation can result in several responses and depending on the cell type involved initiate phagocytosis leading to destruction of the pathogen, production of various cytokines and activation of the immune system via antigen presentation. The main PRRs that are responsible for the initiation of innate immune responses include Toll-like receptors (TLRs), NOD-like receptors (NLRs), C-type lectin receptors (CLRs) and more (84, 100, 101).

The identification of pathogens by PRRs causes the activation of transcription factors such as NF-κB and inflammasome activation resulting in the production of pro-inflammatory cytokines and chemokines as well as type I interferon antiviral

responses (102, 103). The innate system overall playing a vital role in our defense mechanisms against invading pathogens.

1.5 Adaptive immune response

In comparison to innate immune response, adaptive immunity exhibits immunological memory and hence yields the capacity to identify the same pathogen should a second invasion occur (104). The innate immune system complements that adaptive immune response which is vital when innate immunity is inadequate. Notwithstanding the development of immunological memory, adaptive immune system is responsible for classifying antigens to "self" and "non-self" antigens (105).

One of the major targets for therapy in immune-associated diseases are T-cells which are originated from bone marrow and their maturation occurs in thymus (106). Every single T- cell expresses a T-cell receptor (TCR) and need the assistance of antigen presenting cells (APCs) to identify a specific antigen (107).

Upon cellular infection with bacteria or viruses, proteins known as the major histocompatibility complex (MHC) existing on the surface of APCs, present fragments of the corresponding antigens. Those antigens are then recognized by T-cells with the use of unique TCRs leading to their activation (108) and differentiation of T-cells into either cytotoxic T-cells (CD8+ cells) which kill either foreign or cells that have been infected, (109)or into T helper cells (CD4+ cells) which play a pivotal role in adaptive immunity by release cytokines and mediate in the activation of other immune cells (110).

1.6 Classification of macrophages

Arguably the most well described and abundant innate immune cell type found in adipose tissue are macrophages (111, 112). Macrophages are known to originate from primitive

macrophage cells seeded during development in tissues and are known as the tissue resident macrophage population as well as from hematopoietic stem cell precursors in the bone marrow during adulthood. Initially precursor cells exit the bone marrow as undifferentiated cells known as monocytes into circulation (113) having the ability to migrate and differentiate to macrophages in various tissue spaces. Large heterogeneity exists in the macrophage population reflecting their diverse plasticity depending on the environment they encounter and reside in. In mice, monocytes express high levels of CD11b which is associated with chemotaxis, and CD115 which is a macrophage colony stimulation factor (M-CSF) receptor. Previous research has demonstrated that the antigen F4/80 is widely considered to be a good marker for macrophages and it is mainly expressed during the process of monocyte differentiation to macrophages (114, 115).

When tissue is injured or infected, macrophages are responsible for regulating the return of host tissues to homeostasis. Mechanistically this occurs through macrophages engulfing large particulate matter, resembling the capacity of polymorphonuclear neutrophils, which are specialized in the removal of extracellular pathogens and clearance of cellular debris. Macrophages impact the inflammatory response by producing immunosuppressive and inflammatory cytokines upon stimulation of pattern-recognition receptors (PRRs) such as membrane bound TLRs or cytoplasmic Nucleotide oligomerization (NOD) like receptors (NLR) that macrophages express (116).

Previous studies have reported that macrophages are abundant at sites of inflammation, and they can also function as the antigen-presenting cells (APCs). Bone marrow derived macrophages (BMDMs) are an in vitro model of uncommitted cells and depending on the stimuli, they can initiate either a pro- or anti-inflammatory state mirroring the reported functions of

macrophage subsets in vivo. Incubation of macrophages with pro-inflammatory cytokines can induce the state of classically activated macrophages, whereas incubation of BMDMs with anti-inflammatory cytokines can induce the state of alternatively activated macrophages that correspond to an anti-inflammatory phenotype (Fig. 1.2) (116).

More specifically, classically activated macrophages (M1) upon stimulation with pro-inflammatory stimulants such as LPS and IFN-γ that arise from Th1 type subset of T lymphocytes release proinflammatory cytokine and leads to expression of cluster of differentiation (CD)14, CD80/CD86 cell surface markers and inducible nitric oxide synthase (iNOS). The release of pro-inflammatory cytokines and chemokines such as TNF-α, IL-6, IL-1β, CXCL9, CXCL10 is a feature of M1 skewed macrophages (117). Alternatively activated macrophages (M2) differentiate in the presence of Th2 type subset of T lymphocyte derived cytokines and acquire an anti-inflammatory phenotype involved in the resolution of inflammation and tissue repair. Several subtypes of M2 macrophages are described including M2a, M2b, M2c and M2d characterized based on expressing different combinations of cytokines, chemokines, and growth factors. M2 macrophages are triggered directly by IL-4 and IL-13 cytokines resulting in the expression of surface markers such as CD206 and CD209, as well as inducing the release of IL-10 cytokine. M2 macrophages demonstrate immunosuppressive properties, and can also promote angiogenesis (118, 119).

As mentioned above, a primary function of macrophages is phagocytosis. Macrophages can efficiently ingest and eliminate microorganisms, apoptotic cells, and foreign substances (120). Other cell types of the innate immune system include DCs. Similar to macrophages, DCs primarily act as APCs, and can bridge the gap between the innate and adaptive immune responses (121).

Depending on the inflammatory signals present in the adipose tissue microenvironment, macrophages are thought to play a central role in either the enhancement of the inflammatory state (M1), or the promotion of tissue homeostasis (M2) pathways of resolution and repair (122). As such they are considered key orchestrators of inflammation in obesity.

According to previous evidence, macrophages can be contributors to organ failure, when dysregulated activation of repair processes occurs such as cell-independent activation of mTOR signaling occurs (123). It has been established that certain pathogens possess the capacity to prolong the macrophage repairing process which could be detrimental (124).

Chronic diseases which are linked with dysregulation of macrophages tend to be affected by aging (125). To obtain some clarity about the function of macrophages in tissue repair, a better understanding of the age-induced changes in macrophages should be established. Previous researchers have noted that aging is responsible for impairment of pivotal macrophage functions such as phagocytosis, macrophage polarization as well as would healing along with reduced cytokine release (126).

Current evidence has also shown that macrophages can exert a crucial role in heart tissue injury and repair (127). According to previous research, CCR2 macrophages that reside in heart, promote the development of angiogenesis and arteriogenesis as well as cardiac regeneration (128, 129). The diminishment of the CCR2 positive macrophages can promote better clinical outcomes and hence improved cardiac function in a post-myocardial infarction state (130, 131).

Available evidence suggests that macrophages are pivotal in the pathogenesis of atherosclerosis (132). Macrophages, which are derived from monocytes, engulf lipoproteins and they form foam cells. Atheromatous plaque progression is dependent on both the

macrophage population as well as the inflammatory phenotype (133, 134).

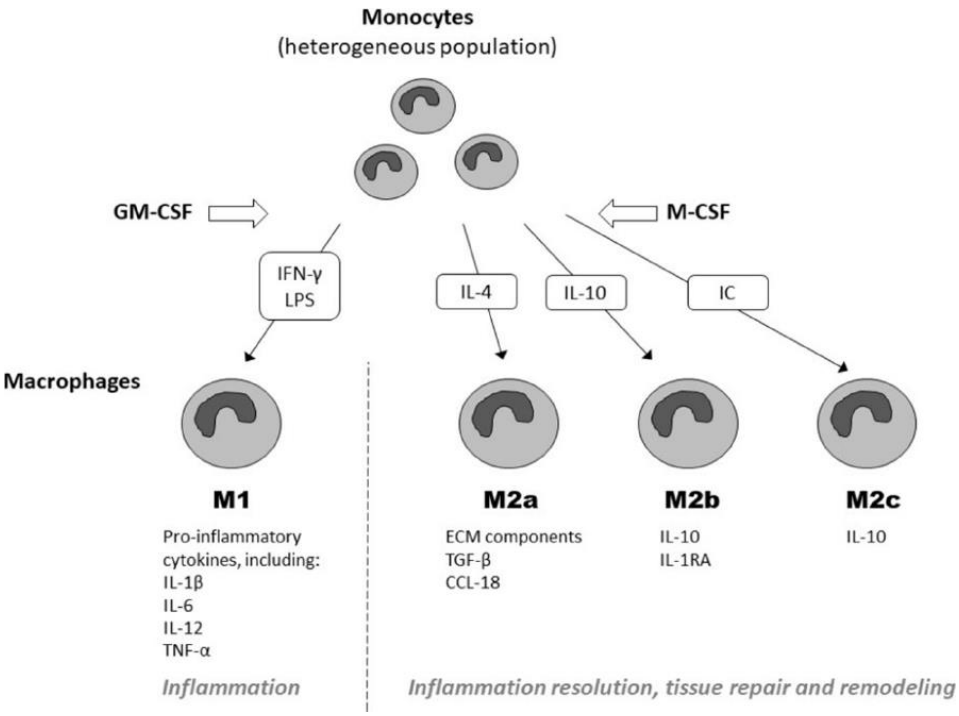

Figure 1.2. Macrophage differentiation into specialized functional subsets. Macrophages, depending on the stimuli, are polarized into either an M1 or M2 state wiht distinct functional phenotypes. M2 is further subdivided into M2a, M2b, M2c and M2d subsets.*Adapted from "Monocyte differentiation and macrophage polarization" by Orekhov AN, Orekhova VA. Vessel Plus. 2019;3:10* (135).

1.7 Pattern-recognition receptors

1.7.1 Toll-like receptors

1.7.1.1 Activation and ligands

Recent investigations focused on inflammation, have highlighted its important role in the pathophysiology of metabolic syndrome (136). Conditions like hypertension and high plasma glucose, as well as lipoprotein abnormalities substantiate a pro-inflammatory state (137). It is well established that inflammation which is a predominant component of repair during tissue injury is a key feature of metabolic and cardiovascular disease exerting detrimental effects if prolonged (2). There is overwhelming evidence corroborating the state of tissue injury in which host molecules or those derived from microorganisms are released and can trigger the activation of PRRs such as TLRs. The TLRs are activated by unique structures present in microbes also known as PAMPs, which originate from bacteria, fungi, and viruses, as well as host derived molecules identified as ELIS (DAMPS) (138).

To date 10 members of TLRs have been found in human, and 13 have been identified in rodents (139). Activation of TLRs by microbial products initiates the activation of NF-kB transcription

factor through mitogen-activated protein kinases (MAPKs) (140). The activation of TLR contributes to a spike of pro-inflammatory cytokines like TNF-alpha, IL-6, and IL-1beta (141-143). PAMP recognition by innate immune cells can also induce expression of a cluster of differentiation 80 (CD80) and 86 (CD86) costimulatory molecules on the surface of these cells which activate the adaptive immune response (144). Lipopolysaccharide (LPS) is one such PAMP located in the outer membrane of Gram-negative bacteria which binds to the cell surface receptor TLR4 stimulating an innate pro-inflammatory immune response (145). Other ligands for TLR4 include a variety of endogenous lipid molecules such as low-density lipoprotein (LDL) and palmitic acid both associated with adverse health effects resulting in dyslipidemia, and hyperglycemia. TLR4 is unique among the TLRs in its ability to signal via multiple adaptor proteins such as Myeloid Differentiation Primary Response Gene 88 (MyD88) and TIR-domain-containing adaptor inducing interferon-β (TRIF), who's signaling pathways are described in detail below.

Bacterial derived PAMPS are also recognized by other cell surface expressed TLR receptors such as TLR2. Ligands for TLR2 include Pam3CSK4 a synthetic diacylated lipopeptide (LP) which mimics the acylated amino terminus of bacterial LP. TLR2 heterodimerizes with TLR1- or TLR6- to signal via the adaptor molecule MyD88 leading to activation of pro-inflammatory transcription factors such as NF-κB and AP-1(146-148). TLR5 recognizes both Gram-positive and Gram-negative bacterial flagellin and signals as a homodimer also via the adaptor molecule MyD88 (149). Endosomal expressed TLRs such as TLR3 recognize viral double-stranded RNA (dsRNA) and signals via the adaptor molecule TRIF (43) whereas endosomal expressed TLR9 ligands include bacterial DNA containing CpG motifs can trigger responses through the adaptor molecule MyD88 (150). Figure 1.3 lists specific

TLR ligands and the associated adaptor molecules involved in downstream signaling events.

In the context of metabolic disease, there is evidence that TLRs play an important role in initiating the inflammatory state both through the increased presence of bacterial endotoxins in the bloodstream of obese individuals as well as endogenous DAMPS resulting from lipolysis (151). The association here is described in greater detail in sections below.

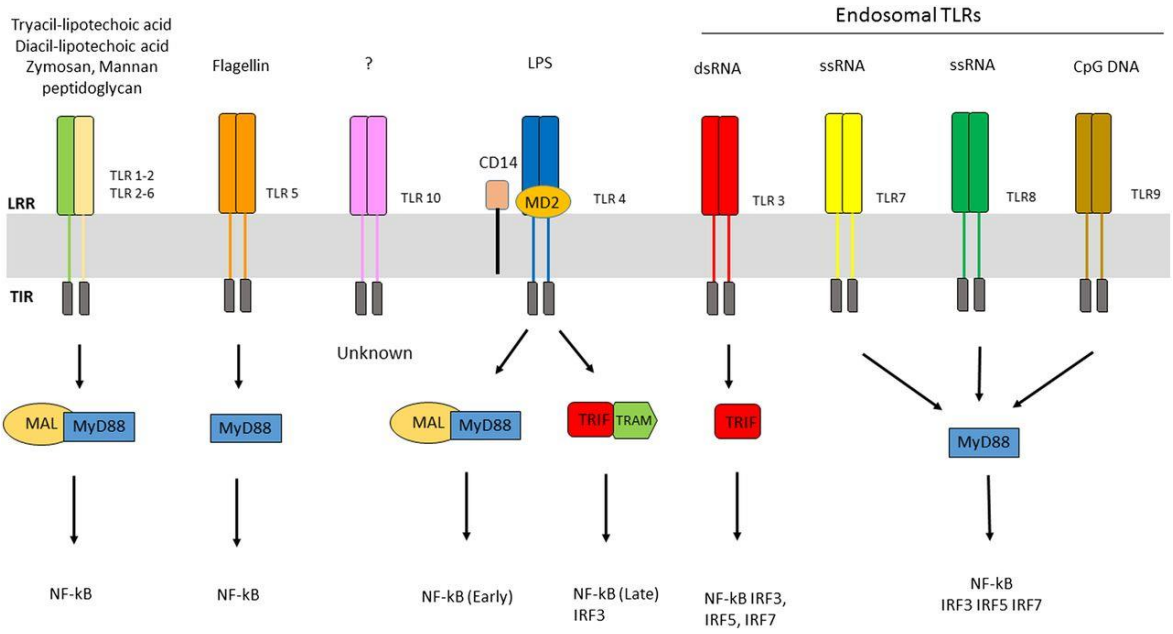

Figure 1.3. TLR adaptor molecules and their corresponding ligands.
Overview of TLRS (1 -10), their cellular locations, known ligands, and associated protein adaptor molecules, MyD88 and TRIF (MyD88-independent) mediating downstream signalling events. *Adapted from "Crosstalk between toll-like receptors and hypoxia-dependent pathways in health and disease" by Crifo B, Taylor CT. Journal of Investigative Medicine. 2016;64(2):369-75* (152).

1.7.1.2 Toll-like receptor - MyD88 adaptor protein pathway

It is generally accepted that TLR ligands produce downstream signals through four different adaptor proteins named Myeloid Differentiation Primary Response Gene 88 (MyD88), MyD88-like adaptor protein (Mal), TIR domain-containing adaptor protein-inducing interferon-β (TRIF), and TRIF-related adaptor molecule (TRAM) (Fig. 1.5) (84). The TLR4 signaling is the most complex among all TLRs. TLR4 is present on the plasma membrane, and its activation effects modulated through the action of all four adaptor proteins. Myeloid Differentiation factor 2 (MD-2) associates with TLR4 on the cell surface and is required for LPS signalling downstream of the TLR4 receptor. The signal transduction through TLR4 is facilitated by an additional protein known as cluster of differentiation 14 (CD14) (153). Conformational change in the TLR4 receptor upon LPS ligand engagement allows TIR domain containing adaptor molecules to be recruited and activated such as Toll Interleukin 1 Receptor Adaptor Protein (TIRAP) followed by the recruitment and subsequent activation of Myeloid differentiation primary-response gene 88 (MyD88).

MyD88 is downstream of all TLRs except TLR3 and it modulates the production of pro-inflammatory cytokines by activation of transcription factors Nuclear Factor kappa – light-

chain-enhancer of activated B cells (NF-kβ), and Activator protein 1 (AP-1) (154, 155). MyD88 is responsible for the formation and activation of Interleukin-1-receptor associated Kinase (IRAK) 1/4 complex which recruits and activates another adaptor protein TNF Receptor Associated Factor 6 (TRAF-6) which can then bind and activate TGF-β-activated kinase 1 (TAK1) (156). The corresponding downstream kinases that are activated under TAK1 include Mitogen-activated protein kinases (MAPKs) resulting in AP-1 transcriptional activation and IκB kinase (IKK) complex regulating early NF-kβ transcriptional activation. The IKK activated complex phosphorylates the inhibitor of nuclear factor kappa B (IκBα), which promotes its degradation and releases NF-κB p50/p65 phosphorylated subunit complex. These events allow NF-κB to nuclear translocate to direct NF-κB-dependent transcriptional activity such as increased expression of TNF-α and IL-6 cytokines (Fig. 1.4) (153).

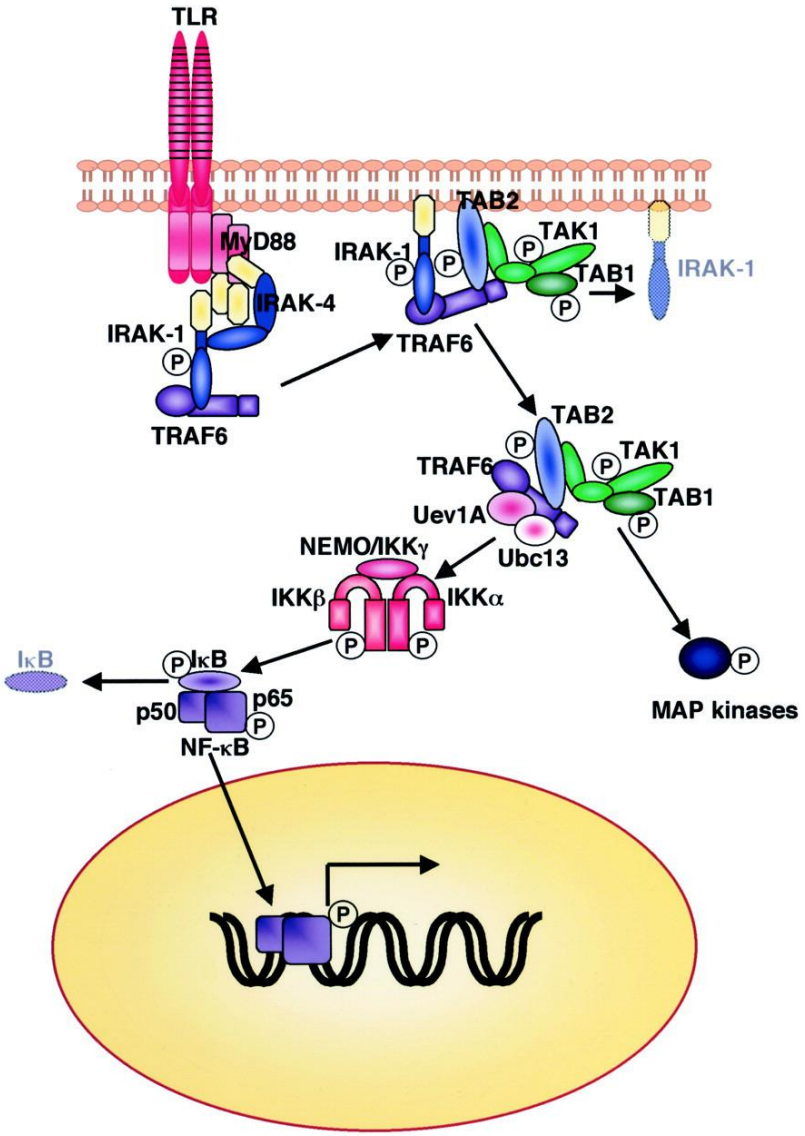

Figure 1.4. TLR and MyD88-adaptor protein dependent signalling.
Overview of TLR MyD88 adaptor protein signalling events that leads to the phosphorylation, nuclear translocation of NF-κB and transcriptional activation of responsive genes. *Adapted from "Toll-like Receptor Signaling" by Akira S. Journal of Biological Chemistry. 2003;278(40):38105-8.* (157)

1.7.1.3 Toll-like receptor - TRIF adaptor protein pathway

TLR4 also can signal via a MyD88 independent pathway via recruitment of the adaptor proteins TRIF (also called TICAM-1) and

the bridging adaptor TRIF related adaptor molecule (TRAM) (158). TRIF dependent (MyD88 independent) TLR signaling via TRAF3 induces type 1 interferon (IFNα and IFNβ) expression through activation of the transcription factor Interferon regulatory factor 3 (IRF3). TLR4 signals through TRIF by recognition of PAMPs like LPS which can also result and contribute to activation of NF-κB compared although delayed compared to MyD88 signaling (159). Activation of TRIF by plasma membrane Toll-like receptors leads to indirect activation of TRAF6 which results in the release of pro-inflammatory cytokines as described previously for MyD88 (153).

Double-stranded RNA is recognized by the endosomal receptor TLR3 (Fig. 1.5), which triggers TLR3 dependent TRIF activation followed by the recruitment of TRAF3 (160, 161). TRAF3 undergoes self-ubiquitination and forms complexes with TANK-binding kinase 1 (TBK1) and IKKi kinase leading to the activation of IRF3 by phosphorylation allowing the transcription factor translocation to the nucleus to induce the expression and release of Type-1-IFNs (159). TRIF is also responsible for TLR3 dependent slow activation of NF-κB by interacting with other signaling molecules such as TRAF6 at the N-terminal region (159, 162).

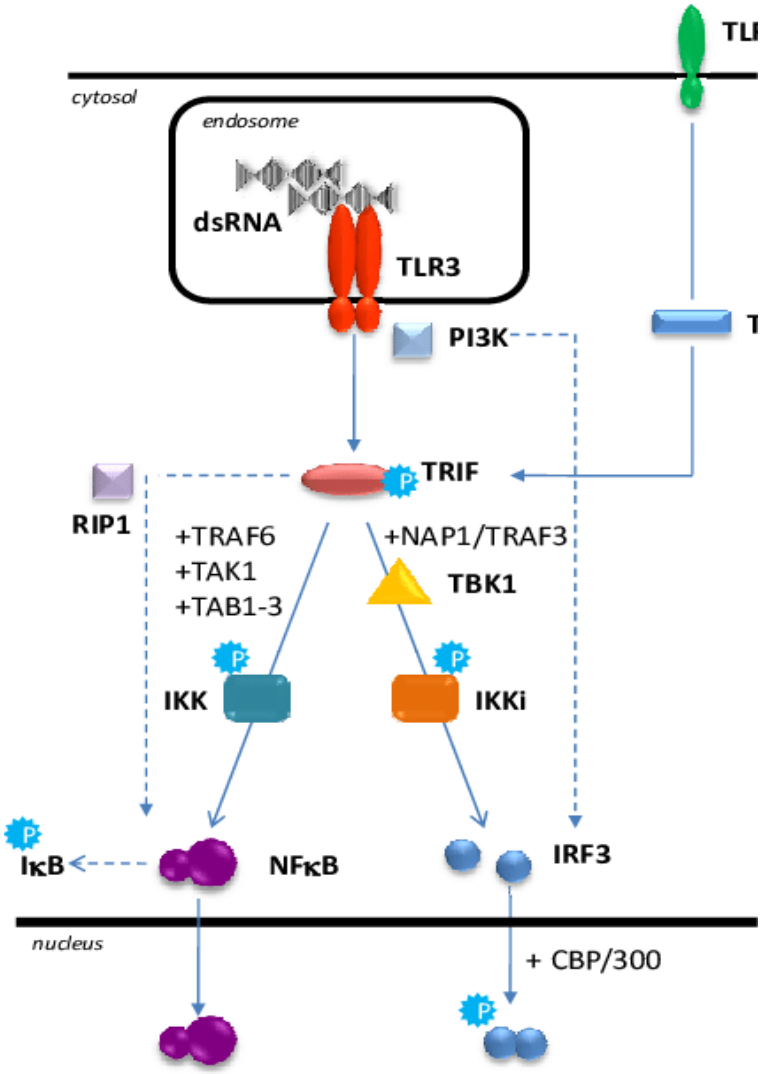

Figure 1.5. TLR and TRIF-adaptor protein dependent signalling.

Overview of TLR3 signalling through TRIF adaptor protein leading to an early IRF3 transcription factor activation and late-phase NF-κB transcriptional activation. *Adapted from "TLR3 Sensing of Viral Infection" by Dunlevy F, McElvaney N, Greene C. The Open Infectious Diseases Journal. 2010;4:1-10.* (163)

1.7.1.4 Toll-like receptors and metabolic disease

Recent papers provide ample support to the claim that TLR signaling plays a substantial role in the pathogenesis of heart and metabolic disease (141-143). In the context of obesity, mice fed a high-fat diet has shown an increase in intestinal permeability, which results in a greater translocation of LPS from the intestinal lumen to the blood circulation. This metabolic endotoxemia is associated with increased body fat, glucose intolerance, and increased expression of proinflammatory mediators and macrophage infiltration in adipose tissue (164). Furthermore, TLR4 gene deletion in diet induced obesity in mice shows a protective effect against adipose tissue inflammation and insulin resistance, supporting a role played by TLR4 in metabolic changes driven by obesity (165, 166).

In type II diabetes and obese individuals there is an increase in TLR2 and TLR4 expression in blood monocytes, and higher concentrations of associated serum cytokines IL-1β, IL-6, IL-8, and TNF-α compared to control lean individuals (167). Obesity gives rise to an increase in systemic inflammation, through an increase also in endogenous DAMPS and PAMPS which can act as TLR ligands. Obesity related saturated fatty acids, can induce inflammation through TLRs, particularly lauric acid and palmitic acid, by stimulating the inflammatory response described above through the TLR4 signaling pathway (168). Saturated fatty acids can also trigger an inflammatory response through the activation of TLR2, which forms heterodimers in the plasma membrane, with TLR1 or TLR6. Inhibition of TLR2 expression as seen above with TLR4 gene deletion in mice fed a high fat diet enhances sensitivity to insulin in the skeletal muscle and in the white adipose tissue, possibly through inhibiting palmitic acid-induced insulin resistance (169).

The transcriptional factor Forkhead box protein O1 (FOXO1) is predominantly expressed in insulin-responsive tissues and organs and can lead to potentiation of the inflammatory state and amplification of TLR4 signaling (170). FOXO1 activity is modulated by undergoing post-transcriptional modifications (171). Insulin stimulation can cause phosphorylation of FOXO1 preventing its nuclear translocation and thus reducing its activity. On the other hand, glucose can increase its nuclear localization (172, 173). FOXO1 exerts a key role within adipose tissue and in glucose metabolism by enhancing the expression of autophagy associated factors and gluconeogenesis enzymes (174). One of those factors, fat-specific protein 27 (FSP27) plays a central role in adipocyte differentiation and expansion, a process that can be reversed by a FOXO1 antagonist exerting anti-inflammatory activity (175). Inhibition of FOXO1 as an anti-inflammatory mechanism has also been explored in prior studies where FOXO1 knockdown in vivo using a rat model has led to downregulation of TLR4 signaling (176). Overall FoxO1 exhibits a central role in adipocyte differentiation and cell cycle control yielding a target for obesity and cancer respectively. Altogether these studies support the role of TLR signaling and its contribution to inflammation associated with the metabolic syndrome.

1.7.2 NOD-like receptor - NLRP3 activation and inflammatory disease involvement

TLRs are bound to the plasma membrane and play a substantive role in initiation of the immune response. However, another key family of PRRs associated with immune responses is NOD-like receptors which are found in the cell cytoplasm. NOD-like receptors are involved in the formation of protein complexes that

amplify immune responses causing apoptosis and are known as inflammasomes. The human genome codes for 23 NOD-like receptor proteins. NOD-like receptors are known to be divided into NOD like receptors with a pyrine domain (NLRP), as well as NOD-like receptors with a Caspase recruitment domain (NLRC). The most widely investigated NOD-like receptor is NLRP3 which is found as a monomer in an inactive form. In response to PAMPS and DAMPS, NLRP3 recruits adaptor proteins apoptosis-associated speck-like protein containing a caspase-recruitment domain (ASC) and pro-caspase-1, in a process known as oligomerization. Inflammasome is the structure that is produced from the oligomerization (177, 178). The inflammasome complex causes the activation of caspace-1 and subsequent cleavage of pro-IL-18 and pro-IL-1β into their active secreted forms (Fig. 1.7) (178, 179).

The activation of NLRP3 inflammasome is tightly regulated and occurs in a two-step process, firstly a priming step followed by second activation step. TLR PAMPs like LPS and cytokines induce the cellular priming events which leads to the upregulation and expression of the NLRP3 components, caspase 1 and pro-IL-1beta (180). The second step allows for full inflammasome activation and formation triggered by various stimuli from cellular stresses sensed by the inflammasome complex such as potassium efflux from PAMP pore forming toxins, DAMPs like ATP and crystal particulates (beta-amyloid, urate and cholesterol).

NLRP3 activation is known to be involved in the pathogenesis of metabolic disorders such as obesity, atherosclerosis and type 2 diabetes exerting a proinflammatory role (181). Previous studies that were conducted in the field of atherosclerosis have revealed the presence of cholesterol crystals (CC) in atheromatous plaque. Since then, CC were found to be involved in other cardiovascular pathologies with a strong correlation to lipid metabolism (182). Investigations assessing the

effect of CC on macrophage polarization provide evidence for the capacity of CC to skew human macrophages towards a M1 pro-inflammatory activation state (183). The presence of CC as well as other particulate matter triggers the formation and full activation of NLRP3 inflammasome in macrophages resulting in the production of IL-1β (184-186). There is a strong correlation between NLRP3 dysregulation with human inflammation driven pathophysiology's which promotes the need for NLRP3 inhibitors (187). As previously mentioned, atherosclerosis is a major driver of NLRP3 inflammasome activation. Dangerous signals derived from the atherosclerotic lesions such ad CC trigger the activation of NLRP3 and subsequent release of IL-1β (188).

Previous research has also emphasized the link between diet induced obesity and metabolic syndrome with NLRP3 inflammasome activation(189). Metabolic DAMPS such as ox LDL, as well as CC are prominent in obese phenotypes and they facilitate the activation of NLRP3 and pro-inflammatory response contributing to insulin resistance and MetS (190). Previous literature has demonstrated that inflammasome activation is also a feature of other diseases such as inflammatory bowel disease (IBD) (191) by displaying a link between NOD2 variants and susceptibility to Crohn's Disease which is the major type of IBD (192). Furthermore, signature cytokines of NLRP3 activation have also been found to contribute to the pathology of IBD (193).

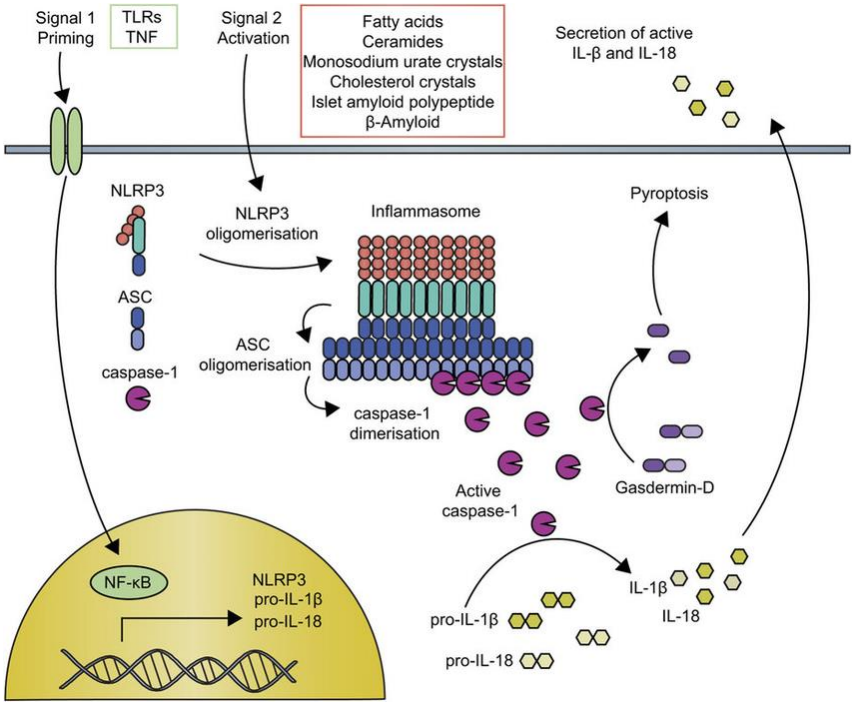

Figure 1.7. NLRP3 inflammasome priming and activation steps.

Overview of the two step events leading to priming and activation of the NLRP3 inflammasome complex. Step one initially involves cellular priming from microbial pathogen recognition leading to upregulation and expression of the inflammasome components. This is followed by step two producing inflammasome full activation facilitated by cellular sensing of various metabolic DAMPS and the cleavage and release of proinflammatory cytokines, IL-1beta and IL-18. *Adapted from "Questions and controversies in innate immune research: what is the physiological role of NLRP3?" by Coll R, O'Neill LAJ, Schroder K. Cell Death Discovery. 2016;2:16019.* (194).

1.8 Associated inflammatory pathways

Receptor activation causes subsequent activation of intracellular pathways. Notwithstanding the activation of NF-κB that was discussed previously, additional pathways modulate inflammation as a result of pro-inflammatory stimuli like TNF-α, IL-6 and IL-1β (195). Consequently to a pro-inflammatory cytokine stimulation, a family of serine/threonine kinases known as MAPKs are activated. Those kinases are playing a pivotal role in regulation of cell proliferation, differentiation, as well as apoptosis (196, 197). The mammalian MAPK family consists of ERK1/2, c-Jun N- terminal and p38 MAP kinase (198). Unlike JNK and p38 activation which is triggered by pro-inflammatory mediators, the activation of ERKs results from mitogens (199). Upon activation of ERK1/2 and JNK, phosphorylation and subsequent activation of cytoplasmic and nuclear p38 transcription factors occurs, which triggers the inflammatory response (197, 200).

Another pathway that is responsible for the release of cytokines and if dysregulated could lead to metabolic diseases, inflammation and cancer is JAK-STAT pathway (201). Apart from the activation of downstream cytokines as a result of JAK-STAT signaling, the pathway is also known to be involved with growth factors and hormones. JAK-STAT pathway is used by extracellular factors for the modulation of gene expression and there permits the translation of external stimuli into transcriptional responses (202). Transcription factors known as STATs, are localized in the cytoplasm before undergoing phosphorylation and hence translocation to the nucleus (203).

1.9 Current treatment approaches for metabolic disease

A favorable starting point for prevention and treatment of metabolic disease is the implementation of a healthy lifestyle which can be facilitated by improved diet and exercise (204). Ongoing pharmacotherapy for MetS focuses predominantly on the alleviation of the risk factors that contribute to its development by following a multi-drug approach (205-207). The multi-drug regimen for metabolic diseases consists of antilipidemic agents, antidiabetic agents, blood pressure lowering drugs, as well as anti-obesity therapy, with a number of these therapeutic approaches producing anti-inflammatory effects.

There is a considerable amount of literature suggesting that the components of metabolic disease such obesity, type II diabetes and cardiovascular disease are all characterized by chronic inflammation (208). Interestingly, colchicine which is the drug of choice for gout, is shown to exert anti-inflammatory effects by antagonizing NLRP3 inflammasome and if used at lower doses can yield a protective role against the occurrence of cardiovascular events (209). Studies also suggested that apart from its antirheumatic properties, the anti-inflammatory effect of methotrexate is beneficiary for the reduction of cardiovascular risk. Methotrexate causes anti-inflammatory effects by lowering the levels of inflammatory mediators such as CRP, TNF-α and IL-6 (210, 211).

Several years ago, research showed that salicylates could be used to reduce glucose levels in diabetic patients. This was further supported more recently by use of Salsalate a salicylate compound that exerts anti-glycemic properties (212, 213). Salicylates are well recognized to produce an anti-inflammatory effect by blocking the activation of NF-κB through specifically antagonizing IκK-β upstream of the transcription factor (214). How the anti-inflammatory effects with the agents described here contributes to their overall protective benefits in cardiovascular disease is still under investigation.

Exercise triggers the activation of a protein complex known as AMPK which has serine/threonine kinase activity. To that end research has focused on the effect of adenosine monophosphate-activated protein kinase (AMPK) in cardiometabolic disease and inflammation (135, 136). Interestingly it was found that activation of AMPK is associated with anti-atherosclerotic effects and reduces the accumulation of inflammatory cells induced by oxidized lipids as well as promoting antioxidant responses (137). Researchers have demonstrated that metformin which is the drug of choice for type II diabetes can also cause activation of AMPK (136). Taken together, activation of AMPK naturally or using pharmaceutical agents like metformin provides positive anti-inflammatory effects associated with the MetS (138).

Specific anti-inflammatory targeting approaches such as through targeting TNF-α are also investigated for cardiovascular and metabolic syndrome benefit Examples of anti-TNF-α agents are etanercept as well as monoclonal antibodies such as infliximab and adalimumab which are predominantly indicated for the treatment of psoriasis and rheumatoid arthritis (215, 216). In a previous study conducted in obese patients with MetS that received prolonged treatment of etanercept, improvement of fasting glucose was observed without any alterations in the levels of IL-6 and CRP (217).

However, agents that reduce the levels of TNF-α could increase the risk of infection as a potential adverse effect.

Other targeted anti-inflammatory approaches involve the IL-1 family of cytokines (208). Previous evidence supports that IL-1β is involved in obesity-linked inflammation (218). To this day, three anti-IL-1 compounds have been approved for their anti-inflammatory properties: anakinra which is an IL-1 receptor antagonist, rilonacept and canakinumab being monoclonal antibodies that neutralizes IL-1β (219, 220). Use of these agents in patients with cardiovascular disease and metabolic syndrome show positive protective effects.

IL-6 is an additional pro-inflammatory cytokine which has been recognized as a co-inducer of obesity associated insulin resistance prior to type II diabetes (221) and is also known to be connected with cardiovascular disease (222). Tocilizumab has been identified to block IL-6R and improve insulin sensitivity in juvenile arthritis patients suffering from insulin resistance (223). The various studies described here support a role for dampening down inflammation as a therapeutic approach in improving outcomes associated with the metabolic syndrome.

1.10 Statins: Mechanism of action and indications

The use of statin compounds is one of the most common pharmacological approaches against metabolic disease due to their LDL-lowering capabilities (205, 224). However, statins are gaining widespread attention not only for the plasma cholesterol-lowering capabilities but also for their anti-inflammatory activity (225). They are known to be the drug of choice for the treatment of atherosclerosis and they exhibit antihyperlipidemic effects by

competitively inhibiting HMG-CoA reductase (HMGCR), which is the rate controlling enzyme of the mevalonate pathway responsible for cholesterol production within the liver (226, 227). Thereby the inhibition of the enzyme leads to inhibition of cholesterol synthesis, very effective in reducing cholesterol laden atherosclerotic plaque burden in blood vessels and reduction in cardiovascular events (228).

Previous studies in the field of atherosclerosis that were carried out using apoE deficient mice have shown that simvastatin exhibited anti-inflammatory and anti-atherosclerotic activity independent of its function as a cholesterol-reducing agent (229). The anti-inflammatory effects of statins are multifactorial (Fig. 1.8) (230). Evidently some of those effects are due to the reduction of cholesterol production in the mevalonate pathway by decreasing protein prenylation and thus affecting innate immune response (231). The reduction in protein prenylation promotes an anti-inflammatory response leading to a reduction of cytokines and chemokines as well as blocking C-reactive protein, and adhesion molecules (232). Isolated innate immune cells from patient administrated simvastatin has shown inhibition in expression and activation levels of IL-1β induced by CC (184). The anti-inflammatory properties of simvastatin use are further substantiated by inhibition of pro-inflammatory mediators such as IL-1β and IL-6 in LPS induced monocytes. The same research group conducted an in vivo study using hypercholesterolemic patients that were subjected to simvastatin treatment resulting in notable reduction of TLR4 and TLR2 levels compared to the untreated patients (233). Interestingly, further evidence suggests that statin treatment can cause NLRP3 activation, indicating that the effect of statin treatment in NLRP3 varies (153). Based on the research that is currently available, it could be argued that statins inhibit the inflammasome activation, however the suppression of

inflammasome could depend on the type of statin used (150-152). It has also been asserted that statins reduce the activity of NF-κB (234) and produce epigenetic cellular changes through accumulation of mevalonate during disruption of cholesterol synthesis (235).

Increased cholesterol phenotypes feature impaired regulation of endothelial nitric oxide (NO). The increase of NO has been identified as a key mechanism for vasodilation and is also critical for vascular smooth muscle proliferation (236). Statins have been known to upregulate endothelial NO synthase (eNOS) resulting in the production of NO in pre-clinical models. Specifically mice treated with atorvastatin exhibited higher levels of eNOS, as well as reduced platelet factor 4 and other platelet specific factors (237). However these results cannot be extrapolated to humans as notably higher doses of statins were used in the animal studies compared to statin doses used in clinical practice (238, 239).

However human studies that were focused on patients with coronary artery disease, researchers have also witnessed that statin therapy had led to improved vasodilation (240) and better endothelial function in the context of coronary syndrome (241). Ezetimibe a selective inhibitor of cholesterol absorption a statin-independent cholesterol-reducing drug, does not share the same beneficiary properties in relation to coronary heart disease (242). Indicating for statins the that these vasodilating effects similar to the anti-inflammatory effects are again likely independent of their cholesterol lowering ability.

A large number of existing studies in the broader literature have discussed about Rho kinases (ROCKs) which has been identified as a biomarker in cardiometabolic disease (243-247). It has been reported that treatment with statins decrease ROCK activity in a cholesterol reduction-independent manner (248, 249). It has been well acknowledged by previous literature that the G

protein Rac1 which is a member of Rho family, plays a key role in the activation of nicotinamide adenine dinucleotide phosphate (NADPH) oxidase and thus generates reactive oxygen species (ROS) resulting to cardiac hypertrophy and conversion of LDL to oxLDL (250-252). To that end, inhibition of Rac1 by statins could indicate that statins potentially antagonize ROS production which may justify some of the pleiotropic effects of statins (253).

Apart from cardiometabolic disease studies the field of multiple sclerosis have demonstrated that high dose of simvastatin was beneficiary in reducing brain atrophy (158). Another study elucidates the protective effect of statin treatment against rheumatoid arthritis that further substantiates that use of the immunomodulary and anti-inflammatory effects of statins (159). Although the exact anti-inflammatory mechanism of statins remains to be established, these studies contribute to a better understanding of their anti-inflammatory role.

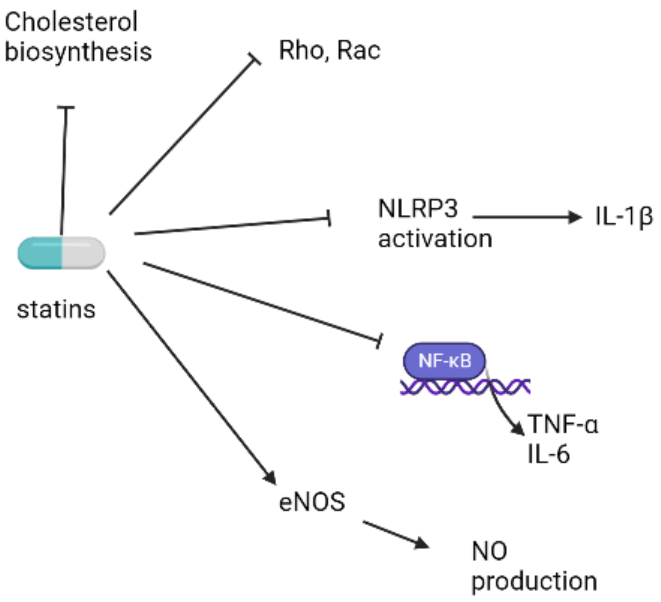

Figure 1.8. Anti-inflammatory mechanisms of statins.

Statins function as HMG-CoA reductase inhibitors and affect cholesterol biosynthesis (254). Statin treatment inhibits Rho signaling and exert anti-

inflammatory properties as well as increases the generation of eNOS (255). Statins suppress the activation of NLPR3 inflammasome (256). Statins reduce the expression of TLR2 and TLR4 and thus supress the NF-κB pathway (230).

Figure created with biorender.com

1.11 Nutraceuticals: Definition, origin and indications

Based on the fact that any compound requires at least 12 years and over $2billion before it gets FDA approval under the current safety paradigm, novel approaches like drug repositioning are needed to make the drug discovery process more affordable and effective (257). Nutraceuticals are components of food with a beneficiary role in the prevention of various pathological conditions. They are mainly derived from plants, animals, multimineral and microbial sources and they are taken orally. They exert their properties in the form of vitamins, phytochemicals, minerals, as well as unsaturated fatty acids (258). The use of nutraceuticals often aids in minimizing the drug complications as well as potentiating the positive effect of pharmaceutical agent in conjunction with their low purchasing cost (259, 260). Unlike drugs which have chemical origin, nutraceuticals facilitate the disease prevention process by restoring essential body micronutrients as well as being derived from natural sources.

The role of nutraceuticals in health is attracting considerable interest for scientists and clinical nutritionists. The high prevalence of obesity and cardiovascular events as a result of modern diet which is rich in sugar and saturated fats has increased the necessity for nutraceutical products which can exert a protective role for the prevention of diseases associated to sedentary lifestyle (Fig. 1.9) (258). Previous studies have demonstrated that intake of

nutraceuticals can yield a cost-effective approach option to minimize the occurrence of events such as atherosclerosis, heart attack and stroke (261).

Apart from the beneficiary role of nutraceuticals in the protection against lifestyle problems, their questionable role against cancer has also been shown. More recently, research has emerged that offers contradictory findings about the use of nutraceuticals in cancer patients. Although food supplements enhance the immune system, they could increase the resistance of cancer cells to chemotherapy and accelerate carcinogenesis (262).

The benefits of nutraceuticals have also been observed against inflammatory diseases such as osteoarthritis (OA). Research has shown that incorporation of unsaturated FAs into the diet can enrich the treatment options for OA by properly regulating the anabolic and catabolic signals associated (263). A previous study has reported that intake of fish oil exerts anti-inflammatory activity in vitro in a dose-dependent manner (264).

The studies described in this thesis focus on an analysis of how a currently available nutraceutical product, Aquamin may be beneficial towards metabolic health through potentially altering the innate inflammatory response.

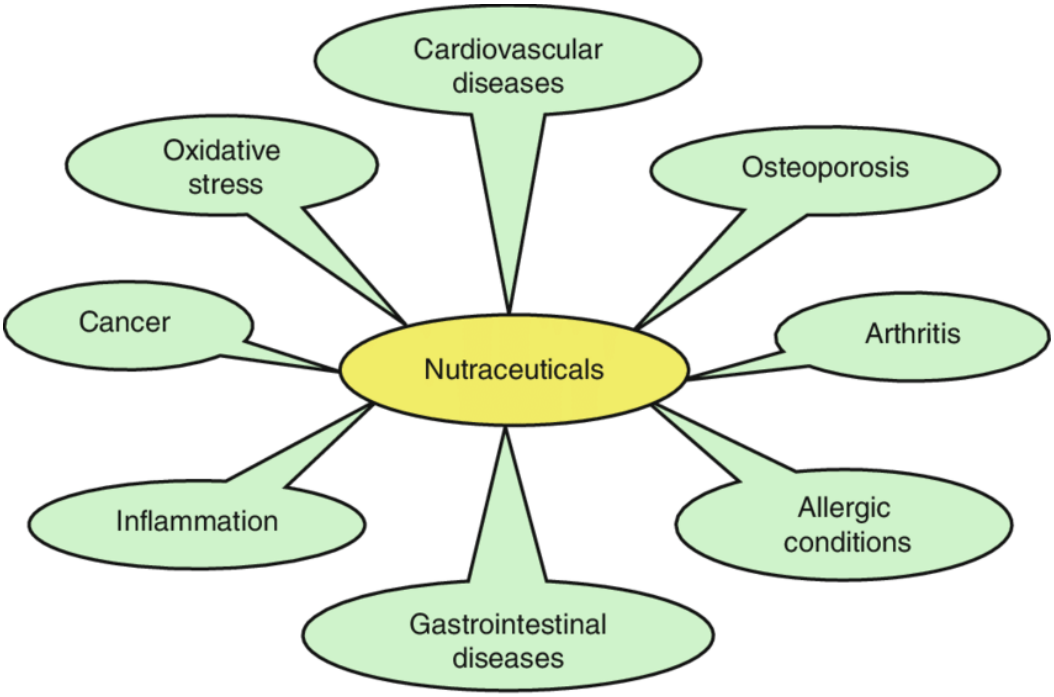

Figure 1.9. Nutraceuticals as beneficial agents across several disease areas.

A list of diseases associated with beneficial outcomes during nutraceutical use, providing support for nutraceutical supplementation along with conventional therapy in these disease areas. *Adapted from "Nutraceuticals and antioxidants in prevention of diseases" by Jain N, Ramawat K. Nat Prod. 2013:2560-80.*(265)

1.12 Benefits of Aquamin consumption and current evidence

Aquamin is a marine multi-mineral nutraceutical derived from the Lithothamnion plant which is rich in magnesium but having calcium as its predominant component (Table 1.1). It is plant based and has a vegetative cell structure in contrast with calcium carbonate which is extracted from limestone or rock. Previous research that was carried out in mice had demonstrated that a single dose of Aquamin did not cause any side effects in mice and no pathological lesions in organs such as liver and kidneys were detected. Similarly, no detrimental effect on eyes and skin was observed and no mortality occurred. In addition, no hypertrophy was observed in any of the organs upon treatment with Aquamin (266).

Aquamin has demonstrated notable bone health benefits exerting a protective role against osteoarthritis and osteoporosis (267). In vitro studies using pre-osteoblastic cells, demonstrated that treatment of cells with Aquamin led to increased mineralization. This evidence provided further support to the beneficiary properties of Aquamin in bone health (268). The osteogenic effect of Aquamin was further empowered by a study that was conducted in a rat model of osteoporosis. In comparison to calcium, the corresponding study demonstrated that Aquamin was more effective against bone loss (269).

Recent evidence has demonstrated that Aquamin might exert a protective role against fatty liver disease. In research

conducted by Harber et. Al, immunohistochemical analysis of liver tissue revealed that incorporation of Aquamin into high-fat Western diet is beneficiary against the development of nonalcoholic steatohepatitis (270).

Previous studies that were performed in IL-$10^{-/-}$ mice of C57BL/J background that received Aquamin, have shown that it provides protective against colitis in that mouse strain. More specifically Aquamin reduced the expression of the pro-inflammatory cytokine IL-1β in colon samples (271).

There is no existing evidence to corroborate whether Aquamin's therapeutic effects are based on a certain element or on a synergy among elements. Research has shown that Ca which is the main component of Aquamin, apart from preventing bone loss , it can also cause a modest decrease to the incidence of colon cancer (272-274). Similarly to calcium supplementation, a recent study published by Aslam, et al. conducted in human subjects, concluded that daily intake of Aquamin is also beneficiary for colonic health and thus exerts a protective role against colon cancer (275).

A previous study has examined the effects of Aquamin on IBS by assessing potential changes in short chain fatty acid production. The authors suggest that Aquamin may exert a beneficiary role in the microbial function of the gastrointestinal tract (276).

Experiments conducted on RAW 264.7 macrophage cells to investigate if there is a link between Aquamin and the transcription factor NF-kB. The results demonstrated that Aquamin reduces the phosphorylation of IkBa which is an upstream blocker of NF-kB, thus suppressing the LPS-driven activation of NF-kB. This indicated Aquamin potentially having an anti-inflammatory effect (277). Additional evidence supporting the anti-inflammatory activity of Aquamin in vitro has been provided by a study that was carried out

in glial primary rat cells where Aquamin supplementation significantly blocked the LPS-induced release of TNF-α and IL-1β (278).

Within the framework of these criteria concerning the drug discovery process, this thesis aims to outline the potential protective role that Aquamin might yield against cardiovascular and metabolic disease as well as assessing its mechanism of action.

Table 1. Mineral composition of the soluble form of aquamin
(Available from: http://aquamin.com/).

Mineral	Dry Salt Weight
Calcium Carbonate	85% (34% calcium)
Magnesium Carbonate	8.5% (2.4% magnesium)
Salt (as chloride)	1.5%
Moisture	3.0%
Trace Minerals**	2.0%
Sulphur	0.7%
Potassium	0.6%
Phosphorus	0.05%
Sodium	0.25%
Manganese	100 ppm.
Zinc	20 ppm
Iron	800 ppm
Iodine	30 ppm
Boron	17 ppm.
Copper	8 ppm.
Cobalt	0.1 ppm.
Selenium	1.0 ppm.

*Aquamin is a natural ingredient and the trace minerals that bind to Aquamin may vary over time.

1.13 Hypothesis and Aims

Research in the past number of years provides evidence that Aquamin can act to restrict inflammation, however many of these studies have been observational to date using Aquamin as a supplement. The main objective of this thesis work is to investigate the immunomodulatory effects of Aquamin in macrophage cellular responses and whether Aquamin supplementation can improve outcomes in the context of the metabolic syndrome. Altogether exploring the possibility for Aquamin as a nutraceutical to be used as a stand-alone agent or combined with existing therapeutic medicines.

Specific aims:

1. To characterize the immunomodulatory effects of Aquamin in both human and murine macrophage cells.

2. To evaluate the global immune mediated macrophage response using Aquamin compared to statin treatment utilising a non-targeted RNA sequencing approach.

3. To investigate whether Aquamin supplementation alters the development of metabolic disease in a relevant animal model of obesity driven type II diabetes.

2. MATERIALS

2.1 Equipment

Table 2.1. Equipment

Equipment	Company, model
Analytical balance	Mettler, AE240
Autoclave	Dixon
Automated pipettes	Gilson, Inc. [2µl, 10µl, 100µl, 200µl, 1000µl, 5000µl, Pipettman Ultra 8-channel (20 – 300 µl)]
Centrifuge	Hettich Zentrfugen, EBA 12R/mikro 22R
Cytell ™ imaging system	GE Healthcare
Digital imaging	Fusion FX imaging system, Vilber Lourmat
Fluorescence microscope	EVOS
Freezer (-80)	Thermofischer Scientific, Revco Valure Plus
Gel electrophoresis system	Bio-Rad, Mini-Protean
Heat block	ThermoScientific
Incubator (37C, 5% CO2, 95% rh)	HERAcell 240i
Inverted microscope	VWR, VistaVision™
Laminar flow hood	Mason Technology, BioBan 48
Micro-volume UV-Vis	Thermofisher Scientific, Nanodrop ND 8000
Microplate reader	BioTek EL 808
Microplate washer	BioTek ELx405
MX3000p, Real Time PCR machine	Applied Biosystem
Neubauer haemocytometer, improved	BRAND GMBH + CO KG, Blaubrand
pH meter	Mettler-Toledo Inc., MP320
Thermocycler	MJ research Inc, PTC-100

2.2 Consumables

Table 2.2: Consumables

Product	Manufacturer
6-well plate	Sarstedt
48-well plate	Sarstedt
96-well plate	Sarstedt
Micro 96 well plates	Sarstedt
T-25 cell culture flasks, filter cap	Nunc
T-75 cell culture flasks, filter cap	Nunc
50 mL tubes	Sarstedt
15 mL tubes	Sarstedt
Cell scraper	Sarstedt
Chromatography paper	Sarstedt
Polyvylidene difluoride (PVDF) membrane	GE Healthcare
PCR 8 tube strips	Applied Biosciences
PCR 8 tube caps	Applied Biosciences
Serological pipettes	Sarstedt
Cryogenic vials	Corning
MicroAmp Optical 8-Cap strip/cap	Applied Biosciences
Hybond-P, Hydrophobic polyvinylidene difluoride membrane (PVDF)	GE Healthcare

2.3 Material and Methods

2.3.1 Cell culture general

Cell culture was carried out under the following conditions temperature at 37^0C, humidity at 95% and 5% CO_2. All primary cells and cell lines were cultured in Dulbecco's modified eagle's medium (DMEM) (Sigma-Aldrich, St. Louis, MO, US) cell culture media

except for PBMCs which were cultured in Roswell Park Memorial Institute (RPMI) 1640 (Sigma-Aldrich, St. Louis, MO, US) media. All culture media was supplemented with 10% Fetal bovine Serum (FBS), 2 mM L-Glutamine, 100U/ml penicillin and 100 µg/ml streptomycin (all purchased from Sigma).

2.3.2 Cell counting

Cell numbers and viability was determined by performing cell counts following trypan blue staining. Briefly 1 part of 0.4% trypan blue (Thermo Fisher Scientific, Waltham, MA, US) and 1 part cell suspension (dilution of cells 1 in 2) were mixed. The mixture was incubated for ∼3 min at room temperature (RT). Cells were counted within 3 to 5 min of mixing with trypan blue by adding 10 µl to both chambers of a hemocytometer mounted with a glass coverslip and viewed under a light microscope with a 10X objective. Cells stained with trypan blue were excluded during counting. Unstained viable cell counts were obtained from 4 areas containing 16 squares marked by gridlines on the hemocytometer and averaged. The number of viable cells per ml was determined from the average number of cells counted multiplied by the trypan blue dilution factor and expressed as cell count ^10^4.

2.3.3 Peripheral blood mononuclear cell (PBMC) isolation

Buffy coats processed from blood donor donations and not suitable for therapeutic purposes were obtained for research purposes under an indemnity agreement between Trinity College Dublin (TCD) and the Irish Blood Transfusion Service (IBTS) at St. James's Hospital in Dublin 8. Buffy coats were diluted 1:1 with sterile PBS.

Histopaque 1077 Hybrimax (Sigma-Aldrich) density gradient was placed in 15 ml conical tubes and overlayed gently without mixing with 2 volumes of diluted buffy coat, centrifuged at 1650 rpm for 25 min at RT with the brake off. The plasma top layer was discarded and the clear interphase buffy coat layer was transferred to 50 ml tube using a sterile pasture pipette. Media was added to 30 ml as a wash step, aliquots taken for cell counting and calculations of cell number for re-suspension volumes before spinning at 2000 rpm, at RT for 8 min with brake on. This wash step was repeated followed by cell pellet re-suspension in desired volume of fresh RPMI media supplemented with 10% FBS, 2 mM L-Glutamine, 100U/ml penicillin and 100 µg/ml streptomycin for plating.

2.3.4 Culturing Mϕ, M1 and M2 macrophages from human PBMC

PBMCs (as described in PBMC isolation method above) were cultured for 6 days in RPMI media supplemented with 10% FBS, 2 mM L-Glutamine, 100U/ml penicillin, 100 µg/ml streptomycin and 20 ng/ml of recombinant human macrophage colony-stimulating factor (rhM-CSF). On day 2 fresh RPMI supplemented media was added to adherent cells to facilitate growth and survival of macrophage Mϕ cells. On days 6 Mϕ cells were stimulated with either 20 ng/ml Interferon gamma (IFN-y) and 10 ng/ml lipopolysaccharides (LPS) to produce M1 skewed macrophages or stimulated with 20 ng/ml interleukin (IL)-4 to produce a M2 skewed macrophage phenotype.

2.3.5 Culturing Murine Immortalized Bone Marrow Derived Macrophage (iBMDM) cell line

iBMDMs were kindly gifted from Prof Doyle's lab at TCD. The iBMDM previously described (279), were generated from wild type C57BL/6 primary bone marrow cells transfected with J2 recombinant retrovirus carrying v-myc and v-raf/mil oncogenes. Macrophage phenotype was based on surface expression of cluster of differentiation (CD)11b and F4/80 markers as well as a range of functional parameters, including responsiveness to Toll-like receptor (TLR) ligands and bacterial uptake. The murine iBMDM cell line was stored cryopreserved in liquid nitrogen, at a concentration of 3 x 10^6 cells/ml in freezing medium (FBS supplemented with 10% DMSO) in plastic cryovials. iBMDM were cultured in DMEM supplemented with 10% FBS, 2 mM L-glutamine, 100 U/ml penicillin and 100 µg/ml streptomycin. iBMDMs were grown in 75 cm^2 flasks and passaged every 3-4 days by trypsinisation. For use in *in vitro* assays IBMDMs were seeded at a cell density of 2×10^6 cells /ml one day prior to treatment and left to adhere overnight.

2.3.6 Culturing Metabolically activated macrophages (MMes)

MMe iBMDMs were generated by incubating iBMDM in DMEM supplemented media as described above with the addition of palmitate (40 µM), insulin (20 nM) and glucose (30 mM) (all purchased from Sigma-Aldrich) overnight.

2.3.7 Isolation and culturing primary murine bone marrow derived macrophages (BMDM)

Hind legs were dissected from adult C57BL/6 mice. Removal of epiphyses of each femur and tibia was performed, so that the bone marrow could be accessed from the ends with a 23 Gauge needle. Bone marrow from the tibiae and femurs were flushed into a 50 ml conical tube with 2-3 ml of DMEM using a 23 Gauge needle. The cell suspension was passed through a 70 µm pore size cell strainer. Bone marrow flushing's from 3 individual mice were combined and then centrifuged at 200 g for 5 minutes. Cell pellets were re suspended in 10 ml of DMEM supplemented with 10% FBS, 2 mM L-Glutamine, 100U/ml penicillin, 100 µg/ml streptomycin and 20 ng/ml recombinant mouse macrophage colony-stimulating factor (rmM-CSF), transferred to T-75 flask and incubated for 72 h in a humidified 5% CO_2 cell culture incubator at 37^{O}C. After 72 h 5ml of DMEM media supplemented as above was added and cells incubated for a further 72 h as above. On day 6 each T-75 flask were viewed under a light microscope for cell confluence and morphology. Once cells reached 70 % confluence in T-75 flasks they were harvested and replated for used in experiments.

2.3.8 Isolation and culturing primary murine bone marrow derived dentritic cells (BMDCs)

Methods as described above for murine BMDM with the exception of DMEM supplementation with 10% FBS, 2 mM L-Glutamine, 100U/ml penicillin, 100 µg/ml streptomycin and 20 ng/ml rmGM-CSF.

2.3.9 Trypsinization of cells

Extraction of adherent cells from culture flasks or plates for harvesting or replating was carried out by firstly removing culture media, washing by the addition of sterile PBS, gently swirling and aspirating. This was followed by the adding 2 ml of sterile 1x trypsin EDTA solution (purchased from Sigma-Aldrich), incubating for 5min in a humidified 5% CO_2 cell culture incubator at $37^{O}C$. Cell culture media (e.g 10 mL for T-75 flask) was added and cells dislodged using a cell scraper, and transferred to 15 ml or 50 ml conical tube or Eppendorfs depending on downstream application.

2.3.10 Cell Stimulation

Cell culture experiments were carried out by plating cells at the following density prior to treatments, 50 X 10^4 cells/ml. Aquamin (Marigot LTD) treatment concentrations (0.125- 2 mg/ml) were prepared fresh prior to use in culture media. A 10 mM simvastatin (5 mg/1.09 ml) stock solution in H_2O was diluted in culture media to give the following treatment concentrations 12.5 µM, 25 µM and 50 µM. Toll like receptor (TLR) agonists were reconstituted according to manufactures instructions as follows. TLR3 agonist, Poly(I:C) HMW (InvivoGen) provided lyophilized, reconstituted to 1 mg/ml in physiological water (NaCl 0.9%), heated for 10 minutes at 65 - 70°C, aliquoted and store at -20°C. CpG ODN 1826 a synthetic unmethylated CpG dinucleotides (InvivoGen) specific for mouse Toll-like receptor 9 (TLR9) and Pam3CSK4 (Pam3CysSerLys4) (InvivoGen) a synthetic triacylated lipopeptide (LP) and TLR2/TLR1 ligand both provided lyophilized, reconstituted to 2 mg/ml in physiological water (NaCl 0.9%), aliquoted and store at -20°C. Lipopolysaccharides from Escherichia coli O55:B5 (Sigma Aldrich, L6529), γ-irradiated, suitable for cell culture and a TLR4 agonist provided lyophilized, reconstituted to 1mg/ml in physiological

water (NaCl 0.9%), aliquoted and store at -20°C. Working concentration for all TLR agonists were prepared prior to use in cell culture media and added to cell cultures for times as indicated in results chapter.

2.3.11 Resazurin assay for Cell viability

Cytotoxic or anti-proliferative capacity of Aquamin was tested using Resazurin assay, which measures cell viability by oxidation/reduction reaction in living cells. The blue resazurin reagent (purchased from Thermo Fisher Scientific) is added to cell culture media and is reduced by metabolically active cells to pink resorufin with a spectrophotometer absorbance reading at 560nm. Measuring the level of pink resorufin absorbance at 56Onm in cell culture media is therefore a measure of cell viability. Cells 100 µl were plated at 100,000 cells/well in 96-well plate and treated with various concentrations of Aquamin (0.1-2mg/ml dissolved in culture media) and incubated for a number of h (4 -24hr). At the end of incubation period 20 µl of resazurin solution was added to each well and incubation continued in standard culture conditions for further 4 h at 37^{o}C. The absorbance was recorded at 560nm excitation / 590nm emission filter set. Aquamin treated cell viability results are presented relative to control untreated cells, untreated cells taken as having 100% viability for each assay performed.

2.3.12 Protein cell extraction for western blot

Firstly, cell culture media was removed followed by a washing step by the addition of sterile ice-cold PBS by gently swirling and aspirating. Cell lysis using RIPA buffer (Trizma Base 50 mM; NaCl

150 mM; EDTA 2 mM, NP-40 0.5% S) supplemented with 1× protease/phospphatase inhibitor cocktail on day of use was added to wells in a culture plate (approx. 100 µL/well for a 12 well plate), cells dislodged using a cell scraper and transfered to a 1.5 mL sampling tube and incubated on ice for 15 min. Two freeze thaw cycles of each sample was then carried out at -20^{0}C to promote complete cell lysis. Sampes were centrifuged for 10 min at 10,000 × g and supernatants transfered to a clean 1.5 mL sampling tube and stored at -20^{0}C for protein quantification and downstream western blot analysis.

2.3.13 The Bicinchoninic acid (BCA) assay for protein quantification

The Pierce BCA (purchased from Thermo Fisher Scientific) protein assay was used to measure the total protein in a sample. The basic principle of this method is that proteins in the sample can reduce Cu+2 to Cu+1 in an alkaline solution (the biuret reaction) resulting in a purple color formation in the presence bicinchoninic acid (BCA) whose absorbance can be detected by a spectrophotometer at 562nm. To quantify sample protein concentrations using this method a Pierce BCA (Thermo fisher) assay kit was used. Standards were prepared in sample lysis buffer in the following range (2000, 1500, 1000, 750, 500, 250, 125, 25, 0 µg/ml) by dilution of 3 mg/ml BSA stock (Sigma Aldrich, A2153). Samples were diluted in sample lysis buffer as follows 1:10, 1:50, 1:100 or left neat. 25 µl of standards and samples were added in duplicate to a 96 well plate with 25 µl of sample lysis buffer added as a blank. 50 parts of BCA reagent A was mixed with 1 part of BCA Reagent B (50:1). 200 µl of this reagent mix was added to each well containing samples and standards. The plate was then incubated for approximately 30 minutes at 37^{o}C followed by absorbance readings measured on a

spectrophotometer at 562nm. A standard curve was prepared using absorbance values obtained for standards and used to extrapolate concentrations for unknown samples on the plate. Concentrations of unknown samples were multiplied by dilution factor where applicable.

2.3.14 RNA cell extraction

Cell culture and adipose tissue RNA sample extraction was carried out on ice using Bioline RNA extraction kit (London, UK). For RNAlater preserved adipose tissue the samples were placed in eppendorf tubes containing 1.5 mm Zirconium beads (Benchmark Scientific, Inc.). 600 µl of Bioline's RNA lysis RLT buffer containing ß-mercaptoethanol (ME) was added and homogenized using BeadBug homogenizer (Benchmark Scientific, Inc.) by mechanical shear. For cell culture, samples were trypsinized according to the protocol described above and transferred to 2ml Eppendorf tube. Cell pellets were obtained by centrifugation (5 min at 300 x g), supernatant removal followed by addition of 350 µl of RLT lysis buffer containing ß-ME and vortexed vigorously. Both tissue and cell lysates were first filtered using the bioline ISOLATE filter column before addition of 70% ethanol to the flow through to adjust RNA binding conditions in the sample. ISOLATE II RNA Mini Column (blue) was placed on a collection tube (2 mL) before loading ethanol adjusted lysates onto the column and centrifuged for 30sec at 11,000g. Membrane Desalting Buffer (MEM) were added to the column and it was centrifuged to dryness, before removing any contamination with genomic DNA by adding DNase 1 treatment step for 15min to the silica membrane. Inactivation of DNase 1 and membrane washing was carried out 3 times with the bioline kit wash buffer supplied with a 2 min, @ 11,000g centrifiguation step

between each wash cycle. Final step of RNA elution from mini columns was carried out using 60 µl RNase-free water and centrifugation @ 11,000 g for 1 min. RNA extracted sample were stored at −80°C until RNA quantification and gene expression analysis.

2.3.15 Nanodrop RNA quantification

The NanoDrop software, "ND1000" was opened and "Nucleic Acids" selected. The instrument was initialized followed by the upper and lower pedestal surfaces cleaning by wiping using a Kim Wipe. 2 µL of NanoPure water was placed on the lower pedestal followed by lowering of the sampling arm and pressing OK. When complete, the upper and lower pedestals were again cleaned with a Kim Wipe. The instrument was next calibrated by placing 2 µL of sample elution buffer on the pedestal and «Blank" clicked. When complete, the upper and lower pedestals were again cleaned with a Kim Wipe. The sample measurements were carried out by adding 2 µL of sample on the pedestal and “Measure” clicked and recorded in lab notebook. In between sample measurements a kim wipe was used to clean the upper and lower pedestals. Ratio of sample absorbance at 260 and 280nm was also noted and used to assess sample purity with a ratio of ~2.0 accepted as pure for RNA.

2.3.16 DNase 1 treatment and cDNA synthesis

Initially each RNA sample underwent a DNase 1 (Invitrogen) treatment step, to digest single- and double-stranded DNA. The DNase treatment reaction was set as follow: 1 µg RNA sample, 1 µl of a 10X DNase I Reaction Buffer, 1 µl DNase I Amp Grade and molecular grade water to 10 µl mixed and incubated for 15 min @ RT. Inactivation of DNase I was by the addition of 1 µl 25 mM EDTA solution to the reaction mixture and heating for 10 min @ 65°C. The

RNA sample was then ready to use in reverse transcription reaction for cDNA synthesis. RevertAid Reverse Transcriptase (Thermofisher, EP0442) kit was used to synthesise cDNA. To each 11 µl RNA DNase 1 treated sample described above 1 µl of random hexamer primers (Thermo Fisher Scientific, SO142) was added and incubated @65°C for 5 min on a thermocycler. To this, 4 µL 5X Reaction Buffer from RevertAid Reverse Transcriptase kit, 0.5 µL (20 U) RiboLock RNase Inhibitor (Thermo Fisher Scientific), 0.2 µL of 100mM dNTP Mix (Thermo Fisher Scientific, R0191) and 1 µL (200 U) RevertAid Reverse Transcriptase was added to give a total reaction volume of 20 µL. Samples were gently mixed, centrifuge briefly, placed on thermocycler and incubated for 10 min at 25°C followed by 60 min at 42°C. The reaction was then terminated by heating at 70°C for 10 min.

2.3.17 Semi quantitative RT-PCR

mRNA expression of genes was analysed by semi-quantitative RT-PCR using target specific primers (Table 2.3) and SYBR green GoTaq DNA polymerase (Promega, A6002) on Mx3000P QPCR System (Agilent Technology). Lyophilized primers were initially reconstituted in molecular grade PCR water to give 100 µM master stocks and 10 µM working primer stocks prepared by diluting master stock 1:10 in molecular grade water for RT-PCR reactions. The RT-PCR sample mix reaction consisted of the following 10 µl of 2X SYBR green mix, 50 ng cDNA template, 500 nM of each primer forward and reverse and volume adjusted to 20 µl with molecular grade water. For each primer set a non-template control sample was included and samples performed in triplicate. Samples were run on Mx3000P QPCR System using the following program settings 1 cycle @ (95 ^{O}C, 2 min), 40 cycles @ (95 ^{O}C for 15 sec, 62 ^{O}C for 1 min, 72 ^{O}C for 15 sec) with final hold step at 4 ^{O}C. Gene expression

was quantified using the comparative Ct method [2^(-ΔΔCt]. In order to optimize each primer, the validity of the primer sequences was verified by nucleotide search (Primer-BLAST; NCBI), while the specificity and size of the amplicons were checked using a dissociation curve added to the end of the PCR run. Reference housekeeping genes such as GAPDH, were used for normalization of the gene of interest, with relative fold expression calculated using the 2 ^(-ΔΔCt) algorithm.

Table 2.3: List of primers for RT-PCR

Primer		Sequence
Gapdh mouse	Forward	5′- AAC AGC AAC TCC CAC TCT TC-3′
	Reverse	5′- CCT GTT GCT GTA GCC GTA TT-3′
TNF-α mouse	Forward	5′- CTA CCT TGT TGC CTC CTC TTT-3′
	Reverse	5′- GAG CAG AGG TTC AGT GAT GTA G-3′
IL-6 mouse	Forward	5′- GTC TGT AGC TCA TTC TGC TCT G-3′
	Reverse	5′- GAA GGC AAC TGG ATG GAA GT-3′
IL-1β mouse	Forward	5′-GGC AGG CAG TAT CAC TCA TT-3′
	Reverse	5′-CCC AAG GCC ACA GGT ATT T-3′
TICAM-1	Forward	5′-GGA CCT CAG CCT CTC ATT ATT C-3′
	Reverse	5′-AGG TTC CCT TCC TCC ACT AT-3′
Myd88	Forward	5′-GTA TCC TGC GGT TCA TCA CTA T-3′
	Reverse	5′GAA CTC TTC CAC TCA GCT ATC C-3′
Tlr3	Forward	5′-TGG AGT CGG TAA AGG GAT AGA-3′
	Reverse	5′-CAG AGG GAG GCA GAG ATA AAT AAG-3′
Tlr4	Forward	5′-TAT TCA GAG CCG TTG GTG TAT C-3′
	Reverse	5′CCA GGT GAG CTG TAG CAT TTA-3′
Cxcl2	Forward	5′-CCA TTG CCC AGA TGT TGT TAT G-3′
	Reverse	5′GCC ATC CGA CTG CAT CTA TT-3′
Ccl2	Forward	5′-GAA GGA ATG GGT CCA GAC ATA C-3′
	Reverse	5′-TCA CAC TGG TCA CTC CTA CA-3′

2.3.18 Cholesterol Crystal preparation

Cholesterol (Sigma Aldrich, C886) was dissolved in 95% ethanol water solution (12.5g/L) and heated to 60 ^{0}C to fully dissolve. Cholesterol solution was filtered, transferred into round glass bottom flask and allowed to crystallize overnight. Next day crystals were placed under vacuum to evaporate liquid. Crystals were removed and ground using pestle and mortal, autoclaved, aliquoted and stored at 4^{o}C. When ready to use cell culture media was added to the powder crystals and sonication applied for 60 sec to break into fine crystal particles. Concentrations of cholesterol crystals used in cell treatment experiments were 1 or 2mg/ml.

2.3.19SDS-PAGE and western blotting

2.3.19.1 Tris-Glycine SDS-PAGE

Prior to tris-glycine SDS-PAGE 20 µl protein samples were prepared. The protein concentration was adjust to contain 20 µg in total with water and 4× sample loading buffer (62.5 mM Tris HCl pH6.8, 2.5% SDS, 10% glycerol, 0.002% bromophenol blue and 5% β-merceptoethanol), mixed and boiled for 10 min. 12% Tris-Glycine SDS-PAGE gel composition was as follows (*Resolving gel 12%* : [3.3ml H_20, 4ml of 30% acrylamide mix, 2.5 ml of 1.5M Tris (pH 8.8), 0.1ml of 10% SDS, 0.1ml of 10 % ammonium persulfate (APS) make fresh on day of use and 4 µl of TEMED]. *Stacking gel 5%*: [2.7 ml H_20, 0.67 ml 30% acrylamide mix, 0.5 ml 1.0 M Tris-HCL (pH 6.8), 0.04 ml 10% SDS, 0.04 ml of 10 % APS made fresh on day of use, 4 µl TEMED]). Samples 20 µg total protein and a molecular weight standard (Fisher BioReag, EZ-Run™ Prestained Protein Ladder, 10-170kDa) was loaded into the gel wells. Electrophoresis was carried out at 100 volts (V) for 70-90 minutes with 1x SDS PAGE running buffer (0.025 M Tris, 0.192 M glycine, 0.10% SDS).

2.3.19.2 Semi-dry gel transfer of proteins onto PVDF membrane

The proteins resolved on tris -glycine gels were transferred onto a polyvinylidene fluoride (PVDF) membrane. A wet transfer sandwich was prepared in the following order: sponge, filter paper, gel, PVDF membrane, filter paper, sponge. PVDF membrane was first activated by submersion in 100% methanol for 5min, distilled water for 5min and transfer buffer (25 mM Tris, 192 mM glycine, 10% methanol) for 15 min. All other components of the transfer

sandwich were submerged in transfer buffer for 15min followed by assembly as stated above and ensuring removal of any air bubbles in the gel sandwich by gently rolling over the surface with 15 ml conical tube to minimize disruption of protein migration from gel to membrane. The transfer sandwich was placed into the dry transfer system with the gel on the cathode (negative) side and the membrane on the anode (positive) side and transfer set at 200 milliamperes (mA) per gel for 90-120 minutes depending on the size of the protein.

2.3.19.3 Immunodetection of proteins

Following the transfer, the PVDF membrane was incubated in blocking buffer, (5% milk in 1 x Tris buffered saline (TBS)), under agitation for 1 h at RT. The membrane was incubated in primary antibody diluted in blocking buffer with agitation, overnight at 4°C. The following primary anti mouse antibodies and dilutions were used: (*iNOS rabbit mAb (1:1,000) (Cat #13120, Cell Signaling, Danvers, MA, USA), IκBα Rabbit mAb (1:1,000) (Cat #4812, Cell Signaling), phospho-NF-κB p65 (Ser536) Rabbit mAb (1:1,000) (Cat #3033, Cell Signaling), NF-κB p65 (Ser536) Rabbit mAb (1:1,000) (Ca #8242, Cell Signaling), Phospho-IRF-3 (Ser396) Rabbit mAb (1:1,000) (Ca #4947, Cell Signaling), IRF-3 Rabbit mAb (1:1,000) (Ca #4302, Cell Signaling), Phospho-p44/42 MAPK (Erk1/2) (Thr202/Tyr204) mAb (1:2,000) (Ca #4370, Cell Signaling), p44/42 MAPK (Erk1/2) Antibody (1:1,000) (Ca #9102, Cell Signaling), Anti-beta -Actin Antibody (C4) (Ca #sc-47778 HRP, Santa Cruz Biotechnology, Santa Cruz, CA, US)*. The membrane was washed 3 times for 5 minutes then twice for 15 min each with 1x TBS with 0.1% Tween® 20 detergent (TBS-T) prior to incubation with secondary antibody (Anti-rabbit IgG, HRP-linked Antibody (1:1000) (Ca#7074, Cell Signaling) for 2 h at RT. The membrane was washed

as above with 1X TBS-T. Immunoreactive bands and using enhanced chemiluminescence (ECL) detection reagent (30% hydrogen peroxide, 250 mM Luminol (Fluka 09253) in DMSO, 90mM 4-Iodophenylboronic acid (Sigma 471933) in DMSO and 100 mM Tris-HCl). Membranes were incubated with ECL soln for 1-2 min, drained, exposed for 1-5 min depending on antibody and image capture on a Fusion FX imaging system (Vilber Lourmat). Densitometry quantification of immune detected bands was carried out using Bio1D software. For re-probing and subsequent immunodetection with other antibodies the membranes were stripped by placing in stripping buffer (62.5 mM Tris-HCl, 2% SDS and 0.8% β-ME) for 45 min at 50 ^{0}C followed by membrane washing with TBS- T twice for 30 min . For each protein of interest a loading control antibody such as β-actin was detected, to normalize the protein of interest.

2.3.20 Flow cytometry

For staining of cells with fluorochrome-conjugated antibodies against extracellular markers, cells were harvested washed and resuspended in FACS buffer (PBS with 5% FBS). Cells were first stained with Live Dead Fixable Aqua Dead Cell stain (LD) ((Ca#L34957, Invitrogen, Waltham, MA, US), a viability dye which binds to dead cells by incubating on ice in the dark for 30 minutes. This LD step allows the distinction of live cells from dead cells to allow for accurate analysis. Cells were then washed in PBS and centrifuged at 300 g for 5 minutes. The supernatant was discarded, and cells were incubated in FACS buffer containing fluorochrome-conjugated antibodies for 30 minutes on ice protected from light. The following fluorochrome-coupled antibodies were applied; APC rat anti mouse CD80 (*Ca #17-0801-82)*, PE rat anti mouse CD86 (*Ca*

#12-0862-82), PE-Cy7 armenian hamster anti mouse-CD11c (Ca #25-0114-82)**,** PerCP/Cyanine5.5 rat anti-mouse CD301 (*Ca #MA1-40071)* (all from eBioscience, San Diego, CA). Following extracellular staining, cells were washed centrifuged at 300 g and resuspended in FACS buffer for acquisition on the flow cytometer LSR Fortessa instrument (BD Biosciences). All flow cytometry data analysis was performed using FlowJo v10 software (TreeStar). Example of gating strategy is illustrated in Figure 2.3.1.

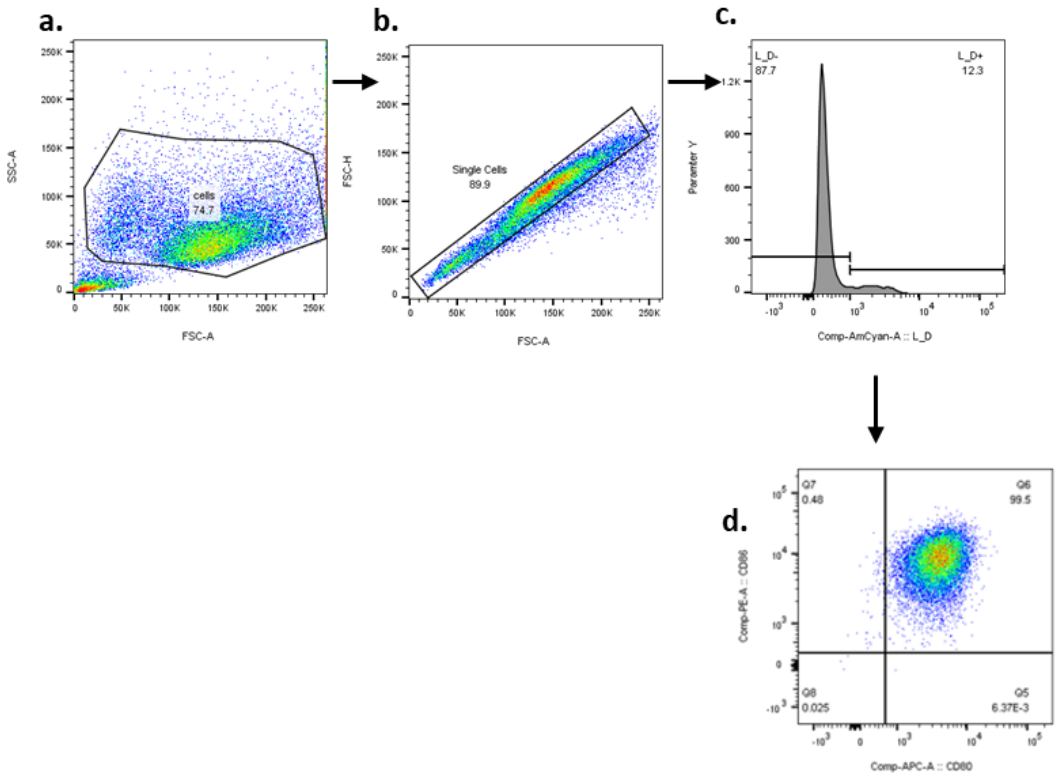

Figure 2.3.1. Representative sequential gating strategy of murine iBMDM cells analysed on a BD LSR Fortessa™ flow cytometer. iBMDM cells are stained with AmCyan LIVE/DEAD® Fixable Aqua Dead cell stain, APC rat anti-mouse CD80, PE rat anti- mouse CD86 and analysed on a BD LSR Fortessa™ flow cytometer. (a) Dot plot showing percentage (74.7%) of cells gated using forward scatter area (FSC-A) versus side scatter area (SSC-A). (b) Of cells gated in (a) doublets are excluded based on forward scatter height (FSC-H) versus forward scatter area (FSC-A) with dot plot gating showing percentage single cells (89.9%). (c) Of single cells gated in (b) cells stained with LIVE/DEAD® stain are shown on histogram plot with percentage live cells gated to the left (87.7%) and percentage dead cells gated on the right (12.3%). (d) Of the live cells gated in (c) dot plot showing percentage of iBMDM cells positive for CD80 versus CD86.

2.3.21 Enzyme-linked immunosorbent assay (ELISA)

The concentrations of cytokines present in cell culture supernatants was quantified by Enzyme-Linked Immunosorbent Assay (ELISA) uncoated ELISA kits (R & D Systems, Minneapolis, MN, US) for TNF-α (Ca #DY210), IL-6 (Ca #DY206), IL-1β (Ca #DY201). Corning® High Binding ELISA plates (Merck, Ca #CLS9018) were coated overnight at 4^{o} C with 100 µl/well of capture antibody diluted in kit coating buffer (Table 2.4). Next day capture antibody was removed washed four times with 300 µl of PBS-tween solution (PBS, 0.05% Tween-20), dried and non-specific binding sites blocked with 1x assay diluent (1% BSA in PBS) for 1 h at RT. After blocking, plates were washed four times in PBS-tween solution and dried. Sample were diluted with 1x assay diluent as follows 1:10, 1:50, 1:100 or left neat and 100 µl of samples added in triplicate to wells. A standard curve of serially diluted standard provided with each kit was also loaded onto the plates in triplicate according to each ELISA kit instructions. Blank wells, containing assay diluent only, were included on each plate to allow the subtraction of any buffer background signal for each sample. Samples and standards were incubated overnight at 4°C or 2 h at RT. Following incubation times, the plate was again washed four times, as above with PBS-tween solution. 100 µl of biotinylated detection antibody diluted in 1x assay diluent (Table 2.4) was added to each well and incubated for 2 h at RT. Plates were again washed four times and 100 µl of horseradish-peroxidase (HRP) conjugated streptavidin diluted in 1x assay diluent was added to wells and incubated for 30 minutes in the dark. Wells were thoroughly washed and 100 µl of substrate, tetramethylbenzidine **(**TMB) solution, was added as required according to kit instructions. The enzyme mediated colour reaction was protected from light

while developing and stopped after a 15min incubation with the addition of 2N H_2SO_4. This was immediately followed by plate absorbance readings measured on a spectrophotometer at 450nm. A standard curve was prepared using absorbance values obtained for standards and used to extrapolate concentrations for unknown samples on the plate. Concentrations of unknown samples were multiplied by dilution factor where applicable. The ELISA for the corresponding mouse ELISA kits (TNF-α, Ca# 88-7324-88), (IL-6, (Ca# 88-7064-88), (IL-1β, (Ca# 88-7013-88) (all purchased from Invitrogen) the samples were analyzed as per manufacturer's instructions.

Table 2.4. List of cytokines analyzed by ELISA for human samples

Cytokine	Description	Working concentration	Dilution
TNF-α	Capture antibody	4 µg/ml	1:120
	Standard	1000 pg/ml	1:130
	Detection antibody	50 ng/ml	1:60
IL-1β	Capture antibody	4 µg/ml	1:120
	Standard	250 pg/ml	1:440
	Detection antibody	150 ng/ml	1:60
IL-6	Capture	2 µg/ml	1:120
	Standard	600 pg/ml	1:300
	Detection antibody	50 ng/ml	1:60

2.3.22 RNA Sequencing: Library Construction, Sequencing workflow and Quality Control

Next generation RNA Sequencing of samples submitted to Novogene (UK) at their Cambridge Science Park center, was

performed following the workflow summarized in figure 2.3.2. Initial sample quality control (QC) was performed on a Qubit® 2.0 fluorometer (Life Technologies, CA, USA) for RNA quality and integrity. PolyA-tailed messenger RNA were enriched to remove ribosomal RNA. An Agilent Bioanalyzer 2100 (Agilent Technologies, Inc., USA) was used to ensure the size of the library fragments and the library quality after a Covaris ultra-sonication (Covaris, Woburn, MA, USA). Sequencing was then performed using a PE150 (2x150bp) sequencing strategy on Illumina's NovaSeq 6000 platform, with 12.0Gb of data (40M PE150 reads) per sample and a Q30 guarantee of >=85%. The sequenced raw reads containing low quality reads or reads with adapters, were removed. The raw read filtering was as follows: 1) Removal of reads containing adapters; 2) Removal of reads containing N > 10% (N represents base that could not be determined); 3) Removal of low-quality reads: The Qscore (Quality value) of over 50% bases of the read is <= 5. Figure 2.3.3 shows a representative sample from the sequenced data set and the percentage of reads filtered before mapping.

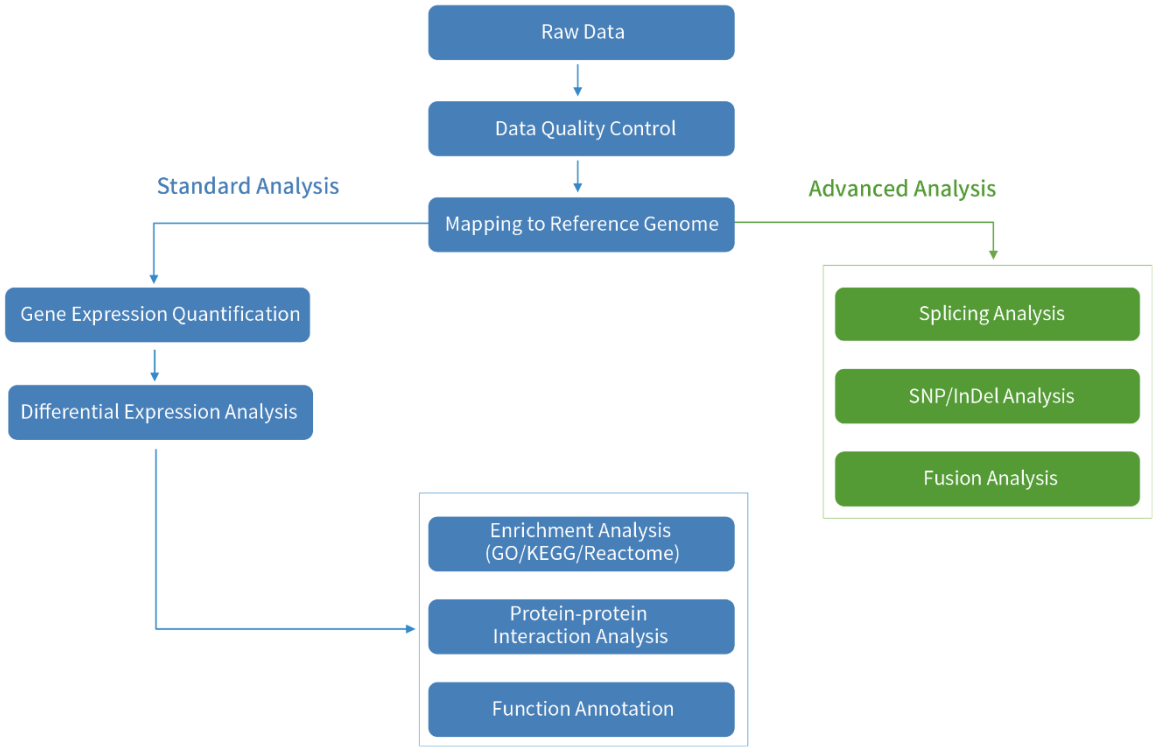

Figure 2.3.2. Schematic representation of next generation RNA sequencing analysis conducted by Novogene (UK).

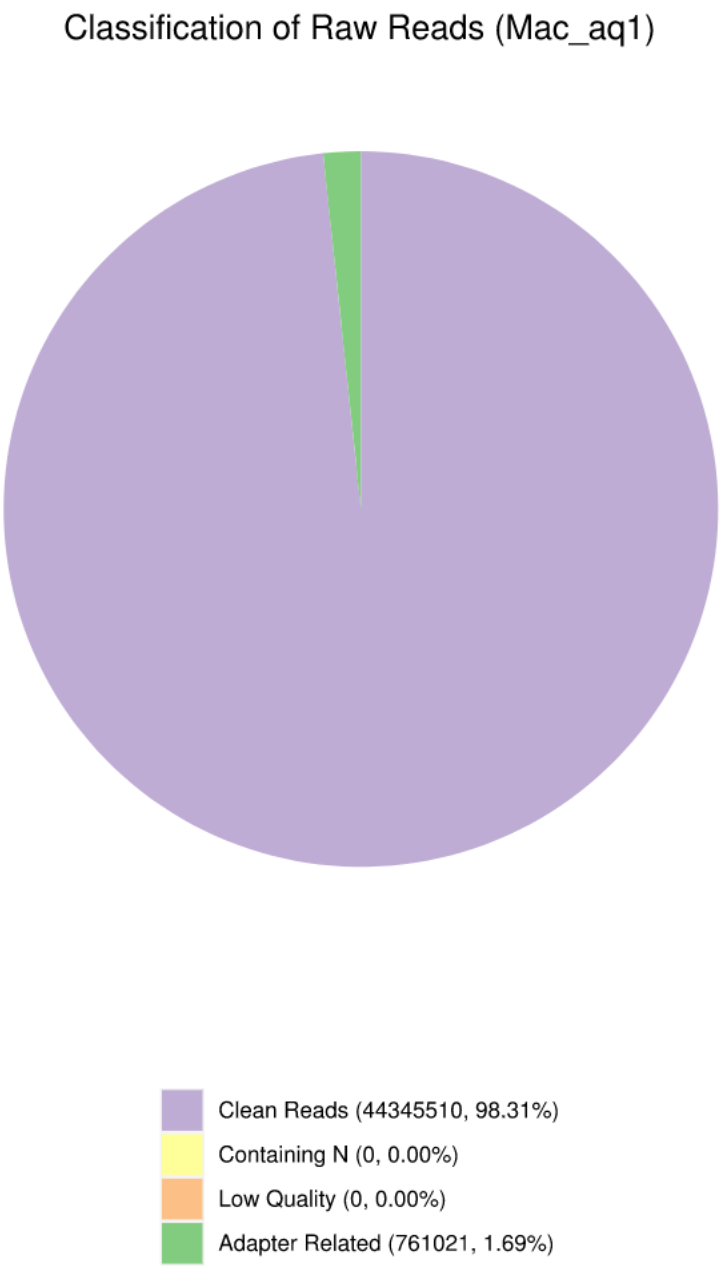

Figure 2.3.3. Representative sample from dataset showing filtering of raw sequenced reads prior to mapping.

Colour key shows over 98% sequenced reads in this sample not filtered and passed QC as denoted by purple area in pie chart. Yellow area represents % N, the number of bases that could not be determined, orange is reads with % low quality in base detection and green area shows % reads containing adapters all filtered prior to sample mapping.

2.3.23 Mapping of sequenced data and gene expression levels

Mapping of the clean filtered reads to the reference transcriptome was performed using HISAT2 alignment program. Mapped regions can be classified as exons, introns, or intergenic regions. The distribution of mapped sequenced reads of a representative sample in the data set is shown in figure 2.3.4. Exon-mapped reads are the most abundant type of reads in the data set (>93 sequences mapped to exon regions in represented sample shown in green Fig. 2.3.4) across samples indicating the reference transcriptome is well annotated and free from pre-mRNA contamination. Gene expression levels in each sample was calculated by the number of mapped reads per gene. Feature Counts v1.5.0-p3 was used to count the read numbers mapped to each gene. The FPKM (Fragments Per Kilobase of transcript sequence per Millions base pairs sequenced) of each gene was calculated based on the length of the gene and reads count mapped to a gene, (Fig. 2.3.5). FPKM is the most used method for estimating gene expression levels and for normalization of RNA sequencing data. Gene expression is generally considered when the FPKM is greater than 1.

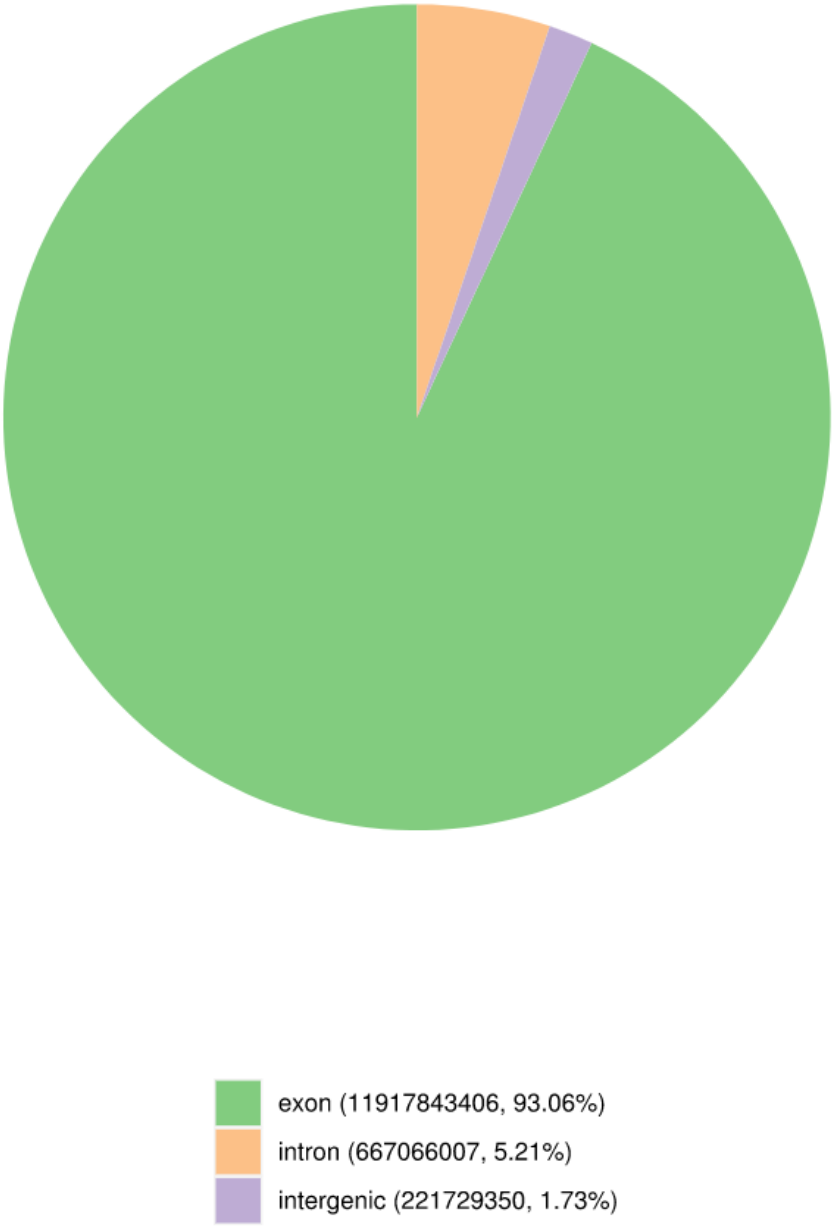

Figure 2.3.4. Sequenced reads in a sample mapped to genomic regions.
The pie chart and its colour key represent the % of read mapped to the different genomic regions. Exon mapping shown in green, intron mapping shown in orange and intergenic mapping in shown in purple.

$$FPKM \sim \frac{Fragment\ counts}{Gene\ length * Total\ read\ counts}$$

Figure 2.3.5. Calculation of FPKM which represents a genes expression level.

FPKM is the normalized gene expression level of each gene in the data set and is based on the length of the gene and reads count mapped to each gene.

2.3.24 Differential gene expression analysis

The DESeq2 R software package was used to perform differential expression analysis on two chosen conditions/groups (three biological replicates for each condition). DESeq2 provided statistical routines for confirming the differential expression in digital gene expression data using models based on the negative binomial distribution. The method of Benjamini and Hochberg was used to adjust the raw generated P value to control the false discovery rate and presented as adjusted P value (Padj) in tables of differentially expressed genes. Genes found by DESeq2 with an adjusted P value of <0.05 were designated as differentially expressed genes (DEG). Log 2 (FC) for differentially expressed genes was also calculated and shown.

Enrichment analysis using GO and KEGG analysis of differentially expressed genes

The cluster Profiler R software package was used to perform gene ontology (GO) enrichment analysis and Kyoto Encyclopedia of Genes and Genomes (KEGG) pathway analysis of differentially expressed genes. GO with corrected P value that is less than 0.05 are a significant enrichment of differentially expressed genes. GO annotates genes to biological processes, molecular functions, and

cellular components, KEGG annotates genes to pathway level. KEGG is a database resource for understanding high-level functions and utilities of the biological system, such as the cell, the organism and the ecosystem, from molecular-level information, especially large-scale molecular datasets generated by genome sequencing and other high-through put experimental technologies (http://www.genome.jp/kegg/).

2.3.25 Mice high fat diet study

This study was approved by the Animal Ethics Committee of Trinity College Dublin, Ireland and performed under license by Irish Health Products Regulatory Authority (project authorization no: AE19136/PO77). All applicable institutional and national guidelines for the care and use of animals were followed. Two diets were used in this study. These included a rodent high-fat Western-style diet (HFWD) composed of 60 kcal % fat with added calcium from salts @1.49 mg/kcal of diet (Research Diets Inc, New Brunswick, NJ, USA, D12492.) designated as control diet. The second comparator diet was formulated as the D12492 HFWD above except supplemented with calcium from Aquamin @1.49mg/kcal of diet, designated as test diet. Both diets contained calcium as well as protein, carbohydrate vitamin and mineral levels at equal amounts. Male wild type mice on a C57BL/6 background, 8-12 weeks of age were fed either the control HFWD or the test HFWD supplemented with Aquamin for 10 weeks. Weights of animals as well as food and water intake were measure weekly during the feeding period.

2.3.26 Glucose and insulin tolerance test

At the end of the study period mice were tested for glucose and insulin tolerance one week apart. For glucose tolerance test, mice were injected intraperitoneal (IP) with 2g/kg glucose (Sigma) after overnight fasting. For insulin tolerance test, mice were injected IP with 1U/kg insulin (recombinant human, Sigma) after overnight fasting. Blood glucose was measured by submandibular bleeding at defined time intervals, for both tests using handheld blood glucose monitor (On Call Vivid, ACON Laboratories or FreeStyle Lite, Abbot Laboratories).

2.3.27Tissue harvest

At the end of the study period epidydimal (EAT) and subcutaneous (SAT) fat pads were dissected and weighted from each animal in the HFWD study. Adipose and liver tissue were also harvested at the end of the study period from each animal and stored at -80^{o} C in RNAlater for RNA expression analysis or snap frozen in liquid N2 for protein analysis.

2.3.28Statistical analysis

Data are expressed as the mean ± standard error of the mean (S.E.M.) for triplicate samples unless specifically mentioned. Data were analysed by an independent Student t-test for the analysis of only two datasets or by 1-way or 2-way analysis of variance (ANOVA) with Dunnett's Post hoc testing with correction for multiple comparisons used to determine differences between specific groups. P values of <0.05 were considered statistically significant and denoted by an asterisk in the figures. Statistical analysis was conducted using GraphPad Prism Version 9 (GraphPad Software Inc., California, USA)

3. AQUAMIN EXERTS ANTI-INFLAMMATORY PROPERTIES BY ANTAGONIZING TRIF-DEPENDENT TLR SIGNALING PATHWAY.

3.1 Introduction

Tissue damage or pathogen invasion instantly trigger the initiation of a defense mechanism by the innate immune system against the corresponding antigens (280). Notwithstanding the protective effect of slow-term activation of the innate immune system which mediates tissue repair mechanisms, its long-term activation is detrimental and can negatively alter organ function as well as structure (281). External PAMPS and internal damage-associated molecular patterns (DAMPS) are identified by a family of recognition receptors knows as TLRs (282, 283). Excess TLR activation dysregulates tissue homeostasis by releasing pro-inflammatory cytokines and chemokines. Elevated cytokine and chemokine levels characterize a variety of auto-immune diseases such as rheumatoid arthritis (284), diabetes (142) and Alzheimer's Disease (285). To that end, antagonizing TLR signaling has been a popular therapeutic approach against inflammation (286).

TLRs possess 20-27 extracellular leucine-rich repeats (LRR) which facilitate the recognition of pathogens that function as stimulants for the activation of downstream signal transduction pathways (286). Until now, ten TLRs in human and 13 TLR members in mice has been identified (287, 288). TLRs such as TLR4, TLR2, TLR1, TLR5, TLR6 and TLR10 are expressed extracellularly on the cell surface (289), whereas TLR3, TLR7, TLR8, TLR9 are intracellularly localized (290). All innate immune cells are known to express TLRs (291). The interaction of PAMPS such as flagellin, lipoteichoic acid (LTA), LPS, peptidoglycan (PGN), double stranded RNA which is derived from viruses, as well as DNA motif like CpG, with TLRs causes the activation of the receptors and hence activation of the innate immune system (292-294).

When TLRs bind to ligands, it triggers the recruitment of TLR signaling adaptor molecules by the receptors Toll-Interleukin-1

receptor (TIR) domain. To this day, five adaptor molecules have been identified to modulate signals downstream of TLRs (292). The most widely studied TLR adaptor protein is MyD88 that exerts its signaling cascade downstream of TLR2,4,5,7,8 and 9 (295). TLR3 is the only TLR that is mediated in a MyD88 independent manner (296). The downstream signaling of MyD88 leads to degradation of IκB allowing nuclear translocation of NFkB to occur and thus subsequent expression of its target genes (292). Previous evidence has led to a profound understanding of the importance MyD88 yields in the production of pro-inflammatory cytokines such as TNF-α and IL-6. In the relevant study, mice lacking MyD88 were not able to produce pro-inflammatory cytokines upon exposure to IL-1β, pinpointing the importance of MyD88 to generate responses when triggered by inflammatory stimulants (297). MyD88 adaptor protein is responsible for the early-phase NF-κB activation downstream of TLR4 in response to LPS stimulation (298).

To elucidate the mechanism of MyD88 independent signaling, scientists used MyD88 deficient macrophages and exposed them to LPS (299). This led to interferon (IFN)-regulatory factor 3 (IRF3) activation and subsequent production of type I interferons such as IFN-β and a late phase NF-κB activation (298). Establishment of the MyD88 independent pathway of TLR4 signaling has resulted in the identification of TIRAP which is another TIR-domain-containing adaptor (140, 300). An earlier study that was conducted on TIRAP deficient mice in response to LPS resulted in low production of pro-inflammatory cytokines, however TIRAP deficiency did not have any effect in the expression of IFN-inducible genes as well as the late phase of NF-κB activation hinting that TIRAP is necessary for the MyD88-dependent signaling but not MyD88-independent signaling downstream of TLR4 (300, 301). Surprisingly, TIRAP deficient mice that were stimulated with TLR2

agonist displayed a defective cytokine production similar to the results derived from the LPS stimulation. On the other hand, the expression of end genes downstream of TLR3, TLR7 and TLR9 was still observed after stimulation with the relevant agonists in TIRAP deficient mice, revealing that TIRAP is crucial for MyD88-dependent signaling downstream of TLR4 and TLR2 (301, 302).

The activation of signaling cascades downstream of TLR which are independent of MyD88 and TIRAP has led to the identification of a third TIR-domain-containing adaptor known as TRIF or TICAM1 (296, 303). Previous research that was carried out in HEK293 cells, has provided evidence that TRIF signaling leads to the induction of IFN-β release in a MyD88- and TIRAP- independent manner (304). TRIF signaling is initiated in response to TLR4 and TLR3 ligands such as LPS and Poly(I:C) respectively (99) and is followed by activation of IRF3 which is MyD88-independent (304). In vitro studies have also reported that a fourth TIR-domain-containing adaptor molecule known as TRAM is involved in the TRIF pathway downstream of TLR4 but not downstream of TLR3 (305, 306), as per previous research that was carried out on TRAM-deficient mice that demonstrated impaired IRF3 activation downstream of the MyD88-independent/TRIF dependent pathway of TLR4. Nonetheless, TLR3 pathway was unaffected (155).

Chronic low grade inflammation is known to be linked with dysregulation of TLRs and excessive production of pro-inflammatory mediators like TNF-α, IL-6 and IL-1β (307, 308). Notwithstanding the excessive release of pro-inflammatory cytokines during inflammation, inflammatory enzymes also play pivotal roles during macrophage activation. Nitric oxide synthase (iNOS) is an inflammatory enzyme which generates nitric oxide (NO) (309). Previous in vitro research that was performed on glial cells provides evidence about the anti-inflammatory effect of Aquamin in LPS driven glial cells by demonstrating a significant reduction of

LPS-induced TNF-α and IL-1β protein expression downstream of TLR in the presence of Aquamin (310). The anti-inflammatory effect of Aquamin was further assessed by stimulating RAW macrophage cells with LPS upon pretreatment with Aquamin. The cells that were treated with Aquamin presented a notable reduction at the levels of NF-κB compared to the LPS stimulated controls (278), which provides support to the claim that Aquamin exerts an anti-inflammatory effect.

To our knowledge, no previous research has investigated the exact molecular mechanisms by which Aquamin modulates TLR signaling to exert its anti-inflammatory effects. This study chapter aims to provide further insight with respect to the mechanism of action of Aquamin and characterize specifically the immunomodulatory effects of Aquamin in both human and murine macrophage cells. The specific objective here was to support the anti-inflammatory effect of Aquamin in LPS-induced innate immune cells and predominantly macrophages. The results suggest that supplementation with Aquamin might potentially contribute to the alleviation of inflammation.

3.2 Results

3.2.1 Aquamin reduces LPS driven pro-inflammatory cytokine levels in human peripheral blood mononuclear cells

To date it has been shown that supplementation with Aquamin provides notable health benefits in protection from ulcerative colitis (311) to osteoporosis (269). The immune system plays a major role in the pathophysiology of these disease states but how Aquamin affects immune cell responses is not clearly elucidated. To investigate whether Aquamin has any effect on the secretion of pro-inflammatory cytokines, human PBMCs were extracted from healthy donors treated with Aquamin (2 mg/ml) and stimulated with LPS (100 ng/ml) overnight. Aquamin contains over 72 minerals in its composition with calcium being the most abundant, therefore calcium concentrations of Aquamin tested were kept within physiological levels. Stimulation with LPS induced as expected an increase in the concentration of TNF-a (Fig. 3.1A) and IL-1b (Fig. 3.1B) in the cellular supernatants of PBMCs compared to untreated controls. LPS is a well characterized trigger of inflammation in innate immune cells through its engagement with TLR4, a pathogen recognition receptor whose signaling results in the activation of the transcription factor NF-κ B. Aquamin alone treatment of PBMCs did not lead to an increase in the concentration of TNF-a (Fig. 3.1A) confirming Aquamin preparations were free of contaminating endotoxins such as LPS. Aquamin treatment however showed a significant reduction in the LPS induced TNF-a (Fig. 3.1A) cytokine levels secreted from PBMCs. On the contrary no significant alteration was caused by Aquamin in the protein expression of IL-1β as depicted in Figure 3.1B, even though a reducing pattern could be observed. Altogether supporting a role for Aquamin having anti-inflammatory effects in human PBMCs.

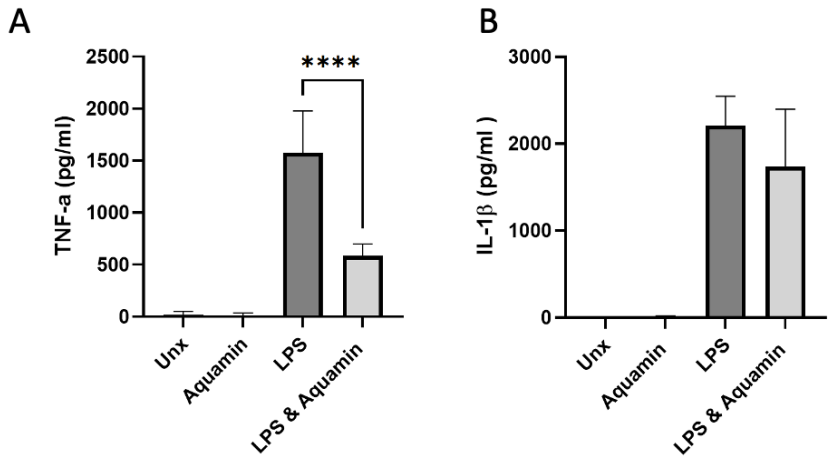

Figure 3.1. Aquamin inhibits LPS driven secretion of TNF-a and IL-1β in human peripheral blood mononuclear cells.

PBMCs treated with Aquamin (2mg/ml) and stimulated with LPS (100ng or 10ng/ml) overnight. The protein release levels of (A) TNF-a and (B) IL-1β in cellular supernatants were determined by ELISA. The bar graph data are Mean ± SEM, n=3. *****p<0.0001 vs LPS alone using one way ANOVA statistical test.*

3.2.2 Aquamin reduces LPS driven pro-inflammatory responses in human M-CSF derived macrophages.

Macrophages are innate cells of the immune system and contribute to important inflammatory responses in a variety of disease states. Investigations in human macrophage cells was carried out to determine whether similar effects with Aquamin also occur as seen in PBMCs above. To investigate the role of Aquamin in macrophages**,** PBMCS were culture for 7 days in the presence of M-CSF (50ng/ml) to generate macrophages. Viability of macrophages treated with Aquamin was initially assessed using the Resazurin assay which measures the mitochondrial respiratory chain in live cells. The resazurin assay showed that Aquamin at 0.5-2mg/ml concentrations did not change the viability of macrophage cells following overnight treatment compared to control untreated cells (Fig. 3.2A). Analysis of LPS (10 ng/ml) stimulation in M-CSF derived human macrophages reveal that treatment with Aquamin at 2mg/ml dose-dependently reduces TNF-a (Fig. 3.2B) and IL -**6 (**Fig. 3.2C) cytokine levels in macrophage cell supernatants. These results further support a role for Aquamin having anti-inflammatory effects in human innate macrophage cells.

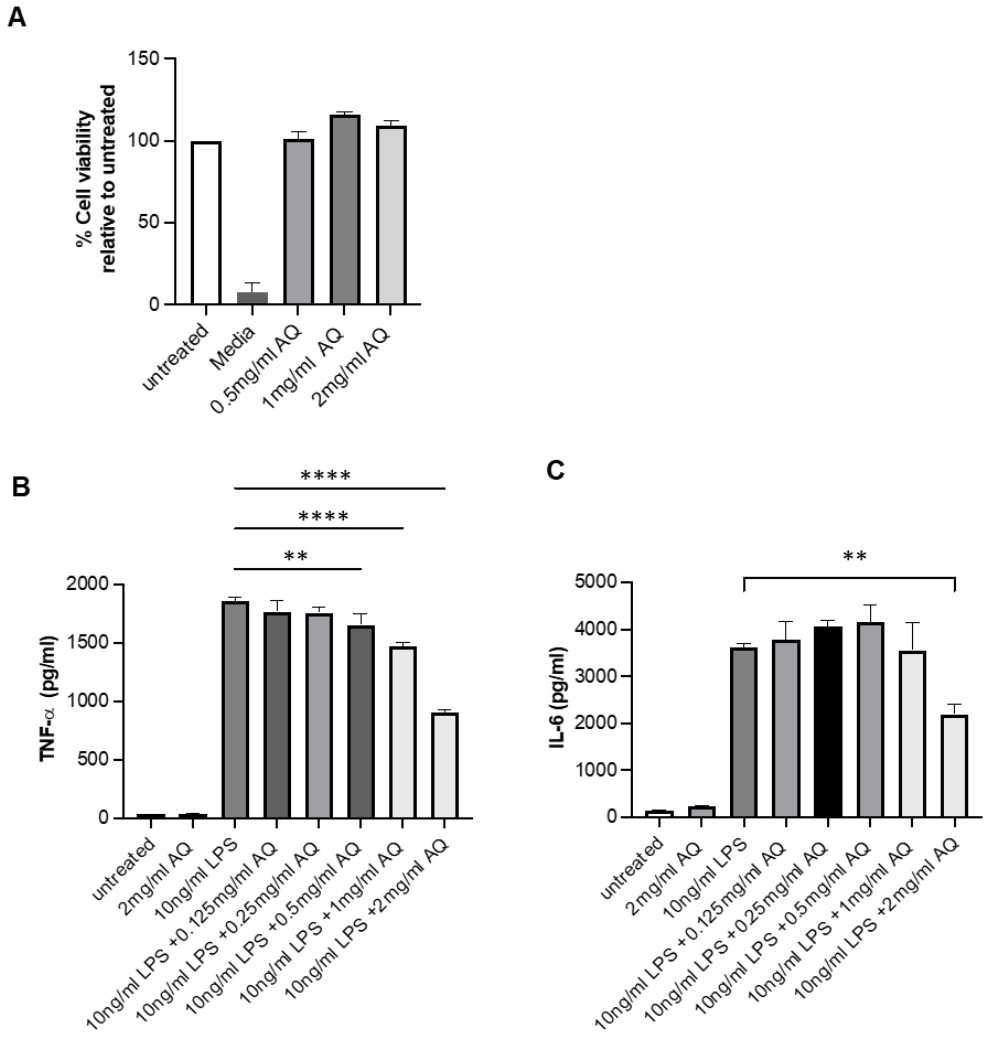

Figure 3.2. The anti-inflammatory effect of aquamin in M-CSF differentiated human macrophages.

Human M-CSF derived macrophage cells treated with varying doses of Aquamin (0.5, 1 and 2mg/ml) overnight followed by assessment of cell viability using the resazurin assay and secretion of inflammatory cytokines TNF alpha and IL-6 by ELISA. (A) Cell viability of Aquamin treated human macrophages is normalized to untreated cells. Secretion of TNF-a (B)and IL-6 (C) under LPS (10 ng/ml) stimulation in human M-CSF differentiated macrophages in the presence and absence of aquamin (0.125-2mg/ml). *The data are mean ±sem, n=3. ****p<0.0001, **p<0.01 vs LPS alone using one way ANOVA statistical test.*

3.2.3 Aquamin reduces LPS driven pro-inflammatory responses in murine immortalized bone marrow derived macrophages.

To extend these analyses murine macrophages were also assessed for inflammatory responses. Immortalized bone marrow derived macrophages (iBMDMs) were treated with Aquamin (0.125-2mg/ml) prior to stimulation with LPS (10ng/ml). As observed in human macrophages, Aquamin using a range of doses (0. 0.125-2mg/ml) did not reduce cell viability with overnight Aquamin treatment compared to untreated cells (Fig 3.3A) as showed by resazurin assay that was carried out in BMDMs. Similarly to results seen above in human macrophages, Aquamin (0.125-2mg/ml) dose dependently attenuated LPS-driven TNF-α (Fig. 3.3B, C) and IL-6 cytokine secretions (Fig. 3.3D, E) at 6 and 24 h post LPS stimulation. Cytokine measurements are from cell culture supernatant using specific ELISA assays.

LPS recognition by innate immune cells can also induce expression of a cluster of differentiation 80 (CD80) and 86 (CD86) costimulatory molecules on the surface of these cells. To determine further whether a change in the activation state of Aquamin treated iBMDM occurs in conjunction with a change in cytokine secretion expression levels of CD80/86 was carried out using FACS analysis. As expected LPS increased expression of CD80 (Fig 3.4A) and CD86 (Fig 3.4B) in iBMDM compared to unstimulated cells. However, no change in the expression of either CD80 (Fig 3.4C, E) or CD86 (Fig. 3.4D, F) was observed by FACS analysis with aquamin (1 and 2mg/ml) treatment in iBMDMs stimulated with LPS (Fig. 3.4C-F). Together these data, demonstrate that Aquamin inhibits LPS/TLR 4 driven innate immune cytokine release responses without affecting activation states in murine BMDM cells with implication for modulating inflammatory disease states.

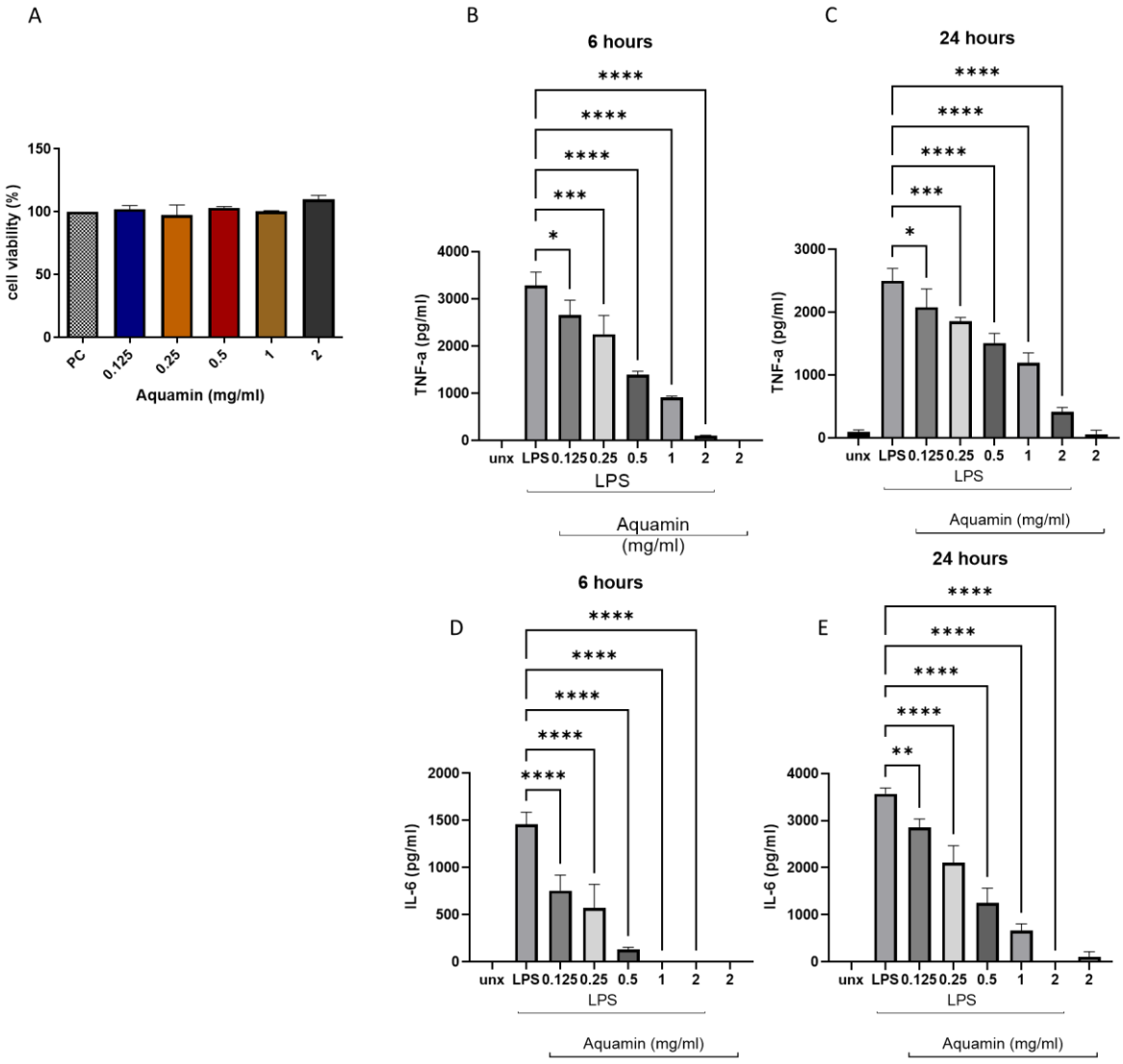

Figure 3.3. Aquamin dose dependently reduces LPS driven TNF-a and IL-6 secretion in murine immortalized bone marrow derived macrophages. iBMDMs were incubated for 3 h with aquamin (0.125-2mg/ml) prior to stimulation with LPS (10ng/ml) for 6 and 24h. (A) Percentage iBMDM cell viability in the presence of aquamin (0.125-2mg/ml) treatment overnight assessed using resazurin assay. TNF-a at 6 (B) and 24 h (C) and IL-6 at 6 (D) and 24 h (E) following Aquamin (0.125-2mg/ml) and LPS (10ng/ml) stimulation in cell culture supernatants from iBMDM, determined by ELISA. Data (A-E) are expressed as mean ±sem from 3 independent experiments. *****p<0.0001, ***p<0.001, **p<0.01; p<0.05 vs LPS alone using one way ANOVA statistical test.*

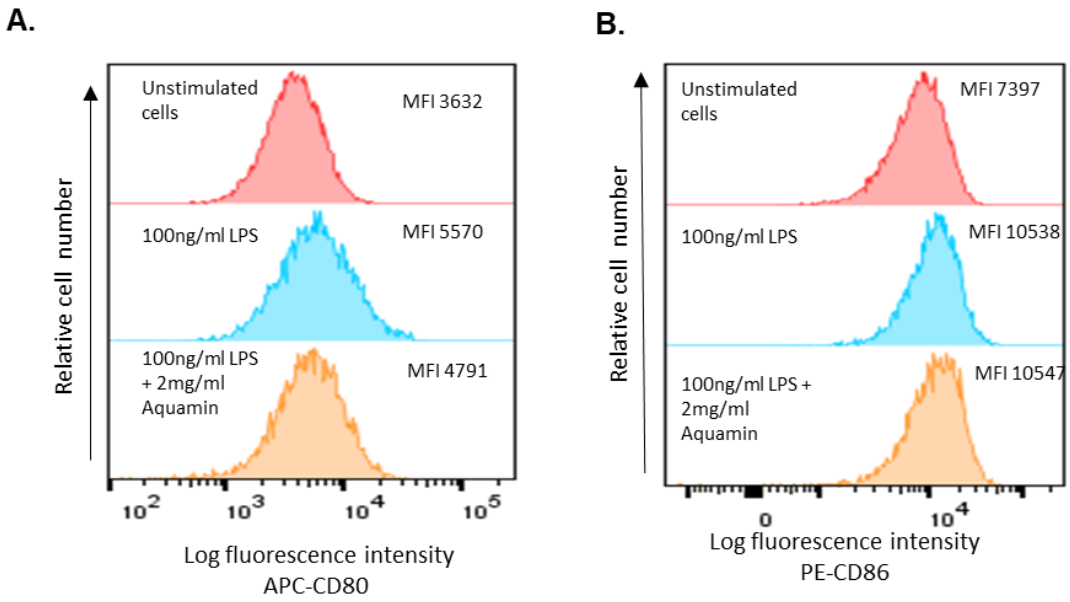

Figure 3.4. Aquamin modulation of CD80 and CD86 expression on murine iBMDM with LPS stimulation.

Murine immortalised bone marrow derived macrophages (iBMDM) treated with Aquamin (2mg/mL) for 3 h followed by stimulation with LPS (10 ng/mL) overnight. iBMDM cells were then stained with fluorescently labelled antibodies, APC rat anti-mouse CD80, PE rat anti- mouse CD86 and analysed on a BD LSR Fortessa™ flow cytometer with cells gated according to figure **2.**3.1. Data was analysed using Flowjo software for positively stained CD80 and CD86 cells. Data is presented as a staggered histogram overlay of log fluorescent intensity of (a) CD80 and (b) CD86 stained cells, with unstimulated cells (red), LPS stimulated cells (blue) and LPS plus Aquamin stimulated cells (yellow). The mean fluorescence intensity (MFI) value for each treatment is indicated to the right on the histogram plots. The staggered histogram plots are shown for a single experiment.

3.2.4 Aquamin inhibits TNF-a released from M1 classically activated murine immortalized bone marrow derived macrophages

Macrophages have great plasticity and a diverse set of functions with distinct phenotypes in reaction to specific stimuli in their microenvironment. Resting macrophages (M0) can be broadly polarized or skewed to either the classically activated M1 state or an alternatively activated M2 state. Classically activated M1 macrophages exhibit a pro-inflammatory phenotype and play an important role in driving the release of pro inflammatory cytokines in the tissue spaces they infiltrate, whereas macrophage that take on the M2 phenotype state are classed as anti-inflammatory. To address whether aquamin has any effect on macrophage polarization, iBMDMs stimulated with both LPS (10ng/ml) and IFN-gamma (20ng/ml) to induce a skewing towards M1 'classically activated' macrophages in the presence and absence of Aquamin for 24 h was carried out. The expression of CD80, CD86 and CD11c, commonly used cell surface markers of M1 polarization was assessed by FACS analysis. Aquamnin (2mg/ml) treatment did not change the expression of CD80 (Fig. 3.5A), CD86 (Fig. 3.5B) and CD11c (Fig. 3.5C), in macrophage cells under M1 polarization conditions. In contrast to M1 cell surface markers, the release of TNF-α demonstrated that Aquamin exhibited a potent inhibitory effect (Fig. 3.5D) on its release upon induction of M1 macrophages. One possible explanation for the inhibition of M1 responses observed is Aquamin induces these cells to preferentially adopt an M2 type response. However, measurement of CD301, a marker of M2 polarization, demonstrated that no significant effects were observed under Aquamin treatment (Fig. 3.5C). Therefore, while Aquamin can inhibit cytokine secretion under M1 polarising conditions, these effects are not the result of alternative activation towards an M2 phenotype or an overall change in the M1 activation

state of the cells.

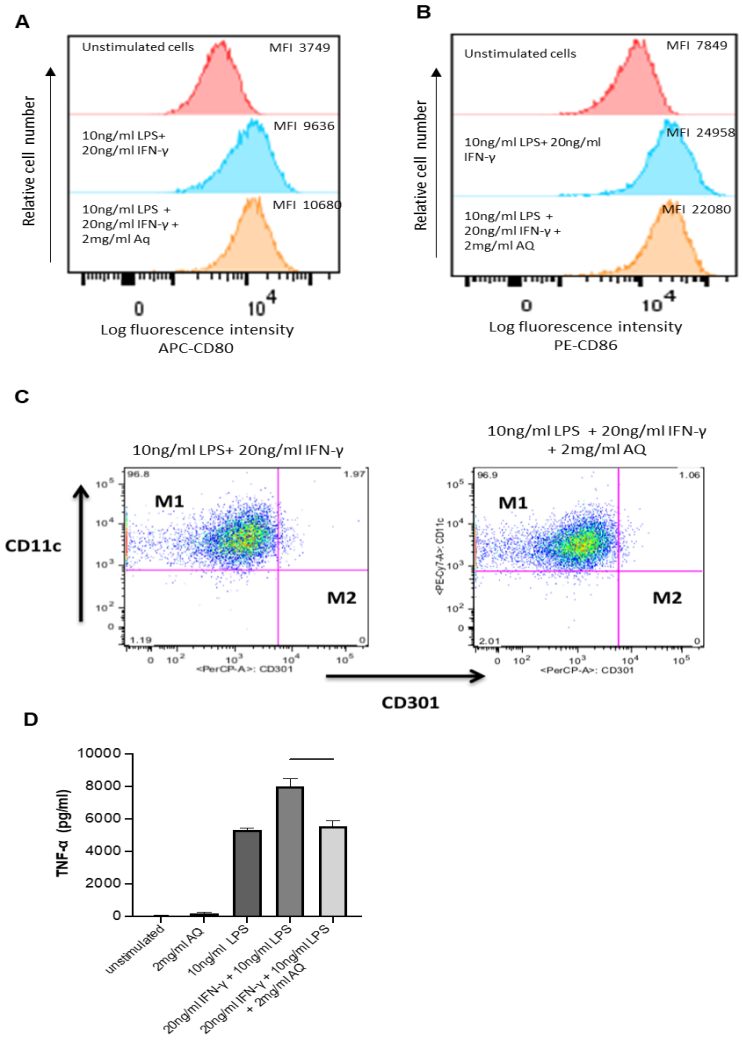

Figure 3.5. Effect of aquamin on M1 polarized macrophages.

Levels of CD80 (A), CD86 (B) and CD11c (C) were estimated by FACS upon overnight stimulation of iBMDMs with LPS (10ng/ml) and IFN-gamma (20ng/ml) after pre-treatment with Aquamin (2mg/ml) for 3 h. In (C), M1 cells are identified in the upper left quadrant, while M2 type cells are found in the bottom right quadrant (CD11c-CD301+). Levels of TNF-a (D) measured by ELISA upon stimulating iBMDMs with LPS (10ng/ml) and IFN-gamma (20ng/ml) and treated with aquamin (2mg/ml). *Data are expressed as mean ±sem from 3 independent experiments. ***p<0.001, **p<0.01 vs LPS+IFN-γ using one way ANOVA statistical test.*

It has recently been reported that 'metabolically' activated macrophages, reflecting the proinflammatory phenotype observed

in the setting of obesity, can be modelled in vitro (312).To make an assessment of aquamin's effect on 'metabolically activated macrophages', iBMDMs were stimulated with insulin, palmitate and glucose to resemble an obesity-like phenotype. The stimulated cells were incubated in the presence and absence of aquamin (0.5-2mg/ml). Inducing a metabolic phenotype led to a significant increase in TNF-a compared to the unstimulated control, however Aquamin had no effect in altering the concentration of TNF-α (Fig. 3.6).

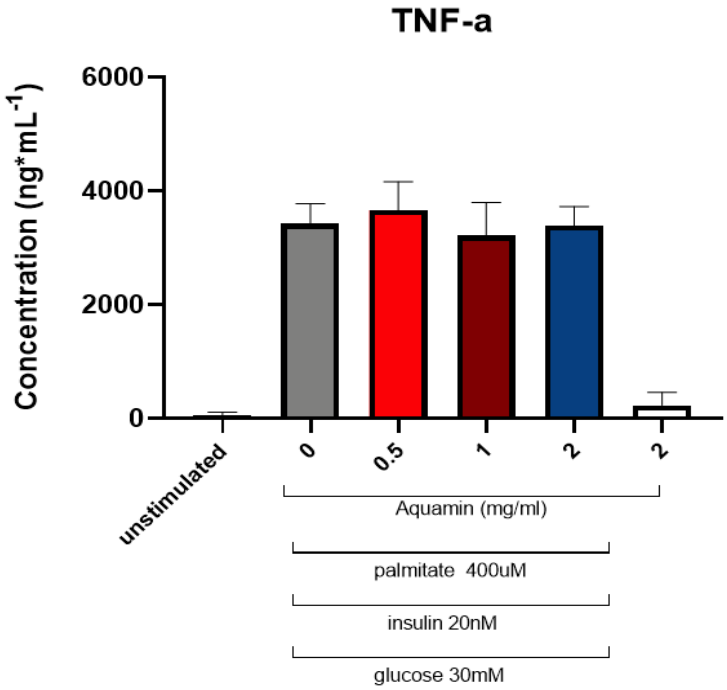

Figure 3.6. Aquamin has no effect on metabolically activated macrophages.

BMDMS were pre-treated with aquamin (0.5-2) mg/ml and stimulated overnight with palmitate (400uM), insulin (20nM) and glucose (30mM) for induction of a metabolic phenotype followed by quantifying TNF-a concentration in the supernatants by ELISA.

3.2.5 Aquamin reduces LPS driven pro-inflammatory responses in primary murine bone marrow dendritic cells

Similar to macrophage cells, the closely related dendritic cells are also important innate cells of the immune system for protective responses against pathogens and associated with driving inflammatory disease states. To extend the effects of Aquamin into different innate immune cell subtypes, bone marrow isolated from mice was cultured to generate dendritic cells using GM-CSF (20ng/ml) treatment for 7-10 days. To assess if the viability of bone marrow dendritic cells (DCs) is affected by Aquamin, DCs were pretreated with Aquamin for 2h followed by LPS stimulation for 24 h. No reduction in the live population of DCs was observed upon treatment of cells with 2mg/ml of Aquamin which was assessed by live/dead dye exclusion (unstimulated 47.4%, LPS 57.8 % and Aquamin 46.3% only treatments) and subsequent FACS analysis (Figure 3.7A). Having established that Aquamin does not affect DC cell viability, we examined the secretion of inflammatory cytokines from these cells by ELISA. The results showed a significant reduction in LPS-induced TNF -a (Fig. 3.7B) and IL-1β (Fig. 3.7C) post Aquamin (2mg/ml) treatment, however no effect observed with LPS induced expression of IL-6 and IL-10 (Fig. 3.7D, E). Expression of surface activation markers CD80 and CD86 was also measure using FACS analysis. The histograms represent the percentages of CD80 and CD86 in DCs. It has been found that LPS-stimulated DCs display an increase percentage of CD80 and CD86 expression compared unstimulated controls. However, as demonstrated by the corresponding cell surface marker percentages in the histograms, treatment of LPS primed cells with Aquamin did not cause any significant effect to the expression of either CD80 or CD86. Taken together, these data indicate that Aquamin can suppress specific

TLR4 driven innate responses in DCs similar to that seen in macrophage cells.

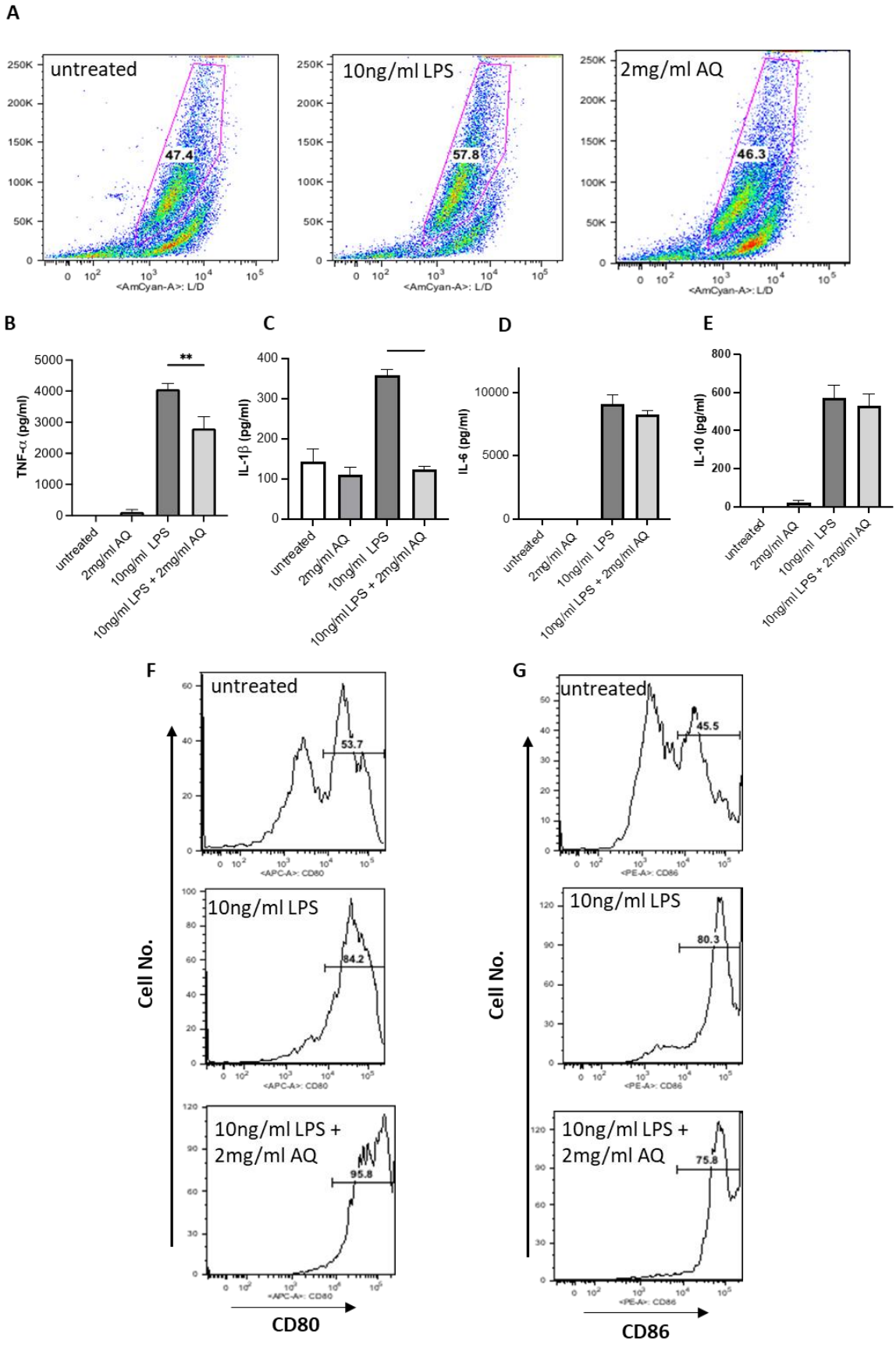
A
untreated
47.4
10ng/ml LPS
57.8
2mg/ml AQ
46.3
<AmCyan-A>: L/D
B
TNF-α (pg/ml)
**
C
IL-1β (pg/ml)
D
IL-6 (pg/ml)
E
IL-10 (pg/ml)
untreated
2mg/ml AQ
10ng/ml LPS
10ng/ml LPS + 2mg/ml AQ
F
untreated
53.7
10ng/ml LPS
84.2
10ng/ml LPS +
2mg/ml AQ
95.8
<APC-A>: CD80
Cell No.
CD80
G
untreated
45.5
10ng/ml LPS
80.3
10ng/ml LPS +
2mg/ml AQ
75.8
<PE-A>: CD86
Cell No.
CD86

Figure 3.7. Aquamin reduces pro-inflammatory cytokines in LPS stimulated DCs.

Viability of murine dendritic cells upon overnight exposure to either LPS or Aquamin assessed by live dead dye exclusion and FACS analysis (A). Expression of TNF-a (B), IL-1β (C), IL-6 (D) and IL-10 (E) on overnight LPS stimulated DCs in the presence and absence of aquamin (2mg/ml). (F) CD80 and (G) CD86 expression in the presence and absence of aquamin (2mg/ml) in LPS-stimulated dendritic cells assessed by FACS. Data are expressed as mean ±sem from 3 independent experiments. ***$p<0.001$; $p<0.05$ vs LPS alone using one way ANOVA statistical test.

3.2.6 Aquamin reduces LPS driven pro-inflammatory cytokine and chemokine responses in primary murine bone marrow derived macrophages.

To examine whether Aquamin affects the expression of cytokines associated with inflammation in primary murine BMDMs, bone

marrow isolated from mice was cultured to generate macrophage cells using M-CSF (50ng/ml) treatment for 7-10 days. Quantitative RT-PCR was carried out to check the mRNA expression of pro-inflammatory cytokines TNF-a (Fig. 3.8A), IL-6 (Fig. 3.8B) and IL-1β (Fig. 3.8C) following Aquamin treatment and LPS stimulation. The TNF-a, IL-6 and IL-1b levels were increased upon LPS exposure compared with those of the control group as expected. The results show that pretreatment with Aquamin reduces the mRNA cytokine expression levels of IL-6 and IL-1b driven by LPS stimulation in primary murine macrophages.

Stimulating BMDM with LPS is also known to increase the mRNA expression levels of chemokines such as CXCL2 and CCL2 (Fig 3.8D, E). These results clearly show a robust increase in the expression levels of these chemokines following 6h LPS stimulation in BMDM which like the cytokine expression levels can also be significantly reduced with Aquamin treatment.

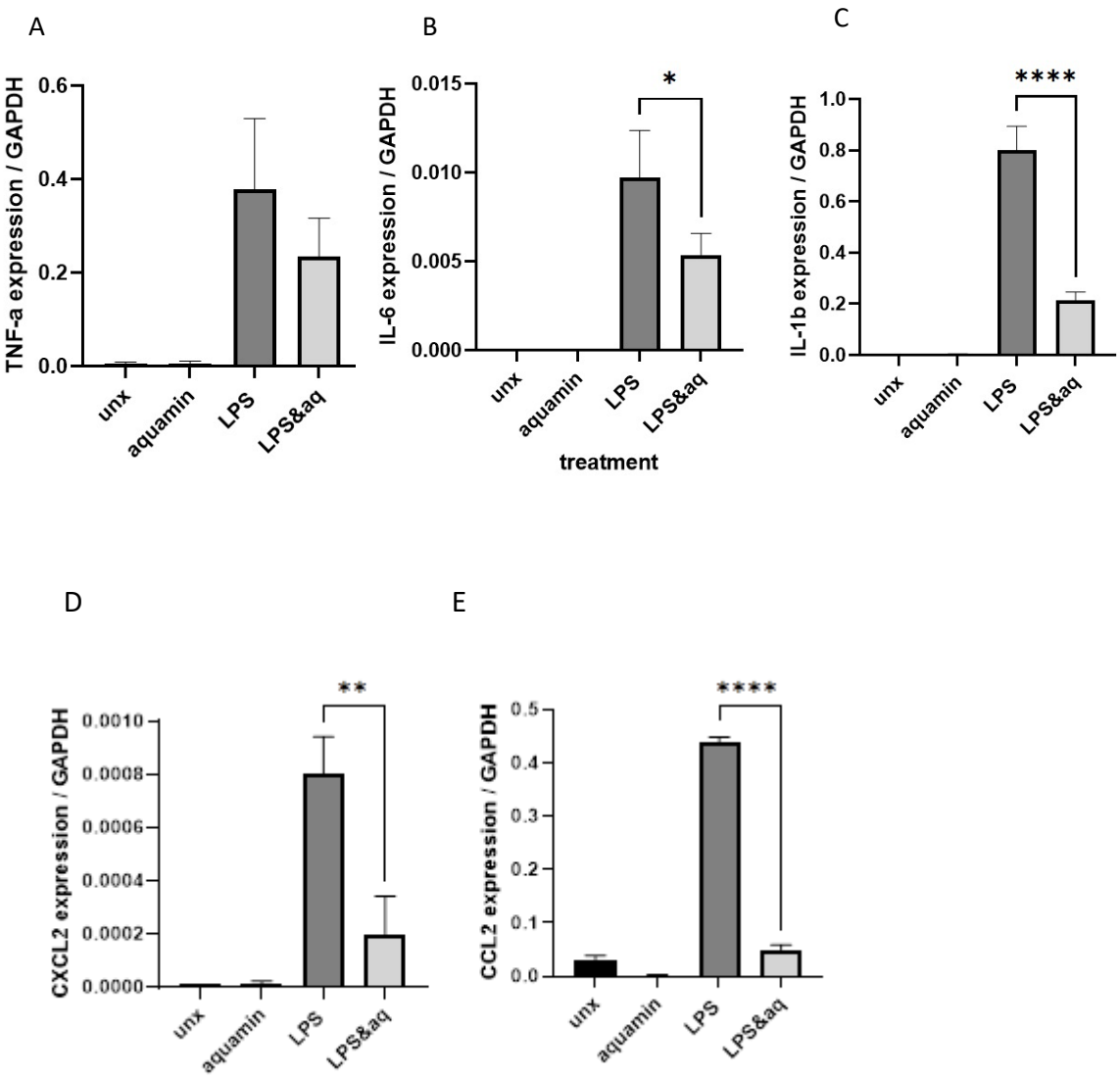

Figure 3.8. Aquamin reduces LPS-induced expression of pro-inflammatory cytokines and chemokines in murine primary BMDMs. BMDMs were pretreated with Aquamin (2mg/ml)) for 3 h and exposed to LPS (100ng/ml) for 4-6 h followed by total RNA extraction. The mRNA expression levels of (A) TNF-a, (B) IL-6, (C) IL-1β at 4h and (D) CXCL2 and (E) CCL2 at 6h following LPS stimulation and assessed using specific primers. Data (A-E) are presented as mean ± sem from 3 independent experiments normalized to GAPDH and expressed relative to untreated cells. *****p<0.0001; ***P<0.001, **p< 0.01, *p<0.05 vs LPS alone using one way ANOVA statistical test.*

3.2.7 Aquamin inhibits iNOS expression in LPS treated primary murine bone marrow derived macrophages.

Nitric Oxide (NO) is a soluble endogenous gas, produced under the enzymatic activity of inducible nitic oxide synthase (iNOS) in macrophage cells in response to inflammatory signals. Macrophages stimulated with LPS a pro-inflammatory stimulus induces expression of the enzyme iNOS and production of NO involved in pathogen killing. To assess the effects of Aquamin on iNOS expression in vitro, murine bone marrow derived macrophages (mBMDMs) were treated with LPS and Aquamin with the indicated concentrations for 12h (Fig 3.9A-C). The expression of iNOS, was assessed using western immunoblotting at the protein level and quantified using densitometric analysis. The data obtained from western blotting show that pretreatment with Aquamin (2mg/ml) significantly inhibits LPS-induced iNOS expression in mBMDMs (Fig. 3.9A representative immunoblot), (Fig, 3.9B densitometric analysis). Protein immunofluorescence staining for iNOS expression in mBMDMs was also carried out under LPS stimulating conditions in the presence and absence of Aquamin (2mg/ml). Consistent with western blot findings, immunofluorescence staining for iNOS protein expression in LPS stimulated mBMDMs is reduced in the presence of Aquamin (2mg/ml) treatment (Fig. 3.9C representative immunofluorescent images). These results indicate that Aquamin reduces LPS driven iNOS expression with the potential to reduce NO production and further strengthens the anti-inflammatory effects of Aquamin in mBMDM.

A

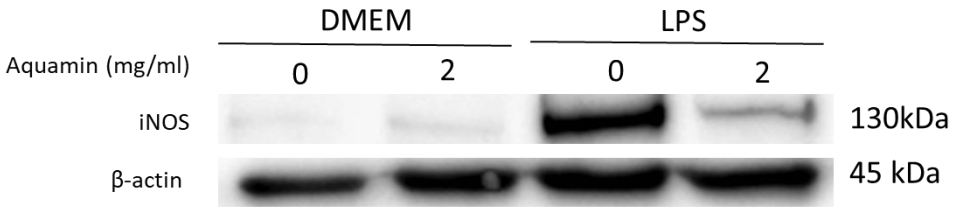

B

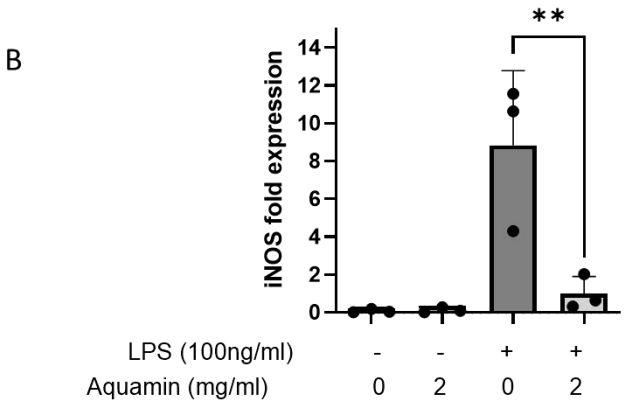

C

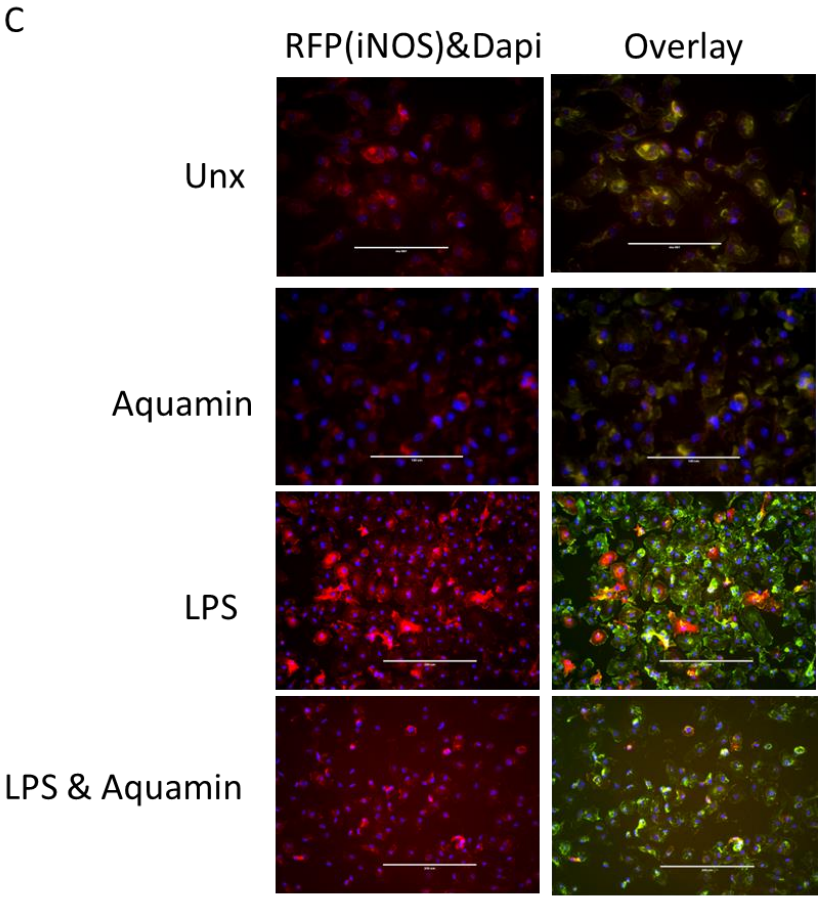

Red: iNOS, blue: Dapi(nuclear), green: actin-cytoplasmic

Figure 3.9. Aquamin suppresses iNOS expression in LPS stimulated murine bone marrow derived macrophages.

mBMDMs pretreated with Aquamin (2mg/ml) for 3 h followed by stimulation with LPS (100ng/ml) for 12 h**.** The protein cell lysates were collected resolved by SDS PAGE for western immunoblotting and additional cells were fixed for immunofluorescence analysis. (A) Representative western blot demonstrating protein expression of iNOS in LPS treated mBMDMs in the presence and absence of Aquamin (2mg/ml). Protein loading assessed assessed by immunoblotting with anti-β-actin antibody (B) Bar graph of densitometric analysis of western blots n=3 showing the mean ± SEM of iNOS protein expression normalised to β-actin and presented as fold change in protein expression relative to untreated control cells. ***p<0.01 versus LPS alone using one-way ANOVA statistical test*. C) Representative immunofluorescence of iNOS protein abundance (Red), DAPI nuclear stain (blue) and actin (green) in mBMDMs, Scale bar (200um).

3.2.8 Aquamin does not affect the phosphorylation of NF-kB transcription factor in LPS stimulated primary murine bone marrow derived macrophages.

It is well established that NF-kB activation plays a crucial role in the signaling mechanisms downstream of LPS/TLR4 in macrophage cells, driving inflammatory cytokine release. The activation of NF-kB induced in response to LPS in macrophages occurs via NF-kB p-65 subunit phosphorylation, allowing its translocation to the nucleus to initiate transcription of regulated genes. In unstimulated cells, IκBα sequesters NF-kB in the cytoplasm keeping NF-kB inactive. Upon phosphorylation, IκBα is targeted for proteasomal degradation with subsequent NF-kB activation. The effect of Aquamin in regulating these events downstream of TLR4 stimulation were investigated by detecting p65 phosphorylation (Fig. 3.10A, B) and IκBα protein expression levels (Fig. 3.10A, C). SDS-Page and Western blotting was performed as described in section 2.3.19. 8% gel was used following electrophoresis at 100 volts for 90 min. Results reveal that Aquamin did not significantly alter either phosphorylation of the NF-kB subunit p65 (Fig. 3.10A, B) or IκBα degradation (Fig. 3.10A, C) post LPS stimulation.

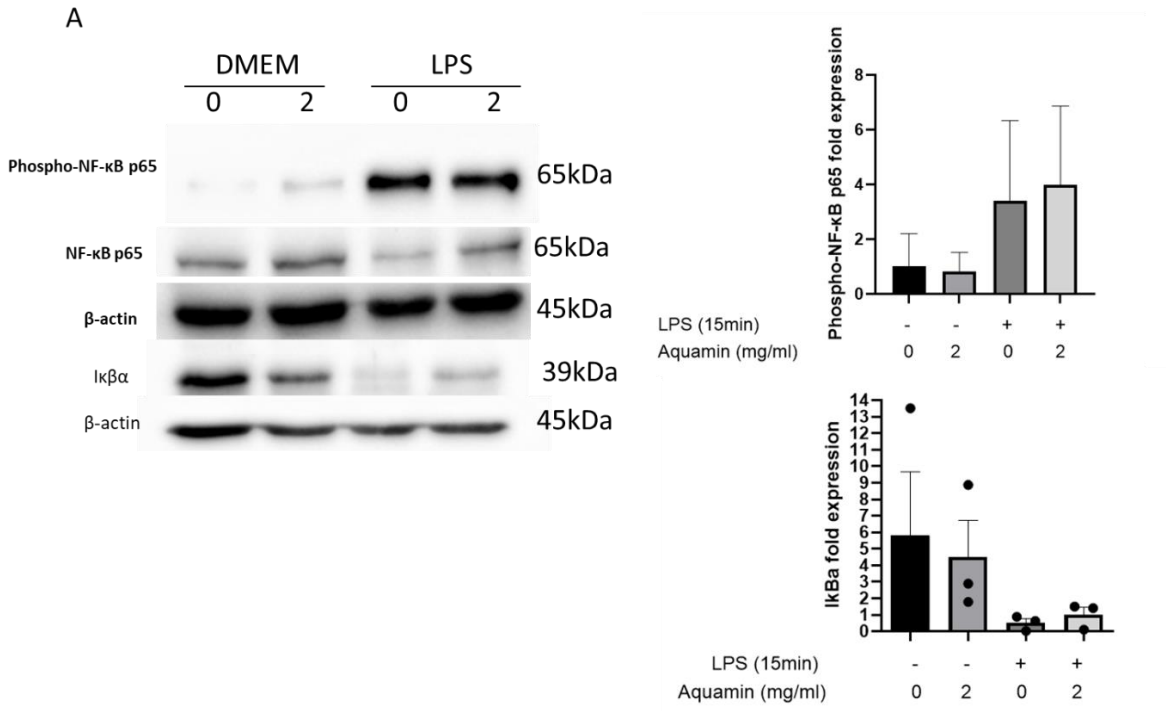

Figure 3.10. Aquamin does not affect activity of NF-kB in LPS stimulated primary murine bone marrow derived macrophages.

BMDMs were pretreated with Aquamin at 2mg/ml for 3 h prior to stimulation with LPS at 100ng/ml for 7 min to detect (p-p65, p65, β-actin), and 15 min to detect (IκBα, β-actin) protein expression levels. The protein cell lysates were collected resolved by SDS PAGE for western immunoblotting. (A) Representative western blots demonstrating protein expression of p-p65, p65, and IκBα in LPS stimulated mBMDMs in the presence and absence of Aquamin (2mg/ml). Protein loading assessed by immunoblotting with anti-β-actin antibody. (B)Bar graph of densitometric analysis of western blots n=3 showing the mean ± SEM of p-p65 protein expression normalised to β-actin/p65? and presented as fold change in protein expression relative to untreated control cells. (C) Bar graph of densitometric analysis of western blots n=3 showing the mean ± SEM of IκBα protein expression normalised to β-actin and presented as fold change in protein expression relative to untreated control cells.

3.2.9 Aquamin does not reduce expression of TLR4 and MyD88 adaptor protein in LPS stimulated primary murine bone marrow derived macrophages

Intracellular events following the interaction of LPS with its TLR4 receptor in macrophage cells is dependent on different sets of adapters. An early response is dependent on MyD88 adaptor protein leading to the activation of nuclear factor-κB (NF-κB) with a later response dependent on TRIF adaptor protein leading to the late activation of NF-κB and IRF3 transcription factors. Our results demonstrate that LPS stimulation resulted to the increase of MyD88 gene expression, however treatment with Aquamin did not exhibit any significant results. The main observation to emerge from Figure 3.11 is that Aquamin does not modulate TLR signaling in a MyD88-dependent manner.

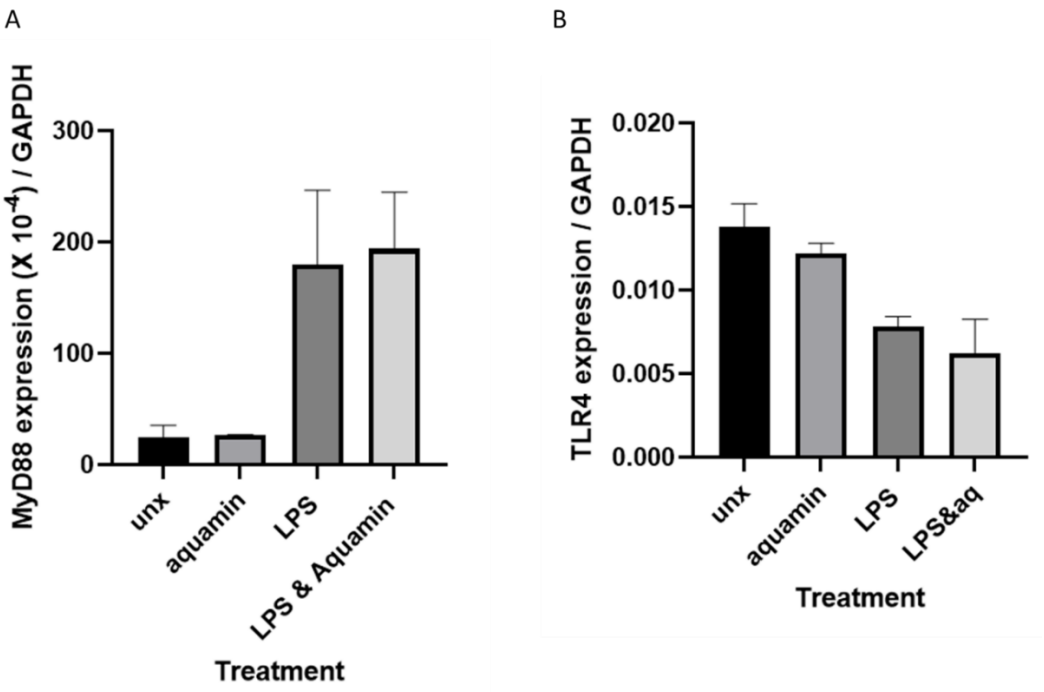

Figure 3.11. Aquamin effects on the expression of TLR4 and Myd88 in LPS stimulated murine primary BMDMs.

BMDMs pretreated with Aquamin (2mg/ml)) for 3 h and exposed to LPS (100ng/ml) for 4h followed by total RNA extraction. The mRNA expression levels of (A) TLR4 and (B) Myd88 was analysed using specific primers and SYBR green qRT-PCR. *Data (A, B) are presented as mean ± sem from 3 independent experiments normalized to GAPDH and expressed relative to untreated cells.*

3.2.10 Aquamin inhibits LPS and Poly(I:C) induced expression of TNF-a and IL-6 in primary murine bone marrow derived macrophages.

The data above demonstrate that Aquamin reduces cytokine release in human and murine innate cells under LPS stimulation. However, these effects appear independent of MyD88 expression or activation of downstream NF- κB mediated signalling. LPS can also signal through TLR4 using a second adaptor protein, TRIF. TLR4 activation of TRIF dependent signaling is a slower response pathway to LPS when compared to Myd88 adaptor protein mediated signalling. TRIF mediated signalling activates the transcription factor IRF3 through phosphorylation and induces robust expression of type 1 interferons such as IFN B while also activating NF-κB dependent gene transcription. While TLR4 is unique in its ability to signal through both adaptor proteins, Myd88 and TRIF, other toll receptors are known to signal specifically through either pathway. For example, TLR3 primarily signals using the adaptor protein TRIF while TLR9 signals using the adaptor protein Myd88. Therefore, to gain a deeper understanding of Aquamin mediated inhibition of TLR family signalling pathways we examined whether Aquamin altered BMDM responses upon stimulation with specific agonists to TLR4, TLR3 and TLR9. Primary murine BMDMs were pretreated with Aquamin for 3h and exposed to specific TLR agonists, Poly(I:C) for TLR3 stimulation (Fig. 3.12B, E), CpG for TLR9 stimulation (Fig. 3.12C, F) and LPS for TLR4 stimulation (Fig. 3.12A, D) overnight. As expected, all TLR agonists increased TNF-a and IL-6 cytokine release from BMDMs compared to untreated cells after an overnight stimulation. While Aquamin treatment significantly reduced TNF-a and IL-6 cytokine release from LPS and Poly (I:C) stimulation, the same inhibitory effect was not evident with Aquamin upon CpG stimulation. These data suggest that mechanistically Aquamin is blocking TRIF dependent

signalling in response to TLR4 and TLR3 stimulation as TLR9/Myd88 dependent cytokine release was not reduced significantly upon Aquamin treatment.

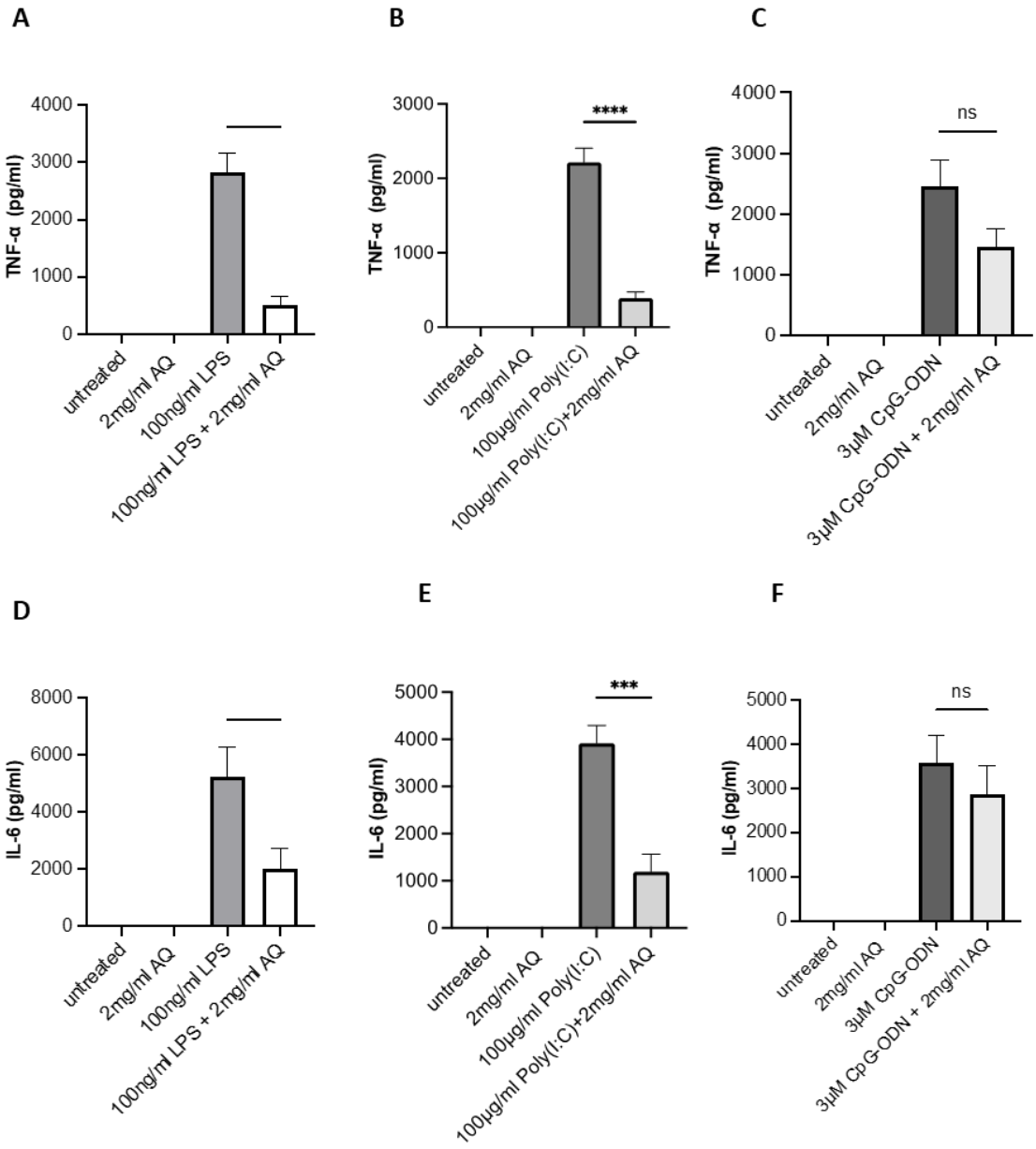

Figure 3.12. Aquamin reduces LPS and Poly(I:C) release of TNF-a and IL-6 in murine BMDMs.

Cells were pretreated with Aquamin (2mg/ml) for 3 h prior to stimulation with the corresponding TLR agonists overnight, LPS (100ng/ml) for TLR4 stimulation, Poly(I:C) (100ug/ml) for TLR3 stimulation and CpG (3µM) for TLR9 stimulation. Cytokine concentrations of TNF-a (A-C) and IL-6 (D-F) detected in the cell culture supernatants by ELISA. *Data (A-F) are expressed as mean ±sem from 3 independent experiments. ***p<0.001, **p<0.01; p<0.05 vs LPS alone using one way ANOVA statistical test.*

3.2.11 Aquamin inhibits expression of TLR3, and TRIF adaptor protein in LPS stimulated primary murine bone marrow derived macrophages

Unlike transcriptional levels of MyD88 that remained unaffected by Aquamin in LPS-induced BMDMs, treatment with 2mg/ml of Aquamin led to significant reduction of both TLR3 and TICAM-1 in LPS-stimulated BMDMs (Fig. 3.13). These findings further hint that the effect of Aquamin in association with TLR signaling is TRIF-dependent.

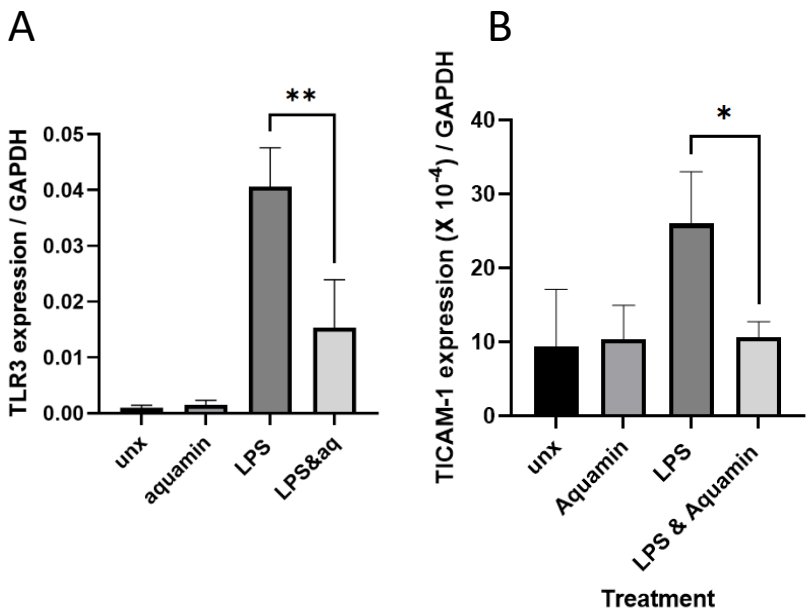

Figure 3.13. Aquamin reduces expression of TLR3, and TRIF in LPS stimulated murine primary BMDMs.

BMDMs were pretreated with Aquamin (2mg/ml)) for 3 h and exposed to LPS (100ng/ml) for 4h followed by total RNA extraction. The mRNA expression levels of (A) TLR3 and (B) TICAM-1 at 4h following LPS stimulation were analysed using specific primers and SYBR green qRT-PCR . Data (A-C) normalized to GAPDH, expressed relative to untreated cells and presented as mean ± sem from 3 independent experiments. ****p<0.001, **p<0.01; *p<0.05 vs LPS alone using one way ANOVA statistical test.*

3.2.12 Aquamin reduces IFN-β expression and nuclear translocation of IRF3 transcription factor under Poly(I:C)-induced TLR3 signaling in BMDMs.

Poly (I:C) TLR3 signalling in macrophages primarily uses the adaptor protein TRIF. To determine if Aquamin regulates TRIF dependent IRF-3 signalling, investigations using Poly (I:C) stimulation were carried out to determine if Aquamin altered the mRNA expression of the IRF-3-dependent gene IFN-β. Using real-time PCR (Fig. 3.14A) the mRNA expression level of IFN-β was analysed in poly (I:C)-stimulated BMDM pre-treated with Aquamin (2mg/ml) The results indicate that Aquamin reduces expression at the mRNA level of IFN-β under poly (I:C) stimulation (Fig. 3.14A). IFN-β expression is dependent on activation of IRF-3 through phosphorylation events, followed by IRF3 dimerization and translocation to the nucleus in macrophage under poly (I:C) stimulation. Protein immunofluorescence staining for IRF3 expression in mBMDMs was also carried out under poly (I:C) stimulating conditions in the presence and absence of Aquamin (2mg/ml). As expected, poly (I:C) increased the level and nuclear localization of IRF3 as evident by nuclear DAPI counterstaining compared to untreated and Aqumain only treated cells. A reduction in the intensity of IRF3 staining as well as a reduction in the nuclear localization of IRF3 in Aquamin (2mg/ml) and poly (I:C) stimulated cells is seem compared to cells treated with poly (I:C) alone. (Fig. 3.14B representative immunofluorescent images and counterstaining overlay). These results indicate that Aquamin inhibits poly (I:C) driven mRNA expression of the IRF-3-dependent IFN-β gene and reduces poly (I:C) driven IRF3 nuclear localization in BMDM.

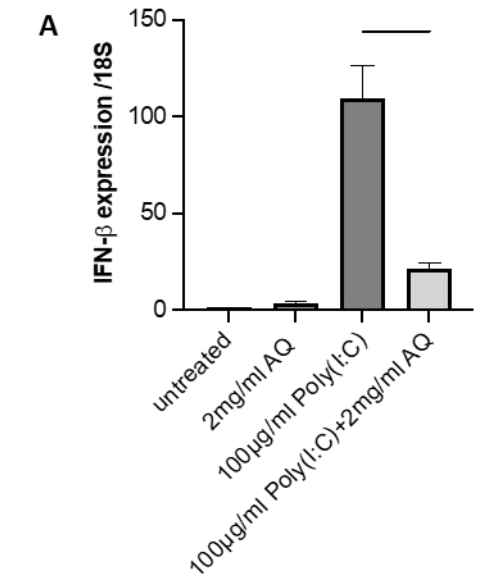

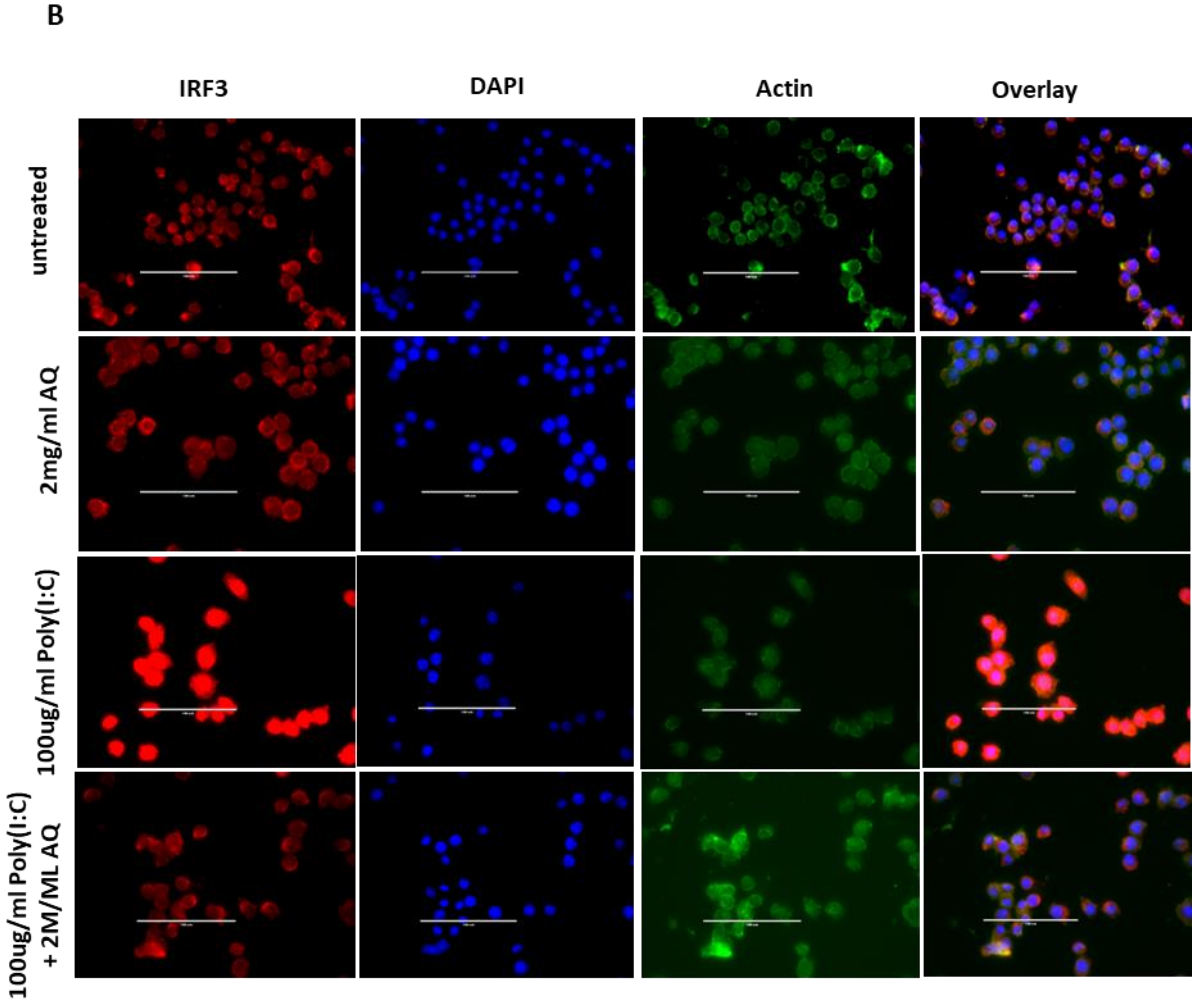

Figure 3.14. Aquamin reduces IFN-β expression and nuclear translocation of IRF3 in Poly (I:C) stimulated iBMDM.

BMDMs were pretreated with Aquamin (2mg/ml) for 3 h before stimulated with Poly(I:C) (100µg/ml) for 6 h. (A) IFN-β mRNA expression normalized to 18S RNA, expressed relative to untreated cells and

presented as mean ± sem from 3 independent experiments. ****p<0.001 vs Poly (I:C) alone using one way ANOVA statistical test.* (B) Representative immunofluorescence of IRF3 protein abundance (Red), DAPI nuclear stain (blue) and actin?? (green) in mBMDMs, Scale bar (100 um).

3.3 Discussion

The health promoting capabilities of aquamin have been studied in several disease models. However, the molecular mechanisms of its immunomodulatory effects in these disease states have not been investigated extensively. Here we investigate the potential therapeutic and health benefits of Aquamin in inflammatory disease states with the aim of gaining a greater understanding of its potential molecular and cellular anti-inflammatory mechanisms.

From previous research it has been shown that Aquamin can modulate inflammation (277, 310). Obesity is a disease of inflammation since excessive fat results in the release of pro-inflammatory cytokines which have a negative correlation with adiponectin and impairs crucial mechanisms for cardiovascular health (313). Therefore, we investigated Aquamin's effect on innate inflammation as a mechanism in contributing to its protection against obesity and possibly cardiovascular disease. To that end we induced a pro-inflammatory phenotype in several innate immune cell types by stimulating with the bacterial endotoxin LPS that acts through the TLR4 signalling pathway. In both murine DCs and iBMDM and in primary human macrophages derived from PBMCs, Aquamin treatment inhibited TNF-a and IL-6 secretion following LPS stimulation. There is overwhelming evidence corroborating the notion that TNF-a and IL-6 levels are significantly higher in obese individuals and hence worsen inflammation in obese subjects (314). Our results agree with previous findings where Aquamin reduced LPS-driven TNF-a and IL-1beta release by glial cells (310) and is also in accordance with reported molecular effect on inhibiting the transcription factor NF-kB and reducing COX-2 gene expression (277). Data obtained in previous studies provides evidence about the connection between inflammation and cancer. Hence control of inflammation could yield an alternative approach for preventing

tumour growth (315, 316). It is evident by previous literature that TNF-a could cause tumorigenesis by promoting cancer cell survival and proliferation(317). It is clear from the data in this thesis, as well as others, that Aquamin is capable of inhibiting inflammation in cells of the innate immune system which plays a role in pathogenesis of not only cardiometabolic disease and obesity but infectious pathogenic insults such as septic shock, tumour growth and autoimmune conditions such as rheumatoid arthritis.

When exposed to LPS, macrophages tend to generate high levels of NO (318). The production of NO occurs due to inflammatory stimuli and exert pro-inflammatory and detrimental effects which are mainly induced by iNOS (319). In this study, it was found that Aquamin blocked the iNOS expression in LPS-induced BMDMs.

To explore more deeply the immunomodulatory role of Aquamin, the effects under conditions of macrophage polarisation were investigated. Again, the current results demonstrated that Aquamin can inhibit signature cytokines when macrophage cells are skewed towards an inflammatory M1 phenotype in the presence of LPS and IFN gamma. As expected, the percentage of cells skewed towards an M1 phenotype as detected by cell surfaces markers (CD11c, CD80/86) was increased in the presence of LPS and IFN gamma but not affected by the presence of Aquamin. Based on these results we conclude that the blocking effect of Aquamin in cytokine levels is not associated with skewed polarization or activation marker expression of macrophages in the conditions tested.

Sedentary lifestyle and dietary intake of saturated fatty acids such as palmitic acid result in subsequent manifestations of hyperglycemia and imbalances in lipid metabolism leading to inflammation and production of pro-inflammatory cytokines such as TNF-a (320). Apart from the dietary intake of free fatty acids, obese individuals are known to exhibit high blood palmitic levels

(321-325). To model the in vivo adipose tissue environment that infiltrating macrophage encounter in obesity we polarized macrophages in vitro towards a metabolic phenotype in the presence of palmitic acid, insulin and glucose. Under these metabolic polarizing conditions an increase in TNF-a secretion was seen however Aquamin treatment did not change the secretion of TNF-a. Unlike LPS, palmitic acid, glucose and insulin act in a complex fashion in modulating macrophage lipid metabolism and the cellular lipidome in priming and skewing the cells down various inflammatory pathways (326). While Aquamin inhibits TLR/LPS immune inflammatory pathways, modelling the obesity inflammatory state in vitro such as that described may mask Aquamin's effects.

It is interesting to note that in spite of the cytokine blocking capabilities of Aquamin, under LPS stimulation in the above cell types, no detectable change in the expression of LPS-driven activation markers CD80/CD86 was detected with Aquamin treatment. These results suggest that Aquamin yields its anti-inflammatory effect through a pathway different to that which induces expression of these surface activation markers. Previous research conducted on DCs and monocytes has shown that increases in CD80/CD86 expression results following activation of either TLR2,TLR4 and TLR9 (327). TLRs signal downstream through recruitment of adaptor proteins such as MyD88, and TRIF which ultimately activate transcription factors and regulate gene transcription. The MyD88 adaptor protein pathway activates early and potently NF-kB transcription and increases expression of signature cytokines such as TNF- a.

As per previous evidence, Aquamin treated RAW264.7 cells that were primed with LPS exhibited a profound reduction at the levels of NF-κB (277). Unlike those previous findings, pretreatment of primary macrophages with Aquamin and exposure to LPS did not

display similar results since no significant effects were observed at the protein expression levels of phospho-NF-κB p65 in our lab. TRIF dependent signalling activates IRF3 and 7 transcription factors increasing type 1 interferons responses such as IFN beta levels. TRIF signalling to a lesser extent can also activate NF-κB transcription. The common mediator of TLR4 and TLR9 signalling is the MyD88 adaptor protein and responsible for CD80/CD86 expression levels. Given that TLR4, unlike TLR9, signals through both MyD88 and TRIF adaptor proteins (328), the suppressive effects of Aquamin on TLR4 induced cytokines could potentially be a result of inhibitory effects on the TRIF dependent arm of TLR4 signalling. No evidence currently available has elaborated on the mechanism that Aquamin modulates inflammation. To acquire a better insight with respect to the mechanistic effect of Aquamin, we examined its effects on the activation of TLR9 which is MyD88-dependent. Aquamin did not block TLR9-driven TNF-a levels suggesting its anti-inflammatory properties is MyD88 independent but possibly blocks TRIF signalling with TLR4 activation. The present study made some noteworthy contributions towards elucidating the anti-inflammatory role of Aquamin. It has been established by previous evidence that Poly(I:C) is the agonist that leads to the release of type I interferons and specifically IFN-β (329). Here in study, it was demonstrated that treatment with Aquamin blocks LPS induced TICAM-1 as well as Poly(I:C) induced IFN-β downstream of TRIF. TLR3 is the only Toll-like receptor which is mediated by TRIF dependent signalling (MyD88 independent) (330). Our results may suggest that Aquamin modulates inflammation by inhibiting TRIF dependent signalling pathways. It is interesting to note that in mouse models of atherosclerosis a functional mutation in the TRIF adaptor protein significantly protected against disease development (331). Similarly, in bone-marrow transplantation models depleting TRIF in haematopoietic cells attenuated vessel inflammation and

protected against atherosclerosis in a murine atherosclerotic model. Furthermore, deleting TLR3 in immune cells here also reduced both aortic inflammation and atherosclerotic lesion burden (332). These studies provide evidence for TLR3 and TRIF dependent signalling as pathways contributing to the pathogenesis of atherosclerosis and cardiovascular disease.

The therapeutic potential for TRIF modulation is explored in agonistic approaches in boosting clearance of a number of viral and bacterial pathogens in infectious diseases such as an adjuvant in vaccine designs (333). On the other hand in a model of sceptic shock , TRIF antagonistic approaches protect mice from a lethal dose of LPS injection (334).

The roles of TRIF and TLR3 signalling in inflammation are divergent, driving inflammatory disease such as tissue specific atherosclerosis versus offering protective functions in host defence mechanism against pathogenic insults (159, 335). A previous in vivo study has examined the significance of TRIF signaling as a factor in the deterioration of cardiovascular events and concluded that TRIF inhibition can play a protective role against worsening of cardiac function attributed to excessive cytokine production and immune cell infiltration (336). Aquamin as a nutraceutical may carry such potential as a TRIF blocking supplement in specific disease states described above. Further investigations of the potential effects of Aquamin in TRIF dependent signalling be conducted to draw firm conclusions about its exact mechanism of action.

4. COMPARATIVE TRANSCRIPTOMIC ANALYSIS OF AQUAMIN VERSUS STATIN TREATMENT ON MONOCYTES USING NEXT GENERATION SEQUENCING ANALYSIS -IDENTIFICATION OF RESPONSIVE GENES AND REGULATORY PATHWAYS INVOLVED.

4.1 Introduction

Based on the results to date, Aquamin imposes profound anti-inflammatory effects exerting TLR signaling pathway inhibition. The presence of PAMPs like LPS can trigger the activation of multiple pathways which are correlated to pathogenesis of inflammatory responses (118). On the basis of the evidence which is currently available, Aquamin can exert anti-inflammatory effects in vitro. According to data that was published in the journal of Phytotherapy Research, Aquamin is shown to block TNF-a and IL-1β release in LPS-primed glial cells (278). Similarly, in a study that was carried out in RAW macrophages, Aquamin had demonstrated anti-inflammatory activity by preventing NF-kB activation (277).

Interleukin-17 (IL-17) is one of the most studied cytokines in immunology contributing to the pathogenesis of diseases associated with inflammation. The release of IL-17 and IL-17F cytokines is mainly attributed to fungal and parasitic infection, and they play key roles in tissue repair, host defense and inflammation (337). Notwithstanding the importance of IL-17 in host defense, much uncertainty still exists on whether IL-17 exerts a pathogenic rather than a protective role during infection (338). Previous research has shown that blockade of IL-17 can be an effective anti-inflammatory treatment alternative to non-steroidal anti-inflammatory drugs (NSAIDS) against the pathogenesis of inflammatory manifestations like ankylosing spondylitis or rheumatoid disease similar to anti-TNF-a treatment (339). IL-17 can also be a driver of airway pathologies such as allergic asthma (340). Lipopolysaccharide-induced systemic inflammation can trigger the release of IL-17A in rat serum (341) thus potential blockade of IL-17 by Aquamin could confer advantageous outcomes against the pathogenesis of inflammatory diseases.

A major public health concern is obesity which is a multi-factorial disorder with increasing prevalence worldwide (342). It is characterized by accumulation of excessive fat and enhances the risk for subsequent pathological events (343, 344). There is substantial amount evidence showing that the state of obesity is characterized by elevated secretion of pro-inflammatory cytokines such as IL-6 and TNF-a attributed to the high intake of macronutrients (345). Inflammation is one of the fundamental features of obesity and can be a consequence of LR family pyrine domain containing 3 (NLRP3) inflammasome activation (346). NLRP3 inflammasome belongs to a family of receptors known as Nod-like family of receptors which recognize non microbial patterns resulting in the secretion of IL-1β and IL-18 (189, 190). Previous research in macrophages has shown that simultaneous exposure of BMDMs to LPS and cholesterol crystals can lead to the activation of NLRP3 inflammasome, linking lipid metabolism and inflammation (347).

Statin compounds are the agents of choice for hypercholesterolemia states and hyperlipidemia states due to their reduction in low-density lipoprotein (LDL)|cholesterol capabilities (348). Apart from their cholesterol lowering capabilities statins exhibit immunomodulatory function demonstrating a potent anti-inflammatory action (225). Cholesterol crystals (CC) is a pathogenic stimulus that triggers the activation of NLRP3 inflammasome. Previous research in PBMCs has shown that simvastatin antagonizes LPS and cholesterol crystal–induced activation of NLRP3 inflammasome by inhibiting IL-1β release (184).

Here in this chapter, we will examine thew transcriptomic profile of murine BMDMs treated with Aquamin and LPS using next generation sequencing technology in the presence and absence of LPS and CCs. The differentially expressed genes were further analysed to provide insight into the main pathways, biological

processes and associated molecular functional changes influenced by Aquamin treatment using Gene Ontology (GO) and Kyoto Encyclopedia of Genes and Genomes (KEGG) pathway analysis platforms. These database resources provide understanding at a high-level functions and utilities of biological system. This chapter also aims to provide details about transcriptomic changes as described for Aquamin above in murine BMDMS treated with simvastatin alone and in the presence and absence of LPS and CC stimulation. These data provide a global insight into the potential anti-inflammatory mechanistic action of Aquamin in monocytes. Furthermore, we aimed to carry out a comparison of Aquamins transcriptomic effects as opposed to those of simvastatin treatment in monocytes, which yields an effective pharmacological treatment of high cholesterol driven disease states associated with cardiometabolic diseases.

4.2 Results

4.2.1 Effect of Aquamin and statin treatment on BMDMs cytokine release when stimulated with LPS and cholesterol crystals.

In a recent study performed by Boland et al., the effect of simvastatin at 50μM was examined in NRLP3 primed PBMCs which occurred by simultaneous exposure to LPS at 100ng/ml and CC at 2mg/ml (184). In the current study, RNA was extracted for global sequencing analysis from primary murine macrophages cultured from bone marrow and treated with either Aquamin (2mg/ml) or simvastatin (50uM) followed by exposure to LPS (100ng/ml) and CC (2mg/ml) for 4 h. Firstly, ELISAs were carried out to measure the concentration of TNF-a and IL-1β in cell culture supernatants under these treatments. The data revealed that treatment with Aquamin but not simvastatin reduced TNF-a release from BMDM when stimulated with LPS or LPS in the presence of CC (Fig. 4.1A). Unlike TNF-a, NLRP3 inflammasome is involved in the release of IL-1β. IL-1β levels increase in cell culture supernatants from stimulation with LPS acting as the NLRP3 priming signal and cholesterol crystals (CCs) driving secondary signals to activate caspase-1 involved in IL-1β maturation and cleavage. The release of IL-1β under LPS and CC stimulating conditions in BMDMs is reduced with both Aquamin and simvastatin treatment (Fig. 4.1B). The overall effect of Aquamin treatment in reducing TNF-a and IL-1β cytokine release from BMDM was greater compared to simvastatin at the doses tested. These data are consistent with that presented for Aquamin in results chapter 3 and previously published data for simvastatin that was carried out in PBMCs (184).

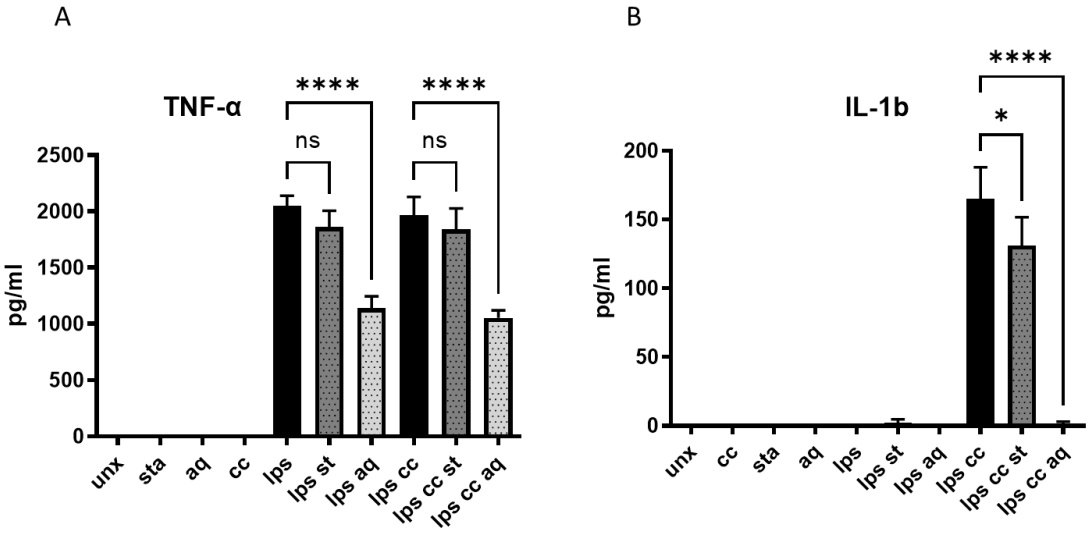

Figure 4.1. Effect of Aquamin and simvastatin treatment on the release of TNF-α and IL-1β from BMDMs exposed to LPS and CC.

BMDMs were pretreated with Aquamin at 2mg/ml and simvastatin at 50μM for 3h prior to stimulation with LPS at 100ng/ml and CC at 2mg/ml for 6h. Protein levels of (A) TNF-α and (B) IL-1β were quantified by ELISA. *Data (A-B) are expressed as mean ±sem from 3 independent experiments. ****p<0.0001; *p<0.05 vs LPS, LPS and CC stimulated controls using one-way ANOVA.*

4.2.2 Distribution of gene expression levels among samples

Upon reproducing the results that support the anti-inflammatory effect of Aquamin as suggested in Chapter 3, as well as providing evidence that our results are similar to previous evidence (184), transcriptome studies were carried out on BMDMs treated with 2mg/ml Aquamin or simvastatin at 50uM followed by LPS stimulation with and without CCs was performed. The transcriptomic studies were conducted using next generation RNA sequencing technology as described in the methods above. The RNA quality control steps revealed indices expected to advance towards a high-quality transcriptome analysis. Distribution of the total gene expression levels of each treatment is represented in the box plot graph (Fig. 4.2) The results demonstrate that BMDMs, even under different treatments have a gene population which is comparable in density and distribution. Comparison of FPKM box plots of gene expression levels of all genes for different experimental conditions revealed that sequencing results were reliable, since every sample exhibited equivalent reads and coverage depth between triplicates. Differences could be observed between treatments while biological replicates were comparable.

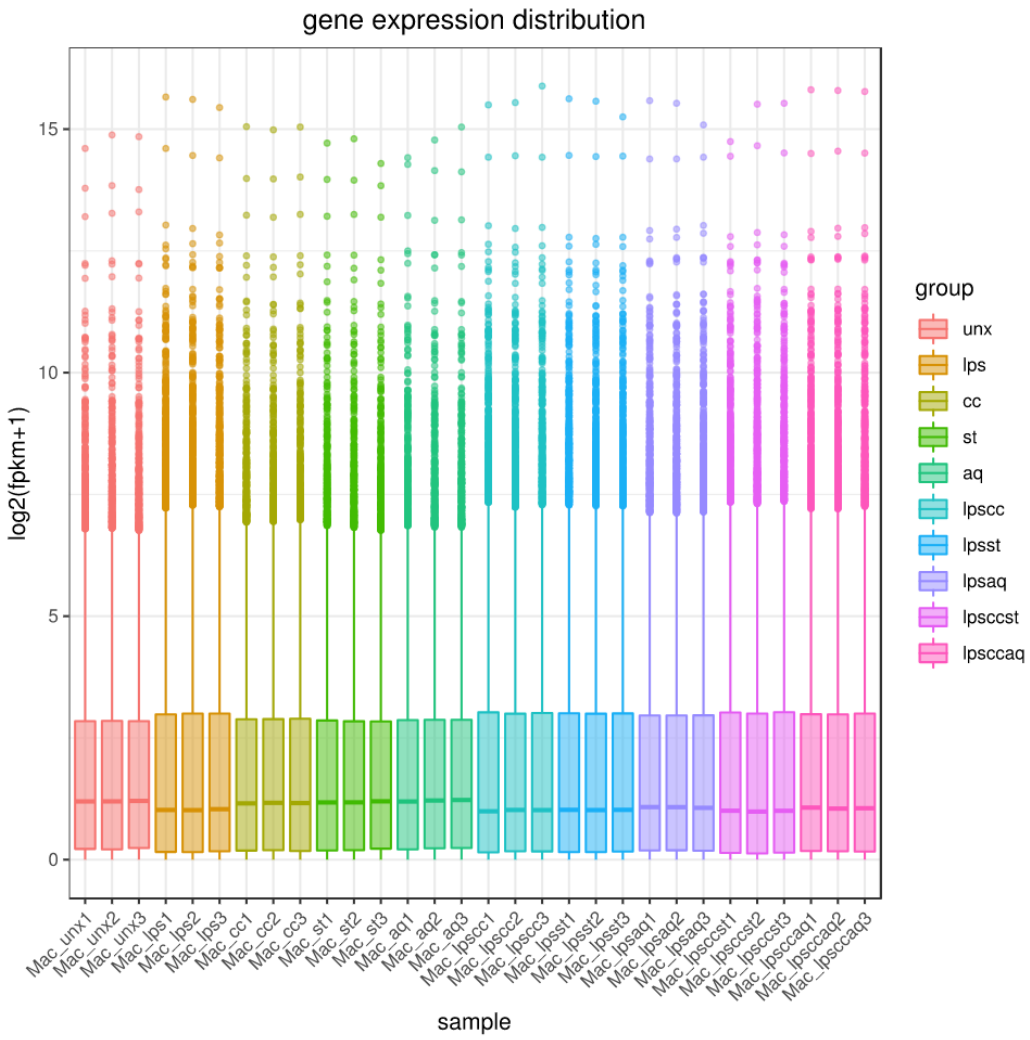

Figure 4.2. Gene expression distribution box plot across the samples in the data set.

X axis represents the name of the sample with biological replicates colour coded. Y axis indicates the log2(FPKM+1). The gene expression distribution plot demonstrates that there was high repeatability among biological replicates of the same treatment in terms of gene expression of every gene, while there is a difference in gene expression values of every gene corresponding to different treatments.

4.2.3 Pearson Correlation and principal component analysis across samples and replicates

The Pearson sample correlation represents the similarity among samples at the gene expression level. The higher the Pearson correlation value indicates greater sample similarity and a smaller number of differentially expressed genes. Figure 4.3 is the Pearson correlation heatmap across samples in the data set. The R^2 (Square of Pearson correlation coefficient(R)) value if closer to 1 and > 0.8 represents greater similarity across samples. Correlation between biological replicates (n=3) in the data set show high R^2 values approaching 1 providing confidence in the reliability and repeatability of the experimental conditions. When comparing samples with different treatments in the data set the R^2 values are less than 0.8 indicating a greater number of differentially expressed genes between these groups.

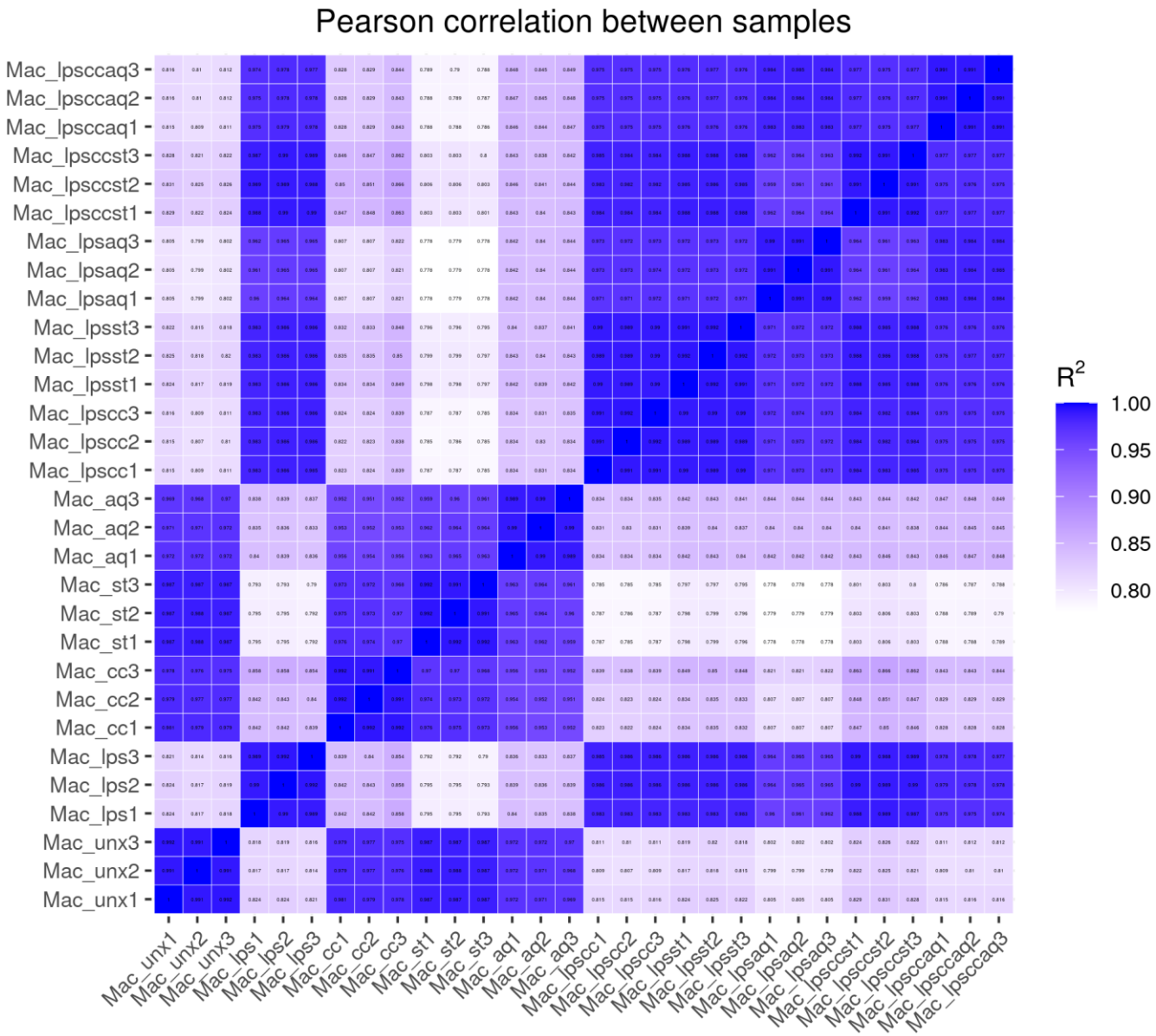

Figure 4.3. Pearson correlation between samples in the data set.

Inter-sample correlation heat map with R^2 (Square of Pearson correlation coefficient(R)) represented with colour coded key. The change of R^2 is displayed by the change of the blue colour. The deeper blue colour corresponds to a higher R^2 value and higher correlation among samples.

Similarly to Pearson correlation analysis, principal component analysis (PCA) was performed to evaluate intergroup differences and intragroup sample duplication. PCA analysis was performed on the gene expression value (FPKM) of all samples, as shown in Figure 4.4. Here the samples within the same treatment groups (biological replicates) are grouped together while the samples between treatment groups are dispersed to a greater extent. Altogether again supporting reproducibility in the biological replicates while showing clear differences in the gene expression pattern across treatment groups.

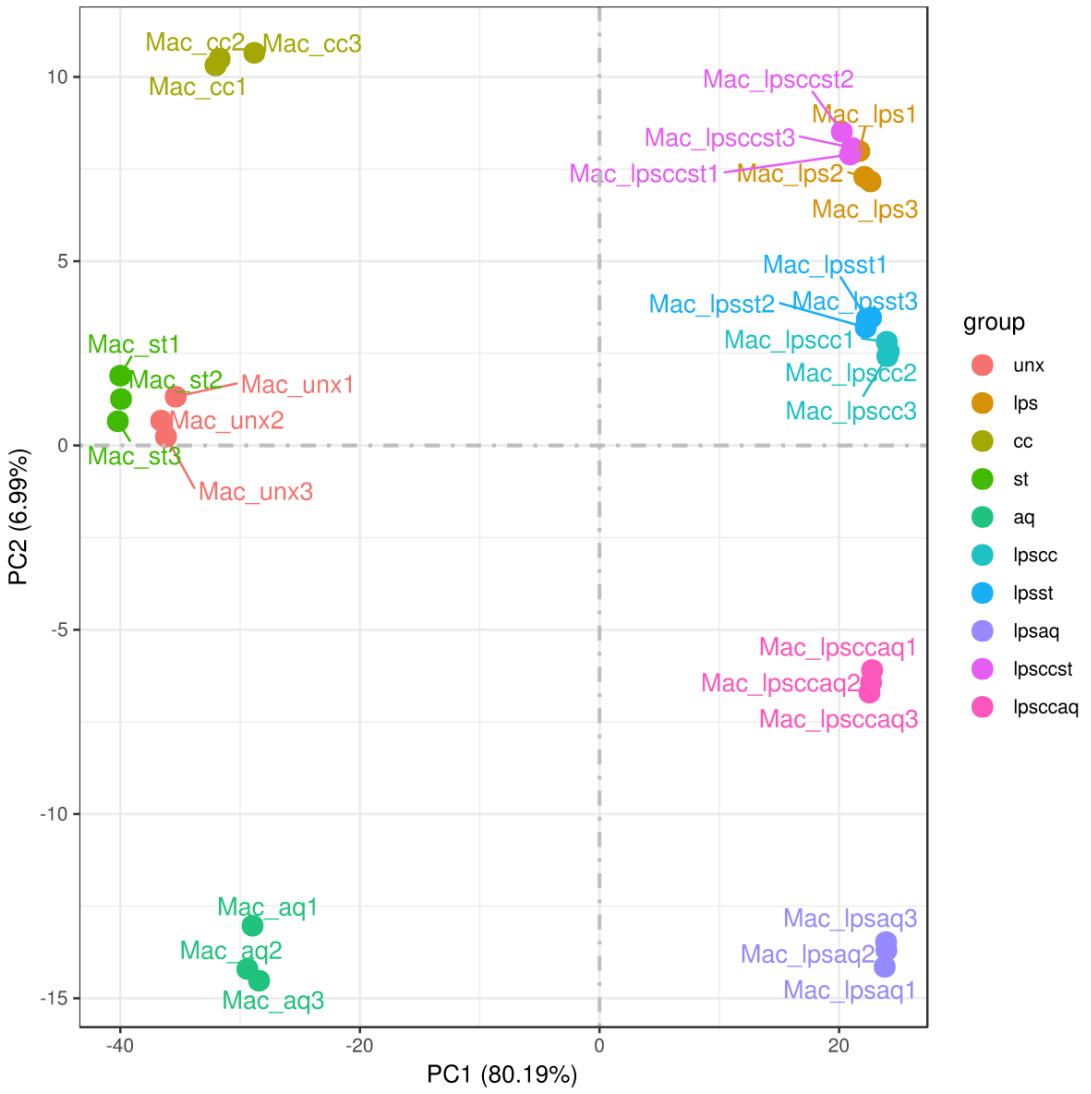

Figure 4.4. Principal component analysis

Untreated (red), LPS (orange), CC (dark green), simvastatin (green), Aquamin (light green), LPS and CC (light blue), LPS and simvastatin (blue), LPS and Aquamin (purple), LPS and CC and simvastatin (light pink), LPS and CC and Aquamin (pink) are shown. PC1 accounts for 80.19% of variance, while PC2 accounts for 6.99%. PC1 clusters untreated samples and simvastatin treatment samples together, while PC2 separates LPS stimulated samples from LPS and Aquamin treatment samples revealing that the heavily influences genes resulted from Aquamin treatment in LPS-primed samples were different than the ones expressed from LPS exposure.

4.2.4 Expression profile of genes across treatment groups

The Venn diagrams shows the number of genes that are uniquely expressed in one treatment, along with the number of co-expressed genes within 2 or more treatments in the overlapping regions (Fig. 4.5A, B). Figure 4.5A reveals that LPS stimulation of BMDMs resulted in the expression of 9,636 genes in total. Of the LPS detected genes, 9,171 are also detected when co-treated with LPS and Aquamin or LPS and simvastatin (Fig. 4.5A). Comparing LPS with LPS and Aquamin, 542 unique genes were further detected in the LPS and Aquamin group. On the other hand, comparing LPS with LPS and simvastatin 234 unique genes were further detected in the LPS and simvastatin group, more than 50% less compared to the same Aquamin comparison with LPS. Of the 234 genes unique to LPS in the presence of simvastatin 146 was also detected in LPS with Aquamin treatment. Altogether LPS and Aquamin treatment resulted in 396 unique genes while LPS and simvastatin treatment fewer genes 88 in total are unique to the simvastatin expression profile. In figure 4.5B, 9,176 genes are commonly detected when BMDMs was stimulated with LPS and CC and treated with either Aquamin or simvastatin. The addition of CC with LPS resulted in a similar number of common genes across the treatment groups as that presented in Figure 4.5A for LPS without CC stimulation which are likely to be similar also in identification. Comparing LPS CC with LPS CC and Aquamin, 307 unique genes was further detected in the LPS CC with Aquamin treatment. On the other hand, comparing LPS CC with LPS CC with simvastatin 226 unique genes was further detected in the LPS CC with simvastatin treatment. Of the 226 genes unique to LPS CC in the presence of simvastatin 134 were also detected in LPS and Aquamin treatment group. Figure 4.5C illustrates that upon comparison of genes resulted from untreated samples with Aquamin only treated genes as well as LPS-stimulated

genes led to 8893 genes that were co-expressed among those three treatments. Aquamin-treated samples displayed 233 genes that were uniquely expressed and led to expression of 351 genes that untreated samples do not express. Altogether LPS CC with Aquamin treatment resulted in 173 unique genes while LPS CC with simvastatin treatment fewer genes 92 in total are unique to the simvastatin expression profile. Overall, the presence of Aquamin produced a higher expression number (2 times) of uniquely expressed genes in LPS-stimulated BMDMs compared to Aquamin with LPS CC comparison. Interestingly Aquamin resulted in a greater number of uniquely expressed genes almost double that when compared to simvastatin. Therefore, Aquamin had a greater magnitude of effect on the overall number of genes expressed compared to simvastatin treatment under these two inflammatory conditions. These unique gene profiles across Aquamin and simvastatin treatments will be useful to investigate potential differences as well as common mechanisms of action in this cell type when comparing treatments.

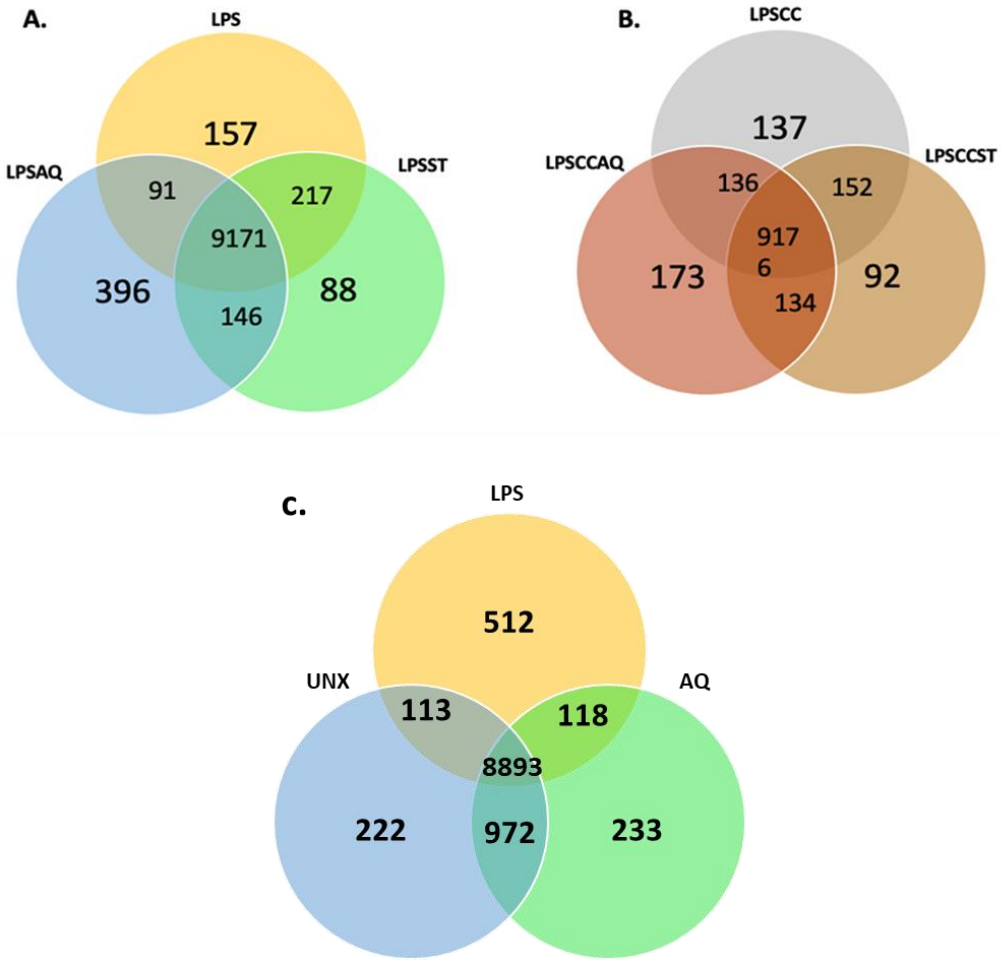

Figure 4.5: Venn diagrams representing unique and coexpression gene numbers.

Comparison of the number of genes that are uniquely expressed within each sample comparing **A)** LPS to LPS+Aquamin and LPS to LPS+Simvastatin treatment, B**)** LPSCC to LPSCC+Aquamin and LPSCC to LPSCC+Simvastatin treatment, C) LPS to Aquamin and LPS to Untreated. Overlapping regions showing the number of genes that are co-expressed in two or three of the sample treatment groups. *LPS: lipopolysaccharide, CC: cholesterol crystals, AQ: Aquamin, UNX: untreated*

4.2.5 Differential gene expression analysis

Following gene expression quantification, statistical analysis of the expression data was carried out to screen the genes whose

expression levels are significantly different across the different conditions. The differential analysis applied the DESeq2 software (349) and considers genes differentially expressed across treatment groups using the following thresholds log2(FoldChange) >= 1 and padj <= 0.05 which controls for the proportion of false positives. Figure 4.10 shows number of differential genes up or down regulated comparing LPS to LPS with Aquamin treatment (Fig. 4.6A) and LPS to LPS with simvastatin treatment (Fig. 4.6B) in BMDM. The differential analysis between LPS and LPS with Aquamin treatment revealed that 709 genes were upregulated, and 781 genes were downregulated in the LPS group (Fig. 4.6A). The differential gene expression profile between LPS and LPS with simvastatin treatment showed fewer upregulated (165) and downregulated (30) genes overall, (Fig. 4.6B). Again, DESeq2 software was used to analyze expression differences between LPS CC against LPS CC with Aquamin as well as LPS CC against LPS CC with simvastatin treatment (Fig. 4.7). In Figure 4.11A a total of 827 genes were identified as differentially regulated in the LPS CC treatment compared to LPS CC with Aquamin group. Of these 827 differentially regulated genes 277 were upregulated and 550 were downregulated in the LPS CC group. In Figure 4.7B, a total of 276 genes were identified as differentially regulated comparing LPS CC with LPS CC and simvastatin. Of these 104 upregulated genes and 172 downregulated genes were identified. Altogether Aquamin has a greater effect on the number of differentially expressed genes up or down regulated from these comparisons compared to simvastatin treatment.

To gain further insight into what the identity of these differentially regulated genes are a list of the top thirty downregulated or upregulated genes in the above comparisons are presented in Tables 4.1—4.9 and they are ranked by log2FoldChange value. As demonstrated in Table 4.1, Aquamin induced upregulation of genes

such as Ifit2 which is positively correlated with response against several viral infections (350-352). Another gene which is upregulation as a result of Aquamin treatment is Ifit3. Recent evidence has shown that Ifit3 plays a pivotal role in antiviral innate immunity (353). Altogether, the data suggests that Aquamin as a nutraceutical potentially exerts intiviral effects. Table 4.2 shows the top 10 downregulated genes in LPS compared to LPS with Aquamin treatment meaning these genes had a greater expression level in LPS with Aquamin treatment and included genes such as Txnip (-3.23-fold), Cited2 (-1.74-fold), Rtl5 (-1.96-fold), Serpine1 (-1.41-fold), Fgl2 (-1.74-fold). Table 4.3 provides a list of the top 10 upregulated genes in LPS compared to LPS with Aquamin meaning the expression of these genes was far less in LPS stimulated samples that were treated with Aquamin and include: Il1rn, Cxcl2, Ccl2, Ccl7 and Plau. These genes are associated with the promotion of inflammation indicating Aquamin reduced the expression levels of these pro inflammatory genes based on this differential gene profile comparison with LPS. When it comes to LPS versus LPS with simvastatin comparison, the overall effect on the number of differential gene expression levels was far less compared to the Aquamin effect. Simvastatin treatment in LPS stimulated BMDMs led to an upregulation of Hmgc1 (-1.31-fold), Stard4 (-1.09-fold) and other genes linked with cholesterol biosynthesis as listed in table 4.4. This is possibly due to a functional compensatory mechanism as intracellular cholesterol synthesis is blocked with simvastatin the cells respond by upregulating the expression of genes involved in lipid synthesis. For example, a well-recognized effect of statin use is the upregulation and expression of low-density lipoprotein receptor (LDLr) to increase the uptake of cholesterol from the bloodstream when intracellular cholesterol synthesis is blocked with statin use. Treatment with simvastatin induces downregulation of genes responsible for cytokine activity like Il1rn,

as well as genes relative to cancer mis regulation such as Plau, (Table 4.5). These gene data support the role associated with statins as having antiproliferative effects in different cancer cell lines as well as the anti-inflammatory pleiotropic associated effects described for statins in the literature. The gene expression results, presented in Tables 4.6-4.9, reveal that co-exposure of cells with LPS, and CC triggered the upregulation of pro-inflammatory genes such as Il1b, Il1a, Il6 and Aquamin treatment here again led to their significant downregulation. Altogether the anti-inflammatory gene expression impact of Aquamin was different compared with simvastatin treatment for both LPS and LPS CC comparisons. To better map functionally the changes in gene expression described in these tables an enrichment analysis of all the differential expressed genes, was carried out to determine which biological functions or pathways are significantly associated with the differentially expressed genes (DEG) across samples. The cluster Profiler (Yu G, 2012) software for enrichment analysis, was applied for GO and KEGG database enrichment analysis and presented in the results sections below.

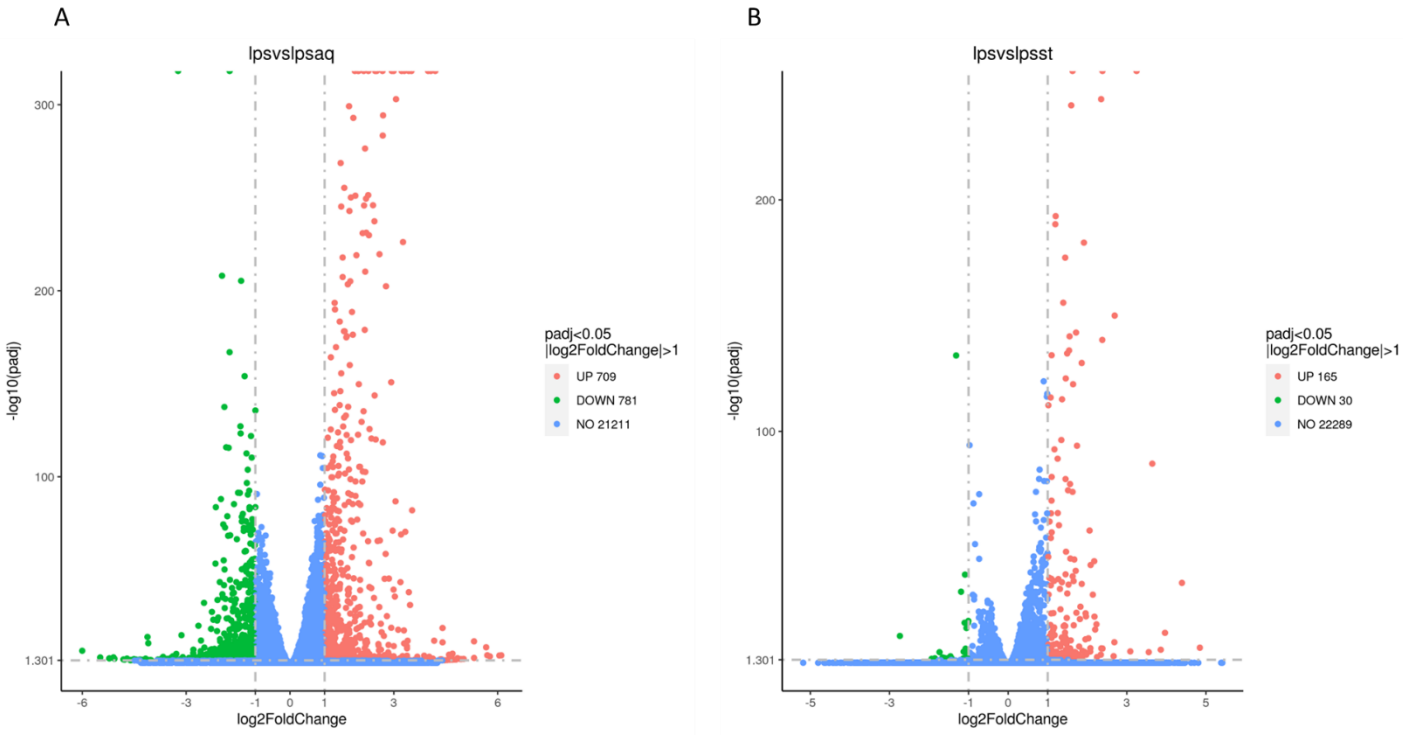

Figure 4.6. Differential Gene Volcano Maps for LPS stimulated samples against Aquamin or simvastatin.

Number of differential expressed genes up and down regulated comparing a) LPS to LPS and Aquamin treatment, b) LPS to LPS and simvastatin treatment. The x axis showing log2(FoldChange), and the y axis is -log10(padj), the blue dashed line indicates the threshold line for differential gene screening criteria.

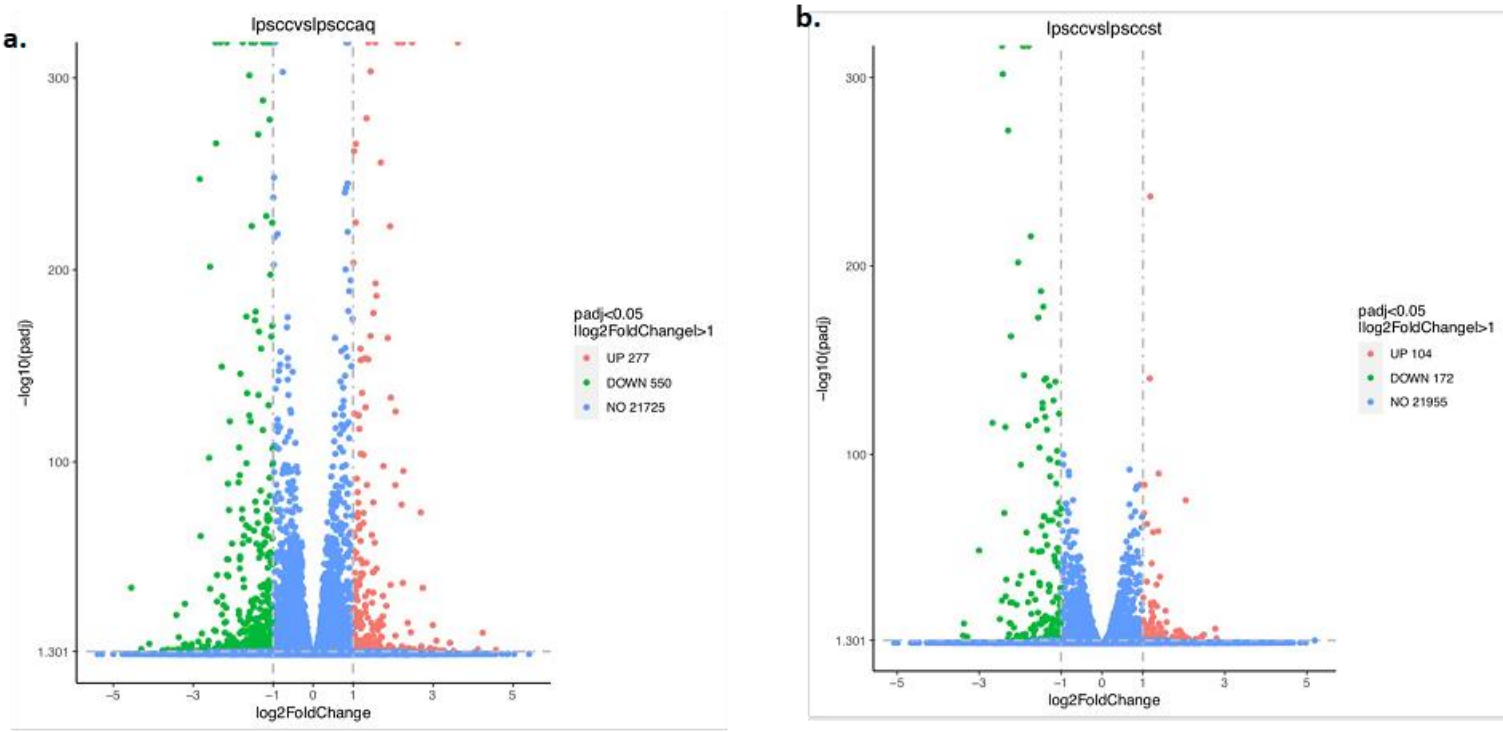

Figure 4.7. Differential Gene Volcano Maps for LPS and CC stimulated samples against Aquamin or simvastatin.

Number of differential expressed genes up and down regulated comparing a) LPSCC to LPSCC and Aquamin treatment, b) LPSCC to LPSCC and simvastatin treatment. The x axis showing log2(FoldChange), and the y axis is -log10(padj), the blue dashed line indicates the threshold line for differential gene screening criteria.

Table 4.1. Top 10 genes that were upregulated by Aquamin as a standalone treatment.

Gene ID	Unx FPKM			Aquamin FPKM			log2Fold Change	padj
Ifit2	54.11837	49.26241	51.21331	351.0377	337.4378	397.1898	2.787245	0
Ifit3	40.92783	43.84228	38.76438	175.9052	161.9534	186.9025	2.062999	8.84E-298
Ifi209	33.61083	32.32834	32.67775	117.6493	115.7829	125.9746	1.841023	0
Ccl5	94.13886	87.60177	88.26629	329.1653	293.3403	306.5819	1.758701	7.34E-270
Klf10	14.84196	13.78319	15.01116	46.09266	47.01117	46.49194	1.652038	0
Txnip	213.8316	199.6211	216.0333	641.5564	636.8687	604.6942	1.556318	0
Ddx58	10.13622	9.708792	9.461244	28.90011	28.34792	30.00344	1.549861	1.29E-267
Mndal	26.91891	25.4561	25.8924	73.66375	73.60313	74.32163	1.476793	0
Oas3	23.03071	23.24849	21.78447	60.93479	60.99876	62.77124	1.416055	4.43E-297
Samhd1	72.80718	75.55302	73.94792	176.9106	183.6297	186.6194	1.274627	0

Table 4.2. LPS versus LPS and Aquamin top 10 downregulated genes.

Gene ID	LPS CC FPKM			LPS CC & Aquamin FPKM			log2FoldChange	padj
Saa3	747.5731	770.5759	755.1614	64.59389	61.24235	60.25413	3.623267	0
Il1a	752.2314	719.2896	674.2413	128.0145	131.5381	127.1496	2.247417	0
Il6	427.3732	426.4363	384.5935	85.76028	88.55103	88.56549	2.247417	0
Il1b	2344.809	2287.256	2153.94	517.2061	521.5111	508.3313	2.144717	0
Edn1	85.43361	83.50981	80.17108	20.29149	19.31373	17.95739	2.126759	0
Hmgcs1	53.58775	51.51899	51.3672	17.64138	18.03023	17.88788	1.557912	0
Ifit1bl1	99.04994	93.67872	96.19392	36.6144	34.66747	35.84148	1.443154	3.96E-304
Mmp13	440.3671	430.546	418.0808	165.6803	173.0892	156.5787	1.391459	0
Rab11fip1	29.87217	27.15357	28.92348	11.50928	11.23949	11.51676	1.338185	1.08E-279
Ccl2	520.0648	497.8648	481.3146	240.0071	241.8541	237.4751	1.07098	2.16E-266

Table 4.3. LPS versus LPS and Aquamin top 10 upregulated genes.

Gene ID	LPS FPKM			LPS & Aquamin FPKM			log2FoldChange	padj
Rab7b	22.44918	22.98766	22.70551	1.043484	1.484592	1.241839	4.198194	0
Ccl7	233.0923	202.9431	200.362	11.74206	13.53847	13.28079	4.069453	0
Egr2	27.06039	27.65257	26.69878	1.780112	1.951916	1.462409	3.991104	0
Edn1	108.0555	98.65186	99.85322	8.467272	9.395423	9.533612	3.509381	0
Plau	234.6627	247.5856	233.5354	24.21058	21.67437	21.69374	3.430364	0
Lhfpl2	57.8081	60.31113	59.44586	6.768485	5.67102	5.874628	3.302996	0
Cxcl2	1309.902	1249.001	1242.253	127.5655	130.0543	156.3509	3.224193	0
Ccl2	702.6934	626.7732	622.7387	75.18241	80.13919	93.96418	2.994809	0
Dusp1	90.85694	85.8021	84.0043	11.12323	12.18561	11.20523	2.941385	0
Il1a	672.197	605.5971	623.5957	94.86761	99.47236	109.3093	2.671983	0

Table 4.4. LPS versus LPS and simvastatin top 10 downregulated genes.

Gene ID	LPS FPKM			LPS & simvastatin FPKM			log2Fold Change	padj
Hmgcs1	20.87017	19.10439	19.58033	50.8054	47.26577	49.54279	-1.31513	1.62E-133
Stard4	3.454202	3.800013	4.071293	8.214024	7.944854	7.934317	-1.09149	7.76E-39
Lss	1.012234	0.991353	1.105573	2.34349	2.406252	2.329478	-1.19087	2.02E-31
Ednrb	2.655955	2.988507	2.506603	5.909511	5.335355	5.094326	-1.00727	8.29E-19
Klf2	3.988396	4.016333	3.77067	8.605712	7.909333	8.648886	-1.10144	5.19E-18
Tmem184c	3.268347	3.479036	3.440352	6.4858	6.706086	7.362951	-1.01761	5.86E-18
Mab21l3	2.206334	1.868085	1.929204	4.038461	4.127981	4.220581	-1.05338	9.86E-16
Fdps	0.071091	0.144998	0.087878	0.773558	0.689673	0.575397	-2.73745	2.54E-12
Sel1l3	0.315094	0.273859	0.244026	0.57305	0.542921	0.629525	-1.07801	8.23E-07
Cdkn2b	1.264393	1.709628	1.26368	3.288517	3.09662	2.846556	-1.12493	1.57E-05

Table 4.5. LPS versus LPS and simvastatin top 10 upregulated genes.

Gene ID	LPS FPKM			LPS & simvastatin FPKM			log2FoldChange	padj
Egr2	27.06039	27.65257	26.69878	2.557946	2.69657	3.25865	3.247457	0
Plau	234.6627	247.5856	233.5354	45.80636	45.40646	45.33321	2.38523	0
Rab7b	22.44918	22.98766	22.70551	4.755508	4.005523	4.55304	2.35111	2.92E-244
Hbegf	58.88766	59.63894	55.6455	14.18435	15.04683	16.68633	1.916636	2.82E-182
Lhfpl2	57.8081	60.31113	59.44586	19.13139	18.697	19.45706	1.627102	0
Abcg1	57.02867	57.75019	57.51672	19.46076	18.88653	18.50384	1.595117	1.33E-241
Lrrc32	39.34	39.60729	38.67125	14.22688	14.00879	14.87093	1.442649	8.74E-176
Dusp1	90.85694	85.8021	84.0043	33.91005	31.77409	33.18446	1.393432	2.52E-156
Il1rn	343.7454	328.3561	338.4755	148.4014	140.861	148.3961	1.202329	1.02E-193
Sgk1	122.9578	119.1001	119.0657	53.27497	51.78229	52.26218	1.193788	3.16E-190

Table 4.6. LPS and CC versus LPS and CC with Aquamin top 10 downregulated genes.

Gene ID	LPS CC FPKM			LPS CC & Aquamin FPKM			log2Fold Change	padj
Atf3	392.1307	394.8739	391.4877	844.6614	808.8389	781.2338	-1.03503	0
Irf8	105.5384	100.2531	103.5479	271.9569	290.505	292.9133	-1.45596	0
Plau	39.93226	39.394	40.8589	191.0785	178.5074	170.3432	-2.15531	0
Plk2	87.50739	85.37861	83.81148	214.7504	201.4235	196.751	-1.24393	0
Sgk1	36.78395	38.30345	38.89795	119.3685	110.1196	105.7123	-1.54394	0
Furin	34.47999	33.09822	34.97199	76.44205	75.79219	75.34222	-1.13826	0
Pcyt1a	12.2616	12.63211	13.05214	36.81455	35.71985	34.70603	-1.4863	0
Tent5c	12.65838	12.05354	12.62133	45.96037	41.03909	40.34065	-1.75801	0
Rcan1	12.69417	12.15443	12.1522	72.09419	65.44857	63.87644	-2.43291	0
Hbegf	16.17658	16.77118	16.89049	84.4012	83.48872	81.0137	-2.30778	0

Table 4.7. LPS and CC versus LPS and CC with Aquamin top 10 upregulated genes.

Gene ID	LPS CC FPKM			LPS CC & Aquamin FPKM			log2FoldChange	padj
Saa3	747.5731	770.5759	755.1614	64.59389	61.24235	60.25413	3.623267	0
Il1a	752.2314	719.2896	674.2413	128.0145	131.5381	127.1496	2.247417	0
Il6	427.3732	426.4363	384.5935	85.76028	88.55103	88.56549	2.247417	0
Il1b	2344.809	2287.256	2153.94	517.2061	521.5111	508.3313	2.144717	0
Edn1	85.43361	83.50981	80.17108	20.29149	19.31373	17.95739	2.126759	0
Hmgcs1	53.58775	51.51899	51.3672	17.64138	18.03023	17.88788	1.557912	0
Ifit1bl1	99.04994	93.67872	96.19392	36.6144	34.66747	35.84148	1.443154	3.96E-304
Mmp13	440.3671	430.546	418.0808	165.6803	173.0892	156.5787	1.391459	0
Rab11fip1	29.87217	27.15357	28.92348	11.50928	11.23949	11.51676	1.338185	1.08E-279
Ccl2	520.0648	497.8648	481.3146	240.0071	241.8541	237.4751	1.07098	2.16E-266

Table 4.8. LPS and CC versus LPS and CC with simvastatin top 10 downregulated genes.

Gene ID	LPS CC FPKM			LPS CC & simvastatin FPKM			log2Fc Chang
Plau	39.93226	39.394	40.8589	211.4995	225.5015	207.4617	-2
Lhfpl2	10.39596	11.37718	12.95579	65.2977	58.51152	60.83938	-2
Gdf15	35.29102	35.8326	37.97302	161.6543	197.0181	171.5885	-2
Rab7b	4.733422	4.604138	4.623816	18.85884	19.97034	18.39899	-2
Sgk1	36.78395	38.30345	38.89795	141.8725	147.6041	141.6165	-1
Plk2	87.50739	85.37861	83.81148	306.6183	327.5921	318.7225	-1
Tent5c	12.65838	12.05354	12.62133	43.31594	41.32948	43.26413	-1
Hbegf	16.17658	16.77118	16.89049	53.90921	55.51503	55.66368	-1
Hmox1	414.3817	383.8325	388.3298	1039.55	1196.626	1070.328	-1
Fnip2	18.24549	16.95771	18.16139	49.63196	44.59536	48.53957	-1

Table 4.9. LPS and CC versus LPS and CC with simvastatin top 10 upregulated genes.

Gene ID	LPS CC FPKM			LPS CC & simvastatin FPKM			log2Fold Change	padj
Gfi1	8.547639	9.077336	9.203627	2.040456	2.035518	2.375239	2.042457	2.43E-76
Pou2f2	8.513186	8.434627	8.499451	3.431516	3.090822	3.145411	1.386205	1.35E-90
Ch25h	34.84515	33.57642	31.304	11.95034	13.10056	13.05348	1.376324	5.93E-60
Cebpd	16.04539	14.73725	14.98431	6.166004	6.869015	6.02965	1.253796	1.74E-59
Saa3	747.5731	770.5759	755.1614	329.5524	339.133	326.8772	1.180828	1.35E-237
Hmgcs1	53.58775	51.51899	51.3672	23.68495	22.23074	23.00883	1.17206	5.17E-141
Rasgrp1	13.30678	12.44972	13.47326	6.174233	5.966873	6.014535	1.101121	8.71E-64
Slc28a2	51.0774	49.57506	48.44373	25.16511	22.2891	24.50037	1.040062	1.54E-84
Gpr85	24.88145	24.74782	24.81916	11.9843	11.5745	12.70779	1.026055	2.06E-69
Shisa3	35.0682	34.02383	34.40555	16.36979	16.83231	17.96033	1.00505	2.30E-84

4.2.6 Functional enrichment analysis of differentially expressed genes (DEGs) downregulated with Aquamin treatment- compared to untreated BMDM

Having demonstrated the most prominent upregulated and downregulated DEGs resulted from each treatment, we aimed to gain better comprehension of the relative pathways associated with Aquamin treatment. Gene Ontology (GO) enrichment analysis was used to categorize the downregulated genes in the presence of Aquamin compared to untreated cell samples, according to biological processes (BP) (red), molecular functions (MF) (blue), and cellular components (green) (Fig. 4.8A). The GO enrichment histogram (Fig. 4.8A) and dot plot (Fig. 4.8B) display an enrichment of 10 terms in the BP category associated with genes downregulated under Aquamin treatment namely neutrophil migration (p = 1.30E-06), positive regulation of neutrophil migration (p = 1.30E-06), positive migration of neutrophil chemotaxis (p = 3.70E-06), positive regulation of granulocyte chemotaxis (p = 4.26E-06), regulation of neutrophil migration (p = 4.26E-06), granulocyte migration (p = 4.95E-06), neutrophil chemotaxis (p = 4.95E-06), regulation of neutrophil chemotaxis (p = 8.03E-06), regulation of granulocyte chemotaxis (p =1.51E-05), and positive regulation of response to external stimulus (p = 3.25E-05). With respect to molecular function the enriched categories associated with downregulated genes in the Aquamin treated samples versus untreated controls, include cytokine activity (p = 0.00047), chemokine activity (p = 0.00142), CXCR chemokine receptor binding (p = 0.003), chemokine receptor binding (p = 0.0047), receptor regulator activity (p = 0.016), receptor ligand activity (p = 0.02), and cytokine receptor binding (p = 0.03).

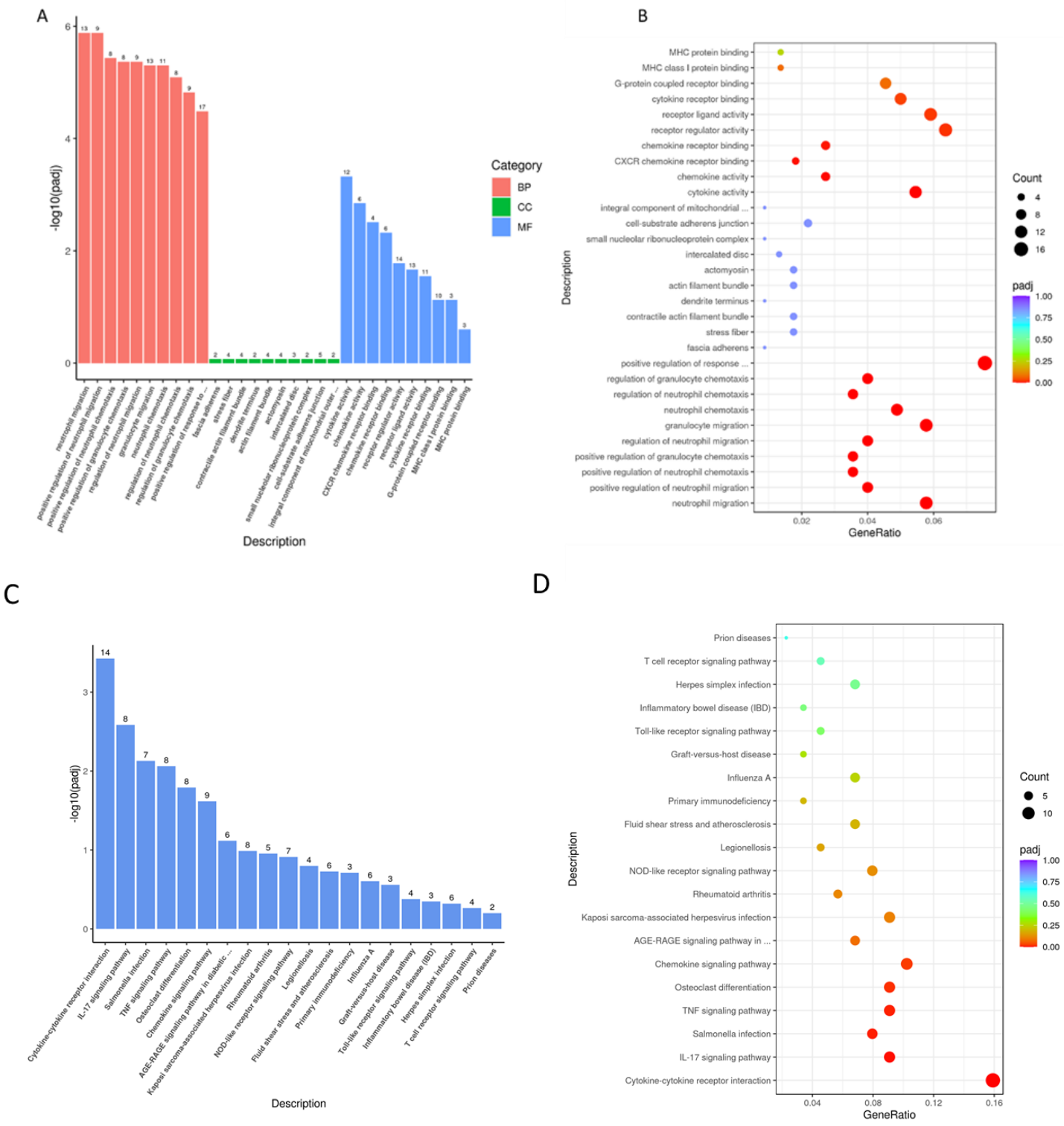

Figure 4.12. Enrichment analysis of all the differentially expressed genes downregulated with Aquamin intervention compared to untreated control samples.

(A) Gene Ontology (GO) histogram enrichment analysis (C) KEGG enrichment analysis histogram of all differentially expressed genes

downregulated with Aquamin treatment versus untreated samples. GO (A) and KEGG (C) Term's on horizontal axis shows level of significance of enrichment expressed as -log10(padj) on vertical axis. Numbers on bars represent number of associated genes. Colours represent different functional categories for (A) GO biological process (BP) red, cellular component (CC) green, and molecular function (MF) blue. GO (B) and KEGG (D) enrichment scatter plots showing the ratio of the differential gene number to the total number of differential genes in the GO or KEGG Term. (B, D) The size and the colour of points in the scatter plots represents the number of target proteins and the padj value respectively.

Differential genes down regulated with Aquamin treatment versus unstimulated cells were also analyzed in the KEGG pathway enrichment database (Fig. 4.8C, D). These down regulated genes mapped to 173 pathways in KEGG and the 20 most significant KEGG pathways were selected for display. The pathways include cytokine-cytokine receptor interaction ($p = 0.00037$), IL-17 signaling pathway ($p = 0.0026$), Salmonella infection ($p = 0.007$), TNF-a signaling pathway ($p = 0.0087$), Osteoclast differentiation ($p = 0.016$), and Chemokine signaling pathway ($p = 0.02$) as the most significant. Lower levels of enriched pathways were also seen in Toll-like receptor signaling pathways and in inflammation associated disorders such as Rheumatoid arthritis and Inflammatory bowel disease (IBD). Altogether the differentially expressed downregulated genes with Aquamin treatment versus untreated control BMDM cells is associated with several inflammatory pathways and terms from GO and KEGG functional enrichment analysis. A panel of genes from the most enriched functional pathways downregulated with Aquamin treatment versus controls is presented in Figure 4.9. Here the FPKM expression level of selected genes primarily associated with proinflammatory states was taken from the sequencing data set and column statistics applied to display the level of significance of individual downregulated genes with Aquamin treatment compared to unstimulated control cells.

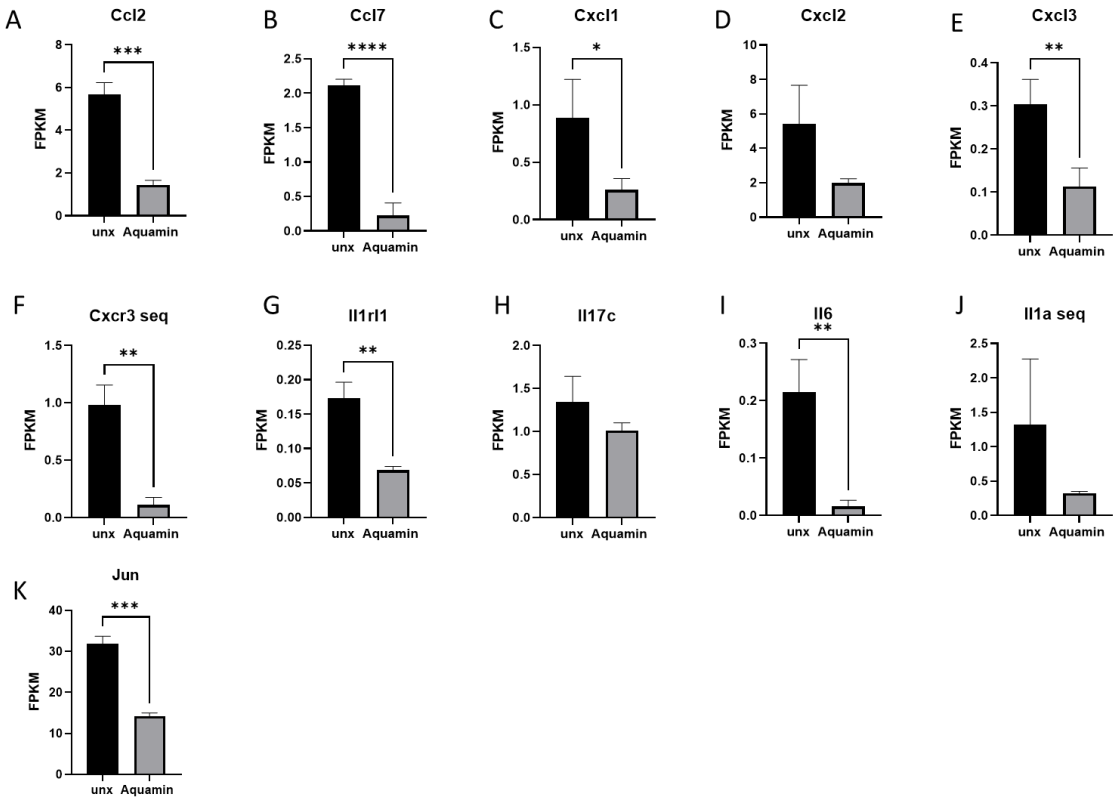

Figure 4.9. Panel of genes from the most enriched functional pathways downregulated with Aquamin treatment versus controls.

FPKM indicates the expression level of each gene from the sequencing data, The identified genes include (A) Ccl2, (B) Ccl7, (C) Cxcl1, (D) Cxcl2, (E) Cxcl3, (F) Cxcr3, (G) Il1rl1, (H) Il17c, (I) Il6, (J) Il1a, (K) Jun. *Data (A-K) are expressed as mean ±sem from 3 independent experiments. ****p<0.0001, **p<0.01; p<0.05 vs unx control using t test.*

4.2.7 Functional enrichment analysis of differentially expressed genes (DEGs) upregulated with Aquamin treatment- compared to untreated BMDM.

The GO enrichment analysis of genes was also examined (Fig. 4.10 A, B) to identified BP and MF associated pathways that were upregulated with Aquamin treatment compared to untreated cells. With BP, the ten most significantly enriched terms were defense response to virus (p = 1.76E-25), response to virus (p = 3.83E-22), defense response to other organism (p = 5.40E-21), response to interferon-beta (p = 2.67E-16), cellular response to interferon-beta (p = 1.10E-12), positive regulation of cytokine production (p = 3.70E-08), regulation of defense response (p = 1.63E-07), regulation of innate immune response (p = 3.33E-06), negative regulation of viral genome replication (p = 5.66E-06), and positive regulation of innate immune response (p = 1.27E-05). With respect to the MF category the most enriched categories were core promoter binding (p = 0.003426), RNA polymerase II proximal promoter sequence-specific DNA binding (p = 0.016209), proximal promoter sequence-specific DNA binding (p = 0.016209), double-stranded RNA binding (p = 0.027303), 2'-5'-oligoadenylate synthetase activity (p = 0.027303), cytokine activity (p = 0.038596), transcription factor activity, RNA polymerase II proximal promoter sequence-specific DNA binding (p = 0.038596), peptide receptor activity (p = 0.038596), antigen binding (p = 0.049891), transcriptional repressor activity, and RNA polymerase II proximal promoter sequence-specific DNA binding (p = 0.049891).

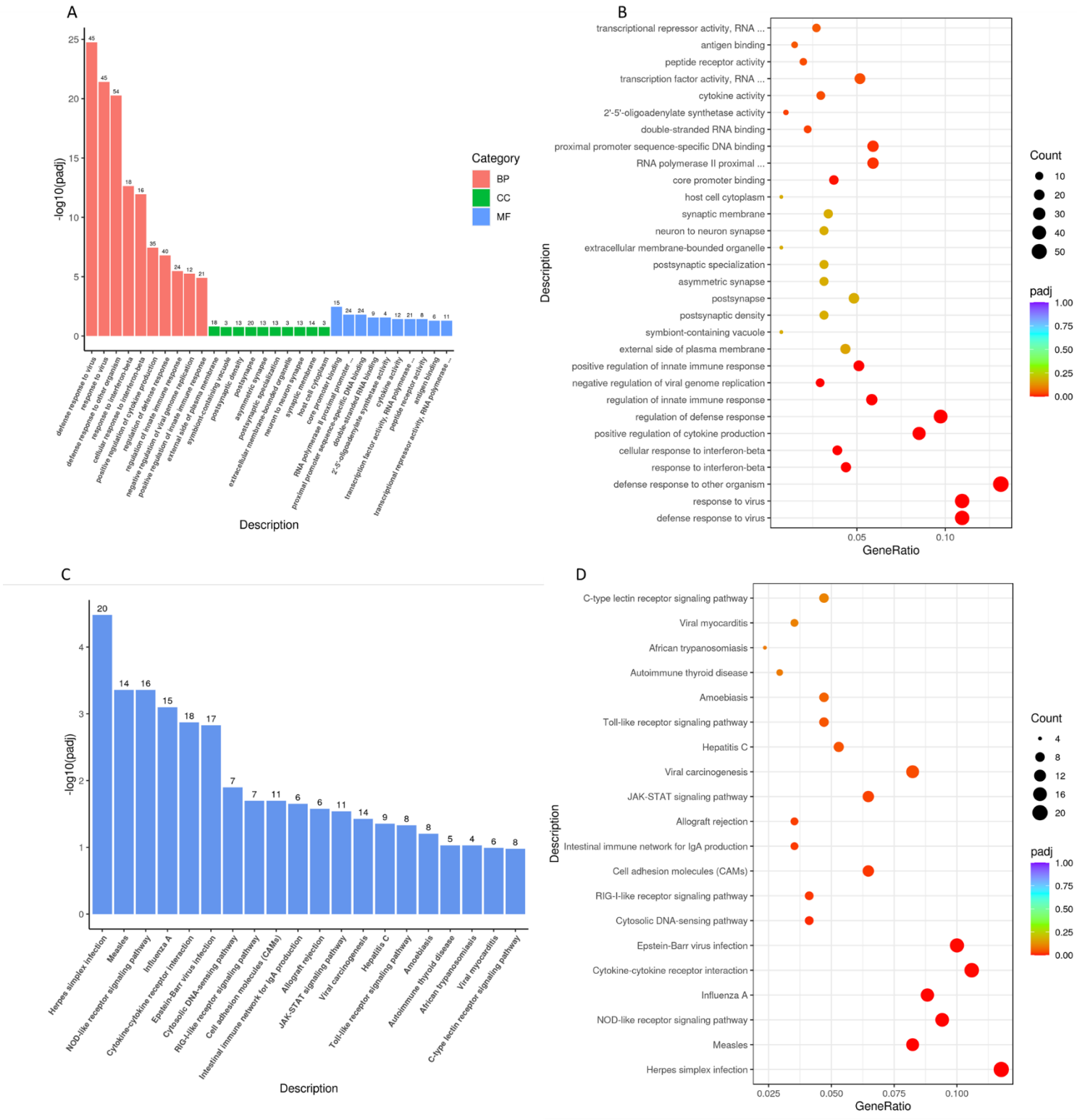

Figure 4.10. Enrichment analysis of all the differentially expressed genes upregulated with Aquamin intervention compared to untreated control samples.

(A) Gene Ontology (GO) histogram enrichment analysis (C) KEGG enrichment analysis histogram of all differentially expressed genes

upregulated by Aquamin treatment versus untreated samples. GO and KEGG Term's on horizontal axis shows level of significance of enrichment expressed as -log10(padj) on vertical axis. Numbers on bars represent number of associated genes. Colours in (A) represent different functional categories for GO, biological process (BP) red, cellular component (CC) green, and molecular function (MF) blue. GO (B) and KEGG (D) enrichment scatter plots showing the ratio of the differential gene number to the total number of differential genes in the GO or KEGG Term. (B, D) The size and the colour of points in the scatter plots represents the number of target proteins and the padj value respectively.

In parallel to the downregulation of genes described above for Aquamin, using the GO pathway analysis, the most enriched pathways associated with Aquamin-induced upregulation of genes compared to the untreated samples are also displayed using KEGG pathway analysis (Fig. 4.10 C, D). The KEGG bars shown an increase in the expression of viral infection associated pathways such as Herpes simplex infection (p = 3.30E-05), NOD-like receptor signaling pathway (p = 0.000438) which is cytoplasmic and yields a crucial role for the innate immune response, Influenza A (p = 0.000794), Cytokine-cytokine receptor interaction (p = 0.00134), Epstein-Barr virus infection (p = 0.001486), are five of the most significantly enriched pathways in the presence of Aquamin. In depth analysis of the corresponding enriched pathways revealed some prominent genes that were upregulated by Aquamin and associated with viral defense mechanisms in these cells. Bar graphs of a panel of genes from the most enriched pathways along with column statistics is shown in (Fig. 4.11) which displays the level of significance of these individual upregulated genes with Aquamin treatment compared to unstimulated control cells.

From the results presented in the previous section it is evident that Aquamin modulates by reducing inflammatory signaling pathways such as TLR, NLR and IL-17 as well as effects on cytokines, chemokines and receptors which are induced by pro inflammatory stimuli. Examples of those genes are Cxcl2, Ccl2, Il6, Il1b, Il17c and presented in Figure 4.9. Treatment with Aquamin also revealed concurrently it can upregulate genes correlated to antiviral responses such as Oas3, Stat1 and Stat2 (Figure 4.11). These data provide evidence altogether for Aquamin's potential to dampen down pro inflammatory responses while preserving antiviral and protective mechanisms in the fight against invading pathogens.

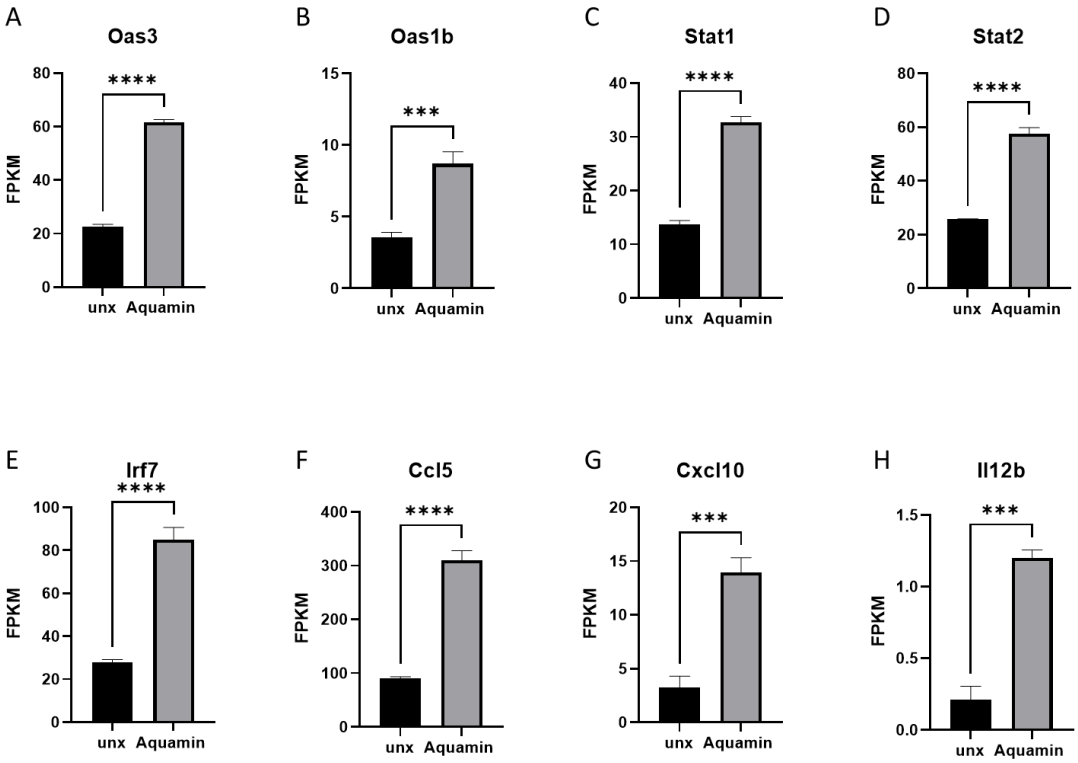

Figure 4.11. Panel of genes from the most enriched functional pathways upregulated under Aquamin treatment versus controls.

FPKM indicates the expression of every gene. The identified genes include (A) Oas3, (B) Oas1b, (C) Stat1, (D) Stat2, (E) Irf7, (F) Ccl5, (G) Cxcl10, (H) Il12b. *Data (A-H) are expressed as mean ±sem from 3 independent experiments. ****p<0.0001; p<0.05 vs unx control using t test.*

4.2.8 Functional enrichment analysis of differentially expressed genes (DEGs) upregulated with LPS treatment- compared to untreated BMDM

Transcriptomic analysis of Aquamin-treated BMDMs under LPS stimulation at 100ng/ml was also conducted. Initially GO and KEGG enrichment analysis of LPS responsive genes was carried out (Fig. 4.12). GO enrichment analysis of LPS induced genes revealed enrichment of 7119 genes of which 1214 were significantly enriched compared to untreated cells. The results are in accordance with previous evidence supporting the induced LPS genes in this data set are mapped to cytokine and chemokine pathways from GO functional pathway analysis (Fig. 4.12 A, B) as expected. KEGG enrichment analysis of upregulated DEGs also derived from LPS stimulated BMDMs were mapped to pathways such as TNF signaling as well as the enrichment of viral infection responsive genes associated with pathways such as Influenza A, Herpes simplex infection and Epstein Barr virus infection. Enrichment of inflammation associated pathways such as NOD-like receptor signaling pathways and cytokine-cytokine receptor interaction was also obtained from the KEGG enrichment analysis of LPS upregulated genes compared to untreated BMDM (Fig 4.12 C, D). These expected results for LPS driving the expression of proinflammatory genes provides confidence in the reliability of the results obtained particularly in looking for gene expression patterns with Aquamin.

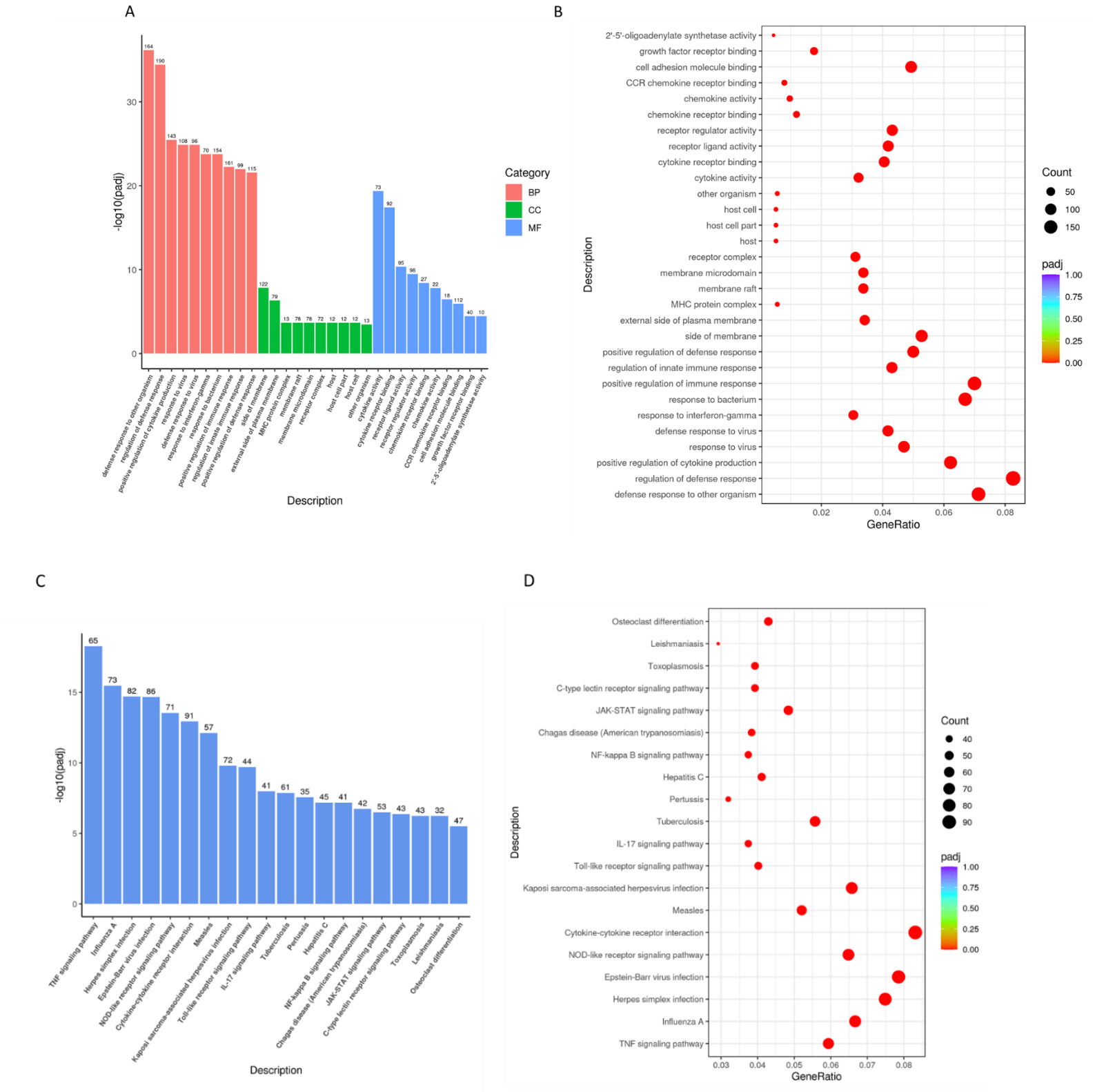
A
-log10(padj)
Description
Category
BP
CC
MF
B
Description
GeneRatio
Count
padj
C
-log10(padj)
Description
D
Description
GeneRatio
Count
padj

Figure 4.12. Enrichment analysis of all the differentially expressed genes upregulated with LPS stimulation compared to untreated control samples.

(A) Gene Ontology (GO) histogram enrichment analysis (C) KEGG enrichment analysis histogram of all differentially expressed genes upregulated by LPS stimulation versus untreated samples. GO and KEGG Term's on horizontal axis shows level of significance of enrichment expressed as -log10(padj) on vertical axis. Numbers on bars represent number of associated genes. Colours represent different functional categories for GO, (A) Biological Process (BP) red, cellular component (CC) green, and molecular function(MF) blue. GO (B) and KEGG (D) enrichment scatter plots showing the ratio of the differential gene number to the total number of differential genes in the GO or KEGG Term. (B, D) The size and the colour of points in the scatter plots represents the number of target proteins and the padj value respectively.

4.2.9 Functional enrichment analysis of differentially expressed genes (DEGs) downregulated with Aquamin treatment- compared to LPS-stimulated BMDM

To gain an insight into the biological roles of the most significantly downregulated genes regarding the comparison of LPS versus LPS with Aquamin, GO enrichment analysis was conducted. As shown in Fig. 4.13A and Fig. 4.13B, the ten most significantly enriched terms with respect to DEGs that were downregulated by Aquamin treatment compared to LPS stimulated controls in the BP category were positive regulation of cellular component movement (p = 2.15E-10), positive regulation of locomotion (p = 3.47E-10), positive regulation of cell motility (p = 3.47E-10), positive regulation of cell migration (p = 3.47E-10), cell chemotaxis (p = 1.80E-9), leukocyte chemotaxis (p = 3.30E-09), myeloid leukocyte migration (p = 6.78E-09), granulocyte migration (p = 2.24E-08), leukocyte migration (p = 3.23E-08), and positive regulation of response to external stimulus (p = 9.67E-08). In the MF category, cytokine receptor binding (p = 1.25E-07), cytokine activity (p = 1.77E-07), receptor ligand activity (p = 1.77E-07), receptor regulator activity (p = 9.83E-07), G-protein coupled receptor activity (p = 1.26E-06), chemokine activity (p = 3.92E-05), chemokine receptor binding (p = 5.36E-05), chemokine binding (p = 0.000487), G-protein coupled chemoattractant receptor activity (p = 0.000566), and chemokine receptor activity (p = 0.000566) were significantly enriched. Altogether here mapped genes downregulated with Aquamin treatment in LPS stimulated BMDM were mainly associated with pro-inflammatory pathways.

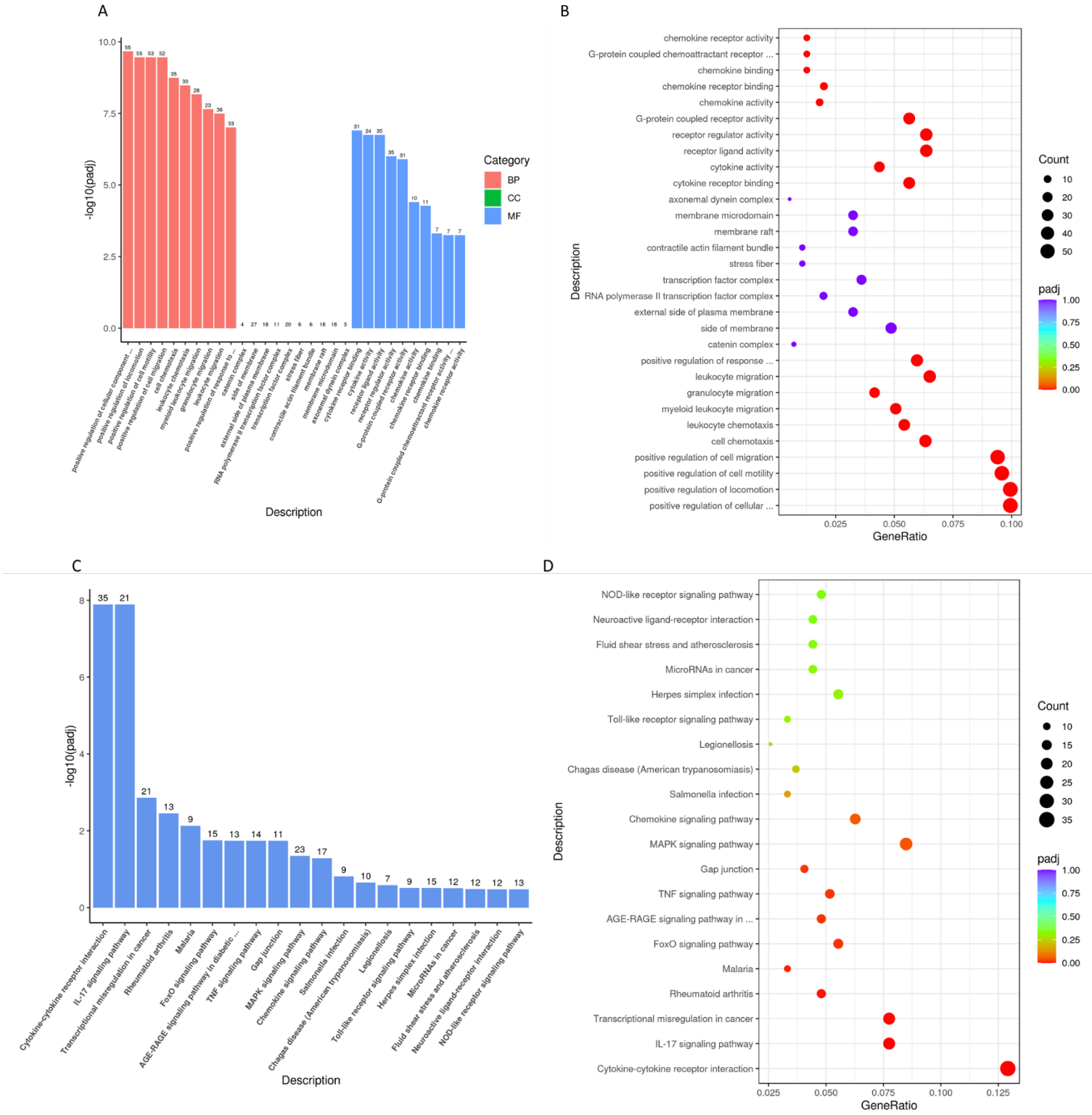

Figure 4.13. Enrichment analysis of all the differentially expressed genes downregulated with LPS Aquamin intervention compared to LPS.

(A) Gene Ontology (GO) histogram enrichment analysis (C) KEGG enrichment analysis histogram of all differentially expressed genes downregulated with LPS Aquamin treatment versus LPS. GO and KEGG

Term's on horizontal axis shows level of significance of enrichment expressed as -log10(padj) on vertical axis. Numbers on bars represent number of associated genes. Colours represent different functional categories for GO, (A) Biological Process (BP) red, cellular component (CC) green, and molecular function (MF) blue. GO (B) and KEGG (D) enrichment scatter plots showing the ratio of the differential gene number to the total number of differential genes in the GO or KEGG Term. (B, D) The size and the colour of points in the scatter plots represents the number of target proteins and the padj value respectively.

Functional enrichment of the downregulated DEG under LPS Aquamin treatment versus LPS in BMDM was carried out using KEGG functional analysis (Fig. 4.13 C, D). KEGG analysis here revealed that 253 KEGG pathways were enriched of which 10 were significantly enriched ($p < 0.05$). The significantly enriched pathways of LPS treated BMDMs that were downregulated by Aquamin intervention were Cytokine-cytokine receptor interaction ($p = 1.27E-08$), IL-17 signaling pathway ($p = 1.27E-08$), Transcriptional misregulation in cancer ($p = 0.0014$), Rheumatoid arthritis ($p = 0.0035$), Malaria ($p = 0.0073$), FoxO signaling pathway ($p = 0.017$), AGE-RAGE signaling pathway in diabetic complications ($p = 0.018$), TNF signaling pathway ($p = 0.018$), Gap junction ($p = 0.018$), and MAPK signaling pathway ($p = 0.045$). Key genes of the most enriched pathways from figure 4.13) were identified and illustrated in column graphs (Fig. 4.14) to provide additional evidence for the anti-inflammatory impact of Aquamin in vitro in relation to individual genes.

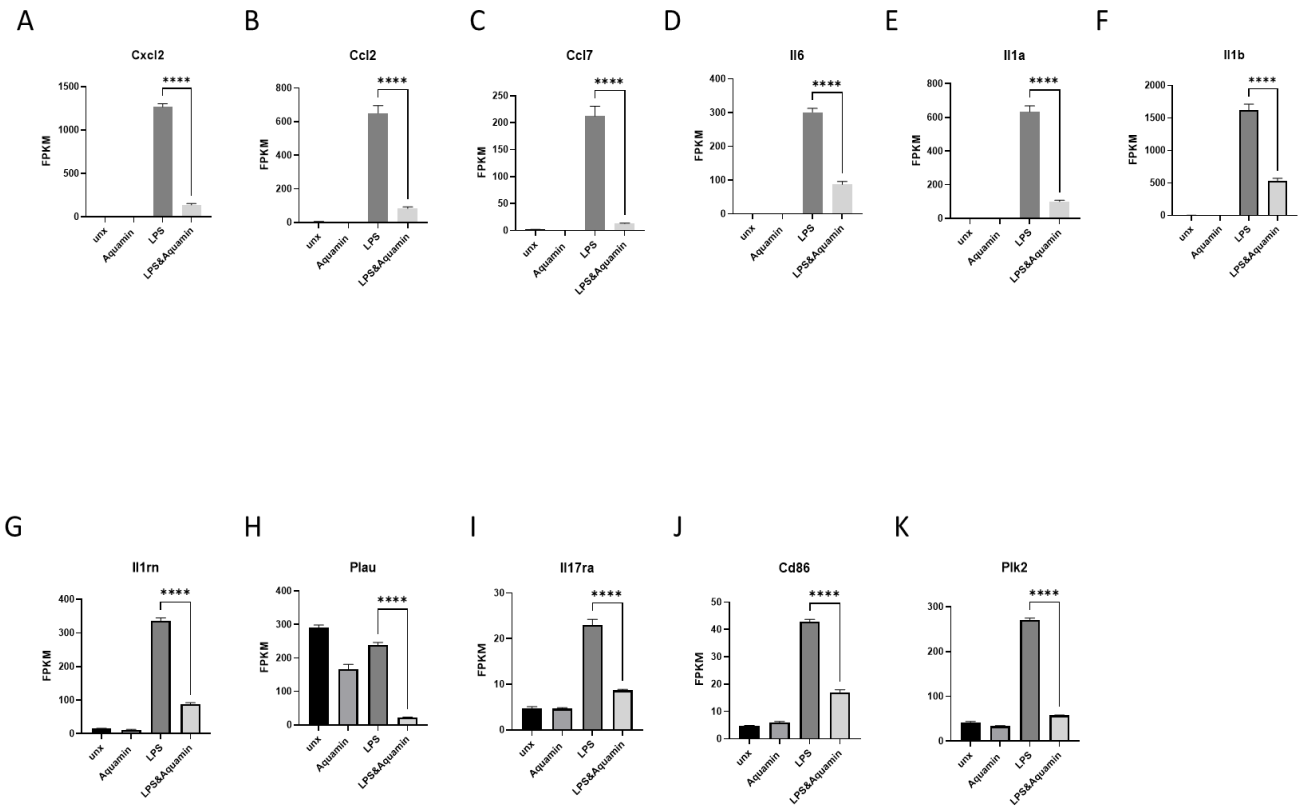

Figure 4.14. Panel of genes from the most enriched functional pathways downregulated by Aquamin treatment compared to LPS in BMDM.

FPKM indicates the expression of every gene. The identified genes include (A) Cxcl2, (B) Ccl2, (C) Ccl7, (D) Il6, (E) Il1a, (F) Il1b, (G) Il1rn, (H) Plau, (I) Il17ra, (J) Cd86, (K) Plk2. *Data (A-H) are expressed as mean ±sem from 3 independent experiments. ****p<0.0001; p<0.05 vs LPS stimulated control using 1 way ANOVA.*

4.2.10 Functional enrichment analysis of differentially expressed genes (DEGs) downregulated with simvastatin treatment- compared to LPS stimulated BMDM

GO enrichment analysis was conducted to provide a list of the ten most enriched BP, CC and MF as a result of the DEGs that were downregulated by simvastatin treatment compared to LPS stimulated BMDMs (Fig. 4.15 A, B). In the category of BP, the most enriched terms were blood vessel morphogenesis (p = 2.59E-08), angiogenesis (p = 2.59E-08), regulation of vasculature development (p = 2.92E-08), regulation of angiogenesis (p = 5.30E-07), leukocyte differentiation, (p = 7.76E-07), positive regulation of vasculature development (p = 1.46E-05), positive regulation of cellular component movement (p = 1.59E-05), chemotaxis (p = 1.96E-05), taxis (p = 1.96E-05), positive regulation of cell migration (p = 2.86E-05). In the CC category no term was significantly enriched. On the other hand in the category of MF, significant enrichment was obtained on transcriptional activator activity, RNA polymerase II transcription regulatory region sequence-specific DNA binding (p = 0.000123), RNA polymerase II proximal promoter sequence-specific DNA binding (p = 0.000123), proximal promoter sequence-specific DNA binding (p = 0.000123), receptor ligand activity (p = 0.000152), MAP kinase tyrosine/serine/threonine phosphatase activity (p = 0.000152), MAP kinase phosphatase activity (p = 0.000189), receptor regulator activity (p = 0.000216), cytokine receptor binding (p = 0.000223), transcription factor activity, RNA polymerase II proximal promoter sequence-specific DNA binding (p = 0.000481), and growth factor activity (p = 0.000707).

KEGG enrichment analysis for the above treatment comparison was also carried out to detect the enriched pathways associated with gene downregulation resulting from statin intervention in LPS stimulated BMDM samples (Fig. 4.15 C, D). Out of the 153 pathways

that were found to be enriched, 3 pathways were significantly enriched. The most significantly enriched pathways were cytokine-cytokine receptor interaction ($p = 0.001138$), MAPK signaling pathway ($p = 0.002581$), transcriptional misregulation in cancer ($p = 0.026515$). Altogether further supporting the protective role statins have been associated with in cancer studies and the pleotropic beneficial role as anti-inflammatory agents.

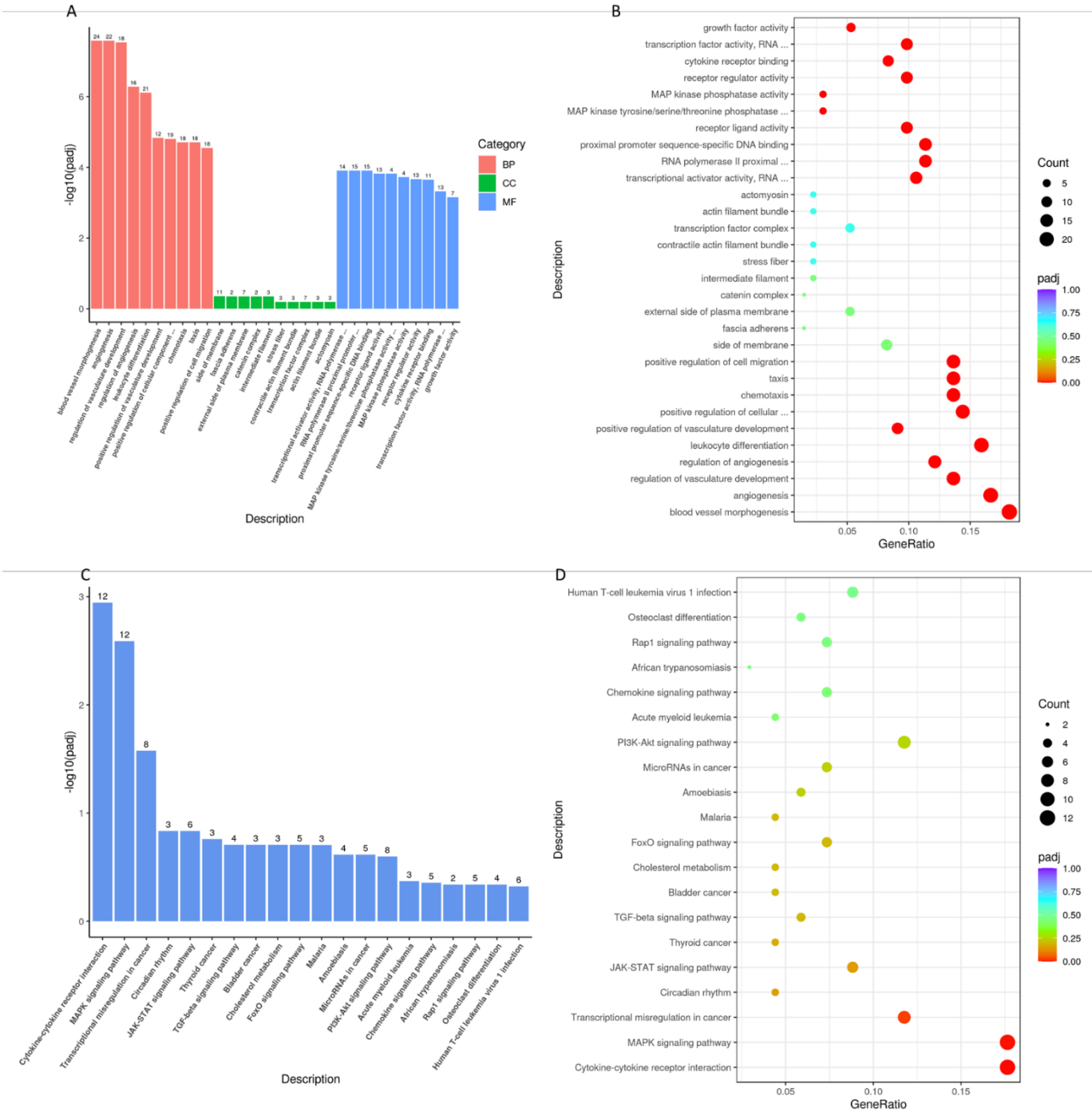

Figure 4.15. Enrichment analysis of all the differentially expressed genes that were downregulated with LPS simvastatin intervention compared to LPS.

(A) Gene Ontology (GO) histogram enrichment analysis (C) KEGG enrichment analysis histogram of all differentially expressed genes downregulated with LPS Aquamin treatment versus LPS. GO and KEGG Term's on horizontal axis shows level of significance of enrichment

expressed as -log10(padj) on vertical axis. Numbers on bars represent number of associated genes. Colours represent different functional categories for GO, (A) Biological Process (BP) red, cellular component (CC) green, and molecular function (MF) blue. GO (B) and KEGG (D) enrichment scatter plots showing the ratio of the differential gene number to the total number of differential genes in the GO or KEGG Term. (B, D) The size and the colour of points in the scatter plots represents the number of target proteins and the padj value respectively.

4.2.11 Functional enrichment analysis of differentially expressed genes (DEGs) downregulated with Aquamin or simvastatin treatment- compared to LPSCC treated BMDM

Go annotation demonstrates the BP, CC and MF that were enriched in relation to the downregulated DEGs resulting from Aquamin intervention in LPS and CC-stimulated BMDMs in contrast to LPSCC samples without Aquamin (Fig. 4.16). In this comparison, 173 GO terms were significantly enriched with 155 BP and 18 MF mapped GO terms. The top ten GO terms showing significant differences in relation to BP category included cell chemotaxis (p = 3.49E-13), leukocyte chemotaxis (p = 5.58E-11), leukocyte migration (p = 7.85E-11), granulocyte migration (p = 1.81E-10), myeloid leukocyte migration (p = 3.67E-10), neutrophil migration (p = 1.28E-09), granulocyte chemotaxis (p = 1.29E-09), chemotaxis (p = 2.93E-09), taxis (p = 2.93E-09), and neutrophil chemotaxis (p = 1.25E-08). The top ten most enriched terms in the MF category were cytokine activity (p = 9.04E-08), cytokine receptor binding (p = 3.02E-06), receptor ligand activity (p = 3.07E-06), receptor regulator activity (p = 7.55E-06), chemokine activity (p = 0.000421), growth factor receptor binding (p = 0.000501), chemokine receptor binding (p = 0.00155), fibronectin binding (p = 0.001801), neurotransmitter: sodium symporter activity (p = 0.003811), and G-protein coupled receptor activity (p = 0.009768).

The KEGG pathway enrichment results for the above comparison for Aquamin downregulated DEGs were mapped to 178 KEGG pathways among which 11 pathways considered significantly enriched. These include steroid biosynthesis (p = 9.75E-07), IL-17 signaling pathway (p = 6.45E-06), cytokine-cytokine receptor interaction (p = 6.45E-06), malaria (p = 0.000282), AGE-RAGE signaling pathway in diabetic complications (p = 0.006567), inflammatory bowel disease (IBD) (p = 0.008937), TNF signaling

pathway (p = 0.011242), hematopoietic cell lineage (p = 0.011242), Salmonella infection (p = 0.028372), Rheumatoid arthritis (p = 0.028372). The results from the GO and KEGG pathway analysis here revealed similar pathway mapping enrichment as described above for Aquamin downregulated genes compared to LPS treated BMDM. This further strengthens the confidence of the observed results and the effects of Aquamin in downregulating expression of genes associated with pro inflammatory pathways in BMDM cells.

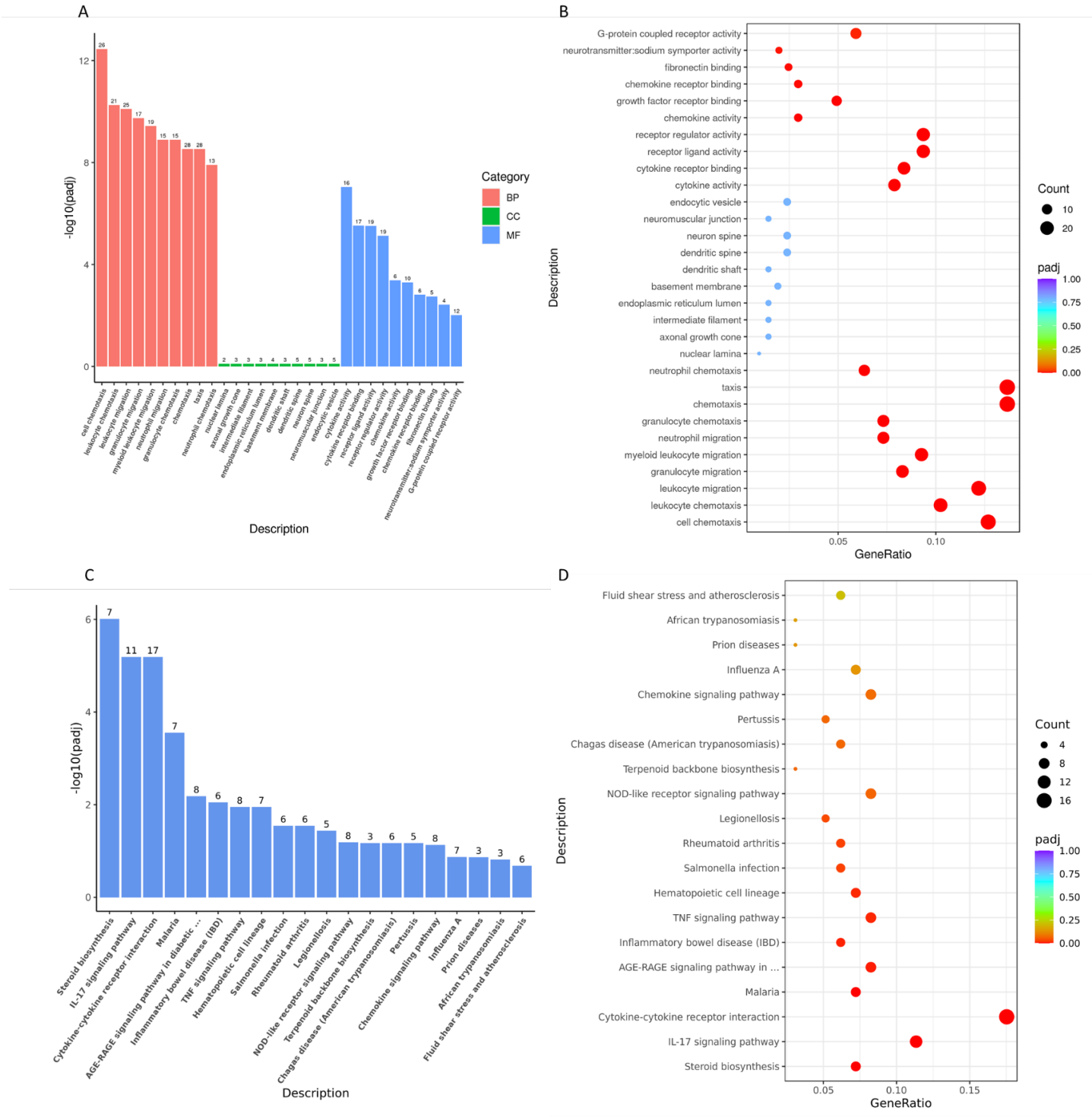

Figure 4.16. Enrichment analysis of all the differentially expressed genes downregulated in the LPS/CC with Aquamin intervention compared to LPS/CC stimulated BMDM.

(A)Gene Ontology (GO) histogram enrichment analysis (C) KEGG enrichment analysis histogram of all differentially expressed genes downregulated with LPS Aquamin treatment versus LPS. GO and KEGG

Term's on horizontal axis shows level of significance of enrichment expressed as -log10(padj) on vertical axis. Numbers on bars represent number of associated genes. Colours represent different functional categories for GO, (A) Biological Process (BP) red, cellular component (CC) green, and molecular function (MF) blue. GO (B) and KEGG (D) enrichment scatter plots showing the ratio of the differential gene number to the total number of differential genes in the GO or KEGG Term. (B, D) The size and the colour of points in the scatter plots represents the number of target proteins and the padj value respectively.

GO and KEGG enrichment of genes downregulated with LPSCC simvastatin treatment versus LPSCC treatment in BMDM was carried out and shown in figure 4.17. GO enrichment analysis identified 1664 enriched terms of which none was considered significantly enriched (Fig. 4.17 A, B). As far as KEGG pathway enrichment is concerned, notwithstanding the enrichment of 78 pathways, no pathway was significantly enriched here also (Fig. 4.17 C, D). This was not surprising as the least number of gene changes across the data set occurred in the LPSCC with simvastatin treatment which provided for reduced power in detecting strong significance in the enrichment analysis (Fig. 4.6, 4.7). However, despite this a similar pattern of potentially enriched pathways downregulated with simvastatin although not significant here was seen above in the LPS simvastatin comparison.

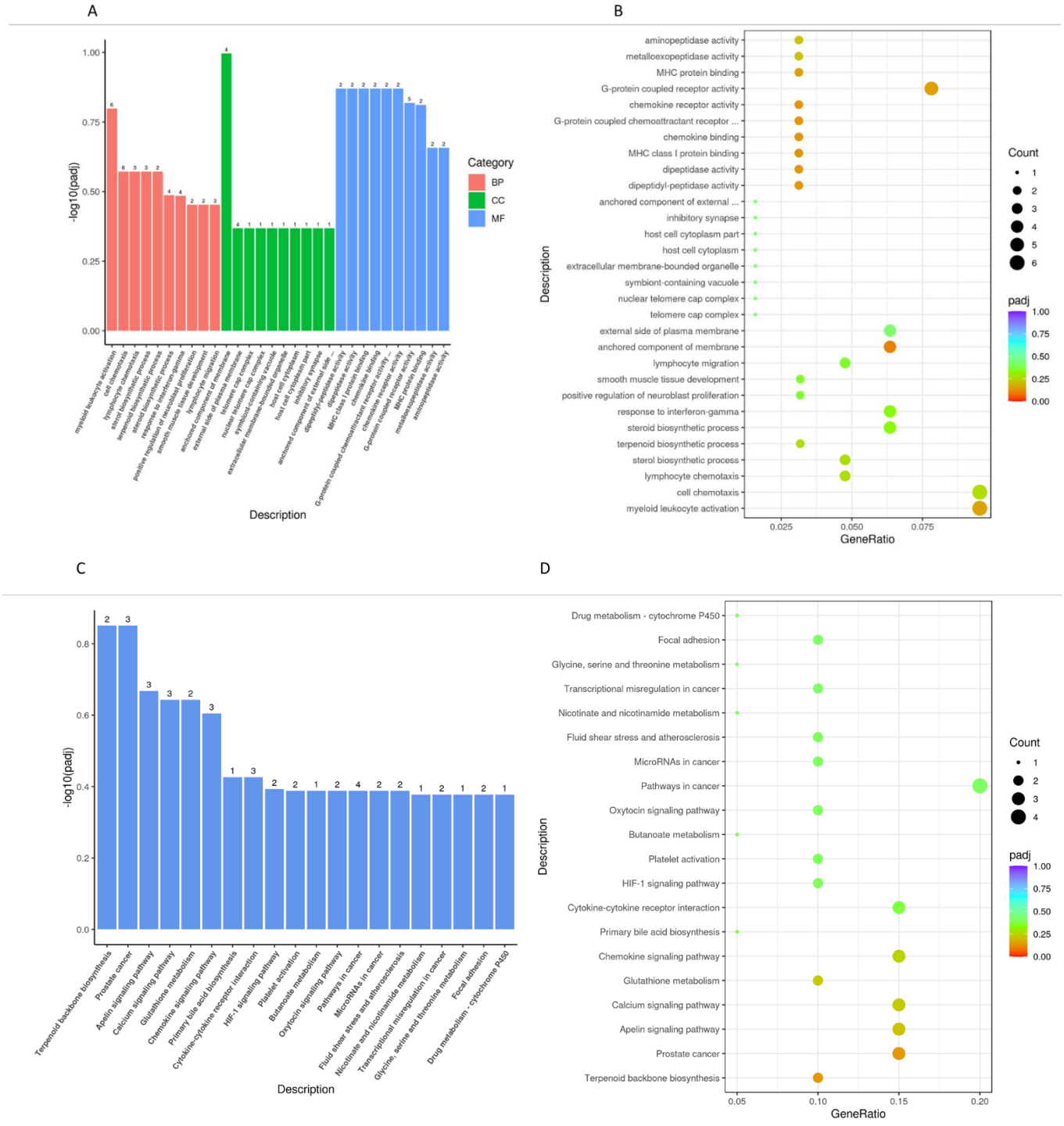

Figure 4.17. Enrichment analysis of all the differentially expressed genes downregulated with LPSCC simvastatin intervention compared to LPSCC.

(A) Gene Ontology (GO) histogram enrichment analysis, (C) KEGG enrichment analysis histogram of all differentially expressed genes downregulated with LPSCC with simvastatin treatment versus LPS and CC.

GO and KEGG Term's on horizontal axis shows level of significance of enrichment expressed as log10(padj) on vertical axis. Numbers on bars represent number of associated genes. Colours represent different functional categories for GO, (A) Biological Process (BP) red, cellular component (CC) green, and molecular function (MF) blue. GO (B) and KEGG (D) enrichment scatter plots showing the ratio of the differential gene number to the total number of differential genes in the GO or KEGG Term. (B, D) The size and the colour of points in the scatter plots represents the number of target proteins and the padj value respectively.

4.2.12 Real-time quantitative PCR (RT-qPCR) verification of gene expression changes

To validate the gene sequencing expression data associated with Aquamin inhibiting pro inflammatory genes quantitative RT-PCR was carried out (Fig. 4.18). The selected markers that were used for validation include chemokines CXCL2, CCL2, cytokines IL-6 and IL-1β as well as TICAM-1 (TRIF) an adaptor molecule associated with TLR signaling. These five DEGs were downregulated by Aquamin intervention from the sequencing data and therefore selected for RT-qPCR due to their significant as pro-inflammatory mediators in chapter 3. Consistent downregulation of expression patterns in these genes were obtained here also under Aquamin treatment using q-RT-PCR confirming validation of RNA –seq results presented above.

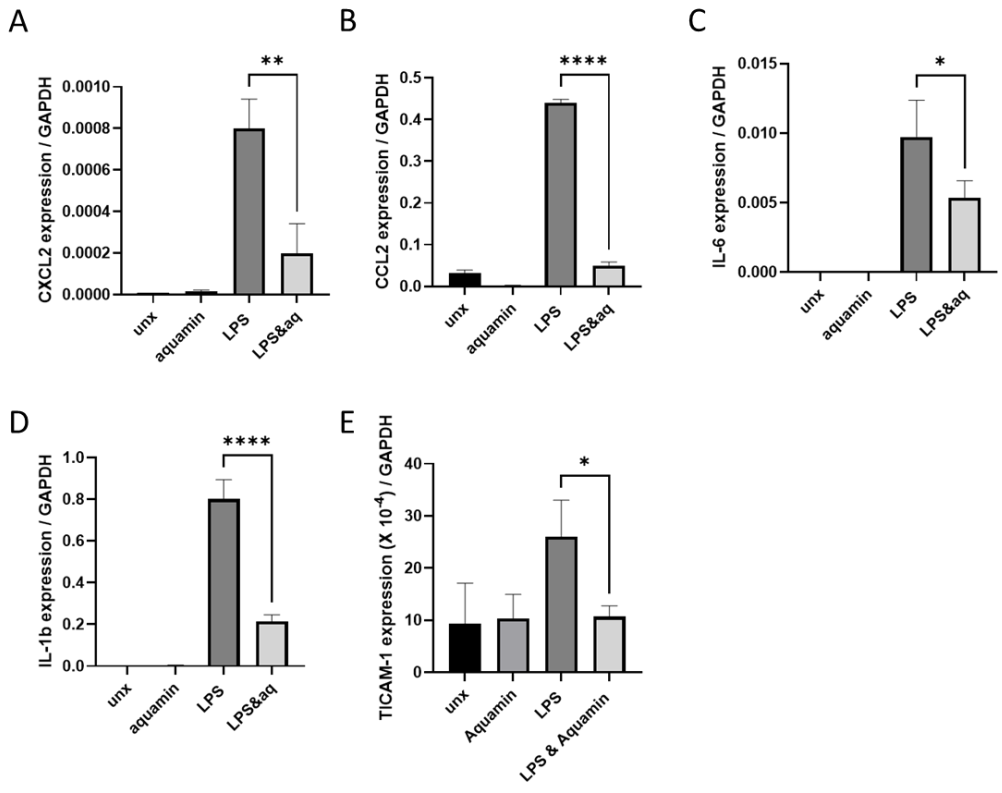

Figure 4.18. Quantitative RT-PCR validations of five genes that were downregulated by Aquamin treatment versus LPS stimulated controls. BMDMs were pretreated with Aquamin 2mg/ml and were exposed to LPS at 100ng/ml for 6 h. RT-PCR was performed to measure the gene expression of A) CXCL2, B) CCL2, C) IL-6, D) IL-1β, E) TICAM-1. Data (A-E) normalized to GAPDH, expressed relative to untreated cells and presented as mean ± sem from 3 independent experiments. *****p<0.0001, **p<0.01; *p<0.05 vs LPS alone using one way ANOVA statistical test.*

4.3 Discussion

The omics technologies are used to explore the roles, relationships and actions of the various types of molecules that make up the cells of an organism (354). Transcriptomic technologies have the capacity to detect genes and corresponding pathways expressed as a result of stimuli. By exhibiting a nontargeted nature, transcriptomics allow recognition of new transcriptional networks (355). Many types of omics data can be produced using New Generation Sequencing (NGS). NGS has been a breakthrough in transcriptomics. It includes RNA analysis through complementary DNA sequencing (356).

Over the last few years, there has been a vast number of papers published on inflammation associated diseases. Numerous genes and pathways have been found to yield a role in those conditions. Aquamin is a nutraceutical that promotes bone health and exerts anti-inflammatory properties in some studies (268, 310). However, there is abundant room for further progress in determining the molecular pathways and the biological processes involved when Aquamin is present. Since the corresponding mechanisms at how Aquamin modulates inflammation have not been established, the aims of the present study were to summarize the most reliable gene set as well as biological processes, molecular functions and associated cellular components involved when BMDMs were treated with Aquamin. NGS analysis is a powerful tool in investigating global gene expression changes across treatments and sample groups.

In the present study, BMDMs were exposed to LPS and treated with Aquamin and simvastatin. Initially, ELISA was carried out to confirm that Aquamin significantly decreases the protein concentration of LPS induced cytokines. Then, the samples were subjected to RNA sequencing to further investigate the whole transcriptome profile

changes of BMDMs in the presence of Aquamin and simvastatin when exposed to LPS or LPS with CCs.

Interestingly across the data set genes that exert crucial roles in inflammatory and viral responses as well as cancer are detected. The results of this study revealed that treatment of cells with Aquamin has induced significant upregulation of Ifit2 gene compared to the unstimulated control. A previous in vivo study has shown that Ifit2 exerts a protective role against neurotropic coronavirus MHV-RSA59 infection in mice (357). From the results in this study it is suggested that supplementation with Aquamin could have beneficial effects against viral infections such as coronavirus. The data of this study also demonstrated that Samhd1 is another gene that is upregulated as a result of Aquamin treatment. Interestingly, a recent study has revealed that Samhd1 could play pivotal role in the connection of neurological manifestations and Covid-19 (358). Hence intake of Aquamin could potentially have an effect on neurodegeneration. When analyzing the data, it was found that stimulation of BMDMs with LPS induces the upregulation of pathways which are popular in inflammatory responses, viral infections, and tumor growth. This provided confidence in the expression results as these pro inflammatory pathway upregulating events are expected with LPS stimulation in BMDM. From the data interpretation a strong anti-inflammatory association is seen when LPS-stimulated BMDMs are treated with Aquamin. Downregulation of chemokines and cytokines participating in pathways like Toll-like receptor, NOD-like receptor, FoxO and IL-17 signaling pathway which are involved in tumorigenesis and immune response mechanisms are seen. Aquamin prevented their upregulation which was induced by LPS. Equally important to the TLR signaling inhibition by Aquamin as described in chapter 3, strong evidence for modulation of the IL-17 signaling pathway was detected. Using KEGG pathway analysis, it

was seen that the IL-17 pathway exhibited significant downregulation with Aquamin treatment and was further supported by reduction in individual gene expression values of Cxcl2, Ccl2, Il6, Il1b which are associated to IL-17 signaling (359). Apart from the beneficial effects of IL-17 signaling, excessive release of IL-17 cytokine could lead to clinical outcomes (360). IL-17 cytokine modulates inflammation in synergy with other cytokines such as TNF-α (361). Hence, downregulation of IL-17 signaling pathway associated genes by Aquamin further supports its anti-inflammatory effect. Previous studies have emphasized that dysregulation of IL-17 pathway is associated with tumour growth which is corroborated by higher expression of IL-17 genes in cervical, colorectal, gastric, as well as esophageal cancer (362, 363). In the future it will be interesting to investigate the effect of Aquamin in modulating disease pathologies associated with IL-17 signaling. Prior research indicated that PLAU enzyme facilitates carcinogenesis, however PLAU inhibition could block tumor progression (364). The findings of the current study hint that Aquamin supplementation might yield anti-cancer effects. The results from the data set indicate altogether that Aquamin as a nutraceutical can yield a protective role against multiple pathologies such a cancer, viral infections, and inflammation related disorders by targeting associated genes.

Metabolic disease is one of the most common pathological conditions in the world and can maximize the risk for further cardiovascular events and various diseases reducing the quality of life (365). High cholesterol is a major risk factor in the pathophysiology of metabolic disease (9). In addition, high levels of cholesterol lead to dysregulation of cellular cholesterol homeostasis which triggers the switch of macrophages to hyperinflammatory cells that are abundant in atherogenesis (366). In the present study we induced a phenotype that resembles a

hypercholesterolemic state in vitro by exposing BMDMs to LPS and cholesterol crystals. Here investigations into the treatment of BMDMs with Aquamin and its effects at antagonizing inflammatory genes and corresponding pathways associated with hypercholesterolemia were carried out.

On the basis of evidence that is currently available, simvastatin is a compound that reduces LDL-cholesterol and associated cardiovascular events. Increasing evidence is supportive of simvastatin also acting as an anti-inflammatory agent by preventing the increase of LPSCC-induced IL-1β in PBMCs by antagonizing NLRP3 inflammasome(184). Further investigations substantiate the anti-inflammatory effect of statins by demonstrating reduction in the activity of the transcription factor NF-κB as well as activator protein 1 (AP-1) that are involved in inflammatory pathways and are linked to atherosclerosis (367).

Simvastatin as a drug of choice for dyslipidemias were used in the study as an established compound to be compared with Aquamin. Aquamin exhibited more potent reduction of TNF-α and IL-1β in BMDMs co-stimulated with LPS and CC compared to simvastatin. Aquamin intervention downregulated inflammation-linked pathways and signature cytokines such as IL-17 which is highly expressed in hypercholesterolemic individuals (368). Steroid biosynthesis was the most significantly enriched pathway with Aquamin downregulated DEGs when compared to LPS and CC stimulated BMDM samples without Aquamin. Enzymes and molecules involved in steroid biosynthesis play key roles in the biosynthesis of cholesterol. Downregulation of steroid associated genes here with Aquamin indicates a possible role in cholesterol lowering capabilities, which needs further investigations yielding a safe additive compound to statins in the protection against hypercholesterolemia. Previous work has shown that Serum amyloid A (SAA) proteins modulate inflammation and metabolism

and they are known to be highly expressed in conditions that are associated with MetS such as high blood glucose, obesity, insulin resistance and heart disease (369-374). That notion was corroborated by a previous research which demonstrated that mice that were exposed to HFD displayed upregulated SAA3 in the adipose tissue (371). A different study revealed that administration of LPS, as well as other products of the indigenous gut microbiota, lead to increased expression of SAA3 in the adipose tissue (375). The present findings re directly in line with the LPS induced Saa3 upregulation that was seen previously and a further novel finding is that treatment with Aquamin induces downregulation of Saa3 which is suggestive of anti-inflammatory effects and potentially beneficial against the development of MetS.

In addition, another pathway which was significantly downregulated as result of Aquamin intervention in LPS and CC stimulated BMDMs was AGE-RAGE signaling pathway in diabetic complications. According to previous literature, RAGE pathway is positively associated with renin-angiotensin system which yields a major drug target in cardiovascular and metabolic diseases (376). Deletion or suppression of RAGE transactivation can lead to attenuation of type 1 angiotensin II receptor (AT_1) and thus pro-inflammatory signaling (377). In other words, the significant downregulation of DEGs associated to AGE-RAGE signaling pathway by Aquamin could mean that Aquamin as a nutraceutical can exert a beneficiary role in heart disease. Further studies using Aquamin in phenotypes that resemble cardiovascular disease should be carried out.

RNA seq provided strong evidence of the notable differences in the gene expression levels during both presence and absence of Aquamin and simvastatin. Strikingly treatment with Aquamin resulted to a notable higher number of DEGs as well as pathways and biological processes compared to simvastatin which pinpoints

suggests that this research could serve as a base for future studies exploring in depth the effect of Aquamin in the corresponding pathways. Treatment with Aquamin has led to the downregulation of genes with yield crucial roles in the pathophysiology of diseases such as obesity, cardiovascular disease, diabetes and inflammatory pathologies. Further gene validation and proteomic analysis needs to be conducted to provide ample support to its beneficiary effect as a nutraceutical. Notwithstanding the fact that transcriptomic analysis yields a noteworthy tool to assess global gene expression, proteomics analysis should be conducted in complement to transcriptomics to provide a thorough intuition into the protein profile of the organism (378). Considering its anti-inflammatory properties, its large accessibility in conjunction with its safety profile could potentially increase the use of Aquamin as a health promoting agent either as an alternative or a synergetic compound to currently approved pharmaceuticals.

5 THE EFFECTS OF AQUAMIN ON DIET INDUCED OBESITY IN MICE

5.1 Introduction

Nowadays, high fat diet is a major public health concern yielding a risk factor for the development of metabolic disorders, obesity and DM II (379). The incidence of those disorders is rising dramatically leading to cardiovascular events because of increased cholesterol, blood glucose and insulin levels as well as hypertension (380). Dietary patterns full of fats are one of the most prominent contributors of atherosclerosis and obesity.

Available evidence has shown that high fat intake contributes to the pathogenesis of cardiovascular disease and diabetes (381). Studies in the field of MetS are investigated using experimental animal models which resemble the disease state in humans. Rodents are the most popular animal models used to investigate MetS which predominantly occurs by diet manipulation (382). Similarly to the MetS, diet-induced obesity (DIO) has been widely studied using in vivo mouse models (383). Administration of a high fat diet (HFD) in mice can induce an obese state in a proportional way that HFD causes obesity in humans along with its associated pathophysiological changes (384). Inflammatory cells are very abundant in the adipose tissue resulting to the production of pro-inflammatory markers which connects obesity, atherosclerosis, as well as insulin resistance (385).

Obesity is regulated by leptin and regulated lipolysis as well as proinflammatory immune responses. Dysregulation of leptin or leptin receptor can lead to early onset obesity (29). Resistance to leptin occurs primarily due to administration of a high fat diet in which elevated levels of plasma leptin and ob gene are observed due to corticosterone and insulin release in mouse and human adipose tissue (386). One of the most popular genes in obesity research is the ob gene which encodes for leptin and to that end, ob/ob mouse, which is leptin deficient, yields one of the most

widely used animal models (387, 388). Along similar lines, the db/db mouse, which is also known as “diabetic mouse”, is leptin receptor-deficient. It manifests a similar phenotype to ob/ob mouse, however it is characterized by increased hyperglycemia compared to the “obese mouse” (387).

To further comprehend the mechanism of MetS and obesity, transgenic models have been produced. Some examples are the corticotropin-releasing factor overexpressing mice (389), serotonin 5-HT-2c overexpressing mice (390), beta-3-adrenergic (391), melanin-concentrating hormone (392), as well as others.

The C57BL/6J (B6J) mouse has received much attention as one of the most susceptible mouse strains to develop obesity, hyperglycaemia, insulin resistance, and impaired glucose tolerance (IGT) when fed a HFD amongst the available strains (393, 394). Previous research has investigated the impact of a high fat diet on different mouse strains. Their results demonstrated increased weight gain in Kunming and ICR mouse compared to C57BL/6 and BALB//c mouse, however all tested mouse strains displayed heavier adipose and liver tissue resulted from the HFD (395). A recent study assessed whether the dietary intake of ginger could yield a protective effect against DIO. In their study Seo et al. exposed C56BL/6 mice to HFD for 7 weeks. Their results revealed that mice that were fed a HFD gained weight as well as high glucose and cholesterol levels. The incorporation of ginger into the diet exerted a significant protective effect against DIO (396).

The prevalence of obesity is on the rise, which pinpoints that current approaches are ineffective against the development of the disease, hence further preclinical studies examining the disease are of utmost importance (397). Notwithstanding the indirect anti-inflammatory activity of statins by decreasing plasma cholesterol, previous studies have pinpointed that statins exert direct anti-inflammatory activity by reducing C-reactive protein (CRP)

concentration (398). Hence, they function as the predominant choice for the treatment of atherosclerosis (399). A Hyperlipidemic state could be a result of insulin resistance and high adiposity which justifies the link between obesity and atherosclerosis (400). Previous authors have demonstrated that immune cells in obesity and specifically macrophages exhibit high levels of IL-1β (401). In a study by Boland et al., it was demonstrated that simvastatin reduces the NLRP3 induced IL-1β release (184). As indicated by previous research, attenuation of NLRP3 inflammasome in mice prevents obesity-induced activation of the inflammasome in liver and adipose tissue and it also increases insulin sensitivity (190). Considering the notable inhibitory effect of Aquamin against the production of cytokines in LPS- and CC-stimulated BMDMs that was interestingly more potent than simvastatin as was outlined in chapter 4, this study aimed to shine new light on the potential synergistic effect of Aquamin and simvastatin in peripheral blood mononuclear cells (PBMCs) exposed to LPS and CC as potential NLRP3 antagonists. The study assessed in this chapter also sought to determine the significance of Aquamin as a prophylactic compound against diet induced obesity in mice which are prone to gain weight by exposing C57BL/6 mice to HFD in the presence and absence of Aquamin.

5.2 Results

5.2.1 Treatment with Aquamin potentiates the effect of simvastatin in NLRP3-primed PBMCs

Previous studies have demonstrated that during the state of obesity molecular pathogens are produced leading to the activation of NLRP3 inflammasome (402). To examine the role Aquamin exerts in the activation of NLRP3, human PBMCs from healthy individuals were exposed to LPS and CC upon treatment with Aquamin and simvastatin (Fig. 5.2). Our results demonstrated that both Aquamin and simvastatin significantly reduce the LPS- and CC-induced release of TNF-α (Fig. 5.2A) and IL-1β (Fig. 5.2B). Another key finding, that can be emerged from figure 5.2 below, is the significant reduction of both NLPR3-primed TNF-α and IL-1β caused by the synergy of Aquamin and simvastatin, even when both Aquamin and simvastatin were used at lower doses (Fig. 5.2). Our results cast a new light on the effect of Aquamin as an additive to simvastatin treatment in vitro, which might suggest that potential supplementation of Aquamin in human subjects treated with statins could be beneficial.

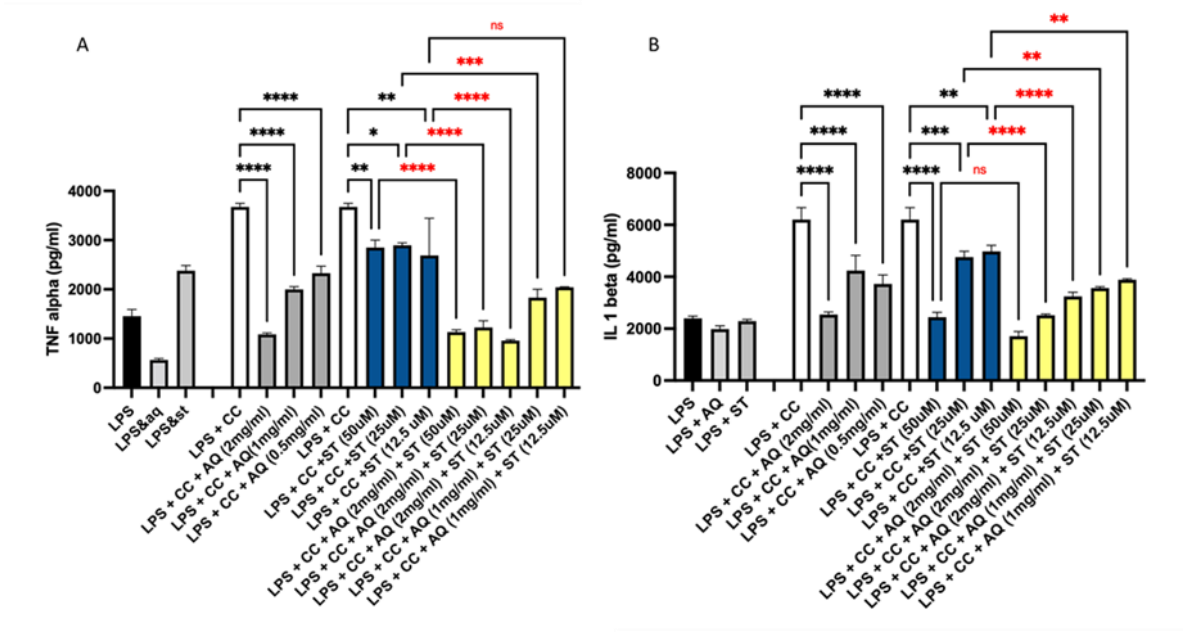

Figure 5.2. In vitro Aquamin treatment inhibits cholesterol crystal-induced expression and activation of TNF-α and IL-1β from healthy peripheral blood mononuclear cells (PBMCs).

Aquamin treatment of healthy PBMCs in vitro inhibits the secretion of (A) TNF-α, (B) IL-1β in response to lipopolysaccharide (100 ng/mL) and cholesterol crystals (CC) (2 mg/mL). Data are shown as mean (standard error of the mean [SEM]). Statistical analysis of significance determined through 1way ANOVA. ns $p>0.05$, *** $p < 0.001$.

5.2.2 The effect of Aquamin on diet induced obesity in mice

To gain an understanding of how Aquamin plays a role in the pathogenesis of obesity and metabolic disease, we placed C57BL/6J mice on a high fat diet with and without Aquamin supplementation for 10 weeks (Fig. 5.3). The results of the experiment found clear support that mice exhibited increased weight gain as expected from HFD feeding. Preliminary findings indicate that inclusion of Aquamin in the HFD diet may lead to a reduction in weight gain compared to the HFD only controls (Fig. 5.3A, 5B). The reduced weight gain in the Aquamin supplemented animals was observed despite similar levels of food and water consumption (Fig. 5.3C, D). No change in mass of epidydimal and subcutaneous white adipose tissue depots was observed between the groups at the end of the study period (Fig. 5.3E). (Carried out with the support of my P.I Dr Lucitt)

As a result of HFD exposure, C57BL/6 mice have been shown to develop signs of metabolic disease such as defective glucose and insulin tolerance. Therefore, we next analysed whether Aquamin supplementation alters metabolic function in these mice. Here, our results demonstrated that mice treated with HFD and Aquamin supplementation were found to have improved glucose tolerance (Fig. 4A, B) and lower insulin resistance (Fig. 5.4C, D) compared to the HFD only control mice at 12 weeks. These results demonstrate that Aquamin supplementation in a model of diet induced obesity can suppress weight gain and protect against development of the metabolic syndrome.

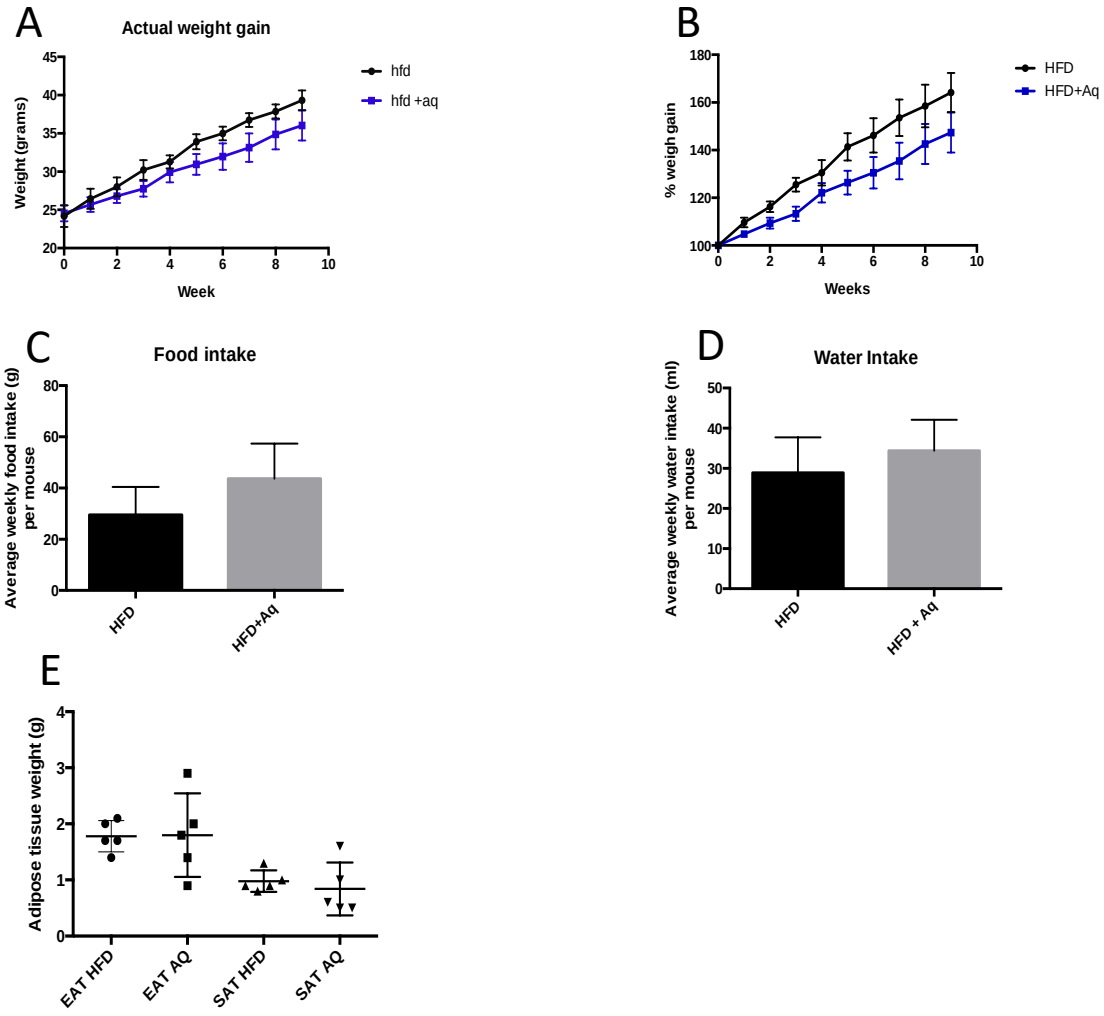

Figure 5.3. AquaminTM supplemental HFD is protective against weight gain.

(A) Actual weight gain, (B) percentage weight gain, (average weekly food intake and (d) average weekly water intake in AquaminTM supplemented HFD animals compared to control HFD animals over 10 weeks. (E) Epidydimal (EAT) and subcutaneous (SAT) adipose tissue weights at the end of study period. The data are mean ±sem, n=5.

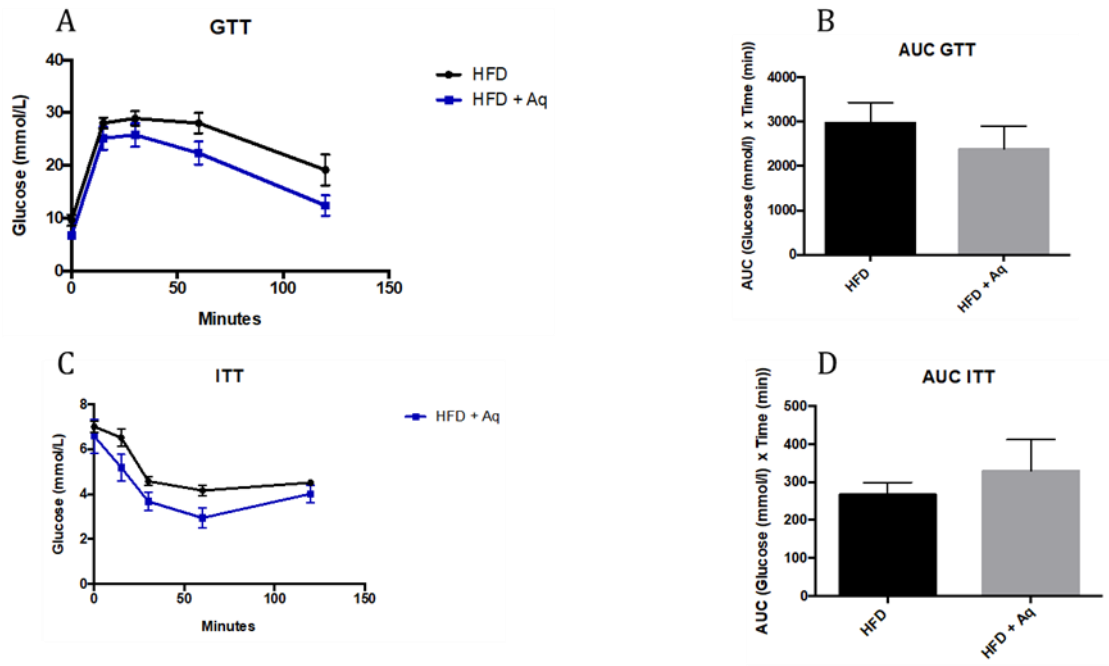

Figure 5.4. AquaminTM supplemented HFD improves glucose tolerance and lowers insulin tolerance.

Glucose tolerance test (GTT) following 10 weeks of HFD; blood glucose over time after i.p. glucose (2g/kg) injection, blue line Aquamin supplemented HFD (A) and AUC (B). Insulin tolerance test (ITT) following 10 weeks on HFD; blood glucose over time after bolus i.p. insulin (1U/kg), blue line Aquamin supplemented HFD (C) and AUC (D) shown. The data are mean ±sem, n=5.

To further determine the gene expression of pro-inflammatory mediators in adipose tissue harvested from mice fed a HFD in comparison, with the mice that received HFD with Aquamin, RNA was extracted from adipose tissue and RT-PCR was carried out to determine the gene expression of TNF-α, IL-6 and IL-1β (Fig. 5.5). Although none of the differences illustrated in figure 5.5 were statistically significant, an observation that could emerge based on the corresponding graphs is that incorporation of Aquamin into HFD potentially exhibits a tendency for reduction of IL-1β compared to HFD alone.

P= 0.1707

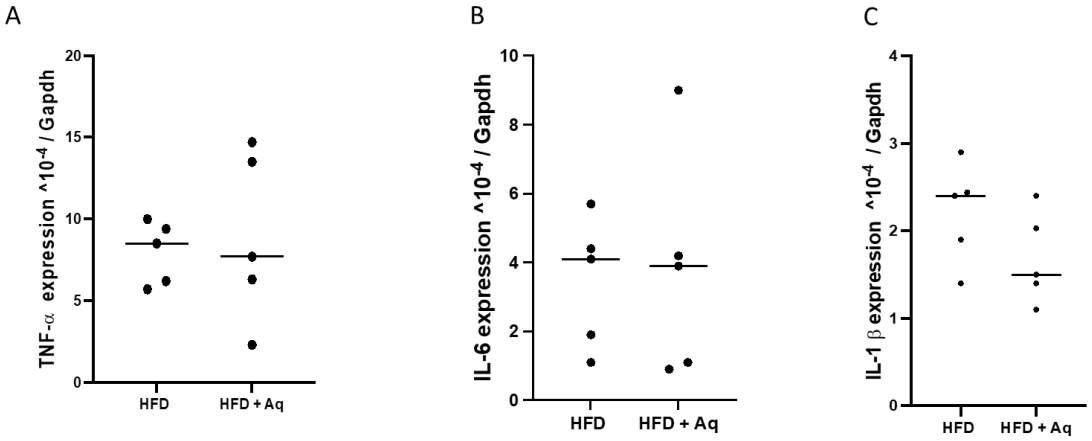

Figure 5.5. Aquamin supplementation did not cause any significant alteration to the gene expression of pro-inflammatory cytokines in the adipose tissue.

(A)TNF-α, (B) IL-6, (C) IL-1β relative gene expression in the adipose tissue of mice fed a HFD and the ones fed a HFD along with Aquamin (*n=5* per group).

5.3 Discussion

It is by now generally accepted that the number of obese patients including children has notably increased leading to further pathological conditions like MetS, diabetes and heart disease (403, 404). Macrophage infiltration occurs as a result of adiposity leading to the release of pro-inflammatory cytokines such as TNF-α, IL-6 (380).

During an obese state the Nod-like receptor including the NLRP3 inflammasome recognizes danger signals leading to the production of IL-1β (190). Cholesterol crystals are the main mediators of NLRP3 activation and signaling (184). Macrophages generate IL-1β which plays a major role in the development of obesity associated insulin resistance (405). A previous research in the field of cardiovascular disease and atherosclerosis has shown that co-stimulation of PBMCs with CC and LPS leads to potent IL-1β and TNF-α production (184). As per previous research that was carried out in NLRP3-activated PBMCs, it was revealed that simvastatin treatment had led to reduced IL-1β levels without any effect on TNF-α protein expression in CC- and LPS-driven cells (184). A study that was performed using diabetes patients demonstrated reduction in the monocyte and lymphocyte levels of pro-inflammatory cytokines (406).

In the present study, NLRP3 spiked PBMCs were formed after exposure to CC and LPS and the effect of simvastatin was also assessed by our lab. The results in this study ties well with previous in vitro studies wherein the combination of LPS and CC induced significant release of IL-1β compared to the untreated controls (347). Findings in the present study are also consistent with the findings of Boland et al. with respect to simvastatin's inhibitory effect against CC- and LPS-induced IL-1β. However, the role of Aquamin with respect to NLRP3 signaling in the context of obesity

has not been established. We demonstrated that PBMCS that were treated with Aquamin prior to stimulation with CC and LPS displayed dramatically reduced levels of TNF-α and IL-1β compared to the positive controls. The results in the current study also indicate that Aquamin exhibited more potent inhibitory effects against both IL-1β and TNF-α compared to simvastatin in vitro. The present study is also significant in the respect of demonstrating that potential synergistic treatment of Aquamin with lower doses of simvastatin can alleviate inflammation in vitro and significantly attenuate TNF-a and IL-1b release in an equivalent manner with higher doses of simvastatin. A growing body of evidence has pinpointed the significance of IL-1β in the pathology of type 2 diabetes (407, 408). Other results have also suggested that IL-1β exerts a key role in cancer pathophysiology by enhancing inflammatory response and hence facilitate in tumor eradication (409, 410). Therefore, total depletion of NLRP3 might exhibit detrimental effects against several pathophysiologies. The results provide novel insights into the anti-inflammatory role of Aquamin and confirm that Aquamin as a standalone compound as well as in combination with simvastatin could exert inhibitory effects in CC-induced activation of NLRP3 pathway. Furthermore, it could conceivably be suggested that intake of Aquamin is a nutraceutical might reduce the risk of occurrence of cardiovascular events. However more research related to the synergistic effect of Aquamin with simvastatin needs to be undertaken to determine whether supplementation with Aquamin could facilitate the administration of lower doses of statins in the future.

In our attempts to explore how Aquamin might regulate obesity and metabolic disease, we examined what role it exhibits in disease pathogenesis in mice treated with HFD. Our pattern of results was in lines with previous findings supporting the susceptibility of C57BL/6J mice to develop diet induced obesity as a result of

exposure to HFD for 10 weeks (383). The results demonstrate that there might be trend towards reduced weight gain and adiposity in mice that were fed a HFD with Aquamin in comparison to HFD alone, as well as having improved glucose and insulin tolerance, without profound alterations to the levels of food and water intake. This result potentially supports our hypothesis that Aquamin plays a protective role by lowering the susceptibility to developing obesity under HFD treatment conditions. This along with its previous reported effects in reducing lipid levels in postmenopausal women are all implying that Aquamin demonstrates protective effects in the metabolic syndrome and obesity. A recent study that was conducted by Han, et al. had shown that C57Bl/6J mice that were subjected to HFD exhibited weight gain after 4 months of diet administration (411), unlike our study in which mice were only subjected to HFD for only 10 weeks. The duration of the exposure to HFD is an apparent limitation of this study and thereby further validation is required to establish the efficacy of Aquamin to significantly prevent weight gain in mice.

As a final remark, the effect of Aquamin on DIO is a domain where much remains to be studied. More studies should be carried out using additional strains with high responsiveness to HFD so that firm conclusions can be drawn about the efficacy of Aquamin to prevent weight gain, insulin resistance as well as glucose tolerance in vivo. Furthermore, the effect of Aquamin supplementation to obese patients should be investigated.

6 GENERAL DISCUSSION/CONCLUSSION

6.1 Discussion and conclusions

The global burden of metabolic syndrome has risen dramatically yielding a clinical concern worldwide. MetS cannot be characterized as a single disease, but it can be defined as the pathological outcome of cardiovascular and metabolic risk factors (412). Since MetS is multifactorial, reduction in prevalence could be achieved by optimal screening and improvement of cardiovascular risk profiles (413). Previous studies have reported that MetS is age-dependent, and it is also more common among certain ethnic groups. During the study, metabolic syndrome prevalence increased from 16.2% to 21.3% for the 20-39 age group while most significant differences were reported for Asian participants (19.9% to 26.2%), as well as Hispanic participants (32.9 to 40.4%) (413). The finding that MetS is more abundant among certain racial group indicates notable health discrepancies which are important because of the ongoing pandemic. Research has shown that some elements of metabolic syndrome such as obesity and high blood pressure are correlated to more severe COVID-19 (414-416). Interestingly, different research reveals that hospitalization and deaths from COVID-19 is more common in Blacks and Hispanic compared to non-Hispanic Caucasian people (417, 418). Similarly to COVID-19, those health disparities indicate that genetic and environmental factors could impact the development of MetS and justify why its prevalence is on the rise.

Due to its multifactorial nature, the reasons associated with the manifestation of MetS are not fully understood. Substantial evidence suggests that sedentary lifestyle might exert a crucial role in its development (419). Implementation of a healthy lifestyle accompanied by regular exercise as well as healthy diet might exhibit a positive impact against obesity. Conventional pharmacotherapy associated with the alleviation of the

components that aggregate the disease such as high lipid levels and blood pressure is an additional approach to manage the disease (420).

The inflammatory response commences in response to an infection and injury. A pro-inflammatory state unfavorably affects MetS and features elevated levels of CRP and other pro-inflammatory mediators (421, 422). According to our limited comprehension of the biological complexity of chronic inflammatory disorders, progress in the development of anti-inflammatory treatment remains a pivotal challenge. Several studies have shown that natural compounds possess a number of biological activities including anti-inflammatory properties (423). In particular, the anti-inflammatory activity of seaweed extracts has been addressed previously demonstrating inhibition of pro-inflammatory cytokine release (424, 425). Previous findings have shown that there has been an improvement in therapeutics and the use of immunomodulators such as anti TNF-a agents are already proving to be beneficial for patients by minimizing the risk of experiencing cardiovascular events (426). Aquamin is a seaweed-originated multimineral with calcium and magnesium as its main components (www.aquamin.com). This study has demonstrated that Aquamin exerts a potent anti-inflammatory effect in a variety of innate immune cells and aimed to provide further evidence in the exact mechanism that Aquamin modulates inflammation in the context of metabolic disease.

In keeping with previous reports from the literature, the initials investigations of this study revealed a significant reduction of pro-inflammatory cytokines such as TNF-a, IL-6 as well as IL-1β in a number of innate immune cells including DCs, monocytes and macrophages that were exposed to LPS (278). Interestingly, no potent inhibition was observed in the expression of cell surface markers in immortalized BMDMs that were exposed to LPS. When

comparing the results of this study to those of an older study that was carried out by Gorman et al. it must be pointed out that we could not replicate the previously reported inhibition of NF-κB activity in LPS stimulated RAW 264.7 macrophages (277). It can be assumed that the reason our results could not tie with the other findings is that our experiment was performed in primary bone marrow derived macrophages in comparison to RAW macrophages. No previous studies have attempted to investigate the effect of Aquamin in macrophage polarization. In this study we induced a classically activate macrophage phenotype by simultaneously exposing M_0 macrophage cells to LPS and IFN-γ. The present findings did not support the current hypothesis that Aquamin prevents skewing of macrophages towards M1 pro-inflammatory state. Contrary to our expectations, FACS analysis of cell surface markers associated with M1 polarization state did not find any significant difference between stimulated samples and the ones that were co-treated with Aquamin.

Activation of Toll-like receptor signaling by PAMPs or DAMPS leads to the production of pro-inflammatory mediators such as TNF-α and IL-6. Taking the data to date into consideration with the known inhibition of pro-inflammatory cytokines downstream of TLR by Aquamin, the next step was to map TLR signaling pathway in order to elucidate the mechanism of action of the compound. Accordingly, it was demonstrated that treatment of primary BMDMs with Aquamin resulted to significant reduction of both TNF-α and IL-6 in TLR4- and TLR3-driven macrophages. TLR4 signaling is known to be mediated by MyD88 and TRIF adaptor proteins (427). Based upon the fact that Aquamin did not cause any significant cytokine alterations in TLR9 (MyD88-dependent) driven macrophages, we set out to test if Aquamin may exert its immunomodulary effect downstream of TRIF adaptor protein. Initially to test this hypothesis RT-PCR was carried out to measure

the transcriptional levels of TLR4, TLR3, MyD88 and TRIF in LPS stimulated macrophages. Our results demonstrate that Aquamin treatment here significantly reduces the gene expression of TLR3 and TICAM-1 (TRIF), without causing any effect in the expression of TLR4 and MyD88. Based on this it was hypothesized that Aquamin induces a TRIF-dependent inhibition of cytokine release. Our next step was to assess the response of IFN-β to Aquamin, which is a TRIF pathway specific readout when murine macrophages are exposed to Poly(I:C), a TLR3 (TRIF-dependent ligand) (329). The results of that study indicated that Aquamin reduces the Poly(I:C)-induced gene expression of IFN-β as well as the Poly(I:C)-induced nuclear translocation of IRF3 in murine BMDMs (Fig. 6.1). Future studies focusing on mapping more precisely TRIF-dependent TLR signaling is therefore suggested to gain a clearer understanding on which level of the pathway Aquamin is producing the observed antagonistic effects.

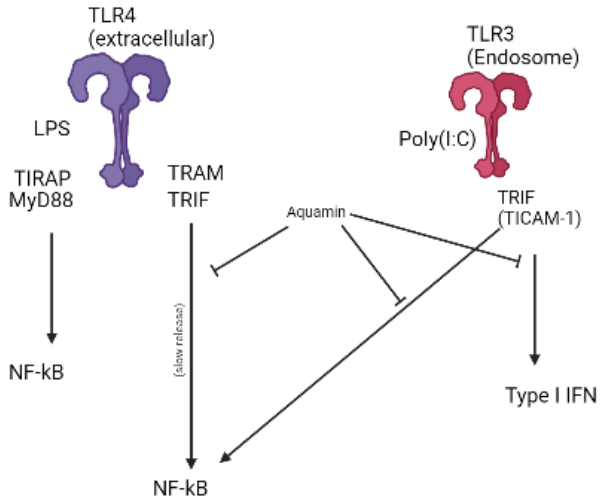

Created in BioRender.com

Figure 6.1. Aquamin potentially exerts its immunomodulary effects downstream of TRIF adaptor protein.

Schematic representation of potential anti-inflammatory mechanism of Aquamin through inhibition of TRIF dependent TLR signaling pathway. TRIF mediates IRF3- and NF-kB-dependent cytokine release which are reduced in the presence of Aquamin.

Created in BioRender.com

Chapter 3 provided support to the claim that Aquamin antagonizes TLR in a TRIF-dependent manner. Despite the activation of TLR post to tissue injury of pathogen invasion, other PRRs are also activated along similar lines. NLR signaling leads to the formation of the inflammasome and further triggers the release of the inflammatory mediator known as IL-1β which is associated with atherogenesis (428, 429).Previous research carried out using an in vivo atherosclerosis mouse model using $ApoE^{-/-}$ mice, demonstrated that attenuation of IL-1β in atherosclerosis is a benefactor to the disease progression (430). The release of IL-1β is dependent initially to stimulation of PRRs by pathogens and secondly by distinct substances like cholesterol crystals in the atherosclerotic lesions (431-433). In agreement with previous findings, the current study showed that cholesterol crystals cause inflammasome activation and production of IL-1β (184, 347).

Statins have become the main option for treatment of heart disease by exhibiting lipid-lowering as well as anti-inflammatory effects (434, 435). In accordance with findings reported by Boland et al, the use of simvastatin in BMDMs resulted in a reduction of LPS- and CC-induced IL-1β (184). The reduction of pro-inflammatory cytokines in monocytes as well as the downregulation of NLRP3 inflammasome by statins have also been demonstrated by further studies carried out in hypercholesterolemia patients under TLR-stimulated conditions (233, 436). Interestingly, treatment of BMDMs with Aquamin under the same conditions demonstrated a more potent reduction of both IL-1β and TNF-α in comparison to simvastatin.

We used RNA-seq to assess the global transcriptome profile of inflammation-driven BMDMs that received Aquamin and simvastatin treatment. We identified 6142 DEGs with LPS stimulation in BMDMs. A pathway analysis of these DEGs revealed that of the induced genes the most notable biofunction was

cytokine activity associated with TNF-α signaling pathway, NOD-like receptor signaling pathway, as well as viral responses such as Influenza A. The enrichment of pathways such as NOD-like receptor and Toll-like receptor resulting from LPS stimulation are consistent with previous literature that LPS is a potent ligand inducing the activation of PRRs and the subsequent production of pro-inflammatory cytokines like TNF-α (118). Comparisons of BMDMs exposed to LPS compared to BMDMs co-treated with Aquamin led to the identification of 1490 DEGs between the two treatments. Here LPS stimulated BMDM cells treated with Aquamin result in downregulation of genes associated with Toll-like receptor as previous evidence suggests (268, 310). Downregulation of NOD-like receptor in Aquamin-treated samples corroborates earlier ELISA results that illustrate significant reduction of IL-1β in vitro. This study has also shed light on additional pathways involved in the inflammation process such as IL-17 signaling pathway as observed by the reduction of corresponding genes like Cxcl2, Ccl2, Il6 and others. Previous authors have substantiated the clinical relevance of IL-17 pathway in auto-immune diseases (437). Existing research has shown that blocking IL-17 with monoclonal antibodies yield an effective approach to the management of auto-immune diseases like psoriasis (438, 439). Our findings support that Aquamin as a nutraceutical significantly downregulates the IL-17 signaling pathway in vitro. Taken together, implementation of dietary Aquamin could play a prophylactic role against the development of auto-immune diseases by blocking IL-17 signaling pathway.

To our knowledge, this is the first report that uses RNA-seq analysis to investigate the transcriptome profile of inflammatory skewed macrophages co-treated with either Aquamin or simvastatin. Unlike the high number of DEGs obtained from LPS versus LPS and Aquamin comparison, replacement of Aquamin with simvastatin as a treatment led to 195 DEGs which is almost 8-fold lower. KEGG

enrichment analysis of relative pathways resulted from simvastatin treatment in LPS stimulated BMDMs has predominantly shown downregulation of cytokine-cytokine receptor interaction which involves interleukin *Il1rn* gene. *Il1rn* is the gene encoding interleukin 1receptor antagonist (IL-1RA) (440) and research has shown that *Il1rn* levels are upregulated in diet-induced obesity (441). High levels of IL-1RA are compatible with the biology of obesity and metabolic disease (442), hence these results corroborate previous findings in this field by Boland et al., suggesting that simvastatin exerts anti-inflammatory effects adding potentially greater benefit for the treatment of cardiovascular and metabolic diseases outside of statins well recognized lipid lowering effects. Pathway enrichment analysis revealed that the presence of simvastatin caused upregulate terpenoid backbone biosynthesis. Terpenoids are known to have anti-inflammatory and immunomodulary properties (443), thus this finding further supports the beneficiary effects of statin as anti-inflammatory compounds.

Overall, the current study has gone some way towards enhancing our existing knowledge regarding the anti-inflammatory effects of Aquamin and simvastatin. Based upon the fact that Aquamin exerted notably more potent inhibitory effects on IL-1β and TNF-α as well as significantly higher number of DEGs compared to simvastatin treatment it is therefore interesting to further explore Aquamin effects in health and disease. Aquamin is a nutraceutical and although it would not replace statins as a conventional therapy in cardiovascular disease and atherosclerosis, intake of Aquamin in combination with administration of statins as pharmaceutical agents would potentially maximize the effect and minimize the risk of statin therapy through dose reduction of statin therapy.

As demonstrated in chapter 4, Aquamin displayed significant reduction of pro-inflammatory cytokines under NLRP3 stimulated

conditions which was strikingly more potent than the reduction caused by simvastatin treatment. To further support our findings, we stimulated human PBMCs with LPS and CC and we investigated the effect of Aquamin and simvastatin treatment. Interestingly, Aquamin consistently achieved a more significant reduction of IL-1β and TNF-α compared to simvastatin. Again, based upon the fact that Aquamin is a nutraceutical and not a pharmaceutical agent, the co-supplementation of simvastatin with dietary intake of Aquamin could reduce the cardiometabolic risk. To that end we assessed the synergistic effect of Aquamin and simvastatin in PBMCs under the same conditions. Our results indicated that synergy of Aquamin and simvastatin induced a robust inhibitory effect in the protein expression of TNF-α and IL-1β in vitro, which remained consistent even when lower concentrations of statin were used. Previous research by Zhang et al. evaluated the toxicity levels of Aquamin in vivo using male and female rats and confirmed that Aquamin is a non-toxic substance (444). Therefore, the synergistic effects of statins along with simultaneous dietary intake of Aquamin in humans might be a research question that could be asked in future studies.

Prompted by the promising results of Aquamin in vitro we decided to explore how Aquamin might regulate obesity and metabolic disease and examined what role, if any, this nutraceutical might play as a protective compound in disease pathogenesis in mice subjected to HFD. We used C57BL/6J mice fed a HFD and obesity readouts such as weight gain with simultaneous monitoring of water and food intake were assessed in mice that received HFD supplemented with and without Aquamin. Even though our results were unable to demonstrate significant results from Aquamin incorporation into the diet, the interpretation of data implies that there is a tendency for weight gain reduction in mice that receive HFD with Aquamin.

Increased adiposity is linked with insulin resistance and glucose tolerance. Mice fed a HFD withAquamin exhibited similar levels of adipose tissue mass with a tendency towards improvements in glucose and insulin intolerancecompared to mice that received HFD without Aquamin. An unanticipated finding was no significant differences in the gene expression of inflammatory mediators involved in obesity-dependent metabolic disease, when adipose tissue of mice that received HFD was compared to those that received HFD with Aquamin. The reader should bear in mind that the exposure to HFD was for 10 weeks, while a previous study in this field was carried out for 4 months to achieve weight gain (411). Furthermore, due to practical constraints associated with low number of samples, this study cannot provide a comprehensive image as far as the effect of Aquamin in vivo is concerned and therefore a deeper investigation including higher number of mice and longer duration of exposure is warranted.

Collectively, the results observed in this thesis mirror those of the previous studies that have examined the effect of Aquamin in LPS driven cells. The most obvious finding to emerge here is that Aquamin exerts significant anti-inflammatory effects in a variety of innate immune cells, and it also extends our knowledge with respect to the mechanism of action of the nutraceutical. It also sheds light to additional pathways modulated by Aquamin and compares it to existing conventional pharmacotherapy of cardiovascular and metabolic disease such as simvastatin. Finally, notwithstanding the apparent limitations of the in vivo study we have demonstrated that Aquamin could potentially exert a beneficiary role in diet-induced obesity. When further research is undertaken, the synergy of Aquamin and statin in vivo should be assessed in the context of cardiovascular and metabolic disease.

6.2 Future directions

This thesis was undertaken to investigate the immunomodulary role of Aquamin in vitro using predominantly murine macrophages in the context of obesity and metabolic disease.

Future studies could fruitfully explore the exact mechanism that Aquamin modulates inflammation further by focusing on TRIF-dependent TLR signaling pathway. Although it was demonstrated that Aquamin significantly blocks nuclear translocation of IRF3 as well as the gene expression of IFN-β downstream of TRIF, future work investigating the phorphorylated levels of IRF3 under LPS and Poly(I:C) stimulation by WB should be conducted. Future research should further test the effect of Aquamin on the NF-κB pathway. Transfection of NF-KB luciferase HEK-293reporter cells or IRF3 reporter cell lines with TRAF3 and TRAF6 which are signaling molecules that regulate NF-κB and IRF3 activation could be an interesting approach for future work. TRAF6 is known to be detected in most TLRs and is associated with the activation of NF-κB and IRF7, while TRAF3-dependent pathway includes the activation of IRF3 and IRF7 (445). Treatment of transfected cells with different concentrations of Aquamin could be done and then measurement of the luciferace activities may be carried out. That study could further disentangle the complexities of TLR. To rule out the possibility that Aquamin exerts its anti-inflammatory effects by blocking MyD88-dependent TLR signaling, macrophages can be pretreated with Aquamin and exposure of cells with additional ligands of TLRs can be done, followed by measurement of TNF-α and IL-6 by ELISA and RT-PCR.

RNA-seq analysis provided evidence that Aquamin triggers the enrichment of several pathways. KEGG pathway enrichment analysis demonstrated that one of the most significantly enriched pathways resulted from Aquamin treatment is IL-17 signaling

pathway. This result provides a good starting point for further research that will unveil the correlation between Aquamin and IL-17 pathway.

Metabolic syndrome is a major contributor of heart disease. As part of this thesis, we were initially planning to investigate whether Aquamin affects inflammation-induced cardiomyocyte dysfunction in vivo. However, due to setbacks resulted from the pandemics, this project was discontinued. A recommendation for future in vitro work would be the exposure of AC16 human cardiomyocytes to Angiotensin II which is a potent vasoconstrictor to assess the effect of Aquamin in these hypertrophic AC16 cells. Initially gene expression of cardiac hypertrophy markers (atrial natriuretic peptide, brain natriuretic peptide, β-MHC) could be used as readouts to confirm Ang II induced hypertrophiceffects. Immunostaining with alpha actin can also be conducted to measure changes in morphology and cellular size. Once the model is established future research could focus on changes in the above markers under Aquamin treatment. As remodeling in heart failure is recognized as an inflammatory environment, the assessment of the Ang II model in the presence of inflammatory cytokines such as TNF alpha and IL-1 beta is also investigated for significant changes when treated with Aquamin, would be interesting.

Looking forward, a number of possible future studies using the same experimental in vivo set up of DIO as utilized in studies presented in this thesis may be of benefit. However, inclusion of more samples as well as a longer duration of exposure to HFD could optimize the setting and prove more informative to Aquamins effects since. Another possible area of future research would be to evaluate the effects of Aquamin supplementation on cardiac failure using a relevant animal model of the disease if results from in vitro cellular studies prove beneficial. Along similar lines with the exposure of cardiac myocytes to Angiotensin II for the in vitro

model, infusion of mice with Angiotensin II could induce a hypertension and cardiac hypertrophy phenotype in vivo. Heart tissue could be harvested for immunohistochemistry analysis and gene expression of relative factors. Altogether these future studies would more precisely map the molecular mechanism of action for Aquamin and measure its potential at improving cardiometabolic disease.

REFERENCES

1. Malakar AK, Choudhury D, Halder B, Paul P, Uddin A, Chakraborty S. A review on coronary artery disease, its risk factors, and therapeutics. J Cell Physiol. 2019;234(10):16812-23.
2. Hotamisligil GS. Inflammation and metabolic disorders. Nature. 2006;444(7121):860-7.
3. Bruce KD, Byrne CD. The metabolic syndrome: common origins of a multifactorial disorder. Postgraduate Medical Journal. 2009;85(1009):614-21.
4. Kim Y, Keogh J, Clifton PM. Nuts and Cardio-Metabolic Disease: A Review of Meta-Analyses. Nutrients. 2018;10(12):1935.
5. Kolb H. Obese visceral fat tissue inflammation: from protective to detrimental? BMC Medicine. 2022;20(1):494.
6. Tylutka A, Morawin B, Walas Ł, Michałek M, Gwara A, Zembron-Lacny A. Assessment of metabolic syndrome predictors in relation to inflammation and visceral fat tissue in older adults. Scientific Reports. 2023;13(1):89.
7. Boden G, Shulman GI. Free fatty acids in obesity and type 2 diabetes: defining their role in the development of insulin resistance and beta-cell dysfunction. European journal of clinical investigation. 2002;32 Suppl 3:14-23.
8. Tripathy D, Mohanty P, Dhindsa S, Syed T, Ghanim H, Aljada A, et al. Elevation of free fatty acids induces inflammation and impairs vascular reactivity in healthy subjects. Diabetes. 2003;52(12):2882-7.
9. Rochlani Y, Pothineni NV, Kovelamudi S, Mehta JL. Metabolic syndrome: pathophysiology, management, and modulation by natural compounds. Therapeutic advances in cardiovascular disease. 2017;11(8):215-25.
10. Poetsch MS, Strano A, Guan K. Role of Leptin in Cardiovascular Diseases. Frontiers in endocrinology. 2020;11:354.
11. Ouchi N, Ohishi M, Kihara S, Funahashi T, Nakamura T, Nagaretani H, et al. Association of hypoadiponectinemia with impaired vasoreactivity. Hypertension (Dallas, Tex : 1979). 2003;42(3):231-4.
12. Pischon T, Girman CJ, Hotamisligil GS, Rifai N, Hu FB, Rimm EB. Plasma adiponectin levels and risk of myocardial infarction in men. Jama. 2004;291(14):1730-7.
13. Lindsay RS, Funahashi T, Hanson RL, Matsuzawa Y, Tanaka S, Tataranni PA, et al. Adiponectin and development of type 2 diabetes in the Pima Indian population. Lancet (London, England). 2002;360(9326):57-8.
14. Tripathy D, Mohanty P, Dhindsa S, Syed T, Ghanim H, Aljada A, et al. Elevation of Free Fatty Acids Induces Inflammation

and Impairs Vascular Reactivity in Healthy Subjects. Diabetes. 2003;52(12):2882-7.
15. Ucak S, Basat O, Satir E, Altuntas Y. Evaluation of various insulin sensitivity indices in lean idiopathic hirsutism patients. Endocrine journal. 2012;59(4):291-6.
16. Hřebíček Ji, Janout Vr, Malinčíková J, Horáková D, Čížek Lk. Detection of Insulin Resistance by Simple Quantitative Insulin Sensitivity Check Index QUICKI for Epidemiological Assessment and Prevention. The Journal of Clinical Endocrinology & Metabolism. 2002;87(1):144-.
17. Matthews DR, Hosker JP, Rudenski AS, Naylor BA, Treacher DF, Turner RC. Homeostasis model assessment: insulin resistance and β-cell function from fasting plasma glucose and insulin concentrations in man. Diabetologia. 1985;28(7):412-9.
18. Vaněčková I, Maletínská L, Behuliak M, Nagelová V, Zicha J, Kuneš J. Obesity-related hypertension: possible pathophysiological mechanisms. The Journal of endocrinology. 2014;223(3):R63-78.
19. Gobal F, Deshmukh A, Shah S, Mehta JL. Triad of metabolic syndrome, chronic kidney disease, and coronary heart disease with a focus on microalbuminuria death by overeating. J Am Coll Cardiol. 2011;57(23):2303-8.
20. Dai Y, Mercanti F, Dai D, Wang X, Ding Z, Pothineni NV, et al. LOX-1, a bridge between GLP-1R and mitochondrial ROS generation in human vascular smooth muscle cells. Biochemical and biophysical research communications. 2013;437(1):62-6.
21. Eckel RH, Grundy SM, Zimmet PZ. The metabolic syndrome. The Lancet. 2005;365(9468):1415-28.
22. McCracken E, Monaghan M, Sreenivasan S. Pathophysiology of the metabolic syndrome. Clinics in Dermatology. 2018;36(1):14-20.
23. Samson SL, Garber AJ. Metabolic Syndrome. Endocrinology and Metabolism Clinics. 2014;43(1):1-23.
24. Gohil BC, Rosenblum LA, Coplan JD, Kral JG. Hypothalamic-pituitary-adrenal axis function and the metabolic syndrome X of obesity. CNS spectrums. 2001;6(7):581-6, 9.
25. Tsigos C, Chrousos GP. Hypothalamic-pituitary-adrenal axis, neuroendocrine factors and stress. Journal of psychosomatic research. 2002;53(4):865-71.
26. Rosmond R, Björntorp P. The hypothalamic-pituitary-adrenal axis activity as a predictor of cardiovascular disease, type 2 diabetes and stroke. Journal of internal medicine. 2000;247(2):188-97.
27. Considine RV, Sinha MK, Heiman ML, Kriauciunas A, Stephens TW, Nyce MR, et al. Serum immunoreactive-leptin concentrations in normal-weight and obese humans. The New England journal of medicine. 1996;334(5):292-5.

28. Berglund ED, Vianna CR, Donato J, Jr., Kim MH, Chuang JC, Lee CE, et al. Direct leptin action on POMC neurons regulates glucose homeostasis and hepatic insulin sensitivity in mice. J Clin Invest. 2012;122(3):1000-9.
29. Obradovic M, Sudar-Milovanovic E, Soskic S, Essack M, Arya S, Stewart AJ, et al. Leptin and Obesity: Role and Clinical Implication. Frontiers in endocrinology. 2021;12:585887.
30. Yamauchi T, Kamon J, Waki H, Imai Y, Shimozawa N, Hioki K, et al. Globular adiponectin protected ob/ob mice from diabetes and ApoE-deficient mice from atherosclerosis. The Journal of biological chemistry. 2003;278(4):2461-8.
31. Esteve E, Ricart W, Fernández-Real JM. Adipocytokines and insulin resistance: the possible role of lipocalin-2, retinol binding protein-4, and adiponectin. Diabetes Care. 2009;32 Suppl 2(Suppl 2):S362-7.
32. Yamauchi T, Kamon J, Waki H, Terauchi Y, Kubota N, Hara K, et al. The fat-derived hormone adiponectin reverses insulin resistance associated with both lipoatrophy and obesity. Nat Med. 2001;7(8):941-6.
33. Ouchi N, Kihara S, Arita Y, Nishida M, Matsuyama A, Okamoto Y, et al. Adipocyte-derived plasma protein, adiponectin, suppresses lipid accumulation and class A scavenger receptor expression in human monocyte-derived macrophages. Circulation. 2001;103(8):1057-63.
34. Kondo H, Shimomura I, Matsukawa Y, Kumada M, Takahashi M, Matsuda M, et al. Association of adiponectin mutation with type 2 diabetes: a candidate gene for the insulin resistance syndrome. Diabetes. 2002;51(7):2325-8.
35. Buechler C, Feder S, Haberl EM, Aslanidis C. Chemerin Isoforms and Activity in Obesity. International journal of molecular sciences. 2019;20(5).
36. Jialal I, Devaraj S, Kaur H, Adams-Huet B, Bremer AA. Increased chemerin and decreased omentin-1 in both adipose tissue and plasma in nascent metabolic syndrome. J Clin Endocrinol Metab. 2013;98(3):E514-7.
37. Wang D, Yuan GY, Wang XZ, Jia J, Di LL, Yang L, et al. Plasma chemerin level in metabolic syndrome. Genetics and molecular research : GMR. 2013;12(4):5986-91.
38. Dong B, Ji W, Zhang Y. Elevated serum chemerin levels are associated with the presence of coronary artery disease in patients with metabolic syndrome. Internal medicine (Tokyo, Japan). 2011;50(10):1093-7.
39. Chu SH, Lee MK, Ahn KY, Im JA, Park MS, Lee DC, et al. Chemerin and adiponectin contribute reciprocally to metabolic syndrome. PloS one. 2012;7(4):e34710.

40. Shi H, Kokoeva MV, Inouye K, Tzameli I, Yin H, Flier JS. TLR4 links innate immunity and fatty acid-induced insulin resistance. J Clin Invest. 2006;116(11):3015-25.
41. Himes RW, Smith CW. Tlr2 is critical for diet-induced metabolic syndrome in a murine model. FASEB journal : official publication of the Federation of American Societies for Experimental Biology. 2010;24(3):731-9.
42. Bennett JM, Reeves G, Billman GE, Sturmberg JP. Inflammation–Nature's Way to Efficiently Respond to All Types of Challenges: Implications for Understanding and Managing "the Epidemic" of Chronic Diseases. Frontiers in Medicine. 2018;5.
43. Kawai T, Akira S. The role of pattern-recognition receptors in innate immunity: update on Toll-like receptors. Nature Immunology. 2010;11(5):373-84.
44. Takeuchi O, Akira S. Pattern Recognition Receptors and Inflammation. Cell. 2010;140(6):805-20.
45. Hannoodee S, Nasuruddin DN. Acute Inflammatory Response. StatPearls. Treasure Island (FL): StatPearls Publishing Copyright © 2023, StatPearls Publishing LLC.; 2023.
46. Branco A, Yoshikawa FSY. Role of Histamine in Modulating the Immune Response and Inflammation. 2018;2018:9524075.
47. Wang H, Kohno T, Amaya F, Brenner GJ, Ito N, Allchorne A, et al. Bradykinin produces pain hypersensitivity by potentiating spinal cord glutamatergic synaptic transmission. The Journal of neuroscience : the official journal of the Society for Neuroscience. 2005;25(35):7986-92.
48. Dubin AE, Patapoutian A. Nociceptors: the sensors of the pain pathway. J Clin Invest. 2010;120(11):3760-72.
49. Webster JI, Tonelli L, Sternberg EM. Neuroendocrine Regulation of Immunity. Annual review of immunology. 2002;20(1):125-63.
50. Barnes PJ, Karin M. Nuclear Factor-κB — A Pivotal Transcription Factor in Chronic Inflammatory Diseases. New England Journal of Medicine. 1997;336(15):1066-71.
51. Cole SW. Social Regulation of Human Gene Expression: Mechanisms and Implications for Public Health. American journal of public health. 2013;103(S1):S84-S92.
52. Mraz M, Haluzik M. The role of adipose tissue immune cells in obesity and low-grade inflammation. Journal of Endocrinology. 2014;222(3):R113-R27.
53. Nteeba J, Ortinau LC, Perfield JW, 2nd, Keating AF. Diet-induced obesity alters immune cell infiltration and expression of inflammatory cytokine genes in mouse ovarian and peri-ovarian adipose depot tissues. Molecular reproduction and development. 2013;80(11):948-58.
54. Choquet H, Meyre D. Genetics of Obesity: What have we Learned? Current genomics. 2011;12(3):169-79.

55. Herrera BM, Lindgren CM. The genetics of obesity. Current diabetes reports. 2010;10(6):498-505.
56. Parlee SD, MacDougald OA. Maternal nutrition and risk of obesity in offspring: the Trojan horse of developmental plasticity. Biochimica et biophysica acta. 2014;1842(3):495-506.
57. Lin X, Li H. Obesity: Epidemiology, Pathophysiology, and Therapeutics. Frontiers in endocrinology. 2021;12:706978.
58. Fuster JJ, Ouchi N, Gokce N, Walsh K. Obesity-Induced Changes in Adipose Tissue Microenvironment and Their Impact on Cardiovascular Disease. Circulation research. 2016;118(11):1786-807.
59. Suleiman JB, Mohamed M, Bakar ABA. A systematic review on different models of inducing obesity in animals: Advantages and limitations. Journal of advanced veterinary and animal research. 2020;7(1):103-14.
60. Chanclón B, Wu Y, Vujičić M, Bauzá-Thorbrügge M, Banke E, Micallef P, et al. Peripancreatic adipose tissue protects against high-fat-diet-induced hepatic steatosis and insulin resistance in mice. International Journal of Obesity. 2020;44(11):2323-34.
61. Sarwar R, Pierce N, Koppe S. Obesity and nonalcoholic fatty liver disease: current perspectives. Diabetes, metabolic syndrome and obesity : targets and therapy. 2018;11:533-42.
62. Schiavo L, Busetto L, Cesaretti M, Zelber-Sagi S, Deutsch L, Iannelli A. Nutritional issues in patients with obesity and cirrhosis. World journal of gastroenterology. 2018;24(30):3330-46.
63. Zhu P, Herrington WG, Haynes R, Emberson J, Landray MJ, Sudlow CLM, et al. Conventional and Genetic Evidence on the Association between Adiposity and CKD. Journal of the American Society of Nephrology. 2021;32(1):127-37.
64. Anjum I, Fayyaz M, Wajid A, Sohail W, Ali A. Does Obesity Increase the Risk of Dementia: A Literature Review. Cureus. 2018;10(5):e2660.
65. Kivipelto M, Ngandu T, Fratiglioni L, Viitanen M, Kåreholt I, Winblad B, et al. Obesity and vascular risk factors at midlife and the risk of dementia and Alzheimer disease. Archives of neurology. 2005;62(10):1556-60.
66. Gorospe EC, Dave JK. The risk of dementia with increased body mass index. Age and ageing. 2007;36(1):23-9.
67. Lumeng CN, Saltiel AR. Inflammatory links between obesity and metabolic disease. J Clin Invest. 2011;121(6):2111-7.
68. Medzhitov R. Inflammation 2010: new adventures of an old flame. Cell. 2010;140(6):771-6.
69. Ferrero-Miliani L, Nielsen OH, Andersen PS, Girardin SE. Chronic inflammation: importance of NOD2 and NALP3 in interleukin-1beta generation. Clinical and experimental immunology. 2007;147(2):227-35.

70. Nathan C, Ding A. Nonresolving inflammation. Cell. 2010;140(6):871-82.
71. Zhou Y, Hong Y, Huang H. Triptolide Attenuates Inflammatory Response in Membranous Glomerulo-Nephritis Rat via Downregulation of NF-κB Signaling Pathway. Kidney & blood pressure research. 2016;41(6):901-10.
72. Furman D, Campisi J, Verdin E, Carrera-Bastos P, Targ S, Franceschi C, et al. Chronic inflammation in the etiology of disease across the life span. Nature Medicine. 2019;25(12):1822-32.
73. Majka Z, Czamara K, Janus J, Kępczyński M, Kaczor A. Prominent hypertrophy of perivascular adipocytes due to short-term high fat diet. Biochimica et Biophysica Acta (BBA) - Molecular Basis of Disease. 2022;1868(2):166315.
74. Kern L, Mittenbühler MJ, Vesting AJ, Ostermann AL, Wunderlich CM, Wunderlich FT. Obesity-Induced TNFα and IL-6 Signaling: The Missing Link between Obesity and Inflammation-Driven Liver and Colorectal Cancers. Cancers. 2018;11(1).
75. Boutens L, Stienstra R. Adipose tissue macrophages: going off track during obesity. Diabetologia. 2016;59(5):879-94.
76. Weisberg SP, McCann D, Desai M, Rosenbaum M, Leibel RL, Ferrante AW, Jr. Obesity is associated with macrophage accumulation in adipose tissue. J Clin Invest. 2003;112(12):1796-808.
77. Xu H, Barnes GT, Yang Q, Tan G, Yang D, Chou CJ, et al. Chronic inflammation in fat plays a crucial role in the development of obesity-related insulin resistance. J Clin Invest. 2003;112(12):1821-30.
78. Stith RD, Luo J. Endocrine and carbohydrate responses to interleukin-6 in vivo. Circulatory shock. 1994;44(4):210-5.
79. Tsigos C, Papanicolaou DA, Kyrou I, Defensor R, Mitsiadis CS, Chrousos GP. Dose-dependent effects of recombinant human interleukin-6 on glucose regulation. J Clin Endocrinol Metab. 1997;82(12):4167-70.
80. Araújo EP, De Souza CuT, Ueno M, Cintra DE, Bertolo MB, Carvalheira JB, et al. Infliximab Restores Glucose Homeostasis in an Animal Model of Diet-Induced Obesity and Diabetes. Endocrinology. 2007;148(12):5991-7.
81. Gonzalez-Gay MA, De Matias JM, Gonzalez-Juanatey C, Garcia-Porrua C, Sanchez-Andrade A, Martin J, et al. Anti-tumor necrosis factor-alpha blockade improves insulin resistance in patients with rheumatoid arthritis. Clinical and experimental rheumatology. 2006;24(1):83-6.
82. Dominguez H, Storgaard H, Rask-Madsen C, Steffen Hermann T, Ihlemann N, Baunbjerg Nielsen D, et al. Metabolic and Vascular Effects of Tumor Necrosis Factor-α Blockade with Etanercept in Obese Patients with Type 2 Diabetes. Journal of Vascular Research. 2005;42(6):517-25.

83. Xiao TS. Innate immunity and inflammation. Cell Mol Immunol. 2017;14(1):1-3.
84. Akira S, Uematsu S, Takeuchi O. Pathogen Recognition and Innate Immunity. Cell. 2006;124(4):783-801.
85. Stokel-Walker C. What do we know about the adaptive immune response to covid-19? BMJ. 2023;380:p19.
86. Diamond MS, Kanneganti T-D. Innate immunity: the first line of defense against SARS-CoV-2. Nature Immunology. 2022;23(2):165-76.
87. Cui J, Chen Y, Wang HY, Wang RF. Mechanisms and pathways of innate immune activation and regulation in health and cancer. Human vaccines & immunotherapeutics. 2014;10(11):3270-85.
88. Kruger P, Saffarzadeh M, Weber AN, Rieber N, Radsak M, von Bernuth H, et al. Neutrophils: Between host defence, immune modulation, and tissue injury. PLoS pathogens. 2015;11(3):e1004651.
89. Häger M, Cowland JB, Borregaard N. Neutrophil granules in health and disease. Journal of internal medicine. 2010;268(1):25-34.
90. Gasteiger G, apos, Osualdo A, Schubert DA, Weber A, Bruscia EM, et al. Cellular Innate Immunity: An Old Game with New Players. Journal of Innate Immunity. 2016;9(2):111-25.
91. Mázló A, Jenei V, Burai S, Molnár T, Bácsi A, Koncz G. Types of necroinflammation, the effect of cell death modalities on sterile inflammation. Cell Death & Disease. 2022;13(5):423.
92. Yipp BG, Kubes P. NETosis: how vital is it? Blood. 2013;122(16):2784-94.
93. Brinkmann V, Reichard U, Goosmann C, Fauler B, Uhlemann Y, Weiss DS, et al. Neutrophil extracellular traps kill bacteria. Science (New York, NY). 2004;303(5663):1532-5.
94. Eiz-Vesper B, Schmetzer HM. Antigen-Presenting Cells: Potential of Proven und New Players in Immune Therapies. Transfusion medicine and hemotherapy : offizielles Organ der Deutschen Gesellschaft fur Transfusionsmedizin und Immunhamatologie. 2020;47(6):429-31.
95. Shortman K, Liu Y-J. Mouse and human dendritic cell subtypes. Nature Reviews Immunology. 2002;2(3):151-61.
96. Jarrossay D, Napolitani G, Colonna M, Sallusto F, Lanzavecchia A. Specialization and complementarity in microbial molecule recognition by human myeloid and plasmacytoid dendritic cells. European Journal of Immunology. 2001;31(11):3388-93.
97. Szabo A, Rajnavolgyi E. Collaboration of Toll-like and RIG-I-like receptors in human dendritic cells: tRIGgering antiviral innate immune responses. American journal of clinical and experimental immunology. 2013;2(3):195-207.

98. Marcenaro E, Carlomagno S, Pesce S, Moretta A, Sivori S. NK/DC crosstalk in anti-viral response. Advances in experimental medicine and biology. 2012;946:295-308.
99. Kawai T, Akira S. The role of pattern-recognition receptors in innate immunity: update on Toll-like receptors. Nat Immunol. 2010;11(5):373-84.
100. Takeuchi O, Akira S. Pattern recognition receptors and inflammation. Cell. 2010;140(6):805-20.
101. Paludan SR, Bowie AG. Immune sensing of DNA. Immunity. 2013;38(5):870-80.
102. Iwasaki A, Medzhitov R. Toll-like receptor control of the adaptive immune responses. Nat Immunol. 2004;5(10):987-95.
103. Takeda K, Akira S. Toll-like receptors in innate immunity. International immunology. 2005;17(1):1-14.
104. Bonilla FA, Oettgen HC. Adaptive immunity. The Journal of allergy and clinical immunology. 2010;125(2 Suppl 2):S33-40.
105. Gonzalez S, González-Rodríguez AP, Suárez-Álvarez B, López-Soto A, Huergo-Zapico L, Lopez-Larrea C. Conceptual aspects of self and nonself discrimination. Self/nonself. 2011;2(1):19-25.
106. Wang H, Zúñiga-Pflücker JC. Thymic Microenvironment: Interactions Between Innate Immune Cells and Developing Thymocytes. Frontiers in Immunology. 2022;13.
107. Gaudino SJ, Kumar P. Cross-Talk Between Antigen Presenting Cells and T Cells Impacts Intestinal Homeostasis, Bacterial Infections, and Tumorigenesis. Frontiers in Immunology. 2019;10.
108. Roche PA, Furuta K. The ins and outs of MHC class II-mediated antigen processing and presentation. Nature Reviews Immunology. 2015;15(4):203-16.
109. Al-Shura AN. 7 - Lymphocytes. In: Al-Shura AN, editor. Advanced Hematology in Integrated Cardiovascular Chinese Medicine: Academic Press; 2020. p. 41-6.
110. Burren OS, Rubio García A, Javierre B-M, Rainbow DB, Cairns J, Cooper NJ, et al. Chromosome contacts in activated T cells identify autoimmune disease candidate genes. Genome Biology. 2017;18(1):165.
111. Roland Osei S, Precious B, Samuel Victor N. The Interactive Role of Macrophages in Innate Immunity. In: Vijay K, editor. Macrophages. Rijeka: IntechOpen; 2022. p. Ch. 3.
112. Cole J, Aberdein J, Jubrail J, Dockrell DH. Chapter Four - The Role of Macrophages in the Innate Immune Response to Streptococcus pneumoniae and Staphylococcus aureus: Mechanisms and Contrasts. In: Poole RK, editor. Advances in Microbial Physiology. 65: Academic Press; 2014. p. 125-202.
113. Fujiwara N, Kobayashi K. Macrophages in inflammation. Current drug targets Inflammation and allergy. 2005;4(3):281-6.

114. Sunderkötter C, Nikolic T, Dillon MJ, Van Rooijen N, Stehling M, Drevets DA, et al. Subpopulations of mouse blood monocytes differ in maturation stage and inflammatory response. J Immunol. 2004;172(7):4410-7.
115. van den Berg TK, Kraal G. A function for the macrophage F4/80 molecule in tolerance induction. Trends in Immunology. 2005;26(10):506-9.
116. Barker RN, Erwig LP, Hill KS, Devine A, Pearce WP, Rees AJ. Antigen presentation by macrophages is enhanced by the uptake of necrotic, but not apoptotic, cells. Clinical and experimental immunology. 2002;127(2):220-5.
117. Yao Y, Xu XH, Jin L. Macrophage Polarization in Physiological and Pathological Pregnancy. Front Immunol. 2019;10:792.
118. Li D, Wu M. Pattern recognition receptors in health and diseases. Signal Transduction and Targeted Therapy. 2021;6(1):291.
119. Liu J, Geng X, Hou J, Wu G. New insights into M1/M2 macrophages: key modulators in cancer progression. Cancer Cell International. 2021;21(1):389.
120. Uribe-Querol E, Rosales C. Phagocytosis: Our Current Understanding of a Universal Biological Process. Frontiers in Immunology. 2020;11.
121. Patente TA, Pinho MP, Oliveira AA, Evangelista GCM, Bergami-Santos PC, Barbuto JAM. Human Dendritic Cells: Their Heterogeneity and Clinical Application Potential in Cancer Immunotherapy. Frontiers in Immunology. 2019;9.
122. Muñoz-Rojas AR, Kelsey I, Pappalardo JL, Chen M, Miller-Jensen K. Co-stimulation with opposing macrophage polarization cues leads to orthogonal secretion programs in individual cells. Nature Communications. 2021;12(1):301.
123. Linke M, Pham HT, Katholnig K, Schnöller T, Miller A, Demel F, et al. Chronic signaling via the metabolic checkpoint kinase mTORC1 induces macrophage granuloma formation and marks sarcoidosis progression. 2017;18(3):293-302.
124. Bah A, Vergne I. Macrophage Autophagy and Bacterial Infections. Front Immunol. 2017;8:1483.
125. Budinger GRS, Kohanski RA, Gan W, Kobor MS, Amaral LA, Armanios M, et al. The Intersection of Aging Biology and the Pathobiology of Lung Diseases: A Joint NHLBI/NIA Workshop. The journals of gerontology Series A, Biological sciences and medical sciences. 2017;72(11):1492-500.
126. Linehan E, Fitzgerald DC. Ageing and the immune system: focus on macrophages. European journal of microbiology & immunology. 2015;5(1):14-24.

127. Dick SA, Macklin JA. Self-renewing resident cardiac macrophages limit adverse remodeling following myocardial infarction. 2019;20(1):29-39.
128. Frantz S, Nahrendorf M. Cardiac macrophages and their role in ischaemic heart disease. Cardiovasc Res. 2014;102(2):240-8.
129. Hulsmans M, Clauss S, Xiao L, Aguirre AD, King KR, Hanley A, et al. Macrophages Facilitate Electrical Conduction in the Heart. Cell. 2017;169(3):510-22.e20.
130. Bajpai G, Bredemeyer A, Li W, Zaitsev K, Koenig AL, Lokshina I, et al. Tissue Resident CCR2- and CCR2+ Cardiac Macrophages Differentially Orchestrate Monocyte Recruitment and Fate Specification Following Myocardial Injury. Circulation research. 2019;124(2):263-78.
131. Panizzi P, Swirski FK, Figueiredo JL, Waterman P, Sosnovik DE, Aikawa E, et al. Impaired infarct healing in atherosclerotic mice with Ly-6C(hi) monocytosis. J Am Coll Cardiol. 2010;55(15):1629-38.
132. Hanna RN, Shaked I, Hubbeling HG, Punt JA, Wu R, Herrley E, et al. NR4A1 (Nur77) deletion polarizes macrophages toward an inflammatory phenotype and increases atherosclerosis. Circulation research. 2012;110(3):416-27.
133. Woollard KJ, Geissmann F. Monocytes in atherosclerosis: subsets and functions. Nat Rev Cardiol. 2010;7(2):77-86.
134. Moore KJ, Sheedy FJ, Fisher EA. Macrophages in atherosclerosis: a dynamic balance. Nature reviews Immunology. 2013;13(10):709-21.
135. Orekhov AN, Orekhova VA, Nikiforov NG, Myasoedova VA, Grechko AV, Romanenko EB, et al. Monocyte differentiation and macrophage polarization. Vessel Plus. 2019;3:10.
136. Rana JS, Nieuwdorp M, Jukema JW, Kastelein JJP. Cardiovascular metabolic syndrome – an interplay of, obesity, inflammation, diabetes and coronary heart disease. Diabetes, Obesity and Metabolism. 2007;9(3):218-32.
137. Alshehri AM. Metabolic syndrome and cardiovascular risk. Journal of family & community medicine. 2010;17(2):73-8.
138. Bell JK, Mullen GED, Leifer CA, Mazzoni A, Davies DR, Segal DM. Leucine-rich repeats and pathogen recognition in Toll-like receptors. Trends in Immunology. 2003;24(10):528-33.
139. Kawai T, Akira S. TLR signaling. Cell Death & Differentiation. 2006;13(5):816-25.
140. Horng T, Barton GM, Medzhitov R. TIRAP: an adapter molecule in the Toll signaling pathway. Nat Immunol. 2001;2(9):835-41.
141. Vallejo Jesus G. Role of Toll-like receptors in cardiovascular diseases. Clinical Science. 2011;121(1):1-10.

142. Jialal I, Kaur H, Devaraj S. Toll-like Receptor Status in Obesity and Metabolic Syndrome: A Translational Perspective. The Journal of Clinical Endocrinology & Metabolism. 2014;99(1):39-48.
143. Katare PB, Banerjee SK. Repositioning of Drugs in Cardiometabolic Disorders: Importance and Current Scenario. Current topics in medicinal chemistry. 2016;16(19):2189-200.
144. Mbongue JC, Nieves HA, Torrez TW, Langridge WHR. The Role of Dendritic Cell Maturation in the Induction of Insulin-Dependent Diabetes Mellitus. Frontiers in Immunology. 2017;8(327).
145. Park BS, Lee J-O. Recognition of lipopolysaccharide pattern by TLR4 complexes. Experimental & Molecular Medicine. 2013;45(12):e66-e.
146. Takeuchi O, Sato S, Horiuchi T, Hoshino K, Takeda K, Dong Z, et al. Cutting Edge: Role of Toll-Like Receptor 1 in Mediating Immune Response to Microbial Lipoproteins. The Journal of Immunology. 2002;169(1):10-4.
147. Farhat K, Riekenberg S, Heine H, Debarry J, Lang R, Mages J, et al. Heterodimerization of TLR2 with TLR1 or TLR6 expands the ligand spectrum but does not lead to differential signaling. Journal of Leukocyte Biology. 2008;83(3):692-701.
148. Tsolmongyn B, Koide N, Jambalganiin U, Odkhuu E, Naiki Y, Komatsu T, et al. A Toll-like receptor 2 ligand, Pam3CSK4, augments interferon-γ-induced nitric oxide production via a physical association between MyD88 and interferon-γ receptor in vascular endothelial cells. Immunology. 2013;140(3):352-61.
149. Hayashi F, Smith KD, Ozinsky A, Hawn TR, Yi EC, Goodlett DR, et al. The innate immune response to bacterial flagellin is mediated by Toll-like receptor 5. Nature. 2001;410(6832):1099-103.
150. Hemmi H, Takeuchi O, Kawai T, Kaisho T, Sato S, Sanjo H, et al. A Toll-like receptor recognizes bacterial DNA. Nature. 2000;408(6813):740-5.
151. Wrba L, Halbgebauer R, Roos J, Huber-Lang M, Fischer-Posovszky P. Adipose tissue: a neglected organ in the response to severe trauma? 2022;79(4):207.
152. Crifo B, Taylor CT. Crosstalk between toll-like receptors and hypoxia-dependent pathways in health and disease. Journal of Investigative Medicine. 2016;64(2):369-75.
153. Wu J, Li L, Sun Y, Huang S, Tang J, Yu P, et al. Altered molecular expression of the TLR4/NF-κB signaling pathway in mammary tissue of Chinese Holstein cattle with mastitis. PloS one. 2015;10(2):e0118458.
154. Hirotani T, Yamamoto M, Kumagai Y, Uematsu S, Kawase I, Takeuchi O, et al. Regulation of lipopolysaccharide-inducible genes by MyD88 and Toll/IL-1 domain containing adaptor inducing IFN-

beta. Biochemical and biophysical research communications. 2005;328(2):383-92.
155. Yamamoto M, Sato S, Hemmi H, Uematsu S, Hoshino K, Kaisho T, et al. TRAM is specifically involved in the Toll-like receptor 4-mediated MyD88-independent signaling pathway. Nat Immunol. 2003;4(11):1144-50.
156. Dainichi T, Matsumoto R, Mostafa A, Kabashima K. Immune Control by TRAF6-Mediated Pathways of Epithelial Cells in the EIME (Epithelial Immune Microenvironment). Frontiers in Immunology. 2019;10.
157. Akira S. Toll-like Receptor Signaling *. Journal of Biological Chemistry. 2003;278(40):38105-8.
158. Milovanovic J, Arsenijevic A, Stojanovic B, Kanjevac T, Arsenijevic D, Radosavljevic G, et al. Interleukin-17 in Chronic Inflammatory Neurological Diseases. Front Immunol. 2020;11:947.
159. Ullah MO, Sweet MJ, Mansell A, Kellie S, Kobe B. TRIF-dependent TLR signaling, its functions in host defense and inflammation, and its potential as a therapeutic target. Journal of Leukocyte Biology. 2016;100(1):27-45.
160. Alexopoulou L, Holt AC, Medzhitov R, Flavell RA. Recognition of double-stranded RNA and activation of NF-κB by Toll-like receptor 3. Nature. 2001;413(6857):732-8.
161. Fitzgerald KA, McWhirter SM, Faia KL, Rowe DC, Latz E, Golenbock DT, et al. IKKε and TBK1 are essential components of the IRF3 signaling pathway. Nature Immunology. 2003;4(5):491-6.
162. Jiang Z, Mak TW, Sen G, Li X. Toll-like receptor 3-mediated activation of NF-κB and IRF3 diverges at Toll-IL-1 receptor domain-containing adapter inducing IFN-&#x3b2. Proceedings of the National Academy of Sciences. 2004;101(10):3533-8.
163. Dunlevy F, McElvaney N, Greene C. TLR3 Sensing of Viral Infection~!2009-10-01~!2010-03-30~!2010-04-28~! The Open Infectious Diseases Journal. 2010;4:1-10.
164. Cani PD, Bibiloni R, Knauf C, Waget A, Neyrinck AM, Delzenne NM, et al. Changes in Gut Microbiota Control Metabolic Endotoxemia-Induced Inflammation in High-Fat Diet–Induced Obesity and Diabetes in Mice. Diabetes. 2008;57(6):1470-81.
165. Saberi M, Woods N-B, de Luca C, Schenk S, Lu JC, Bandyopadhyay G, et al. Hematopoietic cell-specific deletion of toll-like receptor 4 ameliorates hepatic and adipose tissue insulin resistance in high-fat-fed mice. Cell Metab. 2009;10(5):419-29.
166. Shi H, Kokoeva MV, Inouye K, Tzameli I, Yin H, Flier JS. TLR4 links innate immunity and fatty acid-induced insulin resistance. J Clin Invest. 2006;116(11):3015-25.
167. Ahmad R, Al-Mass A, Atizado V, Al-Hubail A, Al-Ghimlas F, Al-Arouj M, et al. Elevated expression of the toll like receptors 2 and 4 in obese individuals: its significance for obesity-induced inflammation. J Inflamm (Lond). 2012;9(1):48-.

168. Hwang DH, Kim J-A, Lee JY. Mechanisms for the activation of Toll-like receptor 2/4 by saturated fatty acids and inhibition by docosahexaenoic acid. Eur J Pharmacol. 2016;785:24-35.
169. Caricilli AM, Nascimento PH, Pauli JR, Tsukumo DML, Velloso LA, Carvalheira JB, et al. Inhibition of toll-like receptor 2 expression improves insulin sensitivity and signaling in muscle and white adipose tissue of mice fed a high-fat diet. 2008;199(3):399.
170. Fan W, Morinaga H, Kim JJ, Bae E, Spann NJ, Heinz S, et al. FoxO1 regulates Tlr4 inflammatory pathway signalling in macrophages. The EMBO journal. 2010;29(24):4223-36.
171. Du S, Zheng H. Role of FoxO transcription factors in aging and age-related metabolic and neurodegenerative diseases. Cell & Bioscience. 2021;11(1):188.
172. Chen J, Lu Y, Tian M, Huang Q. Molecular mechanisms of FOXO1 in adipocyte differentiation. Journal of Molecular Endocrinology. 2019;62(3):R239-R53.
173. Graves DT, Milovanova TN. Mucosal Immunity and the FOXO1 Transcription Factors. Frontiers in Immunology. 2019;10.
174. Xing Y-q, Li A, Yang Y, Li X-x, Zhang L-n, Guo H-c. The regulation of FOXO1 and its role in disease progression. Life Sciences. 2018;193:124-31.
175. Liu L, Zheng LD, Zou P, Brooke J, Smith C, Long YC, et al. FoxO1 antagonist suppresses autophagy and lipid droplet growth in adipocytes. Cell Cycle. 2016;15(15):2033-41.
176. Li Z, He Q, Zhai X, You Y, Li L, Hou Y, et al. Foxo1-mediated inflammatory response after cerebral hemorrhage in rats. Neuroscience Letters. 2016;629:131-6.
177. Fusco R, Siracusa R. Focus on the Role of NLRP3 Inflammasome in Diseases. 2020;21(12).
178. Ohto U, Kamitsukasa Y, Ishida H, Zhang Z, Murakami K, Hirama C, et al. Structural basis for the oligomerization-mediated regulation of NLRP3 inflammasome activation. Proceedings of the National Academy of Sciences. 2022;119(11):e2121353119.
179. Shimizu T, Nakamura H, Kawakami A. Role of the Innate Immunity Signaling Pathway in the Pathogenesis of Sjögren's Syndrome. International journal of molecular sciences. 2021;22:3090.
180. Latz E, Xiao TS, Stutz A. Activation and regulation of the inflammasomes. Nature reviews Immunology. 2013;13(6):397-411.
181. Wang Z, Zhang S. NLRP3 Inflammasome and Inflammatory Diseases. 2020;2020:4063562.
182. Baumer Y, McCurdy SG, Boisvert WA. Formation and Cellular Impact of Cholesterol Crystals in Health and Disease. Advanced Biology. 2021;5(11):2100638.
183. O'Rourke SA, Neto NGB, Devilly E, Shanley LC, Fitzgerald HK, Monaghan MG, et al. Cholesterol crystals drive metabolic

reprogramming and M1 macrophage polarisation in primary human macrophages. Atherosclerosis. 2022;352:35-45.
184. Boland AJ, Gangadharan N, Kavanagh P, Hemeryck L, Kieran J, Barry M, et al. Simvastatin Suppresses Interleukin Iβ Release in Human Peripheral Blood Mononuclear Cells Stimulated With Cholesterol Crystals. 2018;23(6):509-17.
185. Duewell P, Kono H, Rayner KJ, Sirois CM, Vladimer G, Bauernfeind FG, et al. NLRP3 inflammasomes are required for atherogenesis and activated by cholesterol crystals. Nature. 2010;464(7293):1357-61.
186. Dostert C, Pétrilli V, Van Bruggen R, Steele C, Mossman BT, Tschopp J. Innate immune activation through Nalp3 inflammasome sensing of asbestos and silica. Science (New York, NY). 2008;320(5876):674-7.
187. Blevins HM, Xu Y, Biby S, Zhang S. The NLRP3 Inflammasome Pathway: A Review of Mechanisms and Inhibitors for the Treatment of Inflammatory Diseases. Frontiers in aging neuroscience. 2022;14:879021.
188. Grebe A, Hoss F, Latz E. NLRP3 Inflammasome and the IL-1 Pathway in Atherosclerosis. Circulation research. 2018;122(12):1722-40.
189. Wani K, AlHarthi H, Alghamdi A. Role of NLRP3 Inflammasome Activation in Obesity-Mediated Metabolic Disorders. 2021;18(2).
190. Vandanmagsar B, Youm Y-H, Ravussin A, Galgani JE, Stadler K, Mynatt RL, et al. The NLRP3 inflammasome instigates obesity-induced inflammation and insulin resistance. Nature Medicine. 2011;17(2):179-88.
191. Ozaki E, Campbell M, Doyle SL. Targeting the NLRP3 inflammasome in chronic inflammatory diseases: current perspectives. Journal of inflammation research. 2015;8:15-27.
192. Hugot JP, Chamaillard M, Zouali H, Lesage S, Cézard JP, Belaiche J, et al. Association of NOD2 leucine-rich repeat variants with susceptibility to Crohn's disease. Nature. 2001;411(6837):599-603.
193. Aguilera M, Darby T, Melgar S. The complex role of inflammasomes in the pathogenesis of Inflammatory Bowel Diseases – Lessons learned from experimental models. Cytokine & growth factor reviews. 2014;25(6):715-30.
194. Coll R, O'Neill LAJ, Schroder K. Questions and controversies in innate immune research: what is the physiological role of NLRP3? Cell Death Discovery. 2016;2:16019.
195. Chen L, Deng H, Cui H, Fang J, Zuo Z, Deng J, et al. Inflammatory responses and inflammation-associated diseases in organs. Oncotarget. 2018;9(6):7204-18.
196. Kaminska B. MAPK signalling pathways as molecular targets for anti-inflammatory therapy--from molecular

mechanisms to therapeutic benefits. Biochimica et biophysica acta. 2005;1754(1-2):253-62.
197. Pearson G, Robinson F, Beers Gibson T, Xu BE, Karandikar M, Berman K, et al. Mitogen-activated protein (MAP) kinase pathways: regulation and physiological functions. Endocrine reviews. 2001;22(2):153-83.
198. Kim EK, Choi EJ. Pathological roles of MAPK signaling pathways in human diseases. Biochimica et biophysica acta. 2010;1802(4):396-405.
199. Sabio G, Davis RJ. TNF and MAP kinase signalling pathways. Seminars in immunology. 2014;26(3):237-45.
200. Raingeaud J, Whitmarsh AJ, Barrett T, Dérijard B, Davis RJ. MKK3- and MKK6-regulated gene expression is mediated by the p38 mitogen-activated protein kinase signal transduction pathway. Molecular and cellular biology. 1996;16(3):1247-55.
201. Oeckinghaus A, Hayden MS, Ghosh S. Crosstalk in NF-κB signaling pathways. Nat Immunol. 2011;12(8):695-708.
202. O'Shea JJ, Schwartz DM, Villarino AV, Gadina M, McInnes IB, Laurence A. The JAK-STAT pathway: impact on human disease and therapeutic intervention. Annual review of medicine. 2015;66:311-28.
203. Walker JG, Smith MD. The Jak-STAT pathway in rheumatoid arthritis. The Journal of rheumatology. 2005;32(9):1650-3.
204. Pitsavos C, Panagiotakos D, Weinem M, Stefanadis C. Diet, exercise and the metabolic syndrome. The review of diabetic studies : RDS. 2006;3(3):118-26.
205. Grundy SM. Drug therapy of the metabolic syndrome: minimizing the emerging crisis in polypharmacy. Nature reviews Drug discovery. 2006;5(4):295-309.
206. Noale M, Veronese N, Perin PC, Pilotto A, Tiengo A, Crepaldi G, et al. Reply to Letter to the Editor "Polypharmacy in elderly people with diabetes admitted to hospital". Acta diabetologica. 2016;53(5):859-60.
207. Alwhaibi M, Balkhi B, Alhawassi TM, Alkofide H, Alduhaim N, Alabdulali R, et al. Polypharmacy among patients with diabetes: a cross-sectional retrospective study in a tertiary hospital in Saudi Arabia. BMJ open. 2018;8(5):e020852.
208. Esser N, Paquot N, Scheen AJ. Anti-inflammatory agents to treat or prevent type 2 diabetes, metabolic syndrome and cardiovascular disease. Expert opinion on investigational drugs. 2015;24(3):283-307.
209. Nidorf SM, Eikelboom JW, Budgeon CA, Thompson PL. Low-dose colchicine for secondary prevention of cardiovascular disease. J Am Coll Cardiol. 2013;61(4):404-10.
210. Rho YH, Oeser A, Chung CP, Milne GL, Stein CM. Drugs Used in the Treatment of Rheumatoid Arthritis: Relationship

between Current Use and Cardiovascular Risk Factors. Archives of drug information. 2009;2(2):34-40.
211. Micha R, Imamura F, Wyler von Ballmoos M, Solomon DH, Hernán MA, Ridker PM, et al. Systematic review and meta-analysis of methotrexate use and risk of cardiovascular disease. Am J Cardiol. 2011;108(9):1362-70.
212. Rumore MM, Kim KS. Potential role of salicylates in type 2 diabetes. The Annals of pharmacotherapy. 2010;44(7-8):1207-21.
213. Fleischman A, Shoelson SE, Bernier R, Goldfine AB. Salsalate improves glycemia and inflammatory parameters in obese young adults. Diabetes Care. 2008;31(2):289-94.
214. Yin MJ, Yamamoto Y, Gaynor RB. The anti-inflammatory agents aspirin and salicylate inhibit the activity of I(kappa)B kinase-beta. Nature. 1998;396(6706):77-80.
215. Gonzalez-Gay MA, Gonzalez-Juanatey C, Vazquez-Rodriguez TR, Miranda-Filloy JA, Llorca J. Insulin resistance in rheumatoid arthritis: the impact of the anti-TNF-alpha therapy. Annals of the New York Academy of Sciences. 2010;1193:153-9.
216. Channual J, Wu JJ, Dann FJ. Effects of tumor necrosis factor-alpha blockade on metabolic syndrome components in psoriasis and psoriatic arthritis and additional lessons learned from rheumatoid arthritis. Dermatologic therapy. 2009;22(1):61-73.
217. Stanley TL, Zanni MV, Johnsen S, Rasheed S, Makimura H, Lee H, et al. TNF-alpha antagonism with etanercept decreases glucose and increases the proportion of high molecular weight adiponectin in obese subjects with features of the metabolic syndrome. J Clin Endocrinol Metab. 2011;96(1):E146-50.
218. Besedovsky HO, Del Rey A. Physiologic versus diabetogenic effects of interleukin-1: a question of weight. Current pharmaceutical design. 2014;20(29):4733-40.
219. Rydgren T, Öster E, Sandberg M, Sandler S. Administration of IL-1 trap prolongs survival of transplanted pancreatic islets to type 1 diabetic NOD mice. Cytokine. 2013;63(2):123-9.
220. Chakraborty A, Tannenbaum S, Rordorf C, Lowe PJ, Floch D, Gram H, et al. Pharmacokinetic and pharmacodynamic properties of canakinumab, a human anti-interleukin-1β monoclonal antibody. Clinical pharmacokinetics. 2012;51(6):e1-18.
221. Pal M, Febbraio MA, Whitham M. From cytokine to myokine: the emerging role of interleukin-6 in metabolic regulation. Immunology and cell biology. 2014;92(4):331-9.
222. Sarwar N, Butterworth AS, Freitag DF, Gregson J, Willeit P, Gorman DN, et al. Interleukin-6 receptor pathways in coronary heart disease: a collaborative meta-analysis of 82 studies. Lancet (London, England). 2012;379(9822):1205-13.
223. Mirjafari H, Welsh P, Verstappen SM, Wilson P, Marshall T, Edlin H, et al. N-terminal pro-brain-type natriuretic peptide (NT-

pro-BNP) and mortality risk in early inflammatory polyarthritis: results from the Norfolk Arthritis Registry (NOAR). Annals of the rheumatic diseases. 2014;73(4):684-90.
224. Bianchi C, Penno G, Romero F, Del Prato S, Miccoli R. Treating the metabolic syndrome. Expert review of cardiovascular therapy. 2007;5(3):491-506.
225. Lioudakis E, Lucitt M. Statin Disruption of Cholesterol Metabolism and Altered Innate Inflammatory Responses in Atherosclerosis. Immunometabolism. 2021;3(3):e210023.
226. Trub AG, Wagner GR, Anderson KA, Crown SB, Zhang G-F, Thompson JW, et al. Statin therapy inhibits fatty acid synthase via dynamic protein modifications. Nature Communications. 2022;13(1):2542.
227. Brown MS, Goldstein JL. Multivalent feedback regulation of HMG CoA reductase, a control mechanism coordinating isoprenoid synthesis and cell growth. Journal of lipid research. 1980;21(5):505-17.
228. Warita K, Warita T, Beckwitt CH, Schurdak ME, Vazquez A, Wells A, et al. Statin-induced mevalonate pathway inhibition attenuates the growth of mesenchymal-like cancer cells that lack functional E-cadherin mediated cell cohesion. Scientific Reports. 2014;4(1):7593.
229. Sparrow CP, Burton CA, Hernandez M, Mundt S, Hassing H, Patel S, et al. Simvastatin has anti-inflammatory and antiatherosclerotic activities independent of plasma cholesterol lowering. Arteriosclerosis, thrombosis, and vascular biology. 2001;21(1):115-21.
230. Koushki K, Shahbaz SK, Mashayekhi K, Sadeghi M, Zayeri ZD, Taba MY, et al. Anti-inflammatory Action of Statins in Cardiovascular Disease: the Role of Inflammasome and Toll-Like Receptor Pathways. Clinical reviews in allergy & immunology. 2021;60(2):175-99.
231. Greenwood J, Steinman L, Zamvil SS. Statin therapy and autoimmune disease: from protein prenylation to immunomodulation. Nature reviews Immunology. 2006;6(5):358-70.
232. Corsonello A, Garasto S, Abbatecola AM, Rose G, Passarino G, Mazzei B, et al. Targeting inflammation to slow or delay functional decline: where are we? Biogerontology. 2010;11(5):603-14.
233. Moutzouri E, Tellis CC, Rousouli K, Liberopoulos EN, Milionis HJ, Elisaf MS, et al. Effect of simvastatin or its combination with ezetimibe on Toll-like receptor expression and lipopolysaccharide - induced cytokine production in monocytes of hypercholesterolemic patients. Atherosclerosis. 2012;225(2):381-7.

234. Schönbeck U, Libby P. Inflammation, Immunity, and HMG-CoA Reductase Inhibitors. Circulation. 2004;109(21_suppl_1):II-18-II-26.
235. Bekkering S, Arts RJW, Novakovic B, Kourtzelis I, van der Heijden C, Li Y, et al. Metabolic Induction of Trained Immunity through the Mevalonate Pathway. Cell. 2018;172(1-2):135-46.e9.
236. Gauthier TW, Scalia R, Murohara T, Guo J-p, Lefer AM. Nitric Oxide Protects Against Leukocyte-Endothelium Interactions in the Early Stages of Hypercholesterolemia. Arteriosclerosis, thrombosis, and vascular biology. 1995;15(10):1652-9.
237. Laufs U, Gertz K, Huang P, Nickenig G, Böhm M, Dirnagl U, et al. Atorvastatin Upregulates Type III Nitric Oxide Synthase in Thrombocytes, Decreases Platelet Activation, and Protects From Cerebral Ischemia in Normocholesterolemic Mice. Stroke. 2000;31(10):2442-9.
238. Laufs U, Fata VL, Plutzky J, Liao JK. Upregulation of Endothelial Nitric Oxide Synthase by HMG CoA Reductase Inhibitors. Circulation. 1998;97(12):1129-35.
239. Laufs U, Liao JK. Post-transcriptional Regulation of Endothelial Nitric Oxide Synthase mRNA Stability by Rho GTPase *. Journal of Biological Chemistry. 1998;273(37):24266-71.
240. Järvisalo MJ, Toikka JO, Vasankari T, Mikkola J, Viikari JS, Hartiala JJ, et al. HMG CoA reductase inhibitors are related to improved systemic endothelial function in coronary artery disease. Atherosclerosis. 1999;147(2):237-42.
241. Dupuis J, Tardif JC, Cernacek P, Théroux P. Cholesterol reduction rapidly improves endothelial function after acute coronary syndromes. The RECIFE (reduction of cholesterol in ischemia and function of the endothelium) trial. Circulation. 1999;99(25):3227-33.
242. Landmesser U, Bahlmann F, Mueller M, Spiekermann S, Kirchhoff N, Schulz S, et al. Simvastatin versus ezetimibe: pleiotropic and lipid-lowering effects on endothelial function in humans. Circulation. 2005;111(18):2356-63.
243. Shimizu T, Liao JK. Rho Kinases and Cardiac Remodeling. Circulation Journal. 2016;80(7):1491-8.
244. Hata T, Soga J, Hidaka T, Idei N, Fujii Y, Fujimura N, et al. Calcium channel blocker and Rho-associated kinase activity in patients with hypertension. Journal of Hypertension. 2011;29(2):373-9.
245. Liu P-Y, Chen J-H, Lin L-J, Liao JK. Increased Rho Kinase Activity in a Taiwanese Population With Metabolic Syndrome. Journal of the American College of Cardiology. 2007;49(15):1619-24.
246. Nohria A, Grunert ME, Rikitake Y, Noma K, Prsic A, Ganz P, et al. Rho Kinase Inhibition Improves Endothelial Function in

Human Subjects With Coronary Artery Disease. Circulation research. 2006;99(12):1426-32.
247. Gabrielli L, Winter JL, Godoy I, McNab P, Padilla I, Cordova S, et al. Increased Rho-Kinase Activity in Hypertensive Patients With Left Ventricular Hypertrophy. American Journal of Hypertension. 2013;27(6):838-45.
248. Rawlings R, Nohria A, Liu P-Y, Donnelly J, Creager MA, Ganz P, et al. Comparison of Effects of Rosuvastatin (10 mg) Versus Atorvastatin (40 mg) on Rho Kinase Activity in Caucasian Men With a Previous Atherosclerotic Event. American Journal of Cardiology. 2009;103(4):437-41.
249. Nohria A, Prsic A, Liu P-Y, Okamoto R, Creager MA, Selwyn A, et al. Statins inhibit Rho kinase activity in patients with atherosclerosis. Atherosclerosis. 2009;205(2):517-21.
250. Brown JH, Re DPD, Sussman MA. The Rac and Rho Hall of Fame. Circulation research. 2006;98(6):730-42.
251. Takemoto M, Node K, Nakagami H, Liao Y, Grimm M, Takemoto Y, et al. Statins as antioxidant therapy for preventing cardiac myocyte hypertrophy. J Clin Invest. 2001;108(10):1429-37.
252. Miller YI, Choi S-H, Fang L, Tsimikas S. Lipoprotein Modification and Macrophage Uptake: Role of Pathologic Cholesterol Transport in Atherogenesis. In: Harris JR, editor. Cholesterol Binding and Cholesterol Transport Proteins: Structure and Function in Health and Disease. Dordrecht: Springer Netherlands; 2010. p. 229-51.
253. Rac1-Mediated Effects of HMG-CoA Reductase Inhibitors (Statins) in Cardiovascular Disease. Antioxidants & Redox Signaling. 2014;20(8):1238-50.
254. Schonewille M, de Boer JF, Mele L, Wolters H, Bloks VW, Wolters JC, et al. Statins increase hepatic cholesterol synthesis and stimulate fecal cholesterol elimination in mice. Journal of lipid research. 2016;57(8):1455-64.
255. Rikitake Y, Liao JK. Rho GTPases, statins, and nitric oxide. Circulation research. 2005;97(12):1232-5.
256. Wang S, Xie X, Lei T, Zhang K, Lai B, Zhang Z, et al. Statins Attenuate Activation of the NLRP3 Inflammasome by Oxidized LDL or TNFα in Vascular Endothelial Cells through a PXR-Dependent Mechanism. Molecular pharmacology. 2017;92(3):256-64.
257. Savoji H, Mohammadi MH, Rafatian N, Toroghi MK, Wang EY, Zhao Y, et al. Cardiovascular disease models: A game changing paradigm in drug discovery and screening. Biomaterials. 2019;198:3-26.
258. Sachdeva V, Roy A, Bharadvaja N. Current Prospects of Nutraceuticals: A Review. Current pharmaceutical biotechnology. 2020;21(10):884-96.
259. Souyoul SA, Saussy KP, Lupo MP. Nutraceuticals: A Review. Dermatol Ther (Heidelb). 2018;8(1):5-16.

260. Chauhan B, Kumar G, Kalam N, Ansari SH. Current concepts and prospects of herbal nutraceutical: A review. J Adv Pharm Technol Res. 2013;4(1):4-8.
261. Jain S, Buttar HS, Chintameneni M, Kaur G. Prevention of Cardiovascular Diseases with Anti-Inflammatory and Anti- Oxidant Nutraceuticals and Herbal Products: An Overview of Pre-Clinical and Clinical Studies. Recent patents on inflammation & allergy drug discovery. 2018;12(2):145-57.
262. Calvani M, Pasha A, Favre C. Nutraceutical Boom in Cancer: Inside the Labyrinth of Reactive Oxygen Species. International journal of molecular sciences. 2020;21(6).
263. Castrogiovanni P, Trovato FM, Loreto C, Nsir H, Szychlinska MA, Musumeci G. Nutraceutical Supplements in the Management and Prevention of Osteoarthritis. International journal of molecular sciences. 2016;17(12).
264. Boe C, Vangsness CT. Fish Oil and Osteoarthritis: Current Evidence. American journal of orthopedics (Belle Mead, NJ). 2015;44(7):302-5.
265. Jain N, Ramawat K. Nutraceuticals and antioxidants in prevention of diseases. Nat Prod. 2013:2560-80.
266. Zhang Y, Tian R, Wu H, Li X, Li S, Bian L. Evaluation of acute and sub-chronic toxicity of lithothamnion sp. in mice and rats. Toxicology reports. 2020;7:852-8.
267. Frestedt JL, Walsh M, Kuskowski MA, Zenk JL. A natural mineral supplement provides relief from knee osteoarthritis symptoms: a randomized controlled pilot trial. Nutrition Journal. 2008;7(1):9.
268. O'Gorman DM, Tierney CM, Brennan O, O'Brien FJ. The marine-derived, multi-mineral formula, Aquamin, enhances mineralisation of osteoblast cells in vitro. Phytotherapy research : PTR. 2012;26(3):375-80.
269. Brennan O, Sweeney J, O'Meara B, Widaa A, Bonnier F, Byrne HJ, et al. A Natural, Calcium-Rich Marine Multi-mineral Complex Preserves Bone Structure, Composition and Strength in an Ovariectomised Rat Model of Osteoporosis. Calcified Tissue International. 2017;101(4):445-55.
270. Harber I, Zedan D, McClintock S, Varani J, Aslam MN. Liver Proteomic Profile in Mice on a High-Fat Diet: Modulation with Anti-Tumor Intervention. The FASEB Journal. 2022;36(S1).
271. Aviello G, Amu S, Saunders SP, Fallon PG. A Mineral Extract from red Algae Ameliorates Chronic Spontaneous Colitis in IL-10 Deficient Mice in a Mouse Strain Dependent Manner. Phytotherapy Research. 2014;28(2):300-4.
272. Baron JA, Beach M, Mandel JS, van Stolk RU, Haile RW, Sandler RS, et al. Calcium supplements for the prevention of colorectal adenomas. Calcium Polyp Prevention Study Group. The New England journal of medicine. 1999;340(2):101-7.

273. Wallace K, Baron JA, Cole BF, Sandler RS, Karagas MR, Beach MA, et al. Effect of calcium supplementation on the risk of large bowel polyps. Journal of the National Cancer Institute. 2004;96(12):921-5.
274. Grau MV, Baron JA, Sandler RS, Wallace K, Haile RW, Church TR, et al. Prolonged effect of calcium supplementation on risk of colorectal adenomas in a randomized trial. Journal of the National Cancer Institute. 2007;99(2):129-36.
275. Aslam MN, McClintock SD, Jawad-Makki MAH, Knuver K, Ahmad HM, Basrur V, et al. A Multi-Mineral Intervention to Modulate Colonic Mucosal Protein Profile: Results from a 90-Day Trial in Human Subjects. Nutrients. 2021;13(3):939.
276. Felice VD, O'Gorman DM, Apajalahti J, Rinttilä T, O'Brien NM, Hyland NP. A Marine-Derived, Multi-mineral Supplement Influences Bacterial Fermentation and Short Chain Fatty Acid Profile In Vitro. Journal of medicinal food. 2021;24(5):558-62.
277. O'Gorman DM, O'Carroll C, Carmody RJ. Evidence that Marine-derived, Multi-mineral, Aquamin Inhibits the NF-κB Signaling Pathway In Vitro. Phytotherapy Research. 2012;26(4):630-2.
278. Ryan S, O'Gorman DM, Nolan YM. Evidence that the marine-derived multi-mineral Aquamin has anti-inflammatory effects on cortical glial-enriched cultures. Phytotherapy research : PTR. 2011;25(5):765-7.
279. Hornung V, Bauernfeind F, Halle A, Samstad EO, Kono H, Rock KL, et al. Silica crystals and aluminum salts activate the NALP3 inflammasome through phagosomal destabilization. Nat Immunol. 2008;9(8):847-56.
280. El-Zayat SR, Sibaii H, Mannaa FA. Toll-like receptors activation, signaling, and targeting: an overview. Bulletin of the National Research Centre. 2019;43(1):187.
281. Wang Y, Song E, Bai B, Vanhoutte PM. Toll-like receptors mediating vascular malfunction: Lessons from receptor subtypes. Pharmacology & Therapeutics. 2016;158:91-100.
282. Zhang Y, Liang C. Innate recognition of microbial-derived signals in immunity and inflammation. Science China Life sciences. 2016;59(12):1210-7.
283. Yu L, Feng Z. The Role of Toll-Like Receptor Signaling in the Progression of Heart Failure. Mediators of inflammation. 2018;2018:9874109.
284. Huang QQ, Pope RM. The role of toll-like receptors in rheumatoid arthritis. Current rheumatology reports. 2009;11(5):357-64.
285. Zhang YW, Thompson R, Zhang H, Xu H. APP processing in Alzheimer's disease. Molecular brain. 2011;4:3.
286. Gao W, Xiong Y, Li Q, Yang H. Inhibition of Toll-Like Receptor Signaling as a Promising Therapy for Inflammatory

Diseases: A Journey from Molecular to Nano Therapeutics. Front Physiol. 2017;8:508.
287. Mahla RS, Reddy MC, Prasad DV, Kumar H. Sweeten PAMPs: Role of Sugar Complexed PAMPs in Innate Immunity and Vaccine Biology. Front Immunol. 2013;4:248.
288. Yamamoto M, Takeda K. Current Views of Toll-Like Receptor Signaling Pathways. Gastroenterology Research and Practice. 2010;2010:240365.
289. Gay NJ, Symmons MF, Gangloff M, Bryant CE. Assembly and localization of Toll-like receptor signalling complexes. Nature reviews Immunology. 2014;14(8):546-58.
290. Sellge G, Kufer TA. PRR-signaling pathways: Learning from microbial tactics. Seminars in immunology. 2015;27(2):75-84.
291. Delneste Y, Beauvillain C, Jeannin P. Immunité naturelle. Med Sci (Paris). 2007;23(1):67-74.
292. Akira S, Takeda K. Toll-like receptor signalling. Nature Reviews Immunology. 2004;4(7):499-511.
293. Hoebe K, Du X, Georgel P, Janssen E, Tabeta K, Kim SO, et al. Identification of Lps2 as a key transducer of MyD88-independent TIR signalling. Nature. 2003;424(6950):743-8.
294. Ayres JS, Schneider DS. Tolerance of infections. Annual review of immunology. 2012;30:271-94.
295. Burns K, Janssens S, Brissoni B, Olivos N, Beyaert R, Tschopp J. Inhibition of interleukin 1 receptor/Toll-like receptor signaling through the alternatively spliced, short form of MyD88 is due to its failure to recruit IRAK-4. J Exp Med. 2003;197(2):263-8.
296. Yamamoto M, Sato S, Mori K, Hoshino K, Takeuchi O, Takeda K, et al. Cutting Edge: A Novel Toll/IL-1 Receptor Domain-Containing Adapter That Preferentially Activates the IFN-β Promoter in the Toll-Like Receptor Signaling. The Journal of Immunology. 2002;169(12):6668-72.
297. Adachi O, Kawai T, Takeda K, Matsumoto M, Tsutsui H, Sakagami M, et al. Targeted Disruption of the MyD88 Gene Results in Loss of IL-1- and IL-18-Mediated Function. Immunity. 1998;9(1):143-50.
298. Kawai T, Adachi O, Ogawa T, Takeda K, Akira S. Unresponsiveness of MyD88-deficient mice to endotoxin. Immunity. 1999;11(1):115-22.
299. Kawai T, Takeuchi O, Fujita T, Inoue J, Mühlradt PF, Sato S, et al. Lipopolysaccharide stimulates the MyD88-independent pathway and results in activation of IFN-regulatory factor 3 and the expression of a subset of lipopolysaccharide-inducible genes. J Immunol. 2001;167(10):5887-94.
300. Fitzgerald KA, Palsson-McDermott EM, Bowie AG, Jefferies CA, Mansell AS, Brady G, et al. Mal (MyD88-adapter-like) is required for Toll-like receptor-4 signal transduction. Nature. 2001;413(6851):78-83.

301. Yamamoto M, Sato S, Hemmi H, Sanjo H, Uematsu S, Kaisho T, et al. Essential role for TIRAP in activation of the signalling cascade shared by TLR2 and TLR4. Nature. 2002;420(6913):324-9.
302. Horng T, Barton GM, Flavell RA, Medzhitov R. The adaptor molecule TIRAP provides signalling specificity for Toll-like receptors. Nature. 2002;420(6913):329-33.
303. Oshiumi H, Matsumoto M, Funami K, Akazawa T, Seya T. TICAM-1, an adaptor molecule that participates in Toll-like receptor 3–mediated interferon-β induction. Nature Immunology. 2003;4(2):161-7.
304. Yamamoto M, Sato S, Hemmi H, Hoshino K, Kaisho T, Sanjo H, et al. Role of adaptor TRIF in the MyD88-independent toll-like receptor signaling pathway. Science (New York, NY). 2003;301(5633):640-3.
305. Fitzgerald KA, Rowe DC, Barnes BJ, Caffrey DR, Visintin A, Latz E, et al. LPS-TLR4 signaling to IRF-3/7 and NF-kappaB involves the toll adapters TRAM and TRIF. J Exp Med. 2003;198(7):1043-55.
306. Oshiumi H, Sasai M, Shida K, Fujita T, Matsumoto M, Seya T. TIR-containing adapter molecule (TICAM)-2, a bridging adapter recruiting to toll-like receptor 4 TICAM-1 that induces interferon-beta. The Journal of biological chemistry. 2003;278(50):49751-62.
307. Moresco EM, LaVine D, Beutler B. Toll-like receptors. Current biology : CB. 2011;21(13):R488-93.
308. Jaffer U, Wade RG, Gourlay T. Cytokines in the systemic inflammatory response syndrome: a review. HSR proceedings in intensive care & cardiovascular anesthesia. 2010;2(3):161-75.
309. Jiang L, Jiang Q, Yang S, Huang S, Han X, Duan J, et al. GYY4137 attenuates LPS-induced acute lung injury via heme oxygenase-1 modulation. Pulmonary pharmacology & therapeutics. 2019;54:77-86.
310. Ryan S, O'Gorman DM, Nolan YM. Evidence that the marine-derived multi-mineral aquamin has anti-inflammatory effects on cortical glial-enriched cultures. Phytotherapy Research. 2011;25(5):765-7.
311. Aslam MN, McClintock SD, Attili D, Pandya S, Rehman H, Nadeem DM, et al. Ulcerative Colitis-Derived Colonoid Culture: A Multi-Mineral-Approach to Improve Barrier Protein Expression. Front Cell Dev Biol. 2020;8:577221.
312. Coats BR, Schoenfelt KQ, Barbosa-Lorenzi VC, Peris E, Cui C, Hoffman A, et al. Metabolically Activated Adipose Tissue Macrophages Perform Detrimental and Beneficial Functions during Diet-Induced Obesity. Cell Rep. 2017;20(13):3149-61.
313. Ellulu MS, Patimah I, Khaza'ai H, Rahmat A, Abed Y. Obesity and inflammation: the linking mechanism and the complications. Arch Med Sci. 2017;13(4):851-63.

314. Popko K, Gorska E, Stelmaszczyk-Emmel A, Plywaczewski R, Stoklosa A, Gorecka D, et al. Proinflammatory cytokines IL-6 and TNF-α and the development of inflammation in obese subjects. European Journal of Medical Research. 2010;15(2):120.
315. Greten FR, Eckmann L, Greten TF, Park JM, Li ZW, Egan LJ, et al. IKKbeta links inflammation and tumorigenesis in a mouse model of colitis-associated cancer. Cell. 2004;118(3):285-96.
316. Kobelt D, Zhang C, Clayton-Lucey IA, Glauben R, Voss C, Siegmund B, et al. Pro-inflammatory TNF-α and IFN-γ Promote Tumor Growth and Metastasis via Induction of MACC1. Front Immunol. 2020;11:980.
317. Waters JP, Pober JS, Bradley JR. Tumour necrosis factor and cancer. The Journal of Pathology. 2013;230(3):241-8.
318. Lee JH, Ko HJ, Woo ER, Lee SK, Moon BS, Lee CW, et al. Moracin M inhibits airway inflammation by interrupting the JNK/c-Jun and NF-κB pathways in vitro and in vivo. Eur J Pharmacol. 2016;783:64-72.
319. Korhonen R, Lahti A, Kankaanranta H, Moilanen E. Nitric oxide production and signaling in inflammation. Current drug targets Inflammation and allergy. 2005;4(4):471-9.
320. Korbecki J, Bajdak-Rusinek K. The effect of palmitic acid on inflammatory response in macrophages: an overview of molecular mechanisms. Inflammation Research. 2019;68(11):915-32.
321. Mook S, Halkes Cj C, Bilecen S, Cabezas MC. In vivo regulation of plasma free fatty acids in insulin resistance. Metabolism: clinical and experimental. 2004;53(9):1197-201.
322. Pankow JS, Duncan BB, Schmidt MI, Ballantyne CM, Couper DJ, Hoogeveen RC, et al. Fasting plasma free fatty acids and risk of type 2 diabetes: the atherosclerosis risk in communities study. Diabetes Care. 2004;27(1):77-82.
323. Soriguer F, García-Serrano S, García-Almeida JM, Garrido-Sánchez L, García-Arnés J, Tinahones FJ, et al. Changes in the Serum Composition of Free-fatty Acids During an Intravenous Glucose Tolerance Test. Obesity. 2009;17(1):10-5.
324. Kim JY, Park JY, Kim OY, Ham BM, Kim H-J, Kwon DY, et al. Metabolic Profiling of Plasma in Overweight/Obese and Lean Men using Ultra Performance Liquid Chromatography and Q-TOF Mass Spectrometry (UPLC–Q-TOF MS). Journal of Proteome Research. 2010;9(9):4368-75.
325. Feng R, Luo C, Li C, Du S, Okekunle AP, Li Y, et al. Free fatty acids profile among lean, overweight and obese non-alcoholic fatty liver disease patients: a case – control study. Lipids in Health and Disease. 2017;16(1):165.
326. Lancaster GI, Langley KG, Berglund NA, Kammoun HL, Reibe S, Estevez E, et al. Evidence that TLR4 Is Not a Receptor for Saturated Fatty Acids but Mediates Lipid-Induced Inflammation by

Reprogramming Macrophage Metabolism. Cell Metab. 2018;27(5):1096-110.e5.
327. Giraldo DM, Hernandez JC, Urcuqui Inchima S. Impact of in vitro Costimulation with TLR2, TLR4 and TLR9 Agonists and HIV-1 on Antigen-Presenting Cell Activation. Intervirology. 2015;58(2):122-9.
328. Kuzmich NN, Sivak KV, Chubarev VN, Porozov YB, Savateeva-Lyubimova TN, Peri F. TLR4 Signaling Pathway Modulators as Potential Therapeutics in Inflammation and Sepsis. Vaccines (Basel). 2017;5(4):34.
329. Farina GA, York MR, Di Marzio M, Collins CA, Meller S, Homey B, et al. Poly(I:C) drives type I IFN- and TGFβ-mediated inflammation and dermal fibrosis simulating altered gene expression in systemic sclerosis. The Journal of investigative dermatology. 2010;130(11):2583-93.
330. Troutman TD, Bazan JF, Pasare C. Toll-like receptors, signaling adapters and regulation of the pro-inflammatory response by PI3K. Cell Cycle. 2012;11(19):3559-67.
331. Richards MR, Black AS, Bonnet DJ, Barish GD, Woo CW, Tabas I, et al. The LPS2 mutation in TRIF is atheroprotective in hyperlipidemic low density lipoprotein receptor knockout mice. Innate Immun. 2013;19(1):20-9.
332. Lundberg AM, Ketelhuth DFJ, Johansson ME, Gerdes N, Liu S, Yamamoto M, et al. Toll-like receptor 3 and 4 signalling through the TRIF and TRAM adaptors in haematopoietic cells promotes atherosclerosis. Cardiovascular Research. 2013;99(2):364-73.
333. Casella CR, Mitchell TC. Putting endotoxin to work for us: monophosphoryl lipid A as a safe and effective vaccine adjuvant. Cell Mol Life Sci. 2008;65(20):3231-40.
334. Piao W, Vogel SN, Toshchakov VY. Inhibition of TLR4 signaling by TRAM-derived decoy peptides in vitro and in vivo. J Immunol. 2013;190(5):2263-72.
335. Lundberg AM, Ketelhuth DF, Johansson ME, Gerdes N, Liu S, Yamamoto M, et al. Toll-like receptor 3 and 4 signalling through the TRIF and TRAM adaptors in haematopoietic cells promotes atherosclerosis. Cardiovasc Res. 2013;99(2):364-73.
336. Ouyang M-Z, Zhou D, Zhu Y, Zhang M, Li L. The inhibition of MyD88 and TRIF signaling serve equivalent roles in attenuating myocardial deterioration due to acute severe inflammation. Int J Mol Med. 2018;41(1):399-408.
337. Zenobia C, Hajishengallis G. Basic biology and role of interleukin-17 in immunity and inflammation. Periodontology 2000. 2015;69(1):142-59.
338. Qian Y, Kang Z, Liu C, Li X. IL-17 signaling in host defense and inflammatory diseases. Cellular & Molecular Immunology. 2010;7(5):328-33.

339. Chisălău BA, Crînguș LI, Vreju FA, Pârvănescu CD, Firulescu SC, Dinescu Ș C, et al. New insights into IL-17/IL-23 signaling in ankylosing spondylitis (Review). Experimental and therapeutic medicine. 2020;20(4):3493-7.
340. Wilson SC, Caveney NA, Yen M, Pollmann C, Xiang X, Jude KM, et al. Organizing Structural Principles of the Interleukin-17 Ligand-Receptor Axis. Nature. 2022.
341. Sun J, Zhang S, Zhang X, Zhang X, Dong H, Qian Y. IL-17A is implicated in lipopolysaccharide-induced neuroinflammation and cognitive impairment in aged rats via microglial activation. Journal of neuroinflammation. 2015;12:165.
342. Boutari C, Mantzoros CS. A 2022 update on the epidemiology of obesity and a call to action: as its twin COVID-19 pandemic appears to be receding, the obesity and dysmetabolism pandemic continues to rage on. Metabolism: clinical and experimental. 2022;133:155217.
343. González-Muniesa P, Mártinez-González M-A, Hu FB, Després J-P, Matsuzawa Y, Loos RJF, et al. Obesity. Nature Reviews Disease Primers. 2017;3(1):17034.
344. Redinger RN. The pathophysiology of obesity and its clinical manifestations. Gastroenterology & hepatology. 2007;3(11):856-63.
345. Nammi S, Koka S, Chinnala KM, Boini KM. Obesity: An overview on its current perspectives and treatment options. Nutrition Journal. 2004;3(1):3.
346. Lu N, Cheng W, Liu D, Liu G, Cui C, Feng C, et al. NLRP3-Mediated Inflammation in Atherosclerosis and Associated Therapeutics. Frontiers in Cell and Developmental Biology. 2022;10.
347. Rajamäki K, Lappalainen J, Oörni K, Välimäki E, Matikainen S, Kovanen PT, et al. Cholesterol crystals activate the NLRP3 inflammasome in human macrophages: a novel link between cholesterol metabolism and inflammation. PloS one. 2010;5(7):e11765.
348. Stroes E. Statins and LDL-cholesterol lowering: an overview. Current medical research and opinion. 2005;21 Suppl 6:S9-16.
349. Anders C, Niewoehner O, Duerst A, Jinek M. Structural basis of PAM-dependent target DNA recognition by the Cas9 endonuclease. Nature. 2014;513(7519):569-73.
350. Davis BM, Fensterl V, Lawrence TM, Hudacek AW, Sen GC, Schnell MJ. Ifit2 Is a Restriction Factor in Rabies Virus Pathogenicity. 2017;91(17).
351. Fensterl V, Wetzel JL, Ramachandran S, Ogino T, Stohlman SA, Bergmann CC, et al. Interferon-induced Ifit2/ISG54 protects mice from lethal VSV neuropathogenesis. PLoS pathogens. 2012;8(5):e1002712.

352. Fensterl V, Wetzel JL, Sen GC. Interferon-induced protein Ifit2 protects mice from infection of the peripheral nervous system by vesicular stomatitis virus. Journal of virology. 2014;88(18):10303-11.
353. Zhang W, Li Y, Xin S, Yang L, Jiang M, Xin Y, et al. The emerging roles of IFIT3 in antiviral innate immunity and cellular biology. Journal of Medical Virology. 2023;95(1):e28259.
354. Subedi P, Moertl S, Azimzadeh O. Omics in Radiation Biology: Surprised but Not Disappointed. Radiation. 2022;2(1):124-9.
355. Lowe R, Shirley N, Bleackley M, Dolan S, Shafee T. Transcriptomics technologies. PLOS Computational Biology. 2017;13(5):e1005457.
356. Wang T, Zhang Y, Guo Y, Zhang X, Yang H, Tian X, et al. RNA-sequence reveals differentially expressed genes affecting the crested trait of Wumeng crested chicken. Poultry science. 2021;100(9):101357.
357. Das Sarma J, Burrows A, Rayman P, Hwang M-H, Kundu S, Sharma N, et al. Ifit2 deficiency restricts microglial activation and leukocyte migration following murine coronavirus (m-CoV) CNS infection. PLoS pathogens. 2020;16(11):e1009034.
358. Khan A, Sergi C. SAMHD1 as the Potential Link Between SARS-CoV-2 Infection and Neurological Complications. Frontiers in Neurology. 2020;11.
359. Onishi RM, Gaffen SL. Interleukin-17 and its target genes: mechanisms of interleukin-17 function in disease. Immunology. 2010;129(3):311-21.
360. McGeachy MJ, Cua DJ, Gaffen SL. The IL-17 Family of Cytokines in Health and Disease. Immunity. 2019;50(4):892-906.
361. Miossec P. Interleukin-17 in rheumatoid arthritis: if T cells were to contribute to inflammation and destruction through synergy. Arthritis and rheumatism. 2003;48(3):594-601.
362. Le Gouvello S, Bastuji-Garin S, Aloulou N, Mansour H, Chaumette MT, Berrehar F, et al. High prevalence of Foxp3 and IL17 in MMR-proficient colorectal carcinomas. Gut. 2008;57(6):772-9.
363. Miyahara Y, Odunsi K, Chen W, Peng G, Matsuzaki J, Wang RF. Generation and regulation of human CD4+ IL-17-producing T cells in ovarian cancer. Proceedings of the National Academy of Sciences of the United States of America. 2008;105(40):15505-10.
364. Chen G, Sun J, Xie M, Yu S, Tang Q, Chen L. PLAU Promotes Cell Proliferation and Epithelial-Mesenchymal Transition in Head and Neck Squamous Cell Carcinoma. Frontiers in Genetics. 2021;12.
365. Vecchié A, Dallegri F, Carbone F, Bonaventura A, Liberale L, Portincasa P, et al. Obesity phenotypes and their paradoxical

association with cardiovascular diseases. European journal of internal medicine. 2018;48:6-17.
366. Libby P. Inflammation in atherosclerosis. Nature. 2002;420(6917):868-74.
367. Schönbeck U, Libby P. Inflammation, immunity, and HMG-CoA reductase inhibitors: statins as antiinflammatory agents? Circulation. 2004;109(21 Suppl 1):Ii18-26.
368. Ahmed M, Gaffen SL. IL-17 in obesity and adipogenesis. Cytokine & growth factor reviews. 2010;21(6):449-53.
369. Andersson CX, Gustafson B, Hammarstedt A, Hedjazifar S, Smith U. Inflamed adipose tissue, insulin resistance and vascular injury. Diabetes/metabolism research and reviews. 2008;24(8):595-603.
370. Lin Y, Rajala MW, Berger JP, Moller DE, Barzilai N, Scherer PE. Hyperglycemia-induced production of acute phase reactants in adipose tissue. The Journal of biological chemistry. 2001;276(45):42077-83.
371. Scheja L, Heese B, Zitzer H, Michael MD, Siesky AM, Pospisil H, et al. Acute-phase serum amyloid A as a marker of insulin resistance in mice. Experimental diabetes research. 2008;2008:230837.
372. Yang RZ, Lee MJ, Hu H, Pollin TI, Ryan AS, Nicklas BJ, et al. Acute-phase serum amyloid A: an inflammatory adipokine and potential link between obesity and its metabolic complications. PLoS medicine. 2006;3(6):e287.
373. Johnson BD, Kip KE, Marroquin OC, Ridker PM, Kelsey SF, Shaw LJ, et al. Serum amyloid A as a predictor of coronary artery disease and cardiovascular outcome in women: the National Heart, Lung, and Blood Institute-Sponsored Women's Ischemia Syndrome Evaluation (WISE). Circulation. 2004;109(6):726-32.
374. Ogasawara K, Mashiba S, Wada Y, Sahara M, Uchida K, Aizawa T, et al. A serum amyloid A and LDL complex as a new prognostic marker in stable coronary artery disease. Atherosclerosis. 2004;174(2):349-56.
375. Benditt EP, Meek RL. Expression of the third member of the serum amyloid A gene family in mouse adipocytes. J Exp Med. 1989;169(5):1841-6.
376. Cheng CL, Tang Y, Zheng Z, Liu X, Ye ZC, Wang C, et al. Advanced glycation end-products activate the renin-angiotensin system through the RAGE/PI3-K signaling pathway in podocytes. Clinical and investigative medicine Medecine clinique et experimentale. 2012;35(5):E282.
377. Pickering RJ, Tikellis C, Rosado CJ, Tsorotes D, Dimitropoulos A, Smith M, et al. Transactivation of RAGE mediates angiotensin-induced inflammation and atherogenesis. J Clin Invest. 2019;129(1):406-21.

378. Tan KC, Ipcho SV, Trengove RD, Oliver RP, Solomon PS. Assessing the impact of transcriptomics, proteomics and metabolomics on fungal phytopathology. Molecular plant pathology. 2009;10(5):703-15.
379. Kumar A, Sundaram K, Mu J, Dryden GW, Sriwastva MK, Lei C, et al. High-fat diet-induced upregulation of exosomal phosphatidylcholine contributes to insulin resistance. Nature Communications. 2021;12(1):213.
380. Klop B, Elte JW, Cabezas MC. Dyslipidemia in obesity: mechanisms and potential targets. Nutrients. 2013;5(4):1218-40.
381. Wali JA, Jarzebska N, Raubenheimer D, Simpson SJ, Rodionov RN, O'Sullivan JF. Cardio-Metabolic Effects of High-Fat Diets and Their Underlying Mechanisms-A Narrative Review. Nutrients. 2020;12(5).
382. Wong SK, Chin KY, Suhaimi FH, Fairus A, Ima-Nirwana S. Animal models of metabolic syndrome: a review. Nutr Metab (Lond). 2016;13:65.
383. Siersbæk MS, Ditzel N, Hejbøl EK, Præstholm SM, Markussen LK, Avolio F, et al. C57BL/6J substrain differences in response to high-fat diet intervention. Scientific Reports. 2020;10(1):14052.
384. Hariri N, Thibault L. High-fat diet-induced obesity in animal models. Nutrition Research Reviews. 2010;23(2):270-99.
385. Libby P. The changing landscape of atherosclerosis. Nature. 2021;592(7855):524-33.
386. Guerre-Millo M. Regulation of ob gene and overexpression in obesity. Biomedicine & Pharmacotherapy. 1997;51(8):318-23.
387. Lutz TA, Woods SC. Overview of animal models of obesity. Current protocols in pharmacology. 2012;Chapter 5:Unit5.61.
388. Chen H, Charlat O, Tartaglia LA, Woolf EA, Weng X, Ellis SJ, et al. Evidence That the Diabetes Gene Encodes the Leptin Receptor: Identification of a Mutation in the Leptin Receptor Gene in db/db Mice. Cell. 1996;84(3):491-5.
389. Verdouw PM, van Esterik JC, Peeters BW, Millan MJ, Groenink L. CRF(1) but not glucocorticoid receptor antagonists reduce separation-induced distress vocalizations in guinea pig pups and CRF overexpressing mouse pups. A combination study with paroxetine. Pharmacology, biochemistry, and behavior. 2017;154:11-9.
390. Browne CJ, Ji X, Higgins GA, Fletcher PJ, Harvey-Lewis C. Pharmacological Modulation of 5-HT(2C) Receptor Activity Produces Bidirectional Changes in Locomotor Activity, Responding for a Conditioned Reinforcer, and Mesolimbic DA Release in C57BL/6 Mice. Neuropsychopharmacology : official publication of the American College of Neuropsychopharmacology. 2017;42(11):2178-87.

391. de Jong JMA, Wouters RTF, Boulet N, Cannon B, Nedergaard J, Petrovic N. The β(3)-adrenergic receptor is dispensable for browning of adipose tissues. American journal of physiology Endocrinology and metabolism. 2017;312(6):E508-e18.
392. Blanco-Centurion C, Liu M, Konadhode RP, Zhang X, Pelluru D, van den Pol AN, et al. Optogenetic activation of melanin-concentrating hormone neurons increases non-rapid eye movement and rapid eye movement sleep during the night in rats. The European journal of neuroscience. 2016;44(10):2846-57.
393. Wang C-Y, Liao JK. A mouse model of diet-induced obesity and insulin resistance. Methods Mol Biol. 2012;821:421-33.
394. Winzell MS, Ahrén B. The High-Fat Diet–Fed Mouse. A Model for Studying Mechanisms and Treatment of Impaired Glucose Tolerance and Type 2 Diabetes. 2004;53(suppl 3):S215-S9.
395. Li J, Wu H, Liu Y, Yang L. High fat diet induced obesity model using four strainsof mice: Kunming, C57BL/6, BALB/c and ICR. Experimental animals. 2020;69(3):326-35.
396. Seo SH, Fang F, Kang I. Ginger (Zingiber officinale) Attenuates Obesity and Adipose Tissue Remodeling in High-Fat Diet-Fed C57BL/6 Mice. 2021;18(2).
397. Pereira-Lancha LO, Campos-Ferraz PL, Lancha AH, Jr. Obesity: considerations about etiology, metabolism, and the use of experimental models. Diabetes, metabolic syndrome and obesity : targets and therapy. 2012;5:75-87.
398. Kim SW, Kang HJ, Jhon M, Kim JW, Lee JY, Walker AJ, et al. Statins and Inflammation: New Therapeutic Opportunities in Psychiatry. Frontiers in psychiatry. 2019;10:103.
399. Eberhardt N, Giannarelli C. Statins boost the macrophage eat-me signal to keep atherosclerosis at bay. Nature Cardiovascular Research. 2022;1(3):196-7.
400. Vekic J, Zeljkovic A, Stefanovic A, Jelic-Ivanovic Z, Spasojevic-Kalimanovska V. Obesity and dyslipidemia. Metabolism: clinical and experimental. 2019;92:71-81.
401. Thrum S, Sommer M, Raulien N, Gericke M, Massier L, Kovacs P, et al. Macrophages in obesity are characterised by increased IL-1β response to calcium-sensing receptor signals. International Journal of Obesity. 2022;46(10):1883-91.
402. Rheinheimer J, de Souza BM, Cardoso NS, Bauer AC, Crispim D. Current role of the NLRP3 inflammasome on obesity and insulin resistance: A systematic review. Metabolism: clinical and experimental. 2017;74:1-9.
403. O'Donnell A, Buffini M, Kehoe L, Nugent A, Kearney J, Walton J, et al. The prevalence of overweight and obesity in Irish children between 1990 and 2019. Public Health Nutrition. 2020;23(14):2512-20.

404. Scherer PE, Hill JA. Obesity, Diabetes, and Cardiovascular Diseases: A Compendium. Circulation research. 2016;118(11):1703-5.
405. Bing C. Is interleukin-1β a culprit in macrophage-adipocyte crosstalk in obesity? Adipocyte. 2015;4(2):149-52.
406. Krysiak R, Gdula-Dymek A, Okopien B. Effect of Simvastatin and Fenofibrate on Cytokine Release and Systemic Inflammation in Type 2 Diabetes Mellitus With Mixed Dyslipidemia. The American Journal of Cardiology. 2011;107(7):1010-8.e1.
407. Dinarello CA, Donath MY, Mandrup-Poulsen T. Role of IL-1beta in type 2 diabetes. Current opinion in endocrinology, diabetes, and obesity. 2010;17(4):314-21.
408. Larsen CM, Faulenbach M, Vaag A, Vølund A, Ehses JA, Seifert B, et al. Interleukin-1-receptor antagonist in type 2 diabetes mellitus. The New England journal of medicine. 2007;356(15):1517-26.
409. Murphy JE, Morales RE, Scott J, Kupper TS. IL-1 alpha, innate immunity, and skin carcinogenesis: the effect of constitutive expression of IL-1 alpha in epidermis on chemical carcinogenesis. J Immunol. 2003;170(11):5697-703.
410. Ghiringhelli F, Apetoh L, Tesniere A, Aymeric L, Ma Y, Ortiz C, et al. Activation of the NLRP3 inflammasome in dendritic cells induces IL-1beta-dependent adaptive immunity against tumors. Nat Med. 2009;15(10):1170-8.
411. Han J, Nepal P, Odelade A, Freely FD, Belton DM, Graves JL, Jr., et al. High-Fat Diet-Induced Weight Gain, Behavioral Deficits, and Dopamine Changes in Young C57BL/6J Mice. Frontiers in nutrition. 2020;7:591161.
412. Saklayen MG. The Global Epidemic of the Metabolic Syndrome. Current hypertension reports. 2018;20(2):12.
413. Hirode G, Wong RJ. Trends in the Prevalence of Metabolic Syndrome in the United States, 2011-2016. JAMA. 2020;323(24):2526-8.
414. Zheng KI, Gao F, Wang XB, Sun QF, Pan KH, Wang TY, et al. Letter to the Editor: Obesity as a risk factor for greater severity of COVID-19 in patients with metabolic associated fatty liver disease. Metabolism: clinical and experimental. 2020;108:154244.
415. Palaiodimos L, Kokkinidis DG, Li W, Karamanis D, Ognibene J, Arora S, et al. Severe obesity, increasing age and male sex are independently associated with worse in-hospital outcomes, and higher in-hospital mortality, in a cohort of patients with COVID-19 in the Bronx, New York. Metabolism: clinical and experimental. 2020;108:154262.
416. Gallo G, Calvez V, Savoia C. Hypertension and COVID-19: Current Evidence and Perspectives. 2022;29(2):115-23.
417. De Ramos IP, Lazo M, Schnake-Mahl A, Li R, Martinez-Donate AP, Roux AVD, et al. COVID-19 Outcomes Among the

Hispanic Population of 27 Large US Cities, 2020-2021. American journal of public health. 2022;112(7):1034-44.
418. Qeadan F, VanSant-Webb E, Tingey B, Rogers TN, Brooks E, Mensah NA, et al. Racial disparities in COVID-19 outcomes exist despite comparable Elixhauser comorbidity indices between Blacks, Hispanics, Native Americans, and Whites. Sci Rep. 2021;11(1):8738.
419. Bovolini A, Garcia J. Metabolic Syndrome Pathophysiology and Predisposing Factors. 2021;42(3):199-214.
420. Zieve FJ. The metabolic syndrome: diagnosis and treatment. Clinical cornerstone. 2004;6 Suppl 3:S5-13.
421. Reddy P, Lent-Schochet D, Ramakrishnan N, McLaughlin M, Jialal I. Metabolic syndrome is an inflammatory disorder: A conspiracy between adipose tissue and phagocytes. Clinica Chimica Acta. 2019;496:35-44.
422. Sharma P. Inflammation and the metabolic syndrome. Indian journal of clinical biochemistry : IJCB. 2011;26(4):317-8.
423. Chen J-C, Ho F-M, Pei-Dawn Lee C, Chen C-P, Jeng K-CG, Hsu H-B, et al. Inhibition of iNOS gene expression by quercetin is mediated by the inhibition of IκB kinase, nuclear factor-kappa B and STAT1, and depends on heme oxygenase-1 induction in mouse BV-2 microglia. Eur J Pharmacol. 2005;521(1):9-20.
424. Granert C, Raud J, Waage A, Lindquist L. Effects of polysaccharide fucoidin on cerebrospinal fluid interleukin-1 and tumor necrosis factor alpha in pneumococcal meningitis in the rabbit. Infection and immunity. 1999;67(5):2071-4.
425. Jung K, Ha E, Uhm Y, Park H, Kim MJ, Kim H, et al. Suppressive effect by Hizikia fusiforme on the production of tumor necrosis factor in BV2 murine microglial cells. Neurological research. 2007;29 Suppl 1:S88-92.
426. Nurmohamed M, Bao Y, Signorovitch J, Trahey A, Mulani P, Furst DE. Longer durations of antitumour necrosis factor treatment are associated with reduced risk of cardiovascular events in patients with rheumatoid arthritis. RMD Open. 2015;1(1):e000080.
427. Shen H, Tesar BM, Walker WE, Goldstein DR. Dual signaling of MyD88 and TRIF is critical for maximal TLR4-induced dendritic cell maturation. J Immunol. 2008;181(3):1849-58.
428. Kanneganti T-D, Lamkanfi M, Kim Y-G, Chen G, Park J-H, Franchi L, et al. Pannexin-1-Mediated Recognition of Bacterial Molecules Activates the Cryopyrin Inflammasome Independent of Toll-like Receptor Signaling. Immunity. 2007;26(4):433-43.
429. Galea J, Armstrong J, Gadsdon P, Holden H, Francis SE, Holt CM. Interleukin-1 beta in coronary arteries of patients with ischemic heart disease. Arteriosclerosis, thrombosis, and vascular biology. 1996;16(8):1000-6.

430. Kirii H, Niwa T, Yamada Y, Wada H, Saito K, Iwakura Y, et al. Lack of interleukin-1beta decreases the severity of atherosclerosis in ApoE-deficient mice. Arteriosclerosis, thrombosis, and vascular biology. 2003;23(4):656-60.
431. Dinarello CA. Interleukin-1 beta, interleukin-18, and the interleukin-1 beta converting enzyme. Annals of the New York Academy of Sciences. 1998;856:1-11.
432. Katz SS, Shipley GG, Small DM. Physical chemistry of the lipids of human atherosclerotic lesions. Demonstration of a lesion intermediate between fatty streaks and advanced plaques. J Clin Invest. 1976;58(1):200-11.
433. Guyton JR, Klemp KF. Transitional features in human atherosclerosis. Intimal thickening, cholesterol clefts, and cell loss in human aortic fatty streaks. The American journal of pathology. 1993;143(5):1444-57.
434. Catapano AL, Graham I, De Backer G, Wiklund O, Chapman MJ, Drexel H, et al. 2016 ESC/EAS Guidelines for the Management of Dyslipidaemias. Eur Heart J. 2016;37(39):2999-3058.
435. Pasterkamp G, van Lammeren GW. Pleiotropic effects of statins in atherosclerotic disease. Expert review of cardiovascular therapy. 2010;8(9):1235-7.
436. de Bont N, Netea MG, Rovers C, Smilde T, Demacker PN, van der Meer JW, et al. LPS-induced cytokine production and expression of LPS-receptors by peripheral blood mononuclear cells of patients with familial hypercholesterolemia and the effect of HMG-CoA reductase inhibitors. Atherosclerosis. 1998;139(1):147-52.
437. Hirahara K, Poholek A, Vahedi G, Laurence A, Kanno Y, Milner JD, et al. Mechanisms underlying helper T-cell plasticity: implications for immune-mediated disease. The Journal of allergy and clinical immunology. 2013;131(5):1276-87.
438. Langley RG, Elewski BE, Lebwohl M, Reich K, Griffiths CE, Papp K, et al. Secukinumab in plaque psoriasis--results of two phase 3 trials. The New England journal of medicine. 2014;371(4):326-38.
439. Leonardi C, Matheson R, Zachariae C, Cameron G, Li L, Edson-Heredia E, et al. Anti-interleukin-17 monoclonal antibody ixekizumab in chronic plaque psoriasis. The New England journal of medicine. 2012;366(13):1190-9.
440. Steinkasserer A, Spurr NK, Cox S, Jeggo P, Sim RB. The human IL-1 receptor antagonist gene (IL1RN) maps to chromosome 2q14–q21, in the region of the IL-1α and IL-1β loci. Genomics. 1992;13(3):654-7.
441. Somm E, Cettour-Rose P, Asensio C, Charollais A, Klein M, Theander-Carrillo C, et al. Interleukin-1 receptor antagonist is upregulated during diet-induced obesity and regulates insulin sensitivity in rodents. Diabetologia. 2006;49(2):387-93.

442. Meier CA, Bobbioni E, Gabay C, Assimacopoulos-Jeannet F, Golay A, Dayer JM. IL-1 receptor antagonist serum levels are increased in human obesity: a possible link to the resistance to leptin? J Clin Endocrinol Metab. 2002;87(3):1184-8.
443. Ingy IA, Wim JQ. A Glimpse into the Biosynthesis of Terpenoids. KnE Life Sciences. 2017;3(5).
444. Zhang Y, Tian R, Wu H, Li X, Li S, Bian L. Evaluation of acute and sub-chronic toxicity of lithothamnion sp. in mice and rats. Toxicology reports. 2020;7:852-8.
445. Hoebe K, Beutler B. TRAF3: a new component of the TLR-signaling apparatus. Trends in Molecular Medicine. 2006;12(5):187-9.